Definition of the

Early HIV-1 Signalosome

in Dendritic Cells

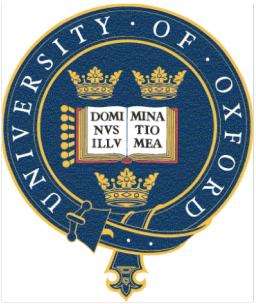

Elham Khatamzas

Trinity College

University of Oxford

Supervisors:
Dr. Alison Simmons
Professor Sarah Rowland-Jones

A DPhil thesis submitted for the degree of

Doctor of Philosophy in Clinical Medicine

Trinity 2012

This dissertation is the result of my own work
and includes nothing, which is the outcome
of work done in collaboration
except where specifically indicated in the text.

This dissertation is not substantially the same
as any submitted by the author for any other
degree or diploma or other qualification
at any other university.

No part of this dissertation has already been,
or is currently being submitted by the author
for any other degree or diploma
or other qualification.

This dissertation does not exceed 50,000 words,
exclusive of appendices, bibliography, diagrams and tables.

Acknowledgements

I would like to thank all the members of the Human Immunology Unit for creating a friendly and creative environment to work in.
Many thanks to all the collaborators for providing reagents and advice, especially the Benedikt Kessler lab for carrying out the proteomics studies and all technical and analytic support.
I thank the Wellcome Trust for funding me.
I'm greatly indebted to Derrick Crook and Paul Klenerman for all the advice and encouragement they provided throughout the years.
A very big thanks goes to Andrew McMichael for being my sponsor and always having his office door open for me.
Thanks to all the members of SRJ and Simmons lab, past and present, in particular Al Leslie and Tica Pichulik, Al for being clever, funny and reliable in your own way, and Tica for sharing all the good times, bad times we've been through. You're both greatly missed.
A big thanks goes to Sarah for supporting me and giving me the opportunity to come to Oxford and introducing me to the amazing Gambia crew.
I'm very grateful to Alison for supervising me and introducing me to a wonderful world of science full of intriguing things to be discovered.
Thanks to mr run-to-be for, well, everything.
Lastly, I thank my parents for supporting their Iranian daughter to do it her way.

Abstract

DCs are critical to the early events of HIV-1 infection. They are the first cells that HIV-1 encounters at mucosal surfaces and as sentinel antigen-presenting cells of the immune system these should alarm the immune system and activate innate immune defences to recruit effective adaptive immunity and viral clearance. A peculiar characteristic of HIV – in contrast to other ssRNA viruses – is its ability to completely evade host innate recognition pathways. Additionally, it has the unique ability to manipulate the endo-lysosomal system of DCs and promote transmission via *trans*-infection to CD4+ T cells across virological synapses. However, it is largely unknown how HIV-1 is sensed by the innate immune system.

Here, a multipronged experimental approach based on phosphoproteomics, transcriptomics and custom RNAi screen was developed to characterize the early signaling complex induced by HIV-1 in DCs. A novel method of phosphoproteomics to identify the HIV-1 phosphoproteome in DCs showed that 342 proteins were differentially phosphorylated following 10 min of HIV-1 infection compared to time-matched mock-infected DCs. Functional analysis of these phosphoproteins showed enrichments in several cellular pathways, including vesicular trafficking, cytoskeletal rearrangements and the secretory pathway and a relative paucity of signaling molecules involved in inflammatory pathways. Proteomics analysis of HIV-1 virions was undertaken to identify host molecules hijacked by HIV-1 during viral replication and revealed a close interaction between the virus and the endo-lysosomal system. Transcriptomics analysis of HIV-1 infected DCs showed a muted immune response with no detectable differentially regulated genes. The results of the phoshoproteomic screen provided the basis for a custom RNAi screen to identify host proteins that are differentially phosphorylated by the virus and required for efficient *trans*-infection from DCs to CD4+ lymphocytes. The results of this screen showed that 54 of the 120 host factors tested were required for efficient viral transfer to CD4+ T cells and contribute to characterization of the compartment that HIV-1 is internalized in on a molecular level. Two host factors identified within the HIV-1 phosphoproteome were chosen for further studies. Studies of BLOC-1 (biogenesis of lysosome-related organelles complex-1) and its subunits

identified a role for snapin in HIV-1 *trans*-infection and HIV-1 and TLR8 sensing. Snapin may act as determinant of sorting of HIV-1 intraluminal vesicles to non-degradative, non-immunogenic compartments by activating mammalian target of rapamycin, mTOR, and inhibiting autophagy. Furthermore, HIV-1 triggered dephosphorylation of the cytosolic tyrosine phosphatase possibly via the interaction of host CD47 incorporated in the virion and the transmembrane glycoprotein SIRPα expressed on DCs. Blocking of this interaction with an inhibitory CD47 antibody resulted in a reduction of HIV-1 replication.

Taken together, this multipronged approach reveals the complexity of the interaction of HIV-1 with the host cell machinery and identifies novel mechanism of the immune evasion tactics usurped by HIV-1.

Contents

List of figures

List of tables

Abbreviations

A	Adenine
Ab	Antibody
AP-1	Activating protein - 1
APC	Antigen presenting cell
AZT	Azidothymidine
BDCA	Blood dendritic cell antigen
BLOC-1	Biogenesis of lysosome-related organelles complex 1
BLOS1	Biogenesis of lysosome-related organelles complex 1, subunit 1
BSA	Bovine serum albumin
C	Cytosine
CA	Capsid
CARD	Caspase recruitment domains
Cbl	Proto-oncogene, E3 ubiquitin protein ligase
CCR	C-C chemokine receptor
CD	Cluster of differentiation
Cdc42	Cell division control protein 42
CXCR	C-X-C chemokine receptor
DC	Dendritic cell
DC-SIGN	Dendritic Cell-Specific Intercellular adhesion molecule-3- Grabbing Non-integrin
DCIR	Dendritic cell immunoreceptor
DDR	DNA damage response
DMEM	Dulbecco's Modified Eagle Medium
DTT	Dithiothreitol
ECL	Enhanced chemiluminescence
EDTA	Ethylenediaminetetraacetic acid
EE	Early endosome
EEA	Early endosomal antigen
EGTA	Ethylene glycol tetraacetic acid
Env	Envelope
ER	endoplasmic reticulum
ERK	extracellular signal-regulated kinases
ESCRT	Endosomal sorting complexes required for transport
ESI	Electrospray ionization
FACS	Fluorescence activated cell sorting
FAK	Focal adhesion kinase
FCS	Foetal calf serum
Fyn	Oncogene related to SRC, FGR, YES
GAPDH	Glyceraldehyde 3-phosphate dehydrogenase
GOI	Gene of interest
Hck	Hemopoietic cell kinase

HEPES	Hydroxyethyl piperazineethanesulfonic acid
HIV	Human Immunodeficiency Virus
IB	Immunoblot
IEF	Isoelectric focussing
IFN	Interferon
IL	Interleukin
ILV	Intraluminal vesicle
IN	Integrase
IP	Immunoprecipitation
IRAK	Interleukin-1 receptor-associated kinase
IRF	Interferon regulatory factor
IS	Immunological synapse
ISG	Interferon Stimulated Gene
ITAM	Immunoreceptor tyrosine-based activation motif
ITIM	Immunoreceptor tyrosine-based inhibitory motif
JAK	Janus Kinase
kb	Kilo base
KSR1	Kinase suppressor of ras 1
LAMP1/2	Lysosomal-associated membrane protein 1
LARG	Rho guanine nucleotide exchange factor (GEF) 12
LB	Luria bertani
LC-MS/MS	Liquid chromatography-tandem mass spectrometry
LC3	Light chain 3
Lck	Leukocyte-specific protein tyrosine kinase
LE	Late endosome
LPS	Lipopolysaccharide
LRR	Leucine-rich repeats
LRRFIP1	Leucine rich repeat (in FLII) interacting protein 1
LSP1	Leukocyte specific protein 1
LTR	Long terminal repeat
m/z	Mass/charge ratio
MALDI	Matrix-assisted laser desorption absorption
MAPK	Mitogen-activated protein kinase
MDDC	Monocyte-derived dendritic cell
MDP	Muramyl dipeptide
MHC	Major histocompatibility complex
MIP-1	Macrophage inflammatory protein-1
MOI	Multiplicity of infection
mRNA	messenger RNA
MTOC	Microtubule organizing centre
mTOR	Mechanistic target of rapamycin (serine/threonine kinase)
MVB	Multivesicular body
MyD88	Myeloid differentiation primary response gene (88)
NF-KB	nuclear factor kappa-light-chain-enhancer of activated B cells
NLR	NOD-like receptor

NOD2	Nucleotide-binding oligomerization domain containing 2
Nup98	Nucleoporin 98kDa
P body	Processing body
PAMP	Pathogen-associated molecular pattern
PBA	Phosphate buffered saline + bovine serum albumin
PBMC	Peripheral blood mononuclear cells
PBS	Phosphate-buffered saline
PCR	Polymerase chain reaction
pDC	Plasmacytoid dendritic cells
PIC	Preintegration complex
PMSF	Phenylmethanesulfonyl fluoride
PR	Protease
PRR	Pattern recognition receptors
Rab	Member RAS oncogene family
Raf-1	v-raf-1 murine leukemia viral oncogene homolog 1
RE	Recycling endosome
RIG-I	Retinoic-acid-inducible gene I
RIN	RNA integrity number
RNAi	RNA interference
rpm	Revolutions per minute
RPMI	Roswell Park Memorial Institute medium
RQ	Relative quantification
RSV	Respiratory syncytial virus
RT	Room temperature
RTC	Reverse transcription complex
SAMHD1	SAM domain and HD domain 1
SD	Standard deviation
SDS	Sodium dodecyl sulfate
SEM	Standard error of the mean
SH2	Src Homology 2
SHP-1	Protein tyrosine phosphatase, non-receptor type 6
SILAC	Stable isotope labeling with amino acids in cell culture
siRNA	Small interfering ribonucleic acid
SIRPα	Signal-regulatory protein alpha
SIV	Simian immunodeficiency virus
Snapin	Soluble N-ethylmaleimide-sensitive factor attachment protein-associated protein
SNP	Single-nucleotide polymorphism
STAT	Suppressor of cytokine signalling
STING	Stimulator of interferon (IFN) genes
TAK1	TGF-β activated kinase 1
Tar	Trans-activation response element
tat	Trans-activating protein
TBK1	TANK binding kinase 1
TBS	Tris buffered saline
TCID50	50% Tissue Culture Infective Dose
TGN	Trans-golgi network

TLR	Toll-like receptor
TNF	Tumor necrosis factor
TNPO3	Transportin 3
TREX1	Three prime repair exonuclease 1
TRIM5	Tripartite motif-containing protein
UbcH7	Ubiquitin-conjugating enzyme E2L 3
Vps	Vacuolar protein sorting
VS	Virological synapse
WASP	Wiskott-Aldrich syndrome family protein
WB	Western blot
WCL	Whole cell lysate
wt	Wild type

Chapter 1

Introduction

In 1989, Charles Janeway in his seminal paper on pathogen-associated molecular patterns predicted, how a virus that does not induce costimulatory activity and does not infect dendritic cells may be particularly dangerous – all characteristics strongly reminiscent of human immunodeficiency virus, HIV (Janeway, 1989).

HIV is the most extensively studied pathogen since its initial discovery in 1982 and has caused an unparalleled pandemic killing more that 30 million people worldwide. Despite the advent of highly active combination therapy and increased accessibility to treatment and public health measures, more than 2.6 million people got infected in 2009[1]. Scientific efforts to develop an effective vaccine or microbicide have been hampered by the unprecedented genetic variability of the virus and its ability to avoid immune recognition (McMichael et al., 2010). Two recent reports showed that the rate of HIV acquisition in young, healthy, mostly female adults was 3 to 5 per 100 person-years in sub-Saharan Africans, making the development of preventive strategies a matter of grave urgency (Cohen and Baden, 2012).

Recognition of the rapid and irreversible damage that occurs at the acute stage of HIV-1 infection constitutes a major change in our understanding of HIV-1 pathogenesis. The current view in the field is, that there is only a small window of opportunity between transmission and peak viremia for a vaccine to be able to prevent viral propagation and the massive and irreversible destruction of the mucosal CD4+ T-cell population as well as the establishment of latent reservoirs (Haase, 2010). Recent reports have revealed the double-edged role of the innate immune system in early immune control and promotion of disease pathology (Li et al., 2009). Therefore, the focus of HIV-1 research has shifted

[1] who.int

towards gaining a basic understanding of the earliest stages of infection and how HIV-1 is sensed by the innate immune system (Medzhitov and Littman, 2008).

1.1 Pathogenesis of early HIV-1 infection

1.1.1 Stages of HIV-1 infection

The clinical phases following HIV-1 acquisition usually follow a set pattern regardless of the acquisition route (reviewed in (Cohen et al., 2011; McMichael et al., 2010)). Recent informative studies of the non-human primate (NHP) model, largely drawn from experiments in Rhesus macaques infected intravaginally with high dose Simian Immunodeficiency Virus (SIV), allow to put the early clinical phases into the context of the highly dynamic viral induced local and systemic pathology, however many gaps remain in understanding the complicated virus-host interactions.

The initial **eclipse phase** - directly following HIV exposure - lasts about 10 days (7 to 21 days) and is characterized by absence of clinical symptoms. During the first week the virus replicates locally in mucosal and submucosal tissues and disseminates to the lymphoreticular system. What ensues is a massive and irreversible depletion of gut CD4+ T cells and probably, although not completely established, the creation of a pool of latently infected cells, that is, resting cells with silently integrated HIV-1 DNA in their genome which persist in the presence of antiretroviral treatment (Chun et al., 1998). In the SIV model the timing of response to post exposure prophylaxis with antiretroviral drugs, that is the time to the establishment of the viral reservoir, may be as short as 24 hours (Cohen et al., 2011; Emau et al., 2006). The important role of the innate immune system in this early phase will be addressed in the following pages.

The eclipse phase ends with the first detection of viral RNA in the plasma. Viral RNA levels rise exponentially reaching **peak viremia** with a maximum at day 21-28 post infection. Patients may develop a flu-like illness, which due to its unspecific nature mostly remains unrecognized. This is due to rapid expansion and massive dissemination of virus and virus-infected cells via draining lymph nodes to other lymphoid tissues, with the gut-associated lymphoid tissue (GALT) being the most severely affected tissue. Antigen-presenting cells (APCs) such as dendritic cells (DCs) capturing virus via C-type lectin receptors play a fundamental role in this process by transmitting HIV to

CD4+ target cells in lymph nodes. The role of other APCs such as B cells is not entirely clear yet, they may bind virus through the complement receptor CD21 and present it to target cells (Moir et al., 2000). It is still unknown whether viral dissemination occurs primarily by release of infectious virions into blood or lymphatics or by migration of infected cells into tissues.

The GALT harbors the bulk of CD4+ T cells in the body. Studies by a number of investigators have demonstrated that these cells undergo a very early and drastic depletion with the GALT being stripped off up to 80% of its CD4+ T-cell population within the first three weeks of infection (reviewed in (Brenchley and Douek, 2008; Dandekar, 2007)). Additionally, B-cell germinal centers are damaged during this early phase and a fibrotic process of lymph node architecture sets in. Importantly, while peripheral blood CD4+ T cells, that had temporarily decreased concomitant to peak viremia return back to normal levels, the GALT CD4+ T-cell numbers never recover. Although antigen-specific cytotoxic CD8+ T cells start to infiltrate lymphoid tissue, the response is considered to be "too little and too late" to prevent the viral induced pathology (Haase, 2005).

Subsequently, viral load decreases over the next 12-20 weeks to establish a **viral set point.** This is determined by a dynamic equilibrium between viral production and viral clearance and coincides with the expansion of HIV-specific T cells that are only partially able to control viremia in most infected individuals (Koup et al., 1994). However, immune pressure exerted by T and Natural killer (NK) cells as well as B cells already selects for viral escape variants (Johnson and Desrosiers, 2002; Price et al., 1997). Multiple investigations have shown the significance of the viral set point for the subsequent rate of disease progression. To envisage the remarkable dynamic nature of the processes so far: Viral particles are cleared within 30 minutes from the blood and half of infected CD4+ T cells die at a rate of 0.7 days, a process that must be maintained by a constant supply of viral production and target cell availability (De Boer et al., 2010; Haase, 2011).

Hallmark of the ensuing **chronic progressive infection** is a cumulative reduction of the CD4+ T-cell population with rising levels of plasma viral load, ultimately leading to the development of opportunistic infections and AIDS.

1.1.2 Early local events in HIV-1 infection

The majority of HIV-1 transmissions (80%) are via mucosal surfaces with the rest being though intravenous and percutaneous exposure. Despite extensive investigation over the past years, it is still uncertain which cells constitute the primary targets for the virus. CD4 is the main receptor for HIV. Given the diverse routes of transmission and the diversity of cell populations in the tissues involved in the transmission event, it is likely that several CD4 expressing cell types may be involved. Candidates are T cells, DCs, Langerhans cells (LC) as well as macrophages. In studies of acutely SIV-infected rhesus macaques, infected CD4+ T cells are found within the first day in vaginal tissue. Other studies of the NHP model and genital explant tissue model have shown that both CD4 as well as LCs are the first targets of the virus in foreskin and vaginal tissue (Ganor et al., 2010). In addition to LCs other dendritic cells have been implicated to play a role (Lackner and Veazey, 2007), especially myeloid DCs, which reside in these tissues in an immature state and are able to extend their dendrites into the lumen to capture antigens (Iwasaki, 2007). The role of submucosal macrophages is not clear, they generally show poor infectivity in *in vitro* studies. Additionally, it still remains to be established if HIV is transmitted as cell free or cell bound virus. Noteworthy are fairly recent findings using single genome amplification and phylogenetic analysis that prove that up to 80% of heterosexual mucosal transmissions arise from a single founder virus (Salazar-Gonzalez et al., 2009). This implicates that once the swarm of virions have breached the epithelial layer of the mucosa, the vast majority do not succeed in establishing infection. This is likely to be multifactorial, for instance due to defective or less fit virions with poor replicative capacity and the mucosal immune system. If and how the local innate responses play a role in selecting the founder virus, e.g. by introducing lethal mutations will be an interesting question for future studies (Keele and Estes, 2011). Interestingly, the single founder virus is responsible for only 40% of infections in injection drug users highlighting the important role of the mucosal barrier during transmission.

It remains unclear how HIV crosses the intact epithelial barrier of the mucosa and studies have provided conflicting results mostly due to the difficulties in setting up a valid experimental system and the different modes of transmission. An ex vivo tissue model suggests that HIV-1 crosses vaginal epithelial cells via transcytosis (Meng et al.,

2002). Studies of the role of epithelial cells (ECs) have provided conflicting results regarding the permissiveness of ECs for viral infection (Boggiano and Littman, 2007). Furthermore, it has been proposed, but not conclusively demonstrated that intraepithelial dendritic cells may capture virions by extending their dendrites into the lumen (Hladik and McElrath, 2008; Shen et al., 2010).

Regardless of the nature of the first cell being infected by the virus, what ensues within the first days appears to be initiated with SIV crossing the epithelial barrier of the mucosal tissue within hours to establish the small founder population of infected cells, these are primarily resting, non-activated CD4+ T cells that also express the integrin α4β7. This is important for a number of reasons: α4β7 engages the viral envelope glycoprotein gp120 resulting in efficient cell-to-cell spread via infectious synapses, it is a marker for the Th17 subset in the mucosa and it regulates cell migration into the GALT (Arthos et al., 2008; Cicala et al., 2009; Nawaz et al., 2011; Wang et al., 2010).

A study by Li et al provided an intriguing insight into the involvement of innate cells early after transmission (Li et al., 2009) (figure 1.1). Intravaginal infection with high dose SIV induces a signaling cascade in vaginal epithelial sells that leads to upregulation of the macrophage inflammatory protein, MIP3-α (CCL20), recruiting plasmacytoid DCs (pDCs) to the local site of infection within 4 days post-exposure. Subsequent production of MIP1-α and β as well as interferon alpha (IFN-α) by activated pDCs attracts more CD4+ target cells resulting in expansion of the localized foci of infection. Importantly, IFN-α, an antiviral cytokine, is fueling viral infection rather than containing its spread. How the virus succeeds in creating this favorable environment for its own expansion is unknown. About 3 weeks post SIV exposure virus specific T cells, most likely primed in local lymph nodes migrate to the mucosal site, however this is “too little, too late” to control the infection (Haase, 2010). By now virus has spread to lymphoid cells in the GALT replicating at high levels in peyer’s patches, the lamina propria and mesenteric lymph nodes and caused massive depletion of the CD4+ T-cell population (Veazey et al., 1998). The exact molecular mechanisms accounting for the massive and irreversible destruction of mucosal CD4 cells are still under investigation. It has been suggested that they are due to a combination of productive viral infection and bystander effects. Immune activation seems to play a role in this, both as a cause and effect.

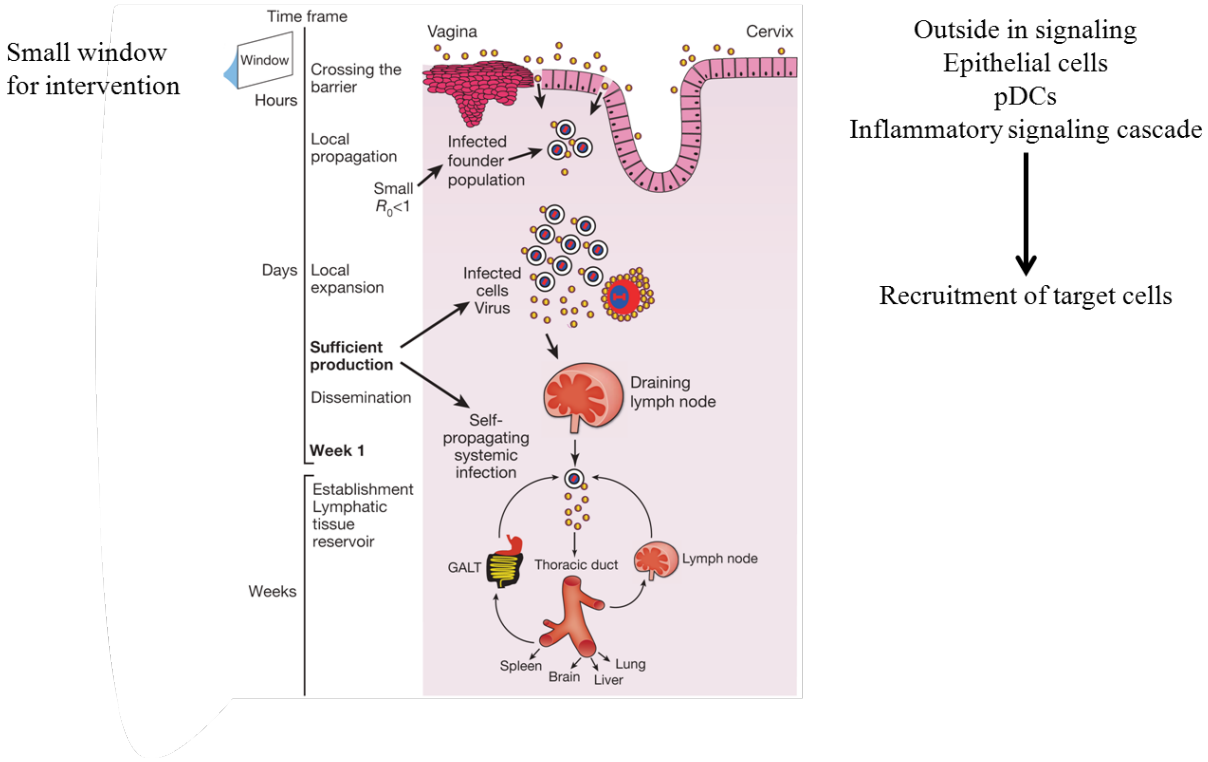

Figure 1.1. Time frame, sites and major events in mucosal SIV transmission. Adapted from (Haase, 2010).

1.2 Role of DCs in HIV-1 infection

DCs are strategically located underneath the epithelial layers throughout the body, where they constantly monitor for invading pathogens. Therefore, they are generally considered to be the first line of defence against incoming virions and HIV-1 is equipped with intricate ways to convert this enemy into a strong ally. Hence, a basic understanding of DC biology and its manipulation by HIV-1 is of paramount importance.

1.2.1 DCs are professional antigen-presenting cells

DCs and other antigen-presenting cells (APC) such as B cells and macrophages are key players in a controlled, specific and efficient T cell response to incoming pathogens (Banchereau and Steinman, 1998). While macrophages are highly efficient at antigen endocytosis and clearance, and B cells fulfill the APC function for induction of a humoral immune response, DCs are exceptionally skilled at antigen presentation and

more competent at activating T cells than any other APC (Mellman and Steinman, 2001). Antigen presentation implies uptake of foreign antigen, its degradation and loading onto the major histocompatibility complex (MHC) class I and II molecules on the surface of the APCs for presentation to T cells (Trombetta and Mellman, 2005). This interaction occurs at stable DC-T cell contact zones, the immunological synapse (IS). Within the IS, T cell receptors (TCR) recognize antigenic peptide-MHC complexes presented on the surface of the T cell (Lanzavecchia and Sallusto, 2001a). Engagement of several pairs of adhesion and costimulatory molecules, e.g. CD86/CD28, DC-SIGN/ICAM-3 present on DC and T cells respectively strengthens the contact. Triggering of the TCR at the synapse induces a signaling cascade that can induce polarization of T cell development or induction of peripheral T cell tolerance (Lanzavecchia and Sallusto, 2001b). In addition to the classical mode of peptide loading of antigens of endogenous and exogenous origin onto MHC class I and class II molecules, respectively, DCs are equipped with alternative pathways to present antigens. Cross presentation refers to a process whereby exogenous antigens are processed in the MHC class I pathway, an important mechanism for DCs to generate either tolerance to self-antigens or immunity to pathogens (Kurts et al., 2010). Furthermore, macroautophagy, which will be discussed in more detail below, can deliver intracellular antigens for MHC class II presentation to CD4+ T cells (Schmid et al., 2007).

1.2.2 DC maturation

Functionally, DCs exist in two distinct states, immature and mature. The majority of DCs in peripheral tissue in situ are immature, the prototype are Langerhans cells in the epidermis (Mellman and Steinman, 2001). Immature DCs (iDC) are highly efficient at endocytosis and express low levels of MHC I and II and costimulatory molecules on the surface (Mellman and Steinman, 2001). MHC class II molecules are sequestered in lysosomal compartments waiting to be loaded with antigenic peptides. Upon encounter with microbial products or proinflammatoy cytokines, iDCs undergo changes consisting of up-regulation of costimulatory (CD80, CD86) and T-cell adhesion (CD54, CD48) molecules, redistribution of MHC class II from intracellular compartment to the cell membrane, acquisition of a migratory phenotype and secretion of soluble mediators

such as chemokines (Guermonprez et al., 2002). The mature DC now has reduced endocytic capacity, but exceptional ability for T cell stimulation and an altered chemokine profile facilitating homing to lymphoid organs as well as change in morphology with formation of dendritic processes (Mellman and Steinman, 2001).

1.2.3 The role of DCs in the innate immune response

Recognition of an invading microbial pathogen as non-self is a first and critical step in programming the host immune system for control of infection (Medzhitov and Janeway, 2000). DCs are equipped with a number of membrane-associated, endosomal and cytosolic intracellular sensors – referred to as pattern-recognition receptors (PRR) - that allow them to detect foreign, pathogen-associated molecular patterns (PAMPs) (reviewed in (Kawai and Akira, 2010)). PAMPs are evolutionary conserved molecular patterns encompassing a wide range of moieties, including nucleic acid, protein, carbohydrates and lipids or combination of each, that differ from host cell macromolecules sufficiently in structure, location, and/or interaction such that they are discriminated as non-self by the PRRs. PAMP-PRR interaction induces the rapid initiation of downstream signaling cascades that results in activation of transcription factors such as NF-κB and phosphorylation of interferon regulatory factors (IRFs) and alterations of host cell gene expression, leading ultimately in the induction of intracellular immune defenses. The innate immune response will modulate the production of inflammatory cytokines, the phagocytic process and intracellular trafficking of the pathogen and DC maturation and shape the subsequent development of the adaptive immune response (van Vliet et al., 2007). Specifically, detection of viral RNA or DNA triggers the induction of interferons that initiate the transcription of interferon-stimulated genes (ISGs), which interfere with various steps of the viral replication cycle and may induce apoptosis in infected cells (Bowie and Unterholzner, 2008; Takaoka et al., 2003). In general, two complementary systems, that detect DNA or RNA exist, the endosomal Toll-like receptors (TLRs) and cytosolic nucleic acid sensors. The TLRs that recognize nucleic acids - TLR3, TLR7, TLR8 and TLR9 - are located in endosomes of APCs and recognize nucleic acids derived from infected apoptotic cells or internalized viruses (Kawai and Akira, 2006). Cytosolic RNA or DNA derived from pathogens can be recognized by the retinoic acid-inducible gene I (RIG-I)-

like receptors (RLRs), the nucleotide-binding oligomerization domain (NOD)-like receptors (NLRs), the more recently identified absent in melanoma 2 (AIM2)-like receptors (ALRs) and an expanding family of DEXDc helicases (DLRs) (Rathinam and Fitzgerald, 2011). Additionally, the proinflammatory antiviral cytokines IL1β and IL18 are generated following cytosolic sensing pathways and activation of the inflammasome (Rathinam and Fitzgerald, 2011).

1.2.4 Endocytic capacity of DCs

The endo-lysosomal system in DCs is distinct from other cells. For instance, macrophages rapidly degrade internalized proteins in lysosomal compartments, DCs however sequester antigens for extended periods of time and regulate antigen degradation for the purpose of formation of peptide-MHC class II complexes (Turley et al., 2000). Regulated control of lysosomal pH and enzyme content such as cathepsins plays a role, the anti-inflammatory cytokine IL10 may also reduce proteolytic capacity by influencing the protease content (Fiebiger et al., 2001).

DCs exhibit different types of endocytosis: phagocytosis, clathrin-mediated endocytosis, caveolar-mediated endocytosis and macropinocytosis (Banchereau and Steinman, 1998). Phagocytosis is from an evolutionary perspective probably the most physiologically relevant mode of antigen uptake, allowing DCs to efficiently internalize large microbes or apoptotic particles or even minute quantities of antigen via a receptor-mediated, actin-dependent process (Carbone and Heath, 2003). Generation of antigenic peptides via phagocytic uptake is particularly efficient. Among the receptors involved in antigen uptake, such as scavenger or Fc receptors, the C-type lectin receptors (CLR) are of particular interest to HIV-1 infection and will be discussed further below. Conversely, macropinocytosis is an unspecific, actin-dependent process that allows DCs to rapidly sample their microenvironment for antigens by engulfing large volumes of extracellular fluid (Guermonprez et al., 2002). Viruses such as Vaccinia and Adenovirus trigger actin-mediated membrane-ruffling and blebbing that induces formation of large vacuoles (macropinosomes) at the plasma membrane and internalization of viral particles through the limiting membrane of these vacuoles into the host cell. The role of macropinocytosis in HIV-1 signaling is not clear, while some work suggests entry of HIV-1 into macrophages via macropinosomes (Marechal et al., 2001), others have

disputed this (Carter et al., 2011). Clathrin-mediated endocytosis represents the most common endocytic route used by viruses including HIV-1 (Cambi et al., 2009; Doherty and McMahon, 2009; McMahon and Boucrot, 2011). It includes a number of complex signaling events such as formation of phosphoinositide-4,5-phosphate that trigger concentration of soluble components such as clathrin around the cargo and to form a characteristic membrane coat at the cytosolic side of the plasma membrane (Doherty and McMahon, 2009). Recruitment of adaptor proteins such as AP2 and Eps15 lead to invagination of the endocytic vesicle, a process that is terminated by fission of the vesicle via the GTPase dynamin (Mercer et al., 2010). This coat then disassembles after the vesicle has pinched off. Lastly, caveolin-mediated endocytosis may play a role in viral entry in pDCs (Pritschet et al., 2012) and ligand-induced endocytosis of CCR5 (Venkatesan et al., 2003). Caveolin 1 is a membrane protein, which forms cholesterol-rich microdomains and invaginations that upon signaling pinch off for endosomal transport (Parton and Simons, 2007).

1.2.5 DC subsets important for HIV-1 pathogenesis

Studies of DCs have shown considerable heterogeneity in ontogeny, localization, function and phenotypic properties among the various subsets (Shortman and Liu, 2002). In humans, DCs are grossly divided into two major subsets, the conventional – also referred to as myeloid – DCs and plasmacytoid DCs (figure 1.2). Plasmacytoid DCs, although only comprising up to 0.2-0.5% of peripheral blood mononuclear cells, are the most potent inducers of type I interferons in response to viral stimulation due to constitutive expression of IRF7 and IRF5 (McKenna et al., 2005; Shortman and Liu, 2002). They are present in blood and secondary lymphoid organs. Their interaction with HIV-1 differs considerably from mDCs due to distinct PRR expression. They take up HIV-1 via CD4 into the endosome (Pritschet et al., 2012), where HIV nucleic acids may be sensed by TLR7 and TLR9 and trigger the production of type I interferons (Altfeld et al., 2011). Unlike other TLR7 agonists, HIV-1 preferentially traffics to early endosomes and skews activation towards IFNα production (O'Brien et al., 2011). They also express the CLR BDCA-2, however the role of this receptor in HIV-1 infection is unknown (Jaehn et al., 2008).

Myeloid DCs reside in peripheral tissue, secondary lymphoid organs and blood (Ueno et al., 2007). In contrast to pDCs, they have high endocytic capacity and express a number of CLRs important in HIV-1 infection. These include DC-specific ICAM3-grabbing non-integrin DC-SIGN (CD209), Langerin (CD207, CLEC4K) and DC immunoreceptor (DCIR, CLEC4A). Furthermore, they are characterized by the expression of the chemokine receptors CCR9, CXCR6, CCR3 and CCR8, which allow migration in tissues and have been implicated in HIV-1 entry and attachment (Wu and KewalRamani, 2006). They are more geared towards production of cytokines such as IL12, important for both the innate and adaptive immune system (Banchereau and Steinman, 1998).

Furthermore, non-mature BDCA-1 positive DCs present in blood can be productively infected by HIV-1 *in vitro*, despite the lack of expression of DC-SIGN and very low levels of CD4 and CCR5 expression (Granelli-Piperno et al., 2006). The *in vivo* relevance of this subset for HIV-1 infection remains to be established.

Owing to the low frequency of mDCs in blood and difficulties in isolating sufficient number and quality of mDCs from peripheral tissues, generation of DCs *in vitro*, either from bone-marrow derived CD34+ cells or blood monocytes, has provided an essential tool to understand DC biology (Sallusto and Lanzavecchia, 1994). The majority of studies investigating the interaction of mDCs with HIV-1 use monocyte-derived DCs (MDDCs) as a valid model for immature DCs residing in peripheral tissues such as the mucosa (Steinman et al., 2003). They are characterized by low expression of maturation markers (CD80, CD83) and MHC class II, but high expression of DC-SIGN and respond to activation with PRR ligands with changes in phenotypic and functional properties. However, while MDDCs have provided invaluable insights into the interaction of HIV-1 with DCs, any results should be interpreted with caution until these can be recapitulated *in vivo*.

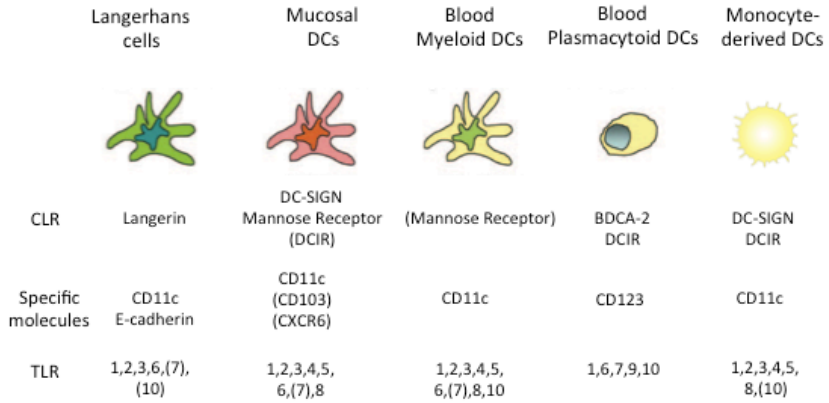

Figure 1.2. Human DC subsets with PRR expression. Adapted from (Kokkinopoulos et al., 2005; Ueno et al., 2007).

1.3 HIV and the innate immune response

Multiple pathogens have evolved mechanisms to subvert the innate immune response to promote their replication and dissemination and increasing evidence is unraveling the mechanisms whereby HIV is exploiting host factors of the innate immune system to remain undetected, and recognized as self (Iwasaki, 2012). HIV-1 is unusual because it does not alert innate host defences that should be triggered by the presence of a ssRNA virus, and it does not induce type I interferons, neither in its major target cells, the CD4+ T cell population, nor in mDCs, which encounter virus during mucosal transmission. Nevertheless, HIV-1-infected individuals display markers of immune activation and elevated levels of cytokines and immunoglobulines during the acute and chronic stages of infection (Altfeld et al., 2011). A finding that is often considered to be due to an antiviral innate immune response. However, the absence of interferon induction and activation in cells directly infected with HIV-1 suggests that systemic immune activation is an indirect consequence of infection that is contributing to disease progression instead of control of infection.

1.3.1 Innate immune recognition of HIV-1 nucleic acids in DCs

Potentially HIV-1 could generate multiple replication intermediates during the viral life cycle that could serve as PAMPs during its life cycle. These include uridine-rich ssRNA sequences from the HIV-1 LTR that have been shown to potently activate endosomal TLR7 and TLR8 (Alter et al., 2007; Heil et al., 2004). Theoretically, double stranded RNA replication intermediates that get access to the endosome during viral endocytosis

or via autophagy could trigger TLR3 in the endosome (Gougeon and Piacentini, 2009). Interestingly, a recent study showed that NOD2 could also recognize viral ssRNA and activate IRF3 and IFNβ (Sabbah et al., 2009). Furthermore, replication intermediates that get access from the RTC to the cytosol, are not shielded by host proteins, and express modifications that differentiate them from self nucleic acid, could trigger cytosolic nucleic acid sensors such as MDA5, LGP2 or RIG-I (Rehwinkel, 2010). However, recent work suggests that the virus has developed numerous strategies to avoid sensing by these PRRs. For instance, purified genomic HIV-1 RNA can be sensed by RIG-I and induce an interferon response, in HIV-1-infected cells however the viral protease sequesters RIG-I and targets it for lysosomal degradation (Solis et al., 2011). Moreover, HIV-1 induces global disruption of innate signaling pathways by degrading IRF3. Altogether our understanding of HIV-1 nucleic acid sensing is still fairly rudimentary.

Table 1.1. Innate HIV-1 sensors.

Type	Sensor	Ligand	Signaling pathway	Location	Cell type
General	TLR7	ssRNA	IRF7, NF-κB	Endosome	pDC, B
	TLR8	ssRNA	IRF7, NF-κB	Endosome	mDC
	Unknown DNA sensor	ISD DNA (RT product)	IRF3	Cytosol	Many cell types
	DC-SIGN	Env	NF-kB	Surface	mDC
Species specific	Cyclophilin A	Capsid	IRF3	Cytosol	DC
	TRIM5, TRIM5-Cyclophilin A	Capsid	AP-1, NF-kB	Cytosol	DC, myeloid cell

For details see text. ISC: interferon-stimulatory DNA. Adapted from (Iwasaki, 2012)

1.3.2 C-type lectin receptors in HIV-1 infection

CLRs recognize glycosylated structures via specific carbodydrate-recognition domains. Mannose molecules of the heavily glycosylated HIV-1 envelope are recognized by CLRs, such as dendritic cell specific ICAM-3 grabbing non-integrin (DC-SIGN, also called CD209), Langerin (also called CD207 or CLEC4K), and the mannose receptor (MR) (Geijtenbeek et al., 2004; van den Berg et al., 2012). Furthermore, a recent study suggests that gp120 is also recognized by DC Immunoreceptor (DCIR, also called CLEC4A), but the exact carbohydrate moieties that are involved remain to be identified (Lambert et al., 2008). MR, DC-SIGN and DCIR are all expressed by specific

macrophage and DC subsets, whereas Langerin is expressed by Langerhans cells (LCs). Witte et al suggested that the interaction of HIV-1 with Langerin may be distinct to the other CLRs, whereby HIV-1 bound by Langerin is routed to Birbeck granules and degraded (de Witte et al., 2007). However, high local concentrations of virus can overcome this effect and vaginal LCs exposed to HIV-1 contribute to viral dissemination by migrating to local lymphatics (Ballweber et al., 2011).

1.3.3 The role of DC-SIGN in HIV-1 infection

Among the CLRs, DC-SIGN fulfills a unique role for HIV-1 pathogenesis. It is highly expressed on mucosal DCs where it may capture HIV-1 and serves as an attachment factor during viral entry (van den Berg et al., 2012). It binds to self-ligands such as ICAM-2 and ICAM-3 and indeed the interaction between ICAM-3 and resting T cells plays a role in potentiating the initial DC-T cell interaction. In addition to HIV-1, it is also involved in recognition of a variety of other pathogens such as Hepatitis C, Dengue virus, *Helicobacter pylori*, *Mycobacterium tuberculosis* as well as *Candida albicans*, pathogens known to subvert the immune response and cause chronic infections (van Vliet et al., 2008).

Usually, mannose-induced stimulation of DC-SIGN activates the serine/threonine protein kinase RAF1 and thereby induces phosphorylation of the NF-kB subunit p65 (reviewed in (van den Berg et al., 2012)). Interestingly, RAF1 activation is independent of TLR signaling; however, phosphorylation of p65 does depend on TLR signaling by triggering prior activation of NF-kB. Of note, the NF-kB family consists of five subunits: p65, c-Rel, RelB, p50, and p52. In steady state, these subunits are retained within the cytosol, and upon PRR activation translocate into the nucleus for initiation or repression of transcription. DC-SIGN signaling by DC-SIGN alone does not lead to NF-kB translocation into the nucleus, but enhances activation of certain canonical NF-kB subunits, and hence promotes transcription of the cytokines IL6, IL12α/β and IL10. This may explain how DC-SIGN is capable to tolerate self-ligands such as ICAM-2 and ICAM-3, as there is no simultaneous TLR signal to activate NF-κB. It also elegantly demonstrates how the combinational signaling mediated by the specific recognition of a PAMP may tailor the immune response towards that pathogen, e.g. the signaling

cascade has been shown to differ between HIV-1 and *M. tuberculosis* (Gringhuis et al., 2009).

HIV-1-mediated signaling via DC-SIGN has been shown to provide an immune escape mechanism for HIV-1 by recruiting the Rho guanine nucleotide-exchange factor LARG to the cytoplasmic domain of DC-SIGN and activating Rho GTPase activity (Hodges et al., 2007). This is associated with downstream activation of cdc42 and hence increased viral synapse formation (Hodges et al., 2007), as well as phosphorylation of Erk1/2 and AKT leading to a Th2 type response (Caparros et al., 2006). One of the most relevant and still elusive mechanisms for DC-SIGN mediated immune evasion, is its ability to capture HIV-1 and divert it to a non-lysosomal compartment to allow a process called *trans*-infection, which will be discussed in more detail below (Garcia et al., 2005; Geijtenbeek et al., 2000b; Geijtenbeek et al., 2000a).

1.3.4 The role of TLR8 in HIV-1 infection

As mentioned above GU-rich sequences from the HIV-1 LTR are readily recognized by TLR7 and TLR8 inducing a signaling cascade via MyD88 leading to the induction of type I interferons. In fact the HIV-1 genome contains multiple U-rich TLR7/8 ligands that induce strong activation in pDCs and monocytes (Meier et al., 2007). Furthermore, the role of TLR8 in HIV-1 pathogenesis is supported by a study demonstrating a favourable course of disease progression in association with a TLR8 polymorphism (Oh et al., 2008). However, myeloid DCs neither mature nor display any signs of activation upon HIV-1 infection (Harman et al., 2011; Hodges et al., 2007), even using excessive viral doses, despite expressing TLR8. It has been suggested that this may be due to low levels of productive viral infection in myeloid DCs, but as outlined below sensing of HIV ssRNA is essential for viral replication in DC-SIGN expressing DCs.

1.3.5 TLR8 and DC-SIGN crosstalk in HIV-1 infection

Gringhuis et al elegantly demonstrated how HIV-1 triggers both DC-SIGN via gp120 and TLR8 via ssRNA to ensure its successful transcription in the host cell (figure 1.3) (Gringhuis et al., 2010). Endosomal TLR8 triggering by HIV ssRNA induces activation and nuclear translocation of NF-κB, which initiates transcription from the integrated provirus. Without a second signal triggered by DC-SIGN and phosphorylated Raf1,

transcription would abort prematurely. DC-SIGN-mediated activation of NF-κB p65 recruits a host transcription elongation-factor called pTEF-b to the transcription complex. This induces phosphorylation of RNA polymerase II allowing generation of full-length transcripts during the first rounds of transcription, where Tat is not present yet. This is a prime example of how HIV-1 selectively usurps elements of the TLR8 signalosome to promote its replication while intriguingly at the same time evading an antiviral response. The *in vivo* relevance of these findings is unknown so far.

1.3.6 DCIR- a recently identified HIV-1 receptor

DCIR is expressed on myeloid DCs and has recently been identified as a novel CLR recognizing HIV-1. Similarly to DC-SIGN it facilitates HIV-1 transmission to CD4 T cells as well as entry to DCs (Lambert et al., 2008). Additionally, its expression is induced on CD4+ T cells following HIV-1 infection (Lambert et al., 2010). DCIR signaling is dependent on the ITIM motif in the cytosolic domain and involves recruitment of the Src homology 2-containing tyrosine phosphatase SHP-1 and SHP-2 as well as the Src kinases Src, Fyn and Hck in CD4 cells to facilitate HIV binding (Lambert et al., 2011). Further details regarding its signaling in DCs remain to be investigated.

1.3.7 TRIM5α – a novel innate PRR?

Recent work has unraveled a new function for the cytoplasmic tripartite motif-containing protein 5α (TRIM5α) showing that it acts as a PRR in myeloid cells (figure 1.4). TRIM5α has been known for its role as a retrovirus restriction factor in Old World monkeys, whereby its interaction with the HIV-1 capsid accelerates uncoating of the

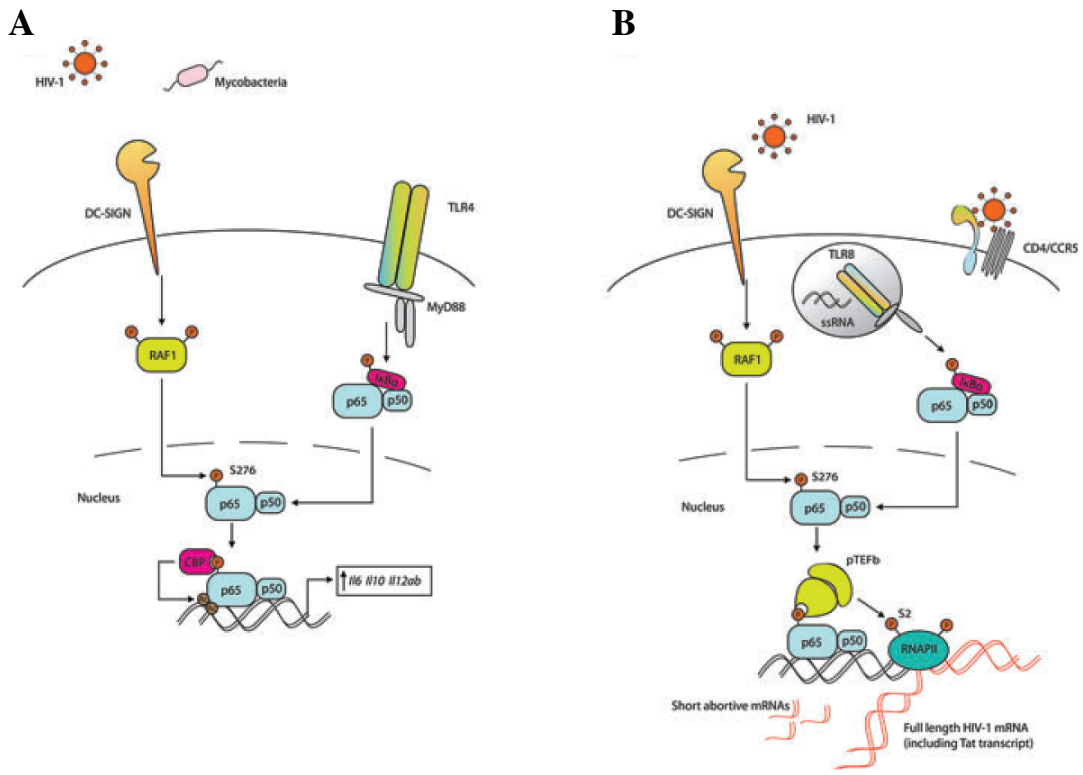

Figure 1.3. DC-SIGN signaling modulates TLR signaling. **A.** DC-SIGN binds ligands such as mycobacteria and HIV-1. DC-SIGN induces RAF1 phosphorylation, which modulates TLR induced NF-kB activation. Upon TLR stimulation the canonical NF-kB subunit p65 is released from its inhibitor and translocates to the nucleus. Phosphorylated RAF1 induces p65 phosphorylation at Ser276, ultimately inducing increased *IL6, IL10* and *IL12αβ* transcription. **B.** HIV-1 enters the host DC via the coreceptors CD4 and CCR5 leading to viral uncoating, reverse transcription and integration into the host genome (host DNA: black; viral DNA/RNA: red). HIV-1 needs the viral protein Tat for transcription elongation, which is encoded in the integrated viral DNA. Without Tat short abortive mRNAs will be produced. By signaling via TLR8 (ssRNA) and DC-SIGN (gp120) HIV-1 recruits host factors to the transcription initiation complex inducing the first HIV-1 transcripts. TLR8 triggering leads to nuclear translocation of p65. DC-SIGN signaling via gp120 induces RAF1 activation and subsequent p65 phosphorylation at Ser276, which functions as a binding site for pTEFb. pTEFb is recruited to the HIV-1 LTR and phosphorylates RNAPII at Ser2, allowing for transcription elongation and full HIV-1 mRNA transcripts. Once Tat is produced, transcription will be more efficient and enhanced. CBP, CREB binding protein; IkBα, inhibitor of NF-kBα; pTEFb, positive transcription elongation factor b; RNAPII, RNA polymerase II. Adapted from (van den Berg et al., 2012)

virus and hence prevents reverse transcription (Stremlau et al., 2004). Human TRIM5α harbors an amino acid substitution that disrupts its interaction with HIV-1 capsid and abrogates its restriction activity (Yap et al., 2005). Pertel et al described how the interaction between HIV-1 capsid with TRIM5α generates ubiquitin chains that activate the TAK1 kinase complex, leading to activation of the transcription factors NF-kB and AP-1 (Pertel et al., 2011). This suggests that TRIM5α is a bona fide PRR that specifically recognizes retroviral capsid (Tareen and Emerman, 2011b). The exact role of TRIM5α in HIV-1 infection remains to be elucidated. Especially, as these authors and a further publication described an additional signaling effect for TRIM5α that was independent of capsid recognition and involved in LPS and NF-κB activation (Tareen and Emerman, 2011a).

1.3.8 The unknown sensor(s) recognizing HIV-1 capsid or DNA?

Capsid recognition as mentioned above has the ability to induce an innate immune response even before viral integration into the host genome. Further evidence for a role of capsid recognition in HIV-1 sensing comes from a study, which demonstrated that newly synthesized capsid is able to interact with cyclophilin and induce IRF3 phosphorylation (Manel et al., 2010). This effect was only mediated after the restriction to HIV-1 infection in mDCs was relieved by delivery of virus like particles expressing vpx from SIV_{MAC}. The authors suggested that the contribution of capsid to sensing of HIV-1 would satisfy the functional definition of a PAMP, however they did not show that capsid itself is the physical substrate for sensing and capsid on its own failed to induce any activation signal, suggesting that a second signal may be required for the capsid to induce an innate immune response (Manel and Littman, 2011).

In addition, recent data strongly suggest that HIV-1 may be sensed by a cytoplasmic DNA sensor, but its identity remains elusive (Yan and Lieberman, 2011). Reverse transcribed viral DNA in the cytoplasm induces a signaling cascade involving this putative receptor, STING and TBK-1 to trigger type I interferon production via IRF3 (Yan et al., 2010). However, excess HIV-1 DNA is digested by cytosolic TREX1, the major 3'-5' DNA-specific exonuclease in mammalian cells, thereby avoiding recognition by the sensor and the induction of interferons.

1.3.9 Restriction to productive HIV-1 infection of mDCs

Myeloid DCs have the unique ability in promoting viral replication via transfer of virions to CD4+ T cells, a phenomenon which will be discussed further below. Early studies on the interaction between HIV-1 with different cell types had demonstrated non-permissiveness of mDCs, resting CD4+ T cells, monocytes and to some extent macrophages to *in vitro* productive infection with high titre HIV-1. Recent exciting developments in the field have identified SAM- and HD-domain-containing protein 1, SAMHD1, as a novel HIV-1-specific restriction factor in myeloid DCs and resting CD4+ T cells that is blocked by the lentiviral accessory protein vpx - expressed by HIV-2 and $SIV_{MAC,}$ but not HIV-1 - and targeted for proteasomal degradation (Baldauf et al., 2012; Laguette et al., 2011). SAMHD1 is a deoxynucleoside triphosphate triphosphohydrolase and restricts viral replication via an intriguing mechanism (Goldstone et al., 2011; Lahouassa et al., 2012): it hydrolyses intracellular dNTPs in non-cycling cells that inherently have low dNTP concentrations in comparison to proliferating cells, hence reducing the amount of key substrates for completion of reverse transcription and viral DNA synthesis. HIV-1 encodes vpu instead of vpx and can therefore not counteract SAMHD1, ultimately providing a mechanism for why mDCs are relatively resistant to productive infection. This is interesting, as SAMHD1 is the only HIV-1 restriction factor against which the virus has not evolved a neutralizing strategy, and raises questions as to what advantage SAMHD1 confers to HIV-1.

SAMHD1 is a key regulator of the interferon pathway and of a rare autoimmune disease called Aicardi-Goutière-Syndrome that is characterized by excessive inflammation and type I interferon production (Laguette and Benkirane, 2012). Whether SAMHD1 plays a role in the evasion of the antiviral interferon response is yet to be determined. Importantly, SAMHD1-mediated restriction to HIV-1 infection in quiescent CD4+ T cells may finally explain the massive depletion of CD4+ T cells during HIV-1 infection: Accumulation of abortive reverse transcripts in resting CD4+ T cells, likely due to the action of SAMHD1, has been shown to cause “bystander death” due to a proapoptotic and proinflammatory response involving caspase 1 and caspase 3 activation (Doitsh et al., 2010).

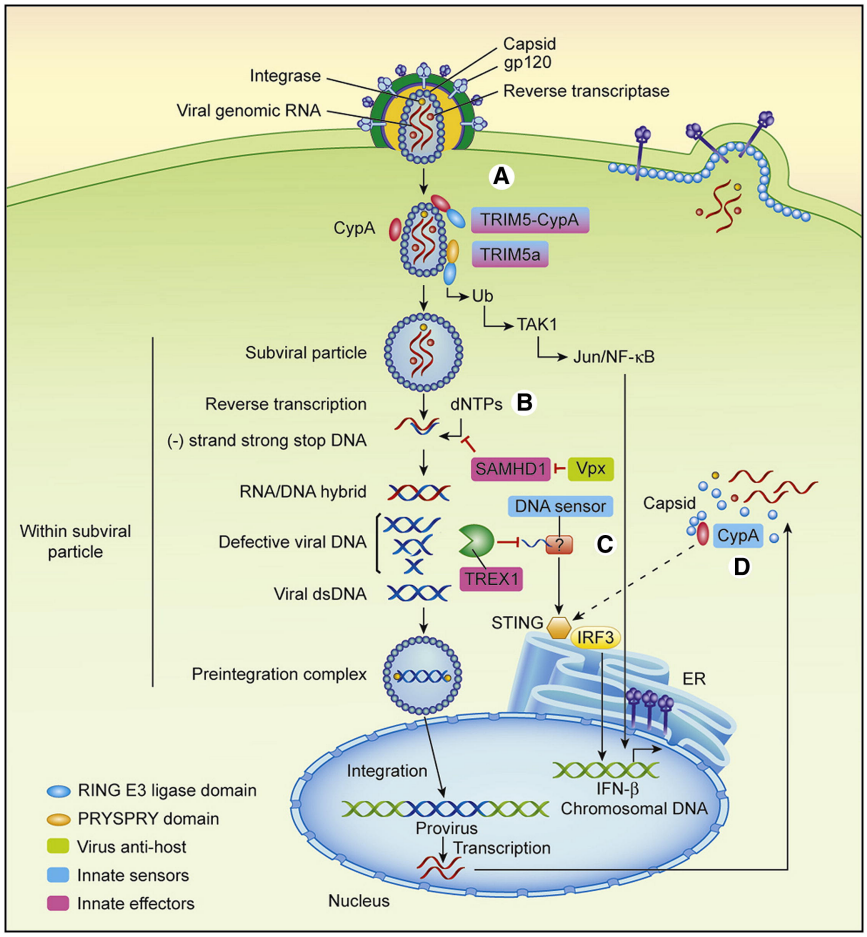

Figure 1.4. Innate Recognition of HIV-1 by Dendritic Cells and Macrophages.
HIV-1 env binds to CD4 and CCR5 expressed on DCs and macrophages and enables viral fusion. **A.** Capsid lattice in the cytosol is bound by TRIM5α and TRIM5-CypA fusion proteins (in certain nonhuman primates) in species-specific manner. This activates E3 ubiquitin ligase function of TRIM5α, to catalyze synthesis of free ubiquitin chains that activate TAK1 kinase complex leading to AP-1 and NF-kB activation. HIV-1 capsid is only weakly recognized by human TRIM5α. Within the subviral particle, cDNA synthesis on HIV-1 genomic RNA begins. **B.** SAMDH1 blocks reverse transcription at the minus strand strong stop DNA stage, by limiting the availability of free dNTPs needed for further cDNA synthesis. However, this is countered by Vpx, which induces SAMDH1 degradation. HIV-1 does not encode Vpx, and thus human DCs are not productively infected. **C.** Defective viral RT-generated DNA products are sensed by a cytosolic DNA sensor. However, accumulation of such DNA intermediates is blocked by TREX1, which degrades such product via its 3′-5′ exonuclease activity. **D.** By introducing Vpx, productively infected DCs stimulate type I IFN synthesis and are properly activated for T cell stimulation, through sensing of de novo synthesized viral capsid via CypA. STING and IRF3 are required to induce type I IFNs downstream of the DNA sensor and the CypA pathways. Viral antihost molecules, innate sensors, and innate effectors are color coded as indicated. Adapted from (Iwasaki, 2012).

1.4 HIV-1 life cycle and replication

1.4.1 Evolution of HIV

HIV belongs to the genus of Lentiviridae of the slow viruses family of *Retroviridae*.
Two types of HIV have been identified to date, HIV-1, the major cause of the pandemic, and HIV-2, which is predominantly confined to West Africa. Recent major advances in phylogenetic techniques and algorithms have greatly improved the identification of the origin and evolution of HIV. SIV from chimpanzees and gorillas has been identified as the likely progenitor of HIV-1 with multiple cross-species transmission events in central Africa between the years 1884 and 1924 (Tebit and Arts, 2011). Based on viral genetic distances and positions in phylogenetic trees HIV-1 is divided into the groups M (major), N (non-major) as well as O (outlier) and P. Group M is the most common strain and is further divided into genetically distinct subtypes or clades termed from A-K, that are typically associated with certain geographical areas (Kuritzkes, 2007). Interestingly, SIV is non-pathogenic in its natural hosts, human on the other hand are a relatively new host for HIV, which potentially explains the lethality of infection in human (Telenti, 2005).
One of the major obstacles in limiting the pandemic is the rapid evolution of HIV-1, whereby the virus is able to rapidly diversify under selective host pressure without compromising its replicative fitness (Wolinsky et al., 1996). The extraordinary diverse viral populations, also termed quasispecies, is the result of a multitude of HIV specific mechanisms, starting with the fast replication cycle with production of 10^{10}-10^{12} newly produced virions per day, an error prone reverse transcriptase without a proofreading activity allowing high mutation rates per genome, and frequent recombination events allowing emergence of new viral variants (Wolinsky et al., 1996).

1.4.2 HIV genomic organization

HIV-1, similar to other lentiviruses, exhibits a more complex genomic organization than simple retroviruses by containing regulatory and auxiliary genes in addition to three essential genes. Its genome is approximately 9.8 kb long and is flanked by two LTR sequences that contain promotors, enhancers and other regions for binding of viral and

cellular transcription factors, such as AP1 and NF-κB (Clever and Parslow, 1997; Pereira et al., 2000). It contains nine open reading frames, which lead to nine primary translation products, but eventually 15 proteins are made in all as a result of cleavage of three of the primary products. The three essential proteins, Gag, Env and Pol are produced first as polyproteins and cleaved by host or viral proteases: The polyprotein pol is cleaved into reverse transcriptase (RT), that is responsible for transcribing the RNA genome into dsDNA, protease (PR), an enzyme essential for proteolytic cleavage of viral proteins and integrase (IN), which integrates the DNA into the host genome. The Gag precursor protein, also called p55, is cleaved into four smaller proteins designated matrix p17 (MA), capsid p24 (CA), nucleocapsid p9 (NC) and p6 (Pettit et al., 2004). The 160kD env (gp160) is cleaved by a host protease called Furin to generate gp41 and gp120 (Freed, 2007). Further, HIV-1 encodes the small proteins tat and rev, which regulate gene expression as well as the accessory proteins Nef, Vpu and Vif, and Vpr (Freed, 2007).

1.4.3 HIV-1 morphology

Retroviral virions are initially assembled and released from the infected cells as immature particles that are spherical with a characteristic electron-lucent center (figure 1.5) (Freed, 2007). The mature retrovirus particle is a spherical structure at about 100nm in diameter with a core that is surrounded by a viral membrane expressing Env trimers (Liu et al., 2008). The viral envelope Env is initially expressed from singly spliced mRNA and further synthesized in the ER migrating though the trans-golgi-network (TGN), where it undergoes glycosylation with the addition of 25-30 complex N-linked carbohydrate side chains. Env glycosylation is crucial to HIV-1 infectivity.

1.4.4 HIV-1 replication life cycle

HIV is an enveloped single-stranded RNA virus with an unusual replication cycle. The life cycle begins with an RNA genome passing through an intracellular intermediate and is completed with a return to RNA into the progeny virus particle (figure 1.5) (reviewed in (Freed, 2001)).

The lifecycle is arbitrarily divided into two distinct stages (Freed, 2007). The early phase starts with viral attachment to the plasma membrane to the integration of viral cDNA as provirus into the host genome, and the late phase consists of expression of viral genes through to viral egress and maturation of progeny virions. The early steps of the HIV-1 lifecycle are, in contrast to the late stage, still poorly defined.

HIV-1 enters cells by sequential binding of the viral envelope glycoprotein gp120 to the main receptor CD4 as well as one of the co-receptors CCR5 or CXCR4 (Doms and Trono, 2000; Wu et al., 1996). Binding of gp120 to CD4, induces a structural change of the hypervariable V3 loop of gp120 exposing the chemokine-binding domain of gp120 allowing interaction to take place (Sattentau and Moore, 1991). Binding triggers formation of the fusion pore and six-helix bundle by gp41 that leads to close apposition of viral and cellular membrane. This ultimately allows fusion of the membranes and release of the viral core into the cytoplasm. Details of viral entry into DCs will be discussed further below. Uncoating, i.e. loss of the viral capsid, is still a poorly defined process and the field is still divided as to the precise location and timing of it (Dvorin and Malim, 2003). It produces the reverse transcription complex (RTC) that is attached to the cytoskeleton via actin filaments (Goff, 2007). The RTC roughly resembles the viral core and contains the viral RNA as well as gag proteins, vpr, NC, RT and IN (Nermut and Fassati, 2003). RT catalyses the reverse transcription of the viral RNA genome into proviral DNA (Jonckheere et al., 2000), which in association with IN, RT, MA, vpr and host proteins forms the pre-integration complex (PIC) (Sherman et al., 2002). This large complex now has to translocate into the nucleus across an intact nuclear membrane by a still poorly defined mechanism involving multiple host proteins, such as importin 7 and Nup98 and TNPO3 and vpr (Lee et al., 2010; Sherman et al., 2003). Inside the nucleus the PIC presumably reassembles and the viral cDNA is incorporated into the host genome by the IN enzyme (Vanegas et al., 2005). This provirus forms the template for viral RNA synthesis and remains in the host cell chromosome for the lifetime of the infected cell. Transcription of full and partial length viral RNA is initiated after binding of multiple cellular factors to the LTR site of the HIV-1 gene by the host RNA Polymerase II (Kingsman and Kingsman, 1996). Basal levels of translation result in small amounts of three small HIV proteins, Tat, Rev and Nef. Tat binds to one of the multiple enhancer sites within the LTR called the TAR

element and increases further HIV-1 transcription (Goff, 2007). Splicing of the transcribed RNA and proteolytic cleavage of translated proteins by the viral protease produces viral proteins.

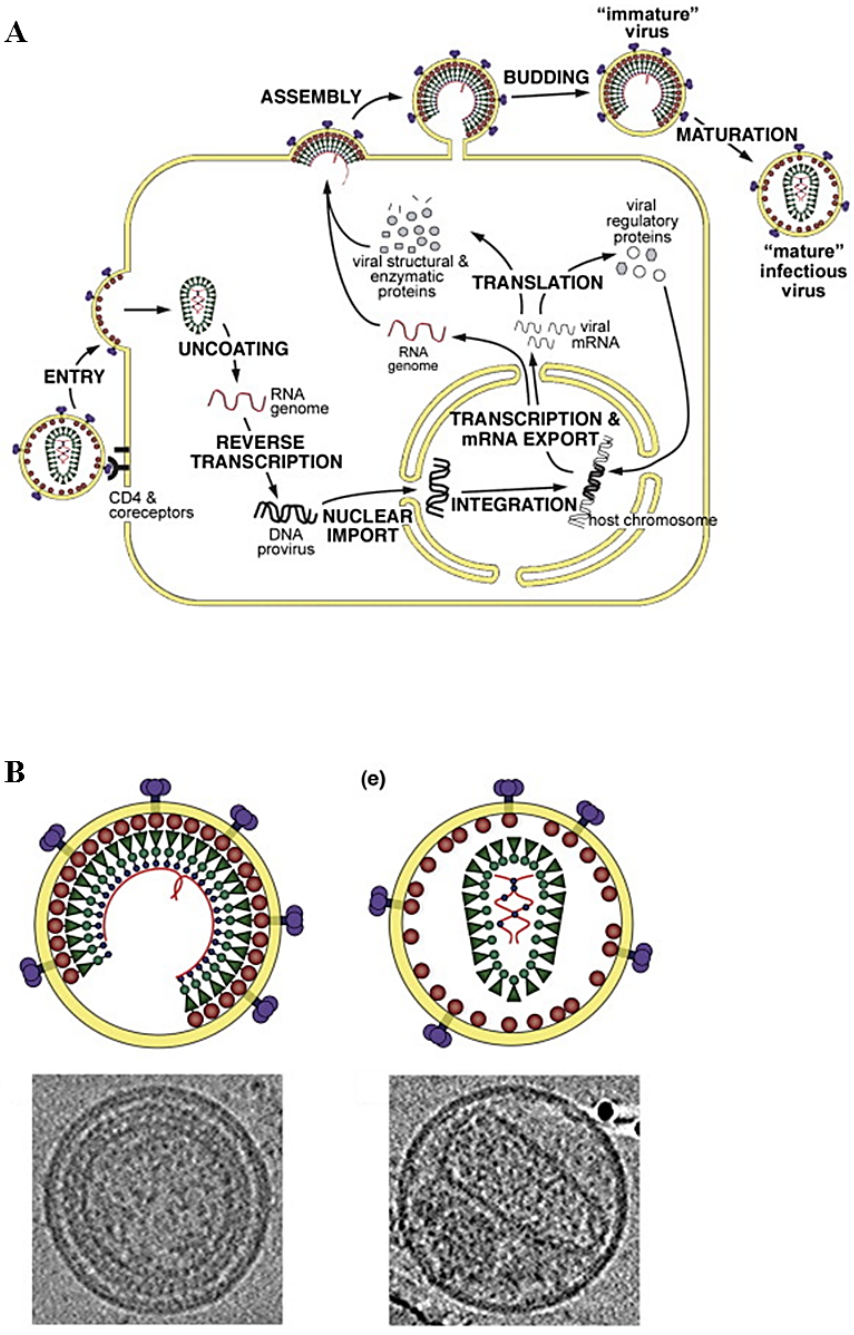

Figure 1.5. Summary of HIV-1 lifecycle and model of HIV-1 virions. A. Summary of the HIV-1 replication cycle. **B**. Schematic models of the immature (left) and mature (right) HIV-1 virions. Lower panel are central slices through cryo-EM tomograms of immature (left) and mature (right) HIV-1 particles. The spherical virions are approximately 130 nm in diameter. Adapted from (Ganser-Pornillos et al., 2008).

Subsequently, full-length RNA transcripts and viral polyproteins assemble at the plasma membrane using well-defined members of the host ESCRT machinery and bud off the cell membrane (Usami et al., 2009). Finally, viral precursor polyproteins are specifically cleaved by the viral protease to produce full infectious mature virions.

1.5 HIV-1 and the trafficking machinery

HIV-1 has developed numerous elaborate strategies to manipulate the host trafficking machinery for its own purposes, which are beyond the scope of this introduction. For instance, viral budding is confined to distinct domains of the cell membrane where viral components converge to assemble and exit. Host ESCRT proteins usually regulate membrane fission during formation of multivesicular bodies and cytokinesis at cellular membranes (Jouvenet et al., 2011). HIV-1 mimics sequences of host cell proteins that usually recruit ESCRT proteins, hereby diverting members of the machinery to sites of viral assembly (Jouvenet et al., 2011). Moreover, the downregulation of CD4 by nef, a myristoylated, membrane-associated HIV-1 auxiliary protein expressed early during infection, is a highly regulated process requiring multiple host factors: Nef interacts with the cytoplasmic domain of CD4 and recruits the adaptor protein complex AP-1 to clathrin coated pits inducing endocytosis of the complex (Piguet et al., 1999). In the endosome nef recruits endosomal coat proteins such as β-COP to target CD4 for lysosomal degradation. In contrast, nef inhibits endocytosis and downregulation of DC-SIGN, hence increasing viral transmission (Sol-Foulon et al., 2002). Nef also triggers the exclusion of the E2 ubiquitin-conjugating enzyme UbcH7 from lipid rafts through inhibition of the Ubiquitin ligase Cbl, which leads to increased CD4+ T cell signaling and promotes HIV-1 replication (Simmons et al., 2005).

1.5.1 Overview of the endolysosomal system

Pathogens that enter the cell within endocytic vesicles, follow the same intracellular pathways as physiological ligands and membrane components, all collectively termed cargo (reviewed in (Lozach et al., 2011; Mercer et al., 2010)). Endocytosis is initiated by the uptake of extracellular material in concert with integral plasma membrane proteins into endocytic vesicles, which then fuse to early endosomes (figure 1.6). The main intracellular organelles are early endosomes (EE), maturing endosomes (ME) and

late endosomes (LE) - that often form multivesicular bodies (MVB) – as well as recycling endosomes (RE) and lysosomes. Although this distinction probably oversimplifies the complex endo-lysosomal system, which should rather be regarded as a spatiotemporal continuum of intermediates that continuously exchange their content and undergo gradual structural and molecular remodeling and functional transformation (Saftig and Klumperman, 2009). EEs are dispersed within the cytosol, whereas MEs, LEs and lysosomes are located in the perinuclear vicinity. Movement of the organelles along microtubules and their motors is fast, e.g. cargo reaches the EE within 2-5 min, the LE within 10-12 min and the lysosomes within 30-60 min (Lakadamyali et al., 2006; Mukherjee and Maxfield, 2004). The lumen of endosomes becomes increasingly acidic from EE to lysosomes mainly through the action of v-ATPases (Lafourcade et al., 2008), whereas the hydrolase and proteinase content increase by active transport from the golgi apparatus.

Fusion of endocytic vesicles with the EE is initiated by a number of different effector molecules, such as the small GTPase Rab5 and the early endosomal antigen1 EEA as well as the phosphatidylinositol 3-kinase Vps34 (Kinchen et al., 2008). In general, the vesicles have a complex structure with tubular or vacuolar elements and expression of functionally distinct domains. The domains determine the destination of the cargo-bearing vesicles, e.g. Rab7 for LEs and Rab9 and the retromer complex for the TGN (Mercer et al., 2010). The formation of intraluminal vesicles (ILV) is mediated by the sequential action of the ESCRT pathway (endosomal sorting complexes required for transport), which refers to a series of four protein complexes (ESCRT-0 to -III) that sort cargo via their ubiquitin-binding domains (Hurley and Emr, 2006). ILVs form by budding of endosomal membranes and monoubiquitin tagged proteins into the lumen of organelles, resulting in the formation of LEs filled with vesicles (MVBs) destined for lysosomal degradation (van Meel and Klumperman, 2008). Fusion with lysosomes in the perinuclear region exposes cargo to acidic hydrolases and degrades them. The glycoprotein LAMP1 remains in the limiting membrane and often serves as a marker for LE/lysosomes.

The endosome network represents a self-organizing machinery of different organelles that converges with multiple different cellular pathways such as autophagy, the ubiquitin system and the secretory pathway. Pathogens have evolved many ways to co-

opt these pathways to evade immune recognition and promote their own replication.

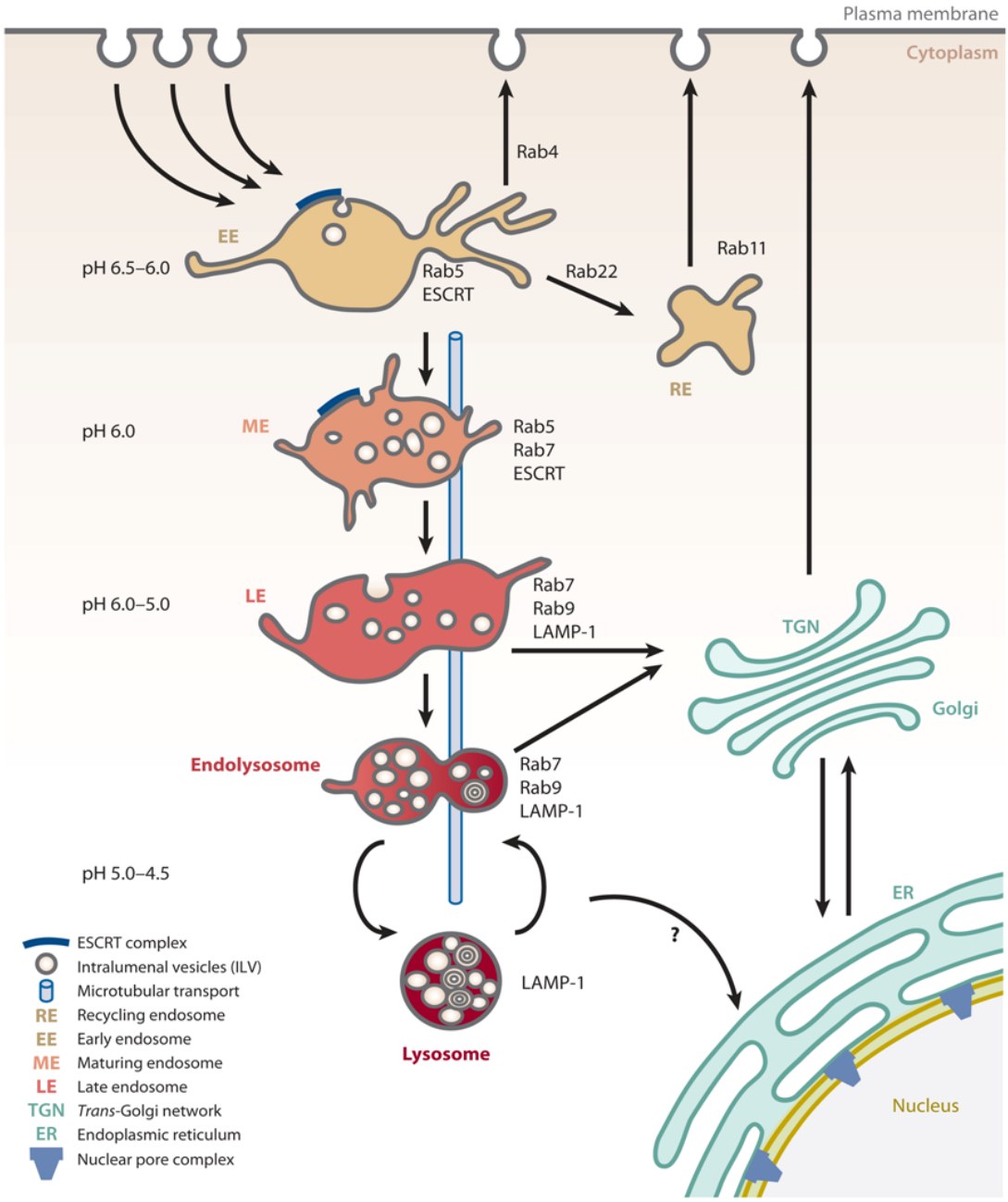

Figure 1.6. The endo-lysosomal system. Adapted from (Mercer et al., 2010).

1.5.2 Interaction of HIV-1 with the autophagy machinery

Autophagy is a process of controlled self-degradation of damaged, redundant, or even dangerous cellular components, ranging from individual proteins (microautophagy) to entire organelles (macroautophagy) (reviewed in (Deretic, 2011; Levine and Deretic, 2007)). Conditions such as starvation and genomic stress initiate this process with engulfment of cytoplasmic portions into an isolation membrane the phagophore, which forms a double-membrane organelle called the autophagosome. The evolutionary conserved serine/threonine kinase mTORC1 (mammalian target of rapamycin) actively suppresses autophagy and, conversely, inhibition of mTORC1 (by small molecules, amino acid withdrawal or pathogens) strongly induces autophagy. Synthesis of the autophagosome involves the interaction of more than 20 autophagy related genes as well as molecules involved in ubiquitination. The fusion of the mature autophagosome with the lysosome leads to degradation of the contents by lysosomal acid hydrolyases and their return back to the cytoplasm via channels in the autophagolysosomal membrane (Levine and Kroemer, 2008; Mizushima et al., 2008). In addition, the autophagosome can also fuse with an endocytic structure, either an early sorting or late MVB endosome to generate an amphisome. Autophagy and the endocytic pathway converge at the stage of fusion of autophagosomes and endosomes with lysosomes (Li et al., 2010; Nair and Klionsky, 2011). Rab GTPases recruit tethering proteins, which in turn coordinate the SNARE family of proteins to regulate membrane fusion. Both pathways require the GTPase Rab7 and homotypic fusion and vacuole protein-sorting (HOPS) complex. The autophagosome essentially becomes an endosome-like organelle that recruits the common fusion machinery for delivery of its cargo to the lysosome.

Accumulating evidence supports the role of autophagy as a general innate defence mechanism. Given the conserved nature of the autophagy pathway, pathogens have been under an evolutionary pressure to develop distinct molecular strategies to subvert this process to their own advantage. Viruses such as poliovirus or influenza require autophagy to complete their replication cycle, whereas other viruses such as HSV-1 actively inhibit autophagy to reduce antigen presentation via MHC class I and II molecules, and establish infection (Espert et al., 2007a; Levine and Deretic, 2007; Yordy and Iwasaki, 2011). The interplay of HIV-1 with autophagy is cell type

dependent and rather complex. In uninfected bystander CD4+ T cells the fusogenic activity of gp41 strongly induces autophagy and apoptosis, providing a mechanism for HIV-induced CD4+ T cell death (Espert et al., 2007b). However, HIV-1 inhibits autophagy in productively infected CD4+ lymphocytes. In macrophages HIV-1 promotes the formation of autophagosomes (Espert and Biard-Piechaczyk, 2009; Espert et al., 2009; Kyei et al., 2009) by inducing the interaction between nef and Beclin-1 as well as the GTPase family M (Gregoire et al., 2011).

Importantly, in the context of this work, in DCs HIV-1 rapidly shuts down autophagy (figure 1.7) (Blanchet et al., 2010). Blanchet et al showed that env leads to activation of negative regulators of autophagy, namely mTOR and S6K, a kinase acting downstream of mTORC1. Viral particles are hereby diverted away from autophagosomes to compartments, which the authors termed immunoamphisomes, before degradation in lysosomes. The consequence is a reduction in MHC class II dependent antigen presentation, downregulation of TLR-mediated responsiveness and increase in viral transfer to CD4+ T cells. The exact molecular mechanism accounting for this rapid inhibition of autophagy was not elucidated, although the authors suggest that the block is induced at the step of autophagy initiation and may be mediated by the interaction of the viral envelope with CD4.

1.6 Viral Entry

While great advances have been made in defining the molecular events occurring on entry to the main target cells CD4+ T cells, the exact nature of the entry process into DCs is less well understood. Traditionally, HIV-1 entry was considered to occur solely at the plasma membrane. Recent work however has shown that HIV-1 fusion occurs at endosomal membranes after endocytic uptake. The precise endocytic routes remain to defined, and it is likely that distinct uptake routes may occur in different target cells (figure 1.8).

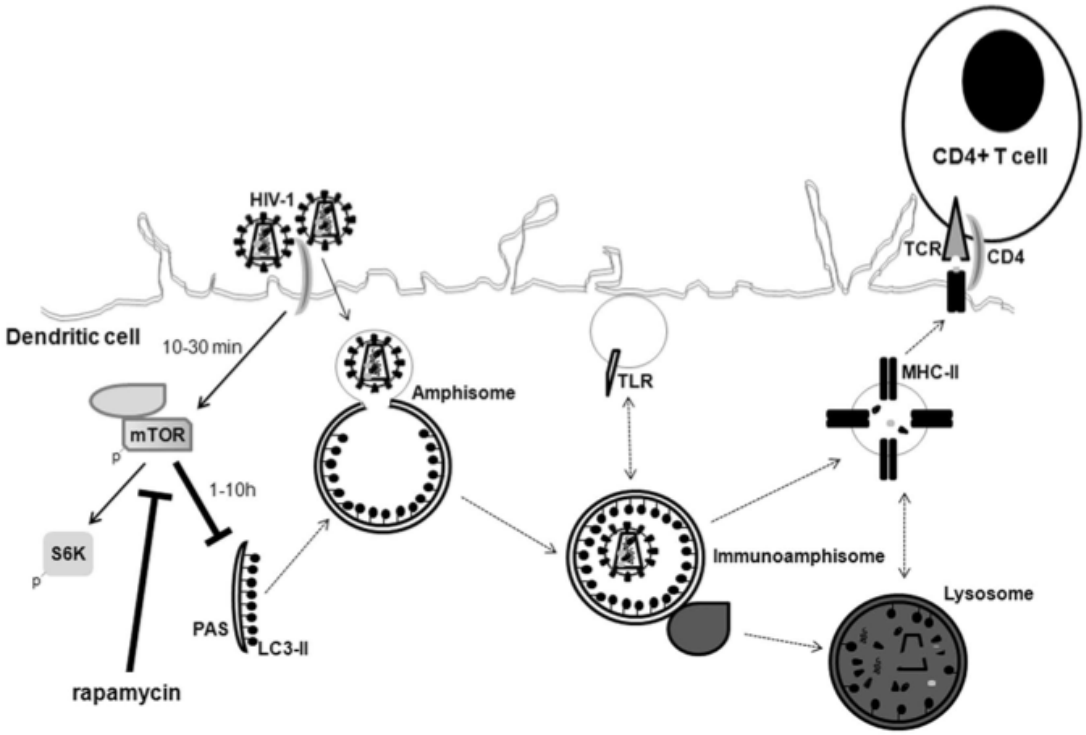

Figure 1.7. HIV-1 inhibits autophagy in DCs. Upon HIV-1 internalization, virions traffic through immunoamphisomes before lysosomal-mediated degradation. Immunoamphisomes are organelles derived from endo/phagosomes and autophagosomes that display potent immunostimulatory properties. Immunoamphisomes are central regulators of some TLR-mediated responses and contribute to optimal exogenous antigen processing and presentation via MHC class II molecules toward specific CD4+ T cells. However, during the very early events (10–30 min) of DC-mediated HIV-1 capture, viral envelope binding to cellular receptor induces mTOR pathway activation leading to blockade of autophagy initiation, which contributes to immunoamphisome decrease at later time points. Consequently, incoming virion degradation and both DC-mediated innate and adaptive immune responses are impaired. The negative impact of HIV-mediated immunoamphisome exhaustion on exogenous antigen presentation can be overcome by Rapamycin, a well-known mTOR inhibitor. Adapted from (Blanchet and Piguet, 2010).

1.6.1 The endocytic route of HIV-1

Endocytosis confers a clear advantageous route for pathogens to enter host cells and is therefore used by most viruses (reviewed in (Mercer et al., 2010)): Endocytosed virus can avoid leaving evidence of their presence on the cell membrane, hence delaying alerting the immune surveillance machinery. Presumably, this pathway would also minimize contact with neutralizing antibodies. Furthermore, the virus utilizes a cell intrinsic trafficking route of cargo uptake to enter the host and bypasses all the potential

cellular obstacles that it would otherwise encounter, such as microfilaments and the actin cytoskeleton. Moreover, some viruses require environmental factors such as alterations in pH and specific proteases to continue their replication cycle.

Entry of HIV-1 like other enveloped viruses is pH-independent and indeed early studies of cell-free virus showed that fusion occurred independent of endocytosis, and hence most likely occurred at the cell membrane via receptor-mediated fusion (Maddon et al., 1988; Sattentau and Moore, 1991; Stein et al., 1987). This was based on work showing that lysomotropic reagents, that normalize the acidic pH of endosomes failed to block HIV-1 entry (Stein et al., 1987) and cell-cell fusion occurred successfully at neutral pH between cells expressing env, CD4 and CCR5. Additional evidence came from work demonstrating that HeLa cells with impaired ability for endocytosis were equally susceptible to infection (Maddon et al., 1988)). Nevertheless, early electron microscopy images had reported binding and internalization of HIV-1 into vesicular structures (Pauza and Price, 1988). Furthermore, a variety of cell types such as macrophages were able to internalize HIV-1 into vesicular structures (Fackler and Peterlin, 2000; Marechal et al., 2001; Schaeffer et al., 2004), however these particles were assumed to be on a dead-end degradative route (Carter et al., 2011). Recent compelling evidence, however, is strongly indicative that HIV-1 fusion can also occur in an endosomal compartment (Miyauchi et al., 2009). Miyauchi et al, used C52L, an inhibitor of the late-stage of viral membrane fusion and a temperature block as well as live cell imaging and demonstrated that in T cell lines and Hela cells three distinct endocytic routes exist: (i) endocytosis of HIV and fusion at the vesicular membrane with subsequent delivery of viral particles into the cytosol (ii) hemifusion at the plasma membrane with completion of fusion occurring after endocytosis into a perinuclear region, (iii) fusion at the plasma membrane without any apparent content mixing indicating immobilization of virus at the plasma membrane. The GTPase dynamin facilitates HIV entry by scission of endocytic vesicles from the plasma membrane (Daecke et al., 2005; Miyauchi et al., 2009). Interestingly, a similar mechanism appears to apply during cell-to-cell transfer (Dale et al., 2011). Dale et al showed that following transfer of HIV-1 across the virological synapse, viral fusion occurs in endosomes and only after a signal induced by particle maturation.

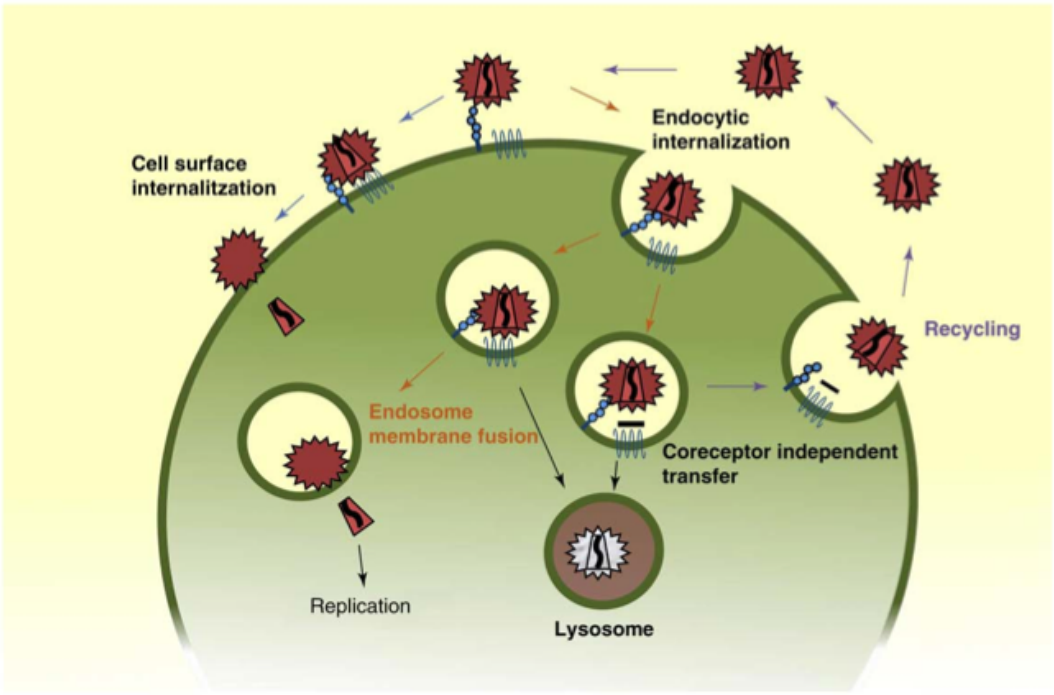

Figure 1.8. Putative HIV entry pathways. After binding of HIV to the CD4 receptor, the virus can enter target cells through three non-exclusive pathways. The first pathway is the canonical of direct fusion of HIV particles with the plasma membrane (cell surface internalization). In the second pathway, endosomal internalization establishes HIV fusion with an endosome membrane following an endocytic uptake of virus particles, or this could lead to endosome maturation and lysis of the virus particle. In the third pathway, coreceptor engagement might lead to virus membrane and endosome membrane fusion and release of the virion into the cytosol; alternatively, in the absence of the appropriate coreceptor or coreceptor independent transfer, viruses might be recycled back to the extracellular medium as infectious particles capable of mediating a productive infection. Adapted from (Permanyer et al., 2010).

1.6.2 Signaling events during viral entry

Entry of HIV into target cells is preceded by viral attachment to cellular adhesion factors such as heparin sulfate and glycosylceramides and in particular the CLR DC-SIGN in mDCs (Sattentau et al., 1999; Ugolini et al., 1999). A number of studies have also reported DC-SIGN independent mechanisms of HIV attachment and entry to DCs (Baribaud et al., 2002; Gummuluru et al., 2003; Wu et al., 2002b). The exact nature of HIV-1-DC-SIGN interaction, especially in situ, is far from clear. Viral attachment induces clustering and enrichment of CD4 and the co-receptors at the site of contact, and fusion is only supposed to occur until sufficient CD4 and coreceptors are recruited (Clapham and McKnight, 2002). Receptor clustering is an active actin-dependent process that uses the Rho-GTPase family to initiate a signaling cascade including RAC1, the WASP-family verprolin-homologous protein 2 (WAVE-2) and the kinase

Abl1, resulting in ARP2/3-triggered actin polymerization and capsid entry (Taylor et al., 2011). Inhibition at any of these steps leads to blockage of viral entry and fusion.

1.6.3 Role of CD4 and the co-receptors in HIV-1 entry to DCs

Despite low levels of CD4 expression on mDCs, CD4 is considered to be the major receptor for viral entry into these cells (Patterson et al., 1994). Binding assays with biotinylated gp120 have shown that 80% of gp120 binds to CLRs such as DC-SIGN with the remainder 20% binding to CD4 (Turville et al., 2001), corroborating the role of DC-SIGN in facilitating viral entry by attachment. Both main co-receptors CCR5 and CXCR4 have also been shown to bind HIV-1, although the general consensus is that CCR5 is the main receptor for HIV-1 in mDCs, particularly immature mDCs, based on studies showing that mDCs are preferentially infected by R5 viruses (Granelli-Piperno et al., 1998; Reece et al., 1998; Rubbert et al., 1998).

In CD4+ lymphocytes env induces remodeling of actin to overcome the cortical actin barrier. This is mediated by filamin A crosslinking the cytoplasmic tails of CD4 and CXCR4 leading to activation of the GTPases RhoA and Rac1 as well as the LIM domain kinase, which induces phosphorylation and inactivation of the actin-binding protein cofilin. Net outcome of this signaling cascade is depolymerization of actin and clustering of receptors (Jimenez-Baranda et al., 2007; Vorster et al., 2011; Yoder et al., 2008). Interestingly, the interaction between chemokine receptors and cofilin has also been implicated in establishment of HIV latency (Cameron et al., 2010). Furthermore, the interaction between R5 and X4 strains with their respective co-receptors induces activation of the ERK pathway that facilitates reverse transcription (Mettling et al., 2008). Binding of env to CD4 also activates moesin of the ezrin/radixin/moesin (ERM) complex that promotes CD4/CXCR4 clustering by tethering transmembrane and cytoplasmic proteins to filamentous actin (F-actin) (Barrero-Villar et al., 2009).

1.6.4 Role of DC-SIGN in HIV-1 capture and entry to mDCs

DC-SIGN is a type II transmembrane protein with the following domains: a cytoplasmic domain, a transmembrane domain, a neck region, a lectin domain. The lectin domain requires calcium for its structural integrity and binds to high mannose and fucose structures (Guo et al., 2004) and has a high affinity for gp120 (Curtis et al., 1992); the

cytoplasmic domain contains motifs that are required for receptor internalization and signaling; and the neck region is important in DC-SIGN tetramerization to ensure high affinity ligand binding (Serrano-Gomez et al., 2008). Internalization mediated by DC-SIGN requires cholesterol, dynamin and clathrin (Cambi et al., 2009).

A large body of evidence, including work from our group, suggests that DC-SIGN is required for efficient capture of HIV-1 by mDCs and transfer to CD4+ lymphocytes. Blocking of DC-SIGN by either RNAi (Arrighi et al., 2004), antibodies or carbohydrates (Baribaud et al., 2002; Wang et al., 2007) diminishes HIV-1 transfer to CD4+ T cells. Furthermore, DC-SIGN is required for HIV-1 uptake and dissemination by migratory cells in a cervical explant model (Hu et al., 2004). However, the requirement for DC-SIGN in HIV infection is controversial, with some work showing that HIV-1 uptake and dissemination occurs independent of DC-SIGN (Boggiano and Littman, 2007; Gummuluru et al., 2003; Wu et al., 2002a). Differences in experimental systems may account for these discrepancies. For instance, DC maturation shifts capture of gp120 from lectins to CD4 (Turville et al., 2002) and differences in composition of host proteins by HIV-1 particles generated in distinct producer lines may affect viral infectivity (Izquierdo-Useros et al., 2009). Moreover, DCIR may play a role as an alternative receptor (Lambert et al., 2008).

1.7 Modes of HIV-1 spread

Generally HIV-1 can infect cells as cell-free or cell-associated virus and it is obviously difficult to ascertain the contribution of either mode of infection *in vivo*.

Whereas cell-free infection involves the classical steps of viral entry as discussed above, cell-to-cell spread occurs via multiple mechanisms. Cell-to-cell infection confers an advantage to viral replication, because it bypasses the rate-limiting step of viral diffusion in the extracellular space, where it may be susceptible to the anti-viral action of neutralizing antibodies or complement factors (Piguet and Sattentau, 2004). HIV-1 infects immune cells, that unlike other cells in the body, neither have a polarized phenotype nor are constitutively in contact with other cells. Polarization is only induced upon contact or activation by other cells or extracellular matrix and HIV-1 has developed intricate pathways to move across these sites of polarization to infect target cells (Martin and Sattentau, 2009).

1.7.1 HIV-1 spreads via virological synapses

The virological synapse (VS) was initially described by Bangham et al as polarized accumulation of HTLV-1 at the contact zone between individual infected and target cells (Igakura et al., 2003). It is reminiscent of the immunological synapse without requiring major histocompatibility antigens (figure 1.9). Both however require polarization of the actin cytoskeleton, use membrane microdomains and are regulated by a range of cellular adhesion factors and tetraspanins. The emerging role of similar synapses in plants, suggests that the VS may be a conserved structure for cell-to-cell spread of animal and plant viruses (Sattentau, 2011).

Mechanistically they provided an explanation why cell-to-cell HIV-1 infection was 100-18,000 times more efficient than cell-free infection and why HIV-1 infection was aggravated in cultures by the addition of DCs (Cameron et al., 1992a; Cameron et al., 1992b). In HIV-1 infection VS formation is initiated when the viral envelope on the surface of the infected cell interacts with CD4 on the surface of the uninfected target cell with accumulation of gag at the contact zone forming an actin-dependent microcluster (Hubner et al., 2009; Jolly and Sattentau, 2005). One HIV-1 infected cell may even form polysynapses by forming synapses with multiple cells (Rudnicka et al., 2009). The sequence of events for viral transfer across the synapse are still not entirely resolved. Live-cell microscopy of fluorescent labeled HIV-1 demonstrated that transfer is mediated via endocytosis of synaptic buttons by target cells. These are packets of donor cell material derived from a gag-positive disc like structure containing membranous proteins and budding virions that have fused in the endosome (Hubner et al., 2009). Accumulation of integrins, tyrosine kinases and cytoskeletal proteins as well as DC-SIGN and the tetraspanin CD81 at these interfaces strongly implicate that adhesion and signaling mediators are required for efficient viral transfer (Jolly et al., 2004; Jolly et al., 2007; Jolly and Sattentau, 2007). Further, in the HTLV-1 VS the microtubule-organizing center (MTOC) is the driving force for viral transfer from cell-to-cell (Igakura et al., 2003). The MTOC and the protein kinase Zap70, the key mediator in TCR signaling, have also been shown to be critical for trafficking of secretory granules across the cell-to-cell interface (Sol-Foulon et al., 2007).

1.7.2 HIV-1 cell-to-cell spread via alternative mechanisms

Alternative modes of HIV-1 spread not involving a cell-cell contact zone such as the VS have been reported. These include transfer of virus via membrane structures that are formed upon changes in the actin-dependent cytoskeleton. Filopodial bridges, that are thin plasma membrane protrusions containing F-actin, bear immature virions on the tip of their extensions (Aggarwal et al., 2012). Dynamics of the filopodial trajectories can induce up to 800 DC to CD4 contacts per hour, with budding virions then infecting selected T cells via filopodial tethering into the T cell membrane. Efficient formations and transfer are dependent on host formin diaphanous 2 and viral nef, respectively (Aggarwal et al., 2012). Furthermore, engagement of viral env with DC-SIGN induces activation of a signaling cascade involving Src kinases, Cdc42, PAK1 and WASP which leads to formation of membrane extensions and efficient transfer of virus across DC-T cell VS (Nikolic et al., 2011).

In contrast to these actively formed membranous structures, HIV can also track along membrane nanotubes to infect target cells via fusion with the target cell membrane in structures that appear as small scale virological synapses (Sowinski et al., 2008). Nanotubes appear to form passively and contain actin, but not tubulin (Abounit and Zurzolo, 2012). They can be up to ten times longer than filopodia, which may provide an intriguing way for the virus to spread under certain conditions.

Furthermore, another still poorly characterized aspect in HIV entry and spread is viral surfing, whereby HIV-1 binds to filopodia and surfs via lateral movements on the outside of these structures to prepared locations, where fusion or entry can occur (Lehmann et al., 2005). It is unclear how common or essential this process is. A recent study quantified the relative contribution of nanotubes, virological synapses and filopodial bridges to HIV-1 transfer between T cells and reported less than 10% of viral transfer across nanotubes or filopodia with VS accounting for the remaining majority of viral transfer (Rudnicka et al., 2009).

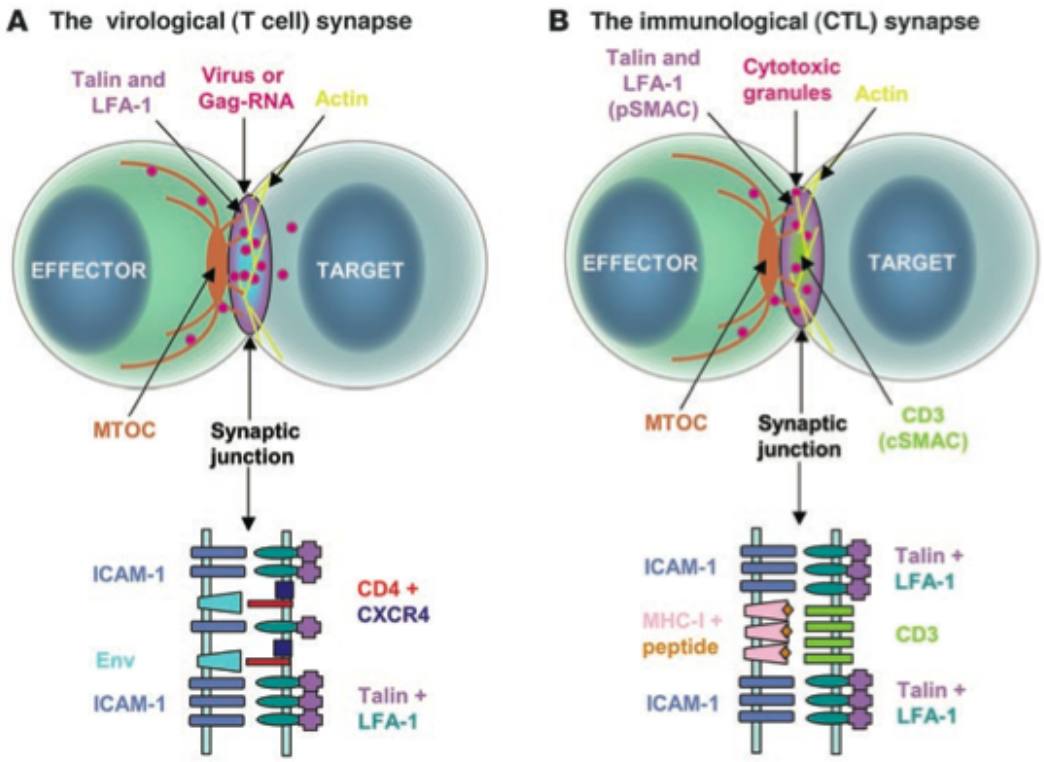

Figure 1.9. Outline of virological and immunological synapse. The upper images of **A** and **B** show stylized features of synapses formed between T cells in the VS (**A**) and the IS (**B**). The VS schematic (**A**) is based on a composite of known features of the HIV-1 and HTLV-1 T cell VSs and highlights features in common with, and divergent from, the IS. Within the VS, Env ligates CD4 and CXCR4 in the target cell and ICAM-1 engages LFA-1 in the target cell. Gag associated with the viral genome present within the effector cell is recruited along microtubules to the site of cell-cell contact and moves across the central zone of the synapse into the target cell. In the target cell, LFA-1–talin complexes and CD4 and CXCR4 are recruited in an actin-dependent manner to the VS. In the IS (**B**), LFA-1–talin complexes form the pSMAC, whereas the T cell receptor (TCR) is recruited to the cSMAC, into which cytotoxic granules are secreted in a microtubule-dependent manner. In the target cell, ICAM-1 engages LFA-1 and peptide–MHC-I complexes ligate the TCR of the effector cell. The lower parts of both panels illustrate a simplified schematic of the molecular arrangements present in the VS (**A**) and IS (**B**). The VS is shown in its partially disordered form with Env-receptor complexes interspersed with ligated adhesion molecules. Adapted from (Piguet and Sattentau, 2004).

1.7.3 HIV-1 spreads via *trans*-infection from DCs to CD4+ T cells

A particularly efficient way to infect T cells *in vitro* is by adding DCs exposed to HIV-1 first, a well known phenomenon in the field that has been known for a number of years and only explained by the description of DC-SIGN as a CLR recognizing HIV (Cameron et al., 1992a; Geijtenbeek et al., 2000a; Geijtenbeek et al., 2000b). Upon capture of the virus by DC-SIGN, HIV-1 is sequestered into a non-classical, non-lysosomal intracellular compartment, that is resistant to proteases and in mature DCs enriched in proteins specific to multivesicular bodies, the tetraspanins CD81 and CD9 (Blauvelt et al., 1997; Garcia et al., 2005; Geijtenbeek et al., 2000a). Virions can survive in this compartment for hours to days, which would provide sufficient time for the DC to undergo maturation and migration to lymph nodes. Upon contact with a CD4+ target cell, virions relocate in conjunction with CD81 to the VS (figure 1.10). This process called "*trans*-infection" explains how DCs can fuel HIV-1 replication without becoming productively infected and indicates how the virus uses the same cells that should effectively fight them into a strong ally. Details of the molecular composition of the *trans* compartment are unknown, but it has been proposed that other viruses, including herpes-, filo and flaviviruses may utilize *trans*-infection for DC mediated infection as well (van Kooyk and Geijtenbeek, 2003). The relevance of *trans*-infection *in vivo* is still unclear, but in early studies of explant tissue models most viral replication was observed in DC-T cell conjugates (Hu et al., 1999; Pope et al., 1994). Some investigators however have challenged the presence of an intracellular compartment containing sequestered virions for DC-T cell infection. Cavrois et al demonstrated full accessibility and susceptibility of HIV to surface applied, membrane impermeable inhibitors, implying that HIV does not get endocytosed and the transfer of virions to CD4 cells is predominantly via virions trapped at the surface of the cell membrane (Cavrois et al., 2007). More recent work attempted to resolve these discrepancies suggesting that the *trans*-compartment is intracellular but nevertheless in a continuum to the plasma membrane (Felts et al., 2010; Yu et al., 2008). Felts et al using superresolution imaging showed elegantly that filopodial extensions emanating from $CD4^+$ T cells make contact with HIV virions sequestered deep within a 3D network of surface-accessible compartments in the dendritic cell (Felts et al., 2010). Yu et al using live cell

microscopy demonstrated that HIV-1 resides in a pocket like domain within the DC, but that it is contiguous to the plasma membrane (Yu et al., 2008).

1.7.4 HIV-1 transfer due to infection *in cis*

Despite the low efficiency of HIV-1 infection of DCs, a small fraction of incoming virus may evade SAMHD1-mediated restriction and lysosomal degradation and lead to *de novo* viral replication in DCs. Hence, several days after viral exposure, progeny virions can be transferred to CD4+ T cells (Garcia et al., 2008; Garcia et al., 2005). Both *cis* and *trans*-infection are likely to contribute to transfer of virus from DCs to CD4+ T cells, and are not two processes that are necessarily sequential or interdependent. However, due to the low efficiency of productive viral replication in DCs and the compelling evidence for *trans*-infection, infection in *cis* is likely to have a smaller contribution to the process of infection.

1.7.5 HIV-1 transfer via exosomes – the Trojan horse model

This metaphor became popular with the findings by Ralph Steinman's group demonstrating that DCs carry HIV without themselves getting infected and induce formation of clusters (syncitia) and eventually death of CD4+ T cells (Cameron et al., 1992b). It basically exemplifies how HIV behaves like a Trojan horse that infiltrates the immune system, in this case DCs, undetected, and exploits the system for its own survival and propagation (reviewed in (Cavrois et al., 2008; Gould et al., 2003; Izquierdo-Useros et al., 2010)). Over the years the model has been extended to include multiple features of HIV, and retroviruses in general, to explain their immune evasion strategies. Studies of retroviral biology have revealed some fundamental differences to basic principles of viral pathogens, including the discovery of host molecules incorporated in retroviral particles, and their ability to utilize a receptor-independent entry pathway. Thus, given the similarities between exosomes and retroviral particles, some investigators suggest that retroviruses are Trojan exosomes.

Exosomes are single membrane organelles, about 100nm in diameter, that mediate intercellular communication by mediating exchange of proteins and genetic material (reviewed in (Belting and Wittrup, 2008; Thery et al., 2009). Their biogenesis is a two-step process initiating with inward budding of an endosomes's limiting membrane into

its lumen, generating MVBs. The outer membrane of these MVBs then fuses with the plasma membrane and releases their intraluminal vesicles into the extracellular space as exosomes (Stoorvogel et al., 2002). Exosomes, in this context, are distinct from intracellular exosomes that are sites for RNA degradation.

The Trojan exosome model encompasses distinct aspects of retroviral biology. Retroviruses such as HIV coopt the exosome biogenesis pathway for virion assembly and budding (Gould et al., 2003). Indirect evidence for this model comes from the strong concordance between the host cell protein profile of exosomes and that of HIV suggesting that HIV and exosomes are indistinguishable (Nguyen et al., 2003), findings that have not been confirmed by other investigators (Coren et al., 2008; Park and He, 2010). Moreover, it has been suggested that exosomes act as vehicles carrying virus/HIV to facilitate env-independent uptake pathways to infect neighboring cells (Izquierdo-Useros et al., 2009; Wiley and Gummuluru, 2006). Studies supporting this notion showed that a significant fraction of endocytosed HIV-1 were targeted for exocytosis and released into the extracellular space in conjunction with 100nm particles, which were identified as exosomes by proteomic profiling. Exosome-associated HIV-1 was more infectious than cell-free virus, however the efficiency of infection of T cells was still considerably less than that achieved by DC-T cell coculture. How HIV bearing exosomes are capable of efficiently infecting target cells is still unresolved. Indirect evidence for a role of adhesion molecules comes from work showing that blocking antibodies to various adhesion molecules and integrins block exosome capture by DCs by up to 30% (Morelli et al., 2004).

A substantial body of recent evidence – not necessarily from the HIV field – argues for a role of exosomes in immune responses and antigen presentation as well as transfer of cellular information such as microRNAs (Mittelbrunn et al., 2011) and signaling molecules such as β-catenin (Chairoungdua et al., 2010). It would be interesting to study the role of HIV-1-bearing exosomes in the context of self and non-self recognition.

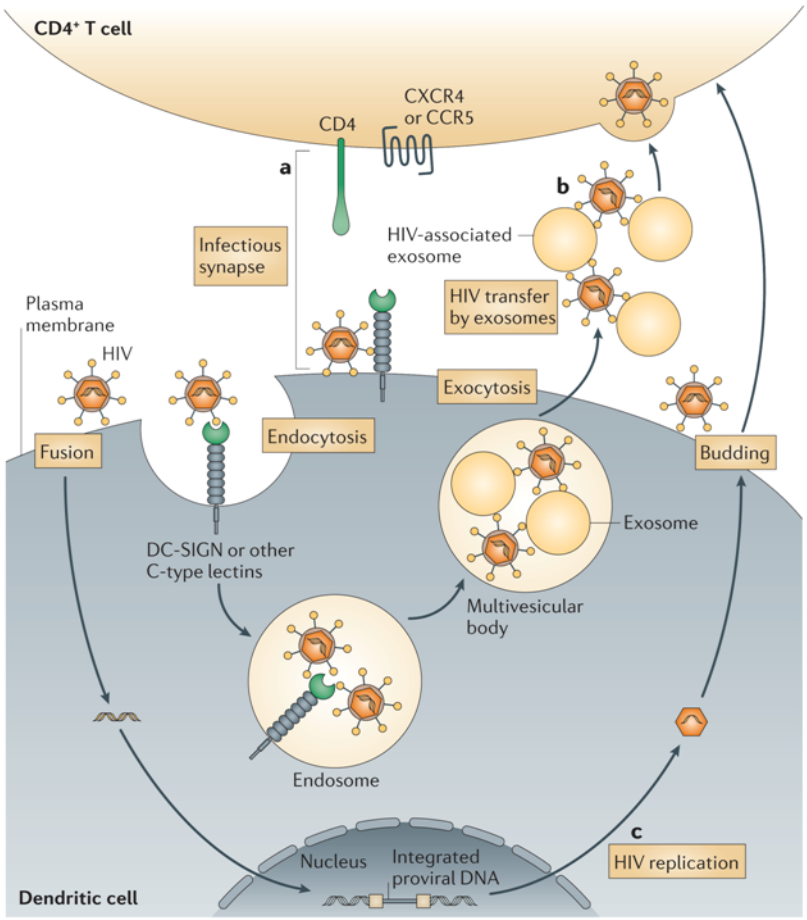

Figure 1.10. DC-mediated HIV transmission to T cells. Two types of DC-mediated HIV transmission have been proposed: *trans*-infection and cis-infection. Trans-infection can occur across the infectious synapse **(a).** Endocytosed HIV can also gain access to endosomal MVBs, enabling the release of HIV associated with exosomes **(b).** *Cis*-infection is the results of de novo viral production in DCs and long-term transmission of HIV. It is conceivable that these three mechanisms of transmission coexist in vitro; however, the relative importance of these pathways in vivo remains to be investigated. Adapted from (Wu and KewalRamani, 2006).

1.8 Conclusion

Despite extensive scientific efforts we still have a fairly incomplete understanding of the early events of HIV-1 infection and how the virus is sensed by the innate immune system.

DCs are the first cells that HIV-1 encounters at mucosal surfaces and as sentinel antigen-presenting cells of the immune system these should alarm the immune system and activate innate immune defences to recruit effective adaptive immunity and viral clearance. A peculiar characteristic of HIV – in contrast to other ssRNA viruses – is its ability to completely evade the antiviral interferon response. Additionally, it has the unique ability to manipulate the endolysosomal system and promote transmission via *trans*-infection in DCs.

Here I perform a comprehensive, unbiased screen to characterize novel signaling pathways that are induced upon HIV-1 infection of DCs – the HIV-1 signalosome - using a novel method of phosphoproteomics. Given the ability of the virus to incorporate host cell proteins to promote viral infection and evade immune recognition, I also carry out a proteomic analysis of HIV-1 virions to complement these studies. The results of these screens will be presented in chapter one and provide the basis for the following two chapters.

Chapter two will investigate the functional significance of components of the HIV-1 signalosome for their role in *trans*-infection and aim to characterize the "*trans*-compartment" on a molecular level. It will identify proteins implicated in the biogenesis of lysosome-related organelles as novel players in the regulation of the secretory pathway and innate immune defence in DCs and demonstrate how these are manipulated by HIV-1.

The third chapter will concentrate on elucidating the role of SHP-1 in manipulation of the innate immune response in DCs. SHP-1 is a negative regulator in multiple signaling cascades and found to be dephosphorylated by HIV-1 within the phosphoproteomic screen.

Chapter 2

Material and Methods

2.1 Cell culture

2.1.1 Tissue culture

All cells were cultured at 37°C in humidified incubators supplemented with 5% CO_2. HEK293T cells were kindly provided by Dr Suneale Banerjee (HIU) and kept in D10 (Dulbecco's Modified Eagle Medium, 10 % Fetal Calf Serum, 2% Glutamine and 1% Penicillin/Streptomycin; Sigma-Aldrich, UK). MDDCs and CD4+ T cells were isolated from buffy coats and kept in R10 (RPMI-1640, 10 % Fetal Calf Serum, 2% Glutamine and 1% Pen/Strep; Sigma-Aldrich, UK). Mucosal mononuclear cells were isolated from normal residual bowel tissue obtained at cancer surgery and kept in R10 and Gentamycin and Amphotericin.

2.1.2 Generation of immature monocyte-derived dendritic cells

Buffy coats were obtained from National Blood Services (Bristol), diluted three fold with RPMI-1640 and separated by centrifugation over a Sodium Diatroziate/Polysaccharide Solution (Lymphoprep, Axis-Shield Oslo). PBMCs were collected at the interface and washed four times with cold RPMI-1640 at decreasing speed (1800, 1500 and 1100 rpm). Monocytes were positively separated with CD14+ microbeads and LS columns (Miltenyi Biotech), in accordance with the manufacturer's instructions. CD14+ monocytes were cultured in 10 cm cell culture dishes in 25 ml R10 as well as 40 ng/ml recombinant IL-4 and GM-CSF (Peprotech) respectively for 5 days. Cells were fed with 40 ng/ml IL-4 and GM-CSF and 5 ml fresh R10 respectively on day 3 and harvested on day 5. Periodic flow cytometry was used to confirm their purity and immature status with low expression of

maturation and activation markers such as CD86, CD83, CD80 and HLA-DR.

2.1.3 Isolation and activation of CD4+ T cells

The CD14 negative fraction isolated during PBMC isolation was washed with cold RPMI-1640, resuspended in 100 ml R10 and transferred to large tissue culture flasks. 72 hours before being used for co-culture experiments PBMCs were blasted by addition of 10 μg/ml phytohemagglutinin (PHA; Rembrel). Isolation of CD4+ T cells was performed by negative selection using the CD4+ T cell Isolation kit II (Miltenyi), according to the manufacturer's instruction. Following collection of the enriched CD4+ T cell effluent, cells were washed and resuspended at 10^6 cells/ml in R10.

2.1.4 Isolation of mucosal mononuclear cells

A piece of macroscopically normal residual bowel tissue was obtained from surgically resected bowel specimens from patients with tumour resections. Patients with a history of neoadjuvant therapy or inflammatory bowel disease were excluded. The study protocol had been approved by the Oxfordshire National Research Ethics Committee.

Initially, tissue specimens were extensively rinsed with sterile PBS, then mucosa was detached from muscularis and serosa. Mucosa tissue was weighed and subsequently incubated with 1 mM ultrapure dithiothreitol (Fisher Scientific) in calcium/magnesium free HBSS with 5% FCS and antibiotics (the antibiotic combination used for mucosal experiments was 1 U/ml Penicillin, 50 μg/ml Streptomycin, 40 μg/ml Gentamycin and 25 ng/ml Amphotericin) for 15 minutes at RT with rapid shaking to remove mucus and crypts. Tissue was incubated with modified HBSS containing 0.75 mM EDTA, 1 M Hepes and antibiotics for two-three 30 minutes incubations, each at 37°C and rapid shaking at 200 rpm, to remove epithelial cells. Subsequently, tissue specimens were washed three times with HBSS with 5% FCS to remove any EDTA, that would otherwise inhibit collagenase. Tissue was dissected into 2-3 mm pieces, distributed among multiple C tubes (Miltenyi) and incubated with a prewarmed enzyme cocktail containing 1-2 mg/ml Collagenase A (Roche) and 1 μg/ml DNAse I (Roche) in RPMI with 5% FCS. C Tubes were attached to the gentleMACS Dissociator (Miltenyi) and ran on program brain

01 once. Further digestion was carried out in a thermal incubator at 37°C at 220 rpm for 60 min, followed by another dissociation step on the gentleMACS dissociator using program C01. The digestion media containing the dissociated cells was collected, filtered through a 70 μm cell strainer (Becton Dickinson) and washed twice with R10 at 4°C. The dissociated cells were resuspended in 2-4 ml of a 40% Percoll solution (GE Healthcare) and placed carefully over a discontinuous Percoll gradient (100%-60%-40%-30% Percoll). Tubes were centrifuged for 25 minutes at 1500 rpm at 4°C and the mononuclear population containing lymphocytes and DCs was collected at the 40-60% Percoll interface, washed twice, counted and either processed immediately or rested overnight in R10 at 37°C.

2.1.5 Activation of MDDCs

MDDCs were stimulated with 0.1-1 μg/ml LPS (LPS from E. coli 0111:B4, Sigma-Aldrich) and 1-10 μg/ml ssRNA40 (5'-GCCCGUCUGUUGUGUGACUC-3'), ssRNA41 (5'-GCCCGACAGAAGAGAGACAC-3'), Poly(I:C)/HMW Lyovec and Lyovec™ (all from Invivogen). For DC-SIGN activation 6 well plates were precoated with 20 μg/ml DC-SIGN antibody (H200, Santa Cruz) in PBS at 37°C, one hour later residual buffer was taken off and the bottom of the well was gently washed 3 times with PBS to remove any unbound antibody and sodium azide. Gp120 activation was performed with 10 μg/ml recombinant gp120 (kind gift from Dr Chris Scanlan, Dept of Biochemistry, Oxford).

2.2 Proteomics

2.2.1 Phosphoprotein purification

MDDCs were harvested with cold RPMI 1640, washed twice, counted and split into 2-4 tubes depending on the experiment. After infection or activation, cells were immediately placed on ice and washed twice with ice-cold Hanks buffered saline containing a 1:100 dilution of a phosphatase inhibitor cocktail I (Sigma-Aldrich). Lysis was carried out at 4°C in 5-7 ml of PhosphoProtein Lysis Buffer supplemented with protease and phosphatase inhibitors for 40 min at 4°C according to the manufacturer's instructions (Phosphoprotein purification kit, Qiagen). During lysis cells were vortexed every 10 min.

Cell debris was pelleted by centrifugation in a microcentrifuge at 13,000 rpm and 4° C for 30 min. Whole-cell lysates were harvested and the protein concentration determined with Bradford Protein Assay (Bio-rad). The concentrations were adjusted to 0.1 mg/ml. Subsequently, a maximum of 2.5 mg lysate was added to resin columns (Qiagen) and the flow-through fraction containing non-phosphorylated proteins discarded. After a wash step, which removed any unbound unphosphorylated proteins, the proteins were eluted with 2 ml of an elution buffer containing PBS. Phosphorylated protein fractions were further concentrated with Pierce 9K ultracentrifuge tubes at 4,000 g to a final volume of ~300 µl (Thermofisher) and either processed immediately or stored at -80°C.

2.2.2 Off gel fractionation by iso-electric focusing (IEF)

Prior to fractionation samples were desalted using ZEBA Spin desalting columns and quantified using Bradford assay. Equal amounts of desalted and concentrated samples (HIV and mock) were loaded onto an iso-electric focusing platform according to the manufacturer's instructions. Phosphoproteins were separated into 12 fractions using the Agilent 3100 OFFGEL Fractionator and the 3100 OFFGEL High Res kit, pH 3–10 (Agilent) by iso-electric focusing (IEF) for 50 kilovolt hours at a maximum current of 50 µA and maximum power of 200 milliwatts. Fractionation was typically completed after 24-36 hours at room temperature, after which fractions were harvested, desalted as described and then either processed for electrophoresis and immunoblotting or mass spectrometry analysis.

2.2.3 Methanol-chloroform precipitation and other desalting protocols

For further analysis, fractions were subjected to methanol-chlorofom precipitation. To 200 µl of each fraction 600 µl of methanol and 150 µl of chloroform were added. Samples were vortexed briefly, 450 µl ultrapure water added to each sample and samples vortexed again. Samples were spun at 13,000 rpm for 1 minute at RT. The upper aqueous layer was carefully removed without disturbing the interface containing protein precipitates. 450 µl of methanol was added to each tube and samples spun for a further 2

minutes in a microcentrifuge. The supernatant was carefully taken off and the protein pellet dried in a speed vacuum.

For some phosphoproteomics experiments, in particular desalting steps before and after IEF, small and large volume Zeba desalting columns (Thermofisher/Pierce) were used as a liquid-phase alternative to methanol-chloroform precipitation according to the manufacturer's instructions. This aided in reducing sample loss and streamlined handling of large number of samples.

2.2.4 In-solution tryptic digestion

Precipitated proteins were dissolved in 100 µl 6M Urea in 0.4M Tris buffer by sonication. 5 µl of reducing agent containing DTT (200 mM DTT in Tris buffer, pH 7.8) was added and samples incubated at RT for 30 minutes. 20 µl of alkylating reagent containing iodoacetamide (200 mM iodoacetamide in Tris buffer, pH 7.8) was added and samples incubated at RT. After 30 minutes another 20 µl of DTT reducing reagent was added to consume any unbound iodoacetamide. After 30 minutes 775 µl water was added to reduce the concentration of urea. 10 µl of a 200 µg/ml sequence grade trypsin solution was added and proteins digested overnight under gentle agitation at 37°C.

2.2.5 SEP-PAK Purification

Sep-Pak Plus C18 cartridges (Waters) were equilibrated with 5 ml of solution B containing 80% Acetonitrile and 0.1% Formic acid followed by 10 ml of solution A containing 98% Acetonitrile and 0.1% Formic acid. Samples were loaded onto columns and washed with 10 ml of solution A. Bound peptides were eluted with 1.5 ml of solution B into eppendorf tubes. Purified peptides were vacuum dried in a vacuum centrifuge before analysis by LC-MS/MS.

2.2.6 Analysis of Mass Spectrometry Data

LC-MS/MS was carried out in collaboration with Dr Benedikt Kessler (Core Proteomics Facility, University of Oxford). Mass spectrometry data were analysed using the Central Proteomics Facility Pipeline (CBRG, Oxford) (Trudgian et al.). Peptides and proteins

were identified by a combination of three different search engines (Mascot, OMSSA, X!Tandem kscore). Spectra were searched with trypsin specificity and stringent filtering criteria such as cysteine carbamidomethylation and phosphorylated residues (Ser, Thr, Tyr). A false discovery rate of maximum 1% was estimated to generate high confidence data. In addition, spectral index quantitation was used to provide a semi-quantitative comparison of protein amounts between samples. Due to the low number of peptide matches for the number of LC-MS/MS runs performed, reliable spectrum identification could only be achieved for the top 1/3 of proteins identified. Pathway analysis was performed with ingenuity, innateDB and STRING databases.

2.2.7 Cell lysis for standard immunoblotting

For standard immunoblotting of non-phosphoproteins pelleted DCs were lysed in 1% Nonidet P-40, 450mM NaCl, 50mM Tris pH 8.0, 5mM EDTA supplemented with protease inhibitors (either 5 μg/ml leupeptin, 5 μg/ml pepstatin, 1mM NaF, 1mM PMSF (all from Sigma-Aldrich) or Roche Complete mini protease (Roche) for 30 min on ice and cleared by centrifugation for 15 min at 13,000 rpm.

2.2.8 Protein Electrophoresis

Concentration-adjusted protein samples were reduced at 95°C with 4x NuPage SDS loading buffer (Invitrogen) for 5 minutes, returned on ice prior to loading onto precast 4-12% or 10% NuPage gels (Invitrogen). Gels were run using NuPage MOPS buffer in NuPage gel tanks (Invitrogen). Gels were initially run at 60V for 10 min, following that they were run at 100-140V until the dye front reached the bottom of the gel.

2.2.9 Immunoblotting

Gels were transferred to nitrocellulose PVDF membranes (Hybond-C-Extra, Amersham Biosciences) in NuPage transfer buffer (Invitrogen) at 30 V for 1 hour using a wet Invitrogen transfer unit. Membranes were washed three times with TBS-0.1%Tween buffer. Membranes were blocked with either 3% Bovine serum albumin in TBS-T (for phosphor-antibodies) or 10% non-fat milk powder in TBS-T with gentle rocking or

rotation. Blocking was either performed overnight at 4°C or for 1 hour at RT. Subsequently, membranes were rinsed three times with TBS-T on a rocker, incubated with primary antibody in 3%BSA/TBS-T for detection of phophoproteins and 10% milk powder in TBS-T for detection of non-phospho-antibodies for one hour at RT or at 4°C overnight, followed by three washing steps. Species-specific HRP-conjugated secondary antibody (Sigma) was diluted 1/10000 and membranes incubated for 1 hour at RT. Finally, membranes were washed at least a further 3 times before being visualized with ECL reaction reagent (Amersham Biosciences) on photographic paper (Amersham) and a Xograph developer (Imaging system).

2.2.10 Silverstaining

Protein electrophoresis was carried out as described above, gels were fixed in fixative solution (50% Methanol, 5% Acetic acid) for 20 min followed by two washing steps, the first for 10 min in 50% Methanol, the second for 2 min in water. Gels were subsequently exposed for 1 min to a sensitizing solution, 0.02% $Na_2S_2O_3$, and washed twice with water for 1 min. This was followed by a 20 min incubation step in cold 0.1% $AgNO_3$ at 4°C in the dark. Development of the silver nitrate protein staining was made using a solution of 2% Formaldehyde, in 2% sodium carbonate for the appropriate length of time, usually between 2-5 min. Development was terminated by addition of a 5% acetic acid solution. Gels were later incubated in ultrapure water for visualization. All reagents from Sigma-Aldrich.

2.3 Molecular biology

2.3.1 Extraction of mRNA

DCs were harvested, washed once with cold PBS and pelleted in an Eppendorf tube. HIV-1-infected cells were lysed using Qiashredder columns (Qiagen), for all other experiments homogenization was performed with a needle. RNA was extracted using an RNeasy Mini kit (Qiagen) according to the manufacturer's instructions. RNA was eluted with nuclease-free water and stored at -80°C until used. RNA concentration and quality was assayed by UV spectrophotometry.

2.3.2 DNase Treatment

Some commercially available primers also amplify genomic DNA (e.g. by not spanning introns or cross intron/exon boundaries), therefore a DNAse treatment step using the DNA-free kit (ABI) was necessary to remove any genomic DNA contamination. Briefly, 1.5 μg RNA were incubated with 1 μl DNAse I enzyme and 10x buffer in a final volume of 22.5 μl for 30 min at 37°C. 2.5 μl inactivation reagent was added to inactivate DNAse I and incubated for 2 min at RT with occasional vortexing. Subsequently, the inactivation reagent was pelleted by centrifugation at 2000 g for 1.5 min. The RNA was taken off and used for reverse transcription accordingly.

2.3.3 Taqman Real-time PCR

Complementary DNA (cDNA) was synthesized from a total of 500 ng RNA in a volume of 20 μl using the High Capacity RNA-to-cDNA kit (ABI), which contains random hexamer primers and MultiScribe Reverse Transcriptase according to the manufacturers instructions. Real-time RT-PCR was performed with pre-designed primers (ABI) using the ABI 7500 real-time PCR system using the standard cycling conditions for 40 cycles. Each reaction contained 25 ng cDNA, 1 μl Taqman primer and 10 μl Taqman Gene expression master mix in a total volume of 20 μl with each sample performed in duplicates or triplicates. The efficiency of each Taqman primer was assessed by performing serial dilution series using cDNA. The C_T (cycling threshold) value is defined as the number of PCR cycles where the fluorescence signal exceeds the detection threshold value. The normalized amount of mRNA of the gene of interest (GOI) was calculated according to the relative quantitation method ($\Delta\Delta$CT) whereby the expression of the glyceraldehyde-3-phosphate-dehydrogenase (GAPDH) amplicon was used as an internal control and the normalizer for the data per following equation:

Relative expression ratio= $(2^{-(C_T GOI - C_T GAPDH)})$treated sample/$(2^{-(C_T GOI - C_T GAPDH)})$control sample.

2.3.4 SYBR-Green Real time PCR for HIV-1 tat-rev transcripts

RNA was extracted at 6 h and 24 h using the RNeasy kit (Qiagen) and subjected to

DNAse digestion and reverse transcription as described above. Early viral tat-rev transcripts and GAPDH were amplified by SYBR green quantitative PCR (SYBR green Master Mix from ABI) using primers published by Gringhuis *et al*. (Table 2.1). A melting curve was generated to ensure amplification of a single product. Finally, gene expression was normalized to GAPDH and relative quantification was performed using the ΔΔCT method.

Table 2.1. Primers used for HIV-1 real-time PCR

Primer	Sequence
tat-rev forward	ATGGCAGGAAGAAGCGGAG
tat-rev reverse	ATTCCTTCGGGCCTGTCG
GAPDH forward	CCATGTTCGTCATGGGTGTG
GAPDH reverse	GGTGCTAAGCAGTTGGTGGTG

2.3.5 Preparation of samples for microarray studies

DCs were activated with 100 ng/ml LPS or mock, harvested 22 h later and infected with HIV-1 or mock for 2 h (MOI=1), washed and pelleted. Each condition was split into two and RNA was extracted as described above. Following quality control samples which satisfied the following criteria were chosen for microarray analysis: 260/280 ≥ 1.8, 230/280 ratio ≥ 1.8 and RNA integrity number (RIN) ≥ 8.

Total RNA was amplified and labelled using the GeneChip WT Terminal Labelling kit (Affymetrix), followed by hybridization to Affymetrix Human Gene 1.0 ST Arrays by Dr. Dilair Baban (Wellcome Trust Centre for Human Genetics, University of Oxford). A total of 2 μg RNA and the appropriate amount of GeneChip Eukaryotic Poly-A spike-in controls were reverse transcribed to double stranded cDNA in two separate steps (1st and 2nd strand cDNA synthesis). The transcripts were amplified by in vitro RNA synthesis. The cRNA yield and size distribution was confirmed by microelectrophoresis using the Bioanalyzer 2100. The cRNA was then purified and reverse transcribed back into cDNA, fragmented and labelled by terminal deoxynucleotidyl transferase (TdT). Each chip was incubated with 10 μg fragmented cDNA for 16 h at 45 °C. Unhybridised probes were removed and fluorescent images were captured using the Gene Array Scanner 3000

(Affymetrix). It was confirmed that all quality controls met the Affymetrix quality assessment guidelines. In addition, on-chip normalization was performed to allow comparison between different arrays and the resulting raw data was analysed using Genespring GX software. Statistical analysis was performed using a two-way ANOVA test with Bonferroni adjustment.

2.4 Protein biochemistry

2.4.1 ELISA

Supernatants were harvested from cell cultures at indicated times and frozen at -80°C until analysis. Samples were cleared by centrifugation before being assayed. ELISA kits for cytokines were from R&D Systems and for p24 from Advances Bioscience Laboratories. Samples were assayed either neat or diluted in duplicates and triplicates. A 7-point serial dilution standard curve was prepared fresh for each plate. Developed ELISA plates were read using a Microplate 680 reader (BioRad).

2.4.2 SHP-1 Phosphatase Assay

MDDCs were harvested with cold RPMI 1640 and split among different 15 ml Falcon tubes at 2 mill cells/condition, washed once and kept on ice after all supernatant was aspirated. HIV-1 (MOI=1) or mock was added to the cell pellets and cells were incubated for the indicated time points at 37°C and then immediately transferred to ice and washed twice with cold TBS. Subsequently, cells were resuspended at 10^7 cells/ml in Phosphatase lysis buffer and allowed to lyse for 15 min on ice and frozen at -80°C. The lysis buffer was prepared fresh before use and contained 50 mM HEPES, 0.1 mM EGTA, 0.1 mM EDTA, 120 mM NaCl, 0.5 % NP-40 (pH 7.5), 25 µg/mL Leupeptin, 25 µg/mL Pepstatin, 2 µg/mL Aprotinin and 1 mM PMSF (all from Sigma-Aldrich). Frozen samples were thawed on ice and centrifuged at 2000 *g* for 5 min. Cell lysate was harvested and protein concentration determined by Bradford assay. Equalized amounts of protein were processed in triplicates for determination of the SHP-1 phosphatase activity, in accordance with the manufacturer's instructions (Human SHP-1 Duoset, R&D Systems).

2.4.3 Flow Cytometry

Cells were initially washed in PBS and dead cells were stained using Violet LIVE/DEAD Cell Stain (Invitrogen). Then, cells were washed in PBA and incubated with titrated amounts of FITC-, PE-, PerCP-, APC-, APC-Cy7-, PE-Cy7-, V450 and PB-conjugated antibodies for 20 minutes at 4°C. After surface staining, cells were washed with PBA and fixed in 1% paraformaldehyde until acquisition on a Cyan flow cytometer (Dako). For intracellular staining with Cytofix/Cytoperm Solution cells were processed according to the manufacturer's instruction (BD Biosciences). Data was analyzed using Flowjo software.

2.4.4 Immunofluorescence confocal microscopy

DCs were transferred onto Poly-L lysine (Sigma-Aldrich) coated slides (BD Bioscience) at 1.5-2x10^5 cells/well and allowed to adhere for 1 h at 37°C. Coverslip adhered cells were fixed in 4% PFA for 10 min at RT or overnight at 4°C and permeabilized in 0.1% TritonX for 7 min. Each well was washed three times with PBS + 2% BSA (2%PBA) before incubation with primary antibodies diluted in 100 µl 2% PBA for 1 h at 37°C or overnight at 4°C. Finally, cells were washed three times with PBA and incubated with appropriate dilutions of secondary antibodies (Molecular Probes) for 1 h at RT. Cells were then washed again with PBA and if appropriate nuclei were stained by adding To-Pro far red (1:4,000 dilution) (Invitrogen) for 10 min. For slides containing ATTO647 labeled HIV-1, nuclear staining was carried out with 5 μm SYTO 82 orange fluorescent nucleic acid stain (Molecular Probes) for 20 min at RT. Slides were prepared with Vectashield without Dapi (Vectorlabs) and images acquired using a Biorad confocal microscope.

2.4.5 Electron microscopy of HIV-1 virions

Staining for electron microscopy and acquisition of images was kindly performed by Dr David Ferguson, Department of Pathology, John Radcliffe Hospital, Oxford. Antibodies used were CD47 (MEM, Abcam) and 2G12 (kind gift from Dr Quentin Sattentau, Dunn School of Pathology, Oxford).

2.5 Bacterial culture

2.5.1 Transformation of competent bacteria

1 µl DNA was added to 50 µl library efficient DH5α cells (Invitrogen) and gently mixed. Cells were incubated on ice for 30 min, heat shocked for 45 sec at 42°C and immediately transferred to ice for another 2 min. The mixture was added to pre-warmed SOC media and incubated for 1 hour at 37°C while shaking at 220rpm. Subsequently, 50 μl of bacteria were plated on LB agar plates containing of selective antibiotic – mostly 100 μg/ml ampicillin - and incubated overnight at 37°C.

2.5.2 Extraction of bacterial plasmid DNA

An initial starter culture was set up by picking singe bacterial colonies from the plates and inoculating them in 5ml LB media and 100μg/ml ampicillin for 12 h at 37°C while shaking at 220rpm. Bacteria were pelleted and plasmid DNA extracted from E.coli using the QIAprep Spin Miniprep kit (Qiagen) in accordance with the manufacturer's instructions.

2.5.3 Digestion of DNA using restriction endonucleases

Successful insertion of the insert was confirmed by performing restriction enzyme digestion using restriction enzymes specific for the insert and plasmid backbone. The reaction was set up with 1μl DNA in the presence of restriction enzymes (Roche and NEB) and the recommended buffers and incubated at 37 °C for 1 hour.

2.5.4 Agarose gel electrophoresis

Digestion products were analyzed by agarose gel electrophoresis. DNA samples were run at 70V in 1% agarose minigels containing 1.5 μl Ethidium bromide in 1x TAE buffer. DNA was visualised using a Stratagene 2040EV UV transilluminator, and photographed using a UVP digital camera.

2.5.5 DNA sequencing

DNA sequencing was performed by the dideoxy termination method at the WIMM or at the Biochemistry Department Sequencing Facility (University of Oxford). To confirm sequence identity and integrity, automatically called base pairs from sequencing traces were analyzed with the online software available at:

(1) http://www.ncbi.nlm.nih.gov/projects/gorf/

and

(2) http://blast.ncbi.nlm.nih.gov/Blast.cgi?PAGE_TYPE=BlastSearch&PROG_DED=blastn&BLAST_PROG_DEF=megaBlast&BLAST_SPEC=blas2seq

2.5.6 Plasmids Used

Plasmids for SHP-1 and RagA were all from Addgene and as follows:

pJ3SHP-1WT, deposited by Ben Neel, Addgene plasmid 8572

pJ3SHP-1 C453S, deposited by Ben Neel, Addgene plasmid 8573

pRK5 HA GST RAGA WT, deposited by David Sabatini, Addgene plasmid 19298

pRK5 HA GST RAGA Q66L, deposited by David Sabatini, Addgene plasmid 19300

pRK5 HA GST RAGA T21L, deposited by David Sabatini, Addgene plasmid 19299

2.6 Transduction of DCs

2.6.1 Transfection of DCs using Amaxa nucleofection

Transient transfection of DCs with Qiagen siRNAs or Dharmacon Smartpool siRNAs was performed using the human DC Nucleofector kit (Amaxa). 3×10^6 DCs were resuspended in 100 µl human dendritic cell transfection solution and mixed with 5 µl siRNA (50 µM stock solution). The mixture was transferred to a cuvette and electroporated using program U-02. Warm R10 was added to the cuvette immediately after nucleofection and cells were transferred to a 6-well plate containing 3 ml of R10. Cells were incubated for 24 h to allow for target gene expression or knockdown before experiments were performed.

2.6.2 Transfection of DCs using Neon™ electroporation

DCs were prepared, counted to resuspend at appropriate cell concentration and washed with PBS. All residual PBS was taken off the cell pellet, which was resuspended in 10 μl transfection solution and 2 μl siRNA (50μM stock solution) or 1-3 μg DNA per 2.5x10^5 DCs. The mixture was aspirated with the electroporation pipette and electroporated at following settings: pulse voltage 1475 V, pulse width 20 ms, pulse number 2. Following electroporation cells were immediately transferred to a 12 well plate with warm R10 without antibiotics and kept at a concentration of 10^6 DCs per ml for 48 h to allow knockdown of gene expression.

2.6.3 Generation of lentiviruses

HEK 293T cells were harvested one day prior to transfection and plated in six well plates at 6x10^5 cells/plate in D10 to achieve a confluency of about 50-70% the following day. Cells were transfected with equal amounts of three plasmids using Genejuice (Novagen Merck): packaging plasmid p8.91 (Zufferey et al., 1997), envelope VSV-G protein-expression plasmid pMD-G (Naldini et al., 1996) and pHR-SIN-GFP2 (Bainbridge et al., 2001) encoding the gene of interest, all kindly provided by the S. J. Davis lab, HIU, WIMM. 48-72 h post transfection viral supernatant was harvested and spun at 3000 rpm to remove any residual cells from the supernatant and added to 1x10^6 cells. Efficient expression of the desired proteins was analyzed by flow cytometry. Virus was filtered (0.45 μm Milipore filter) and depending on cells to be transfected either used immediately or further concentrated by ultracentrifugation.

2.6.4 Generation of CD47shRNA and SIRPα shRNA constructs for lentiviral transduction

The shRNA sequences targeting CD47 and SIRPα were designed after searching for the following pattern in the target mRNA: N2(GC)N(A)N6(UT)N2(ATUC)N5(A)N2 (Table 2.2). The shRNA expression plasmid consists of a nucleotide sense sequence (identical to the target sequence in the mRNA to be downregulated), followed by a loop TTCAAGAGA, an antisense sequence, and a stretch of five Ts as a pol III transcriptional

termination signal, downstream of the U6 promotor. Complementary overhangs from BamHI and EcoRI were included to allow insertion into plasmids digested with these enzymes. The final DNA sequence, and its complementary reverse, were ordered as custom designed primers (Sigma-Aldrich). The two DNA were mixed 1:1 and heated to 95°C and allowed to cool slowly to 10°C. The double-stranded DNA sequence was then cloned into the pHR-U6P lentiviral vector.

Table 2.2. DNA oligos used to generate CD47 and SIRPα shRNA

CD47 shRNA Forward
GAT CCG CCA GGT GAA TAT TCA TTA ATT CAA GAG ATT AAT GAA TAT TCA CCT GGT TTT TTA CGC GTG
CD47 shRNA Reverse
AAT TCA CGC GTA AAA AAC CAG GTG AAT ATT CAT TAA TCT CTT GAA TTA ATG AAT ATT CAC CTG GCG
SIRP α shRNA Forward
GAT CCG CGA GAA GAA TGC CAG AGA ATT CAA GAG ATT CTC TGG CAT TCT TCT CGT TTT TTA CGC GTG
SIRP α shRNA Reverse
AAT TCA CGC GTA AAA AAC GAG AAG AAT GCC AGA GAA TCT CTT GAA TTC TCT GGC ATT CTT CTC GCG

2.6.5 Generation of lentiviruses expressing SHP-1 transgene

SHP-1 Genes were amplified from pJ3 SHP-1 WT and CS, encoding the SHP-1 wild-type and mutant vector templates using oligonucleotide primers that incorporated suitable restriction enzyme sites at both 5' and 3' ends (Table 2.3). Following PCR amplification the gene of interest and the vector pHR-SIN-BX-IRES-Em were digested with BamHI and XhoI. A ligase reaction of the purified DNA fragments was performed to obtain a contiguous plasmid. This product was then used to transform bacteria in the presence of appropriate antibiotics. Confirmation of the size of the DNA was performed with restriction digestion and agarose gel electrophoresis. Furthermore, sequence integrity was verified by the WIMM sequencing facility.

Table 2.3. DNA oligos used to generate SHP-1 transgene

SHP-1 Forward
TAGTAGGGATCCGCCACCATGATGGTGAGGTGGTTCACC
SHP-1 Reverse
CTACTACTCGAGTTCACTTCCTCTTGAGGGAACCC

2.6.6 Infection of DCs with lentiviruses

DCs were harvested on day 3 of differentiation and seeded at 10^5 cells per well in a 96-well flat-bottom plate in 100 µl of R10 supplemented with 40 ng/ml IL4 and GM-CSF, respectively. Lentivirus, expressing the shRNA or transgene of interest, and Vpx-VLPs were added and mixed well with the DCs with a multichannel pipette. After two hours of incubation at 37 °C, plates were centrifuged at 1,800 rpm for 10 min. Medium was carefully aspirated and replaced with fresh R10 supplemented with cytokines. Lentiviral transduction efficiency was assessed by flow cytometry on day 4 p. i. Protocol here described was adapted from that described by Berger *et al*. (Berger et al., 2011)

2.7 Virology

2.7.1 Production of HIV-1 BaL

pNL4.3 BaL strain was originally supplied by Dr Hal Drakesmith, Weatherall Institute, Oxford. The construct contains a full-length HIV-1 provirus. This consists of the backbone of the HXB-3 strain of HIV-1 IIIB containing 2687bp SalI to Bam HI fragment from strain BaL, including the Env sequences. The integrity of the plasmid was verified by restriction digestion and agarose gel electrophoresis. HEK293T cells were grown until 70% confluent and transfection was carried out by calcium phosphate transfection. 30 μg HIV-1 NL4-3 BaL proviral construct was added to 1ml sterile 2.5 M $CaCl_2$ solution and incubated at RT for 10 min. The mixture was added dropwise to 1 ml 2x Hepes buffer (pH 7.08-7.14, pretested for transfection efficiency) while vortexing constantly followed by a further incubation at RT for 20 min. The mixture was then added dropwise to the tissue culture plate while gently moving the plate from side to side to ensure thorough uptake of the transfection solution by the cells. Six to eight hours later the medium was replaced with fresh D10. Viral supernatant was harvested 24 h later, filtered (0.45 μm

Milipore filter) and stored at -80 °C. For some experiments viral stocks were further purified and concentrated (see below). Virus stocks were titrated by p24 ELISA (Immunodiagnostics and ABL) or measurement of HIV Reverse transcriptase activity (QuanT-RT kit GE Healthcare). $TCID_{50}$ of viral stock was measured by limiting dilution infectivity assay on TZM-bl cells (human cervical cancer cells from AIDS Research and Reference Reagent Program).

2.7.2 Purification and ultraconcentration of HIV-1 and lentiviruses

This protocol was adapted from (Kutner et al., 2009). Filtered viral stocks were transferred to pre-sterilized SW28 ultracentrifuge tubes (Beckman Coulter) and underlayed with 4 ml of a cold, sterile 20% sucrose solution (Sigma-Aldrich). Tubes were filled up with sterile PBS and weight adjusted until they were 0.1 g from each other. Tubes were loaded into a Beckman SW28 ultracentrifuge rotor and spun at 25,000 rpm (82,700 g) for 2 h at 4 °C. Tubes were carefully removed, viral supernatant was poured off and tubes left in an inverted position for 10 min for any residual media to dry up. 100-200 μl PBS was added to the bottom of the tubes and the tubes incubated at 4 °C for 2 h on a shaker to allow resuspension of the viral pellet. Concentrated stocks were aliquoted, frozen at -80 °C and titrated accordingly for downstream experiments.

2.7.3 Generation of fluorescently labeled HIV-1

ATTO-647N-maleimide and ATTO-488-maleimide (both ATTO-Tec GmbH, Sigma-Aldrich) were used for labeling of HIV-1 virus. Dyes were reconstituted in DMSO according to manufacturer's instructions and then added dropwise with intermittent vortexing to purified, concentrated HIV-1. The mixture was incubated light protected at RT for 2 hours before being diluted with PBS and underlayed with 100 μl cold 20% sucrose. Virus was purified by centrifugation at 13,000 rpm in a table top centrifuge for 90 min at 4 °C. Subsequently, virus was pelleted again by washing with PBS, aliquoted and stored at -20 °C.

2.7.4 Generation of CD44 positive NL4-3 BaL

HEK 293T cells were transfected with pRc CMV CD44S (kind gift from Dr. Suneale Banerjee (HIU) using Lipofectamine™ 2000 (Invitrogen) according to the manufacturer's instructions. Expression of CD44 was checked by flow cytometry and cells were split and prepared accordingly for generation of HIV-1 NL4-3 BaL according to 2.7.1.

2.7.5 HIV-1 infection of DCs

For phosphopurification and LC-MS/MS experiments DCs were harvested with cold RPMI and $20x10^6$ DCs per condition were incubated with 500 µl HIV-1 BaL (180ng p24) or 500 µl mock (supernatant from mock transfected 293T cells) in a small volume for 10 minutes at 37°C before proceeding for cell lysis and phosphopurification.

Otherwise, MDDCs were pulsed with titrated NL4-3 BaL HIV-1 or labeled HIV-1 at an MOI of 0.1-1. Excessive virus was washed off with R10 after 120 minutes and cells were cultured in R10 in 6-96 well plates depending on the experiment performed. HIV replication was measured in supernatants by (i) reverse transcriptase assay (Quan-T-RT kit, Amersham Biosciences) or (ii) p24 capture ELISA (Immunodiagnostics or Abl, Advances Biosciences) or (iii) flow cytometric intracellular p24 staining (Beckman Coulter).

2.7.6 Co-culture of HIV-1-infected DCs with CD4+ T cell blasts

For co-culture experiments autologous CD14- PBMCs were kept after monocyte isolation in complete medium for the duration of DC generation. Three days prior to planned co-culture experiment, PBMCs were activated with 10 μg/ml phytohaemagglutinin PHA and CD4+ T cells were selected by negative immunomagnetic bead selection according to manufacturer's recommendations. Autologous PHA-activated CD4+ T cells were maintained in R10. MDDCs were infected with HIV-1 for 2 hours, washed twice with PBS and co-cultured in R10 at a ratio of 1:3 (DC:CD4) at $2x10^6$ cells/ml.

2.7.7 RNAi screen for HIV-1 DC-CD4 *trans*-infection

DCs were prepared as above for Neon transfection (2.6.2). 2.2 μl of each siRNA tested

was transferred to prepared Eppendorf tubes. DCs were resuspended at appropriate concentration in transfection solution and 33 μl of cell suspension containing $2.5x10^5$ DCs and mixed with the siRNA. Electroporation was performed with the 10 μl tip in triplicates and cells were transferred to a 96 well plate containing 200 μl warm R10 without antibiotics. 48 h later plates were spun at 1100 rpm for 5 min and media was aspirated. DCs were infected with NL4-3 BaL resuspended in R10 at an MOI of 0.1 (2 μl virus and 48 μl R10 per well) for 2 h, washed twice with R10 and then mixed with $22.5x10^5$ CD4+ T-cell blasts in final volume of 250 μl R10 and kept in culture for 72 h before flow cytometry staining.

2.7.8 HIV-1 entry assay

Cells were transfected as described in 2.7.7 and infected with ATTO488-labeled HIV-1 diluted in R10 for 2 h. Cells were washed twice with RPMI and incubated with 0.25% Trypsin for 10 min at 37°C to remove any cell-surface-bound viral particles, washed twice in R10 and processed for flow cytometry.

2.7.9 Infection of DCs with Influenza

Influenza A/PR/8/34 stock (4,000 HAU/ml) was kindly provided by Prof. John McCauley (NIMR, London) and was stored at -80°C. 10^6 DCs were resuspended in 100 µl RPMI supplemented with 2 µg Trypsin (Sigma). Influenza A/PR8/34 was added to cells and incubated for 2 h at 37°C. After 2 h cells were washed twice with RPMI and resuspended in R10 at a concentration of 10^6 cells/ml for further culture.

2.7.10 Generation of CD47 negative HEK 293T cells

HEK 293T cells were plated out in 6 well plates at $6x10^5$ cells per well the preceding day to achieve a confluency of 70%. Lentivirus expressing shRNA CD47 as well as lentivirus without a gene of interest were generated. All media was removed from cells and cells were infected with 2 ml of virus. The following day 4 ml of fresh media was added, and cells were checked daily for expression of CD47 by flow cytometry and cells were split regularly as required.

Appendix 1: List of antibodies

Table 2.4. List of antibodies used

Antibody target	Species	Clone/Product ID	Company
15-LO	Mouse	11-K/sc130360	Santa Cruz
Actin	Mouse	AC74	Sigma
AHCYL1	Mouse	225/sc-100581	Santa Cruz
Ahnak	Mouse	EM-09/ab68556	Abcam
Akt	Rabbit	9272	Cell Signaling
BLOC1S1	Rabbit	19687-1-AP	Proteintech
c-Cbl	Rabbit	C49H8/2179	Cell Signaling
Calnexin	Rabbit	2679	Cell Signaling
Cappuccino	Mouse	S-5/sc-100683	Santa Cruz
Cappuccino	Mouse	6C3/H00055330-M02	Abnova
CARHSP1	Chicken	ab14245	Abcam
CAS	Mouse	ab54674	Abcam
CD44	Mouse	BRIC236/9407P	NHS BT
CD44	Mouse	156-3C11/3570	Cell Signaling
CD47	Mouse	2D3/14-0478	eBioscience
CD47	Mouse	B6-H12/556044	BD
CD47	Mouse	B6-H12/160479	eBioscience
CD47	Mouse	MEM-122/ab9098	Abcam
CD47	Mouse	C-18/sc-7057	Santa Cruz
CD47	Mouse	S-10/sc-7059	Santa Cruz
CD47	Mouse	B6-H12/BE0019-1	BioXcell
CD47	Mouse	BRIC126/MCA911	AbD Serotec
CD47	Mouse	B6-H12.1/ab3283	Abcam
CD63	Mouse	556019	BD
CD81	Mouse	555675	BD
CD9	Mouse	P1/33/2/sc-20048	Santa Cruz
CHMP4B/C	Rabbit	ab76334	Abcam
COPE	Rabbit	E-20/sc-12104	Santa Cruz
CRMP2	Rabbit	9393	Cell Signaling
DC-SIGN	Rabbit	H-200/sc-20081	Santa Cruz
DC-SIGN	Mouse	1B10/sc-23926	Santa Cruz
EDC4/Ge-1	Rabbit	2548	Cell Signaling
EIF4GI	Rabbit	2858	Cell Signaling
G3BP	Mouse	611126	BD
GABARAP	Rabbit	PAB0730	Abnova
HIP55	Rabbit	Ab77147	Abcam
IRAK1	Rabbit	4504	Cell Signaling
La/SSB	Mouse	44/sc-136258	Santa Cruz
LAMP2	Mouse	H4B4/ab25631	Abcam
MARCKS	Mouse	JK-8/sc-100777	Santa Cruz
Mst3	Rabbit	3723	Cell Signaling
NDRG2	Rabbit	HPA002896	Sigma
Numb	Rabbit	2756	Cell Signaling
p-SH-PTP1	Mouse	14.Tyr536/sc-135780	Santa Cruz
p24 gag	Mouse	ab9071	Abcam
P42/44 MAPK	Rabbit	137F5	Cell Signaling
PAK2	Rabbit	2615	Cell Signaling
PCNP	Mouse	2707C2a/ab70733	Abcam
Phosphotyrosine	Mouse	PY20	Zymed
PPP1R7	Rabbit	ab86508	Abcam
PRAT4A	Rabbit	E-22/sc-102064	Santa Cruz
PSAP	Rabbit	ab68466	Abcam
PSMB6	Mouse	JQ-3/sc-100455	Santa Cruz

RRAGA	Rabbit	4357	Cell Signaling
RRAGA/B	Rabbit	ab91062	Abcam
RRAGC	Rabbit	3360	Cell Signaling
Sam68	Rabbit	C-20/sc-333	Santa Cruz
SHP-1	Mouse	610125	BD
SHP-1	Rabbit	C-19/sc-287	Santa Cruz
SHP-1	Rabbit	C14H6/3759	Cell Signaling
SIRPα	Mouse	ab77061	Abcam
SIRPα	Mouse	SE7C2/sc-23863	Santa Cruz
SIRPα	Mouse	17-7219	eBioscience
SIRPα	Mouse	27-136067	Santa Cruz
SLP-76	Rabbit	4958	Cell Signaling
Snapin	Rabbit	148002	Synaptic Systems
SNX1	Mouse	Ab55776	Abcam
SNX1	Mouse	611482	BD
SNX5	Rabbit	H-40/sc-50375	Santa Cruz
STIP1	Mouse	WH0010963M1	Sigma
SYAP1	Rabbit	HPA000175	Sigma
TGN46	Rabbit	ab50595	Abcam
TIA-1/TIAR	Rabbit	H-120/sc-28237	Santa Cruz
TOM1	Rabbit	HPA001749	Sigma
VAMP1/2/3	Rabbit	104102	Synaptic Systems
VCP	Mouse	ab11433	Abcam
Vinculin	Rabbit	4650	Cell Signaling
VPS4	Rabbit	H-165/sc-32922	Santa Cruz
WAVE-2	Rabbit	D2C8/3659	Cell Signaling
β -Adaptin	Rabbit	H-300/sc-10762	Santa Cruz

Appendix 2: List of buffers and reagents

Solutions

R10: RPMI (Sigma) supplemented with 10% (v/v) heat-inactivated (56°C for 20 min) FCS (Sigma), 2 mM L-glutamine, 1 U/ml penicillin and 50 μg/ml streptomycin.

D10: DMEM (Sigma) supplemented with 10% (v/v) FCS, 2 mM L-glutamine, 1 U/ml penicillin and 50 μg/ml streptomycin.

HEPES-buffered solution 2x: 0.28M NaCl, 0.05M HEPES, 1.5mM Na_2HPO_4, adjusted to pH 7.05-7.12.

MACS buffer: Phosphate-buffered saline (PBS), 2% (v/v) FCS, 0.5M EDTA.

PBA: PBS, 0.5% BSA, 0.01 g NaN3.

FACS fix: PBS, 1% (v/v) formaldehyde.

50× TAE buffer: 242 g of Tris base, 57.1 ml acetic acid, 100 ml of 0.5 M EDTA pH8.

Lysis buffer: 1% NP-40, 50 mM Tris-HCl pH 7.4, 150 mM NaCl, 1 mM EDTA, Sodiumfluoride 1:200, Sodium Orthovanadate 1 in 200, 1 Roche Complete mini per 10ml

TBS - 25 mM Tris, 150 mM NaCl, pH 7.5.

LB (Luria Bertani) medium: 10 g/l bactotryptone (BD Biosciences), 5 g/l yeast extract (Meford) and 10 g/l NaCl (Sigma) in distilled water. The solution was autoclaved at 15 psi for 20 min and cooled before use.

Ampicillin A ready made 100 mg/ml stock solution was obtained from Sigma and stored at -20°C.

Agar plates LB agar (as for LB medium but with the addition of 15 g/l bactoagar (BC Biosciences) was autoclaved at 15 psi for 20 min and cooled to below 50°C before the addition of ampicillin to a final concentration of 100 μg/ml. Agar containing the antibiotic were then poured into 9 cm petri dishes and allowed to cool. Once set, plates were stored at 4°C.

Chapter 3

Characterization of the HIV-1 signalosome in DCs

3.1 Introduction

The life cycle of HIV-1 calls for a multitude of interactions with the host cell (figure 3.1): During the entry process the virus binds to cellular receptors and recruits cellular co-factors to facilitate its entry into the host cytoplasm. Release of the viral nucleocapsid requires interaction with the host cytoskeleton machinery (Naghavi and Goff, 2007). Transfer of virus to target cells involves close relationship with the host' endo-lysosomal system (Blanchet et al., 2011). Devoid of any replication enzymes, the virus depends on the host RNA replication machinery to ensure transcription (Freed, 2001). Integration into the host genome relies upon interactions of the virus' accessory proteins with the host karyopherin system (Brass et al., 2008). To assemble its proteins and egress the host cell, the virus has developed a sophisticated way to use the host ubiquitination system (Martin-Serrano and Neil, 2011; Navare et al., 2012).

Recent technological advances in high throughput "omics" approaches such as functional genomics, transcriptomics and proteomics screens, combined with system-level analysis have greatly expanded our understanding of host-pathogen interactions (Munk et al., 2011). For HIV-1, three groups have conducted large-scale genome-wide RNAi screens that interrogated most of the human genes for effects on HIV-1 infection, within a relatively short time frame of each other (Bushman et al., 2009; Zhou et al., 2008). Zhou at al, for example, identified more than 311 host factors important for HIV-1 replication in an RNAi screen targeting 19,709 genes (Zhou et al., 2008).

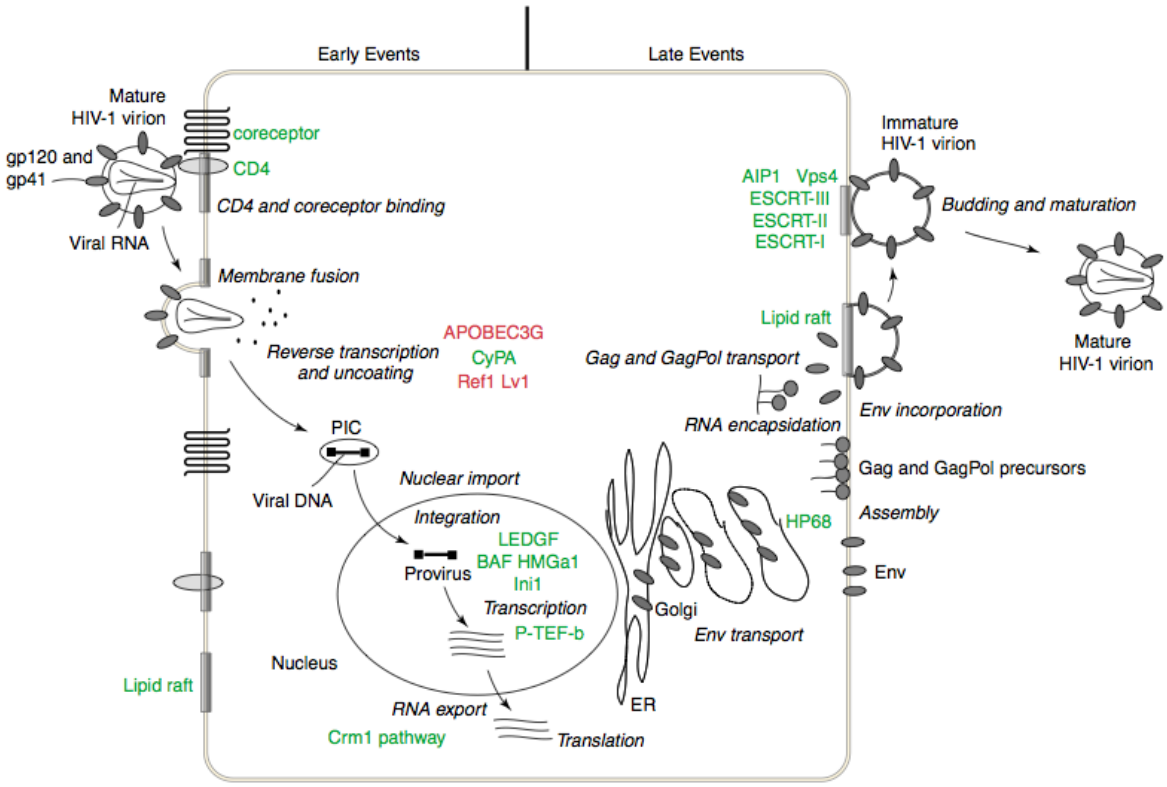

Figure 3.1. Interaction of HIV-1 with host cellular factors during viral life cycle. Positive factors that promote virus replication are indicated in green; negative factors that restrict replication are in red. The steps in the replication cycle are indicated: binding of virus to CD4 and coreceptor; membrane fusion between the lipid bilayers of the viral envelope and the host cell plasma membrane; reverse transcription and uncoating; nuclear import of the viral preintegration complex (PIC); viral DNA integration into the host cell chromosome; transcription; RNA export from the nucleus; transport of Gag, GagPol and Env precursor proteins to the plasma membrane; RNA encapsidation; virus assembly; Env incorporation; virus budding and release; and PR-mediated maturation to generate the mature virus particle. Abbreviations: AIP1, ALG2-interacting protein; APOBEC3G, apolipoprotein B mRNA-editing enzyme, catalytic polypeptide-like 3G; BAF, barrier to autointegration factor; CypA, cyclophilin A; ESCRT, endosomal sorting complex required for transport; HMGa1, high mobility group a1; Ini1, IN interactor 1; LEDGF, lens epithelium-derived growth factor; Lv1, lentivirus susceptibility 1; P-TEF-b, positive transcription factor b; Ref1, restriction factor 1; Vps4, vacuolar protein sorting protein 4. Adapted from (Freed, 2004).

Konig et al performed an extensive screen to examine the early steps of HIV-1 replication, in particular the uncoating step, and characterized 293 genes involved in HIV-1 infection (Konig et al., 2008). However, only an overlap of less than 7% between any pair of the screens could be found, demonstrating the inherent limitations of large scale screening techniques (Bushman et al., 2009). Variations due to experimental noise, timing of sampling and different filtering criteria may explain the discrepancies that

were observed within these studies (Bushman et al., 2009). Nevertheless, a meta-analysis derived from these studies and other relevant literature assembled a host-pathogen interaction network containing several molecular clusters, with the aim to develop a novel therapeutic approach targeting cellular cofactors, which may be more likely to have lower probability of spontaneous mutations than current antiretroviral drug targets (Bushman et al., 2009).

Global expression profiles are another approach to assess the changes of a host in response to specific viral pathogens and again a number of groups have conducted several microarray studies of the host gene signature in response to *in vitro* infection with different HIV-1 and SIV strains as well as in cells and tissues of HIV-1 and SIV-infected subjects taken *ex vivo*. These studies have revealed gene signatures linked to disease progression involving cellular pathways such as apoptosis, metabolism, T-cell signaling and cell-cycle dysregulation (Harman et al., 2009; Izmailova et al., 2003; Mehla and Ayyavoo, 2012; Smith et al., 2010). Despite diversities in experimental protocols, such as viral inoculum, time course of infection as well as target cell populations studied, it is apparent from these studies is that HIV-1 and SIV induce profound changes in gene expression impacting most cellular functions. In particular, a study of MDDCs infected with different strains of HIV-1 showed enhanced expression of genes implicated in signal transduction, cell proliferation and cell cycle, transcription and immune response related-genes at different times post *in vitro* infection (Solis et al., 2006).

To date, it is still unclear how HIV-1 is sensed by innate immune cells, precisely which receptors are involved, if and how they cross talk and how HIV-1 succeeds in manipulating this sensing to its own advantage (discussed in more detail in the introduction). A parallel and complimentary approach to these studies of genetic perturbations and genetic screens to dissect the molecular basis of innate sensing is to look for changes to the cellular proteome upon viral infection. They may be even more informative of the intricate signaling networks that ensue receptor triggering than genetic studies. Given the complexity of the system it may be difficult to clearly define the upstream signaling events that induce a given gene expression profile. Propagation of signals typically lead to protein changes on three different levels: first, protein post-translational modifications (PTMs), that are diverse and include phosphorylation, ubiquitination, glycosylation, methylation and SUMOylation, among others; second,

protein-protein interactions, often due to PTMs; third, alterations in protein expression (Choudhary and Mann, 2010; Mann and Jensen, 2003; Yates et al., 2009). These must be regulated tightly in a both timely and spatially coordinated manner to ensure a tailored immune response while preventing aberrant immune activation.

Transient differential phosphorylation of molecules is one of the most studied PTMs and has provided invaluable insight into cellular signaling pathways and host pathogen interactions (Dengjel et al., 2007; Mumby and Brekken, 2005). It involves transient phosphorylation or dephosphorylation at a Serine, Threonine or Tyrosine residue (in descending order of frequency) resulting in changes of activity or localization of the protein and translating into alteration of the signaling cascade. These may ultimately lead to changes in the expression of specific genes (Olsen et al., 2006).

A comprehensive, unbiased analysis of HIV-1-induced phosphorylation in any cells, and primary innate cells in particular, is missing. In order to understand the signaling cascade initiated by the interaction between the HIV-1 envelope and DC-SIGN as an initial approach to decider the HIV-1 signaling cascade, our group performed a proteomic screen of tyrosine-phosphorylated proteins following DC-SIGN activation of MDDCs (Hodges et al., 2007). This study demonstrated stimulation of the Rho guanine nucleotide exchange factor Leukemia associated Rho GEF (LARG) via the interaction of HIV-1 with DC-SIGN. This interaction was required for successful HIV-1 infection of DCs and affected the efficiency of infectious synapse formation between DCs and T cells, hence corroborating the role of DC-SIGN in viral propagation. Further work complemented the DC-SIGN signaling cascade showing that HIV-1 (and *M. tuberculosis*) induce the recruitment of a signaling complex containing the scaffold proteins LSP1, KSR1 and CNK to activate the kinase Raf-1 leading to phosphorylation of NF-kB and increased transcription of proinflammatory genes (Gringhuis et al., 2009).

The majority of proteomic studies of HIV-1 have employed affinity tagging and purification mass spectrometry to specifically determine the interaction of specific viral proteins complexed with host proteins (Gautier et al., 2009; Jager et al., 2012; Mukerji et al., 2012; Zhang et al., 2010). The most recent and compelling of these studies determined the HIV-1-protein-human protein interaction for all 18 HIV-1 proteins, polyproteins, the corresponding processed products and accessory factors, in two different cell lines. It identified 435 individual host proteins targeted by the virus (Jager et al., 2012). While these findings provide invaluable insight into the manipulation of

the host cell machinery by the virus, their findings are somewhat limited by the fact that single proteins do not work in isolation. They certainly do not allow direct conclusions of the unique patterns of intracellular signaling events that follow binding of HIV-1 to PRRs.

Mass spectrometry based proteomics is a powerful technique that has greatly evolved over the past years, allowing high-throughput analysis of complex samples for accurate quantification of protein expression levels and post-translational modifications (Choudhary and Mann, 2010). One of the great advantages of mass spectrometry based proteomics is that it is unbiased allowing a "hypothesis free" approach to interesting questions. The technique essentially involves obtaining proteins from cellular lysates, followed by a number of concentration and cleaning steps to enrich low abundant proteins and remove detergents and salts, respectively. Subsequently, proteins are enzymatically digested providing peptide fragments of different sizes, which are separated by chromatographic and/or electrophoretic techniques among multiple dimensions, and subsequently loaded into the mass spectrometer to undergo vaporization followed by ionization. Charged particles are separated according to their mass-to-charge *(M/Z)* ratio by an electromagnetic field. Finally, the ions are detected creating a peptide M/Z spectrum that can be processed in peptide spectrum databases, thus allowing identification of the peptide and imputation of the corresponding proteins. Mass spectrometry platforms are continuously evolving (reviewed in (Yates et al., 2009). In this study two instruments were used both employing electrospray ionization (ESI), whereby liquid phase samples are dispersed into an electrically charged spray at the inlet of the machine (Schaeffer-Reiss, 2008; Wilm, 2011). The ESI Ion-Trap was used for the phosphoproteomic analysis of HIV-1-infected DCs, and allows high-throughput analysis with high sensitivity and reasonable resolution of the M/Z (in contrast to MALDI Q-TOF machines). A further proteomic study of HIV-1 virions was carried out with a different instrument, the LTQ Orbitrap Velos, which has the added advantage of high resolution accurate mass detection and increased sensitivity (Olsen et al., 2009).

As outlined in the introduction the interaction of HIV-1 with DCs in the mucosa may be crucial to disease pathogenesis by allowing the virus to remain undetected during the earliest stages of infection, thereby promoting viral dissemination and latency before an effective immune response can take effect (Haase, 2010). Accumulating evidence

suggests that HIV-1 actively avoids recognition by PRRs or actively subverts the classical pathways to prevent activation of a proinflammatory and antiviral immune response (Manel and Littman, 2011; Yan and Lieberman, 2011). Known strategies to achieve this include the inhibition of cytosolic DNA - and in effect PAMPs - accumulation to avoid recognition and interferon induction (Yan et al., 2010) as well as the hijacking of the DC-SIGN-TLR8 crosstalk to support HIV-1 transcription (Gringhuis et al., 2010). In this chapter a novel phosphoproteomic technique is used to perform an unbiased analysis of the full spectrum of phosphorylation following entry of HIV-1 into DCs. It is envisaged that characterization of innate signaling pathways induced by the virus upon early infection will unravel some more of the immune evasive mechanisms that the virus uses to remain undetected and prevent an interferon response. Further, it may also aid in identifying novel host antiviral proteins.

3.2 Aims

The aims of this chapter are:

- to detect proteins differentially phosphorylated by HIV-1 in DCs using mass spectrometry
- to validate proteins identified by LC-MS/MS analysis
- to complement the characterization of the HIV-1 signalosome by identifying host molecules incorporated in HIV-1 virions
- to investigate changes in gene expression profile of DCs upon HIV-1 infection

3.3 Results

3.3.1 Set up experiments for characterization of the HIV-1 phosphoproteome

Previous work in our group characterizing the DC-SIGN signaling complex had used traditional phosphoproteomic techniques based on immunoprecipitation (IP) of tyrosine-phosphorylated proteins followed by LC-MS/MS analysis (Hodges et al., 2007). Although this technique yielded an interesting dataset and identified novel signaling molecules, it is cumbersome and precludes a comprehensive, global picture of the whole phosphoproteome due to purification of tyrosine-phosphorylated proteins only.

While this thesis was in progress, our group (John Baker) successfully developed a protocol that allowed efficient global enrichment of phosphorylated proteins and identification of these proteins with a high sensitivity in primary MDDCs. The technique involves the steps outlined in figure 3.2a. DCs were activated with LPS in a set-up experiment: DCs were harvested with cold media, activated with LPS or mock for 15 min at 37°C, the reaction was quenched with cold buffer followed by two washing steps. Subsequently, cells were lysed with lysis buffer containing a mild CHAPS detergent in the presence of phosphatase and protease inhibitors, cleared cell lysates were quantified and adjusted to equal protein concentrations. A maximum of 2.5 mg of protein were applied to resin-based affinity chromatography phosphoprotein enrichment columns followed by washing steps and elution of phosphoproteins with a PBS-containing elution buffer. Finally, eluates were concentrated and processed for downstream experiments.

Figure 3.2b demonstrates the result of this set up experiment. A western blot was performed for p42/44 MAPK, a known signaling molecule downstream of LPS activation. Successful phosphoenrichment and activation is demonstrated by the increased density of p42/44 MAPK in the phosphofractions following LPS treatment, both visualized on immunoblots using non-phospho-specific and phospho-specific antibodies.

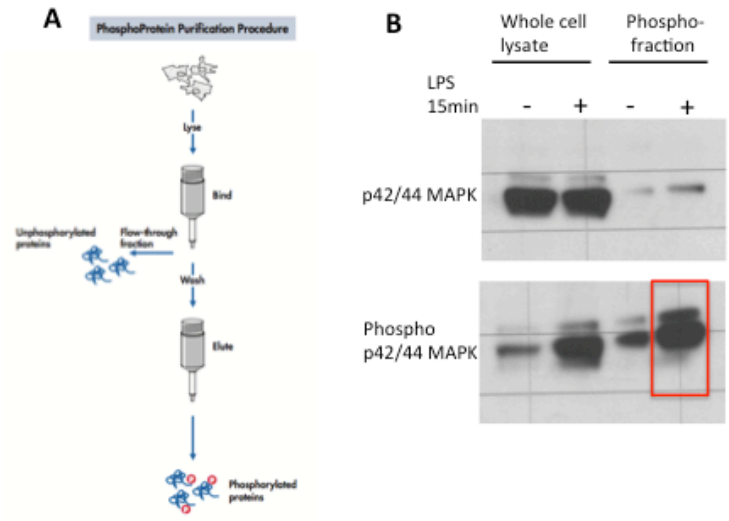

Figure 3.2. The phosphoprotein purification procedure allows efficient enrichment of phosphorylated proteins. A. Principle of the procedure. B. Whole cell lysates of MDDCs activated with LPS are enriched for phosphoproteins by phosphoaffinity columns and further concentrated. Western Blot analysis shows up-regulation of phosphorylated p42/44 MAPK on whole cell lysate following LPS activation that is markedly enriched for in the phosphorylated fractions.

3.3.2 HIV-1 induces changes in the phosphoproteome of DCs

I next used the same protocol to look at changes in protein phosphorylation following infection of MDDCs with HIV-1 NL4-3 BaL for just 10 minutes. This early timepoint allowed direct comparison to the DC-SIGN proteomics data we had already established following activation of DCs with the signaling antibody H200 for 10 min (Hodges et al., 2007). Additionally, this would primarily define changes in phosphorylation induced upon the early steps of HIV-1 encounter with DCs.

Therefore, immature MDDCs (day 5 post differentiation) were pelleted and resuspended with 500μl NL4-3 BaL (corresponding to an MOI of 1) or mock for 10 min and subjected to phosphoprotein enrichment as described above. Importantly, as a negative mock control I used supernatant collected from HEK293T cells that had been treated with an empty plasmid in a similar fashion as pWolf NL4-3 BaL transfected cells to control for any unspecific effects across conditions. Following 10 min of HIV-1 or mock infection clear changes in tyrosine-phosphorylated proteins are visualized following an immunoblot for phosphotyrosines (figure 3.3a). These changes are dramatically enhanced by phosphoenrichment, demonstrated by increased density of

phosphoenriched samples compared to whole cell lysates (WCL). Equal loading of whole cell lysates on to the qiagen phosphocolumns is demonstrated by comparable densities of beta actin in diluted whole cell lysates. Successful enrichment for phosphoproteins can be seen by both increases in densities of phosphotyrosine and reduction of beta-actin within phosphofractions. This was reproducible among multiple donors tested. It is noteworthy, that some changes could also be seen in immunoblots for phospho-serines and threonines of HIV-1-infected phosphoenriched samples, however the immunoblots had too much background and were of too poor quality to be included here.

In order to investigate if this experimental approach would allow me to dissect the HIV-1 signaling complex, I conducted a similar experiment, whereby I activated DCs with ssRNA40, a U-rich single-stranded RNA derived from the HIV-1 long terminal repeat and a known TLR8 agonist (Heil et al., 2004). HIV-1 and ssRNA40 triggered distinct patterns of tyrosine phosphorylation with some changes common to both ligands (figure 3.3b), indicating that assessment of the signaling cascade in response to HIV-1 may inform how the virus is sensed by different PRRs in DCs.

Altogether, the direct visualization of fairly dramatic changes in tyrosine-phosphorylated proteins following only 10 min of HIV-1 infection was encouraging for the ensuing work on the HIV-1 phosphoproteome.

3.3.3 Off gel Fractionation reduces the complexity of the HIV-1 phosphoproteome

One of the problems in using shot gun proteomics of cellular lysates is the complexity of the sample, which precludes reliable identification of signaling molecules that may have an important functional significance, but are typically far less abundant than major cellular proteins, such as those belonging to the cytoskeleton. In-solution isoelectric focusing (IEF) is a technique that is being increasingly used as an adjunct to preparation of complex samples prior to mass spectrometry (reviewed in (Fournier et al., 2007)). It is based on the same principle as 2D gel electrophoresis, whereby proteins are separated

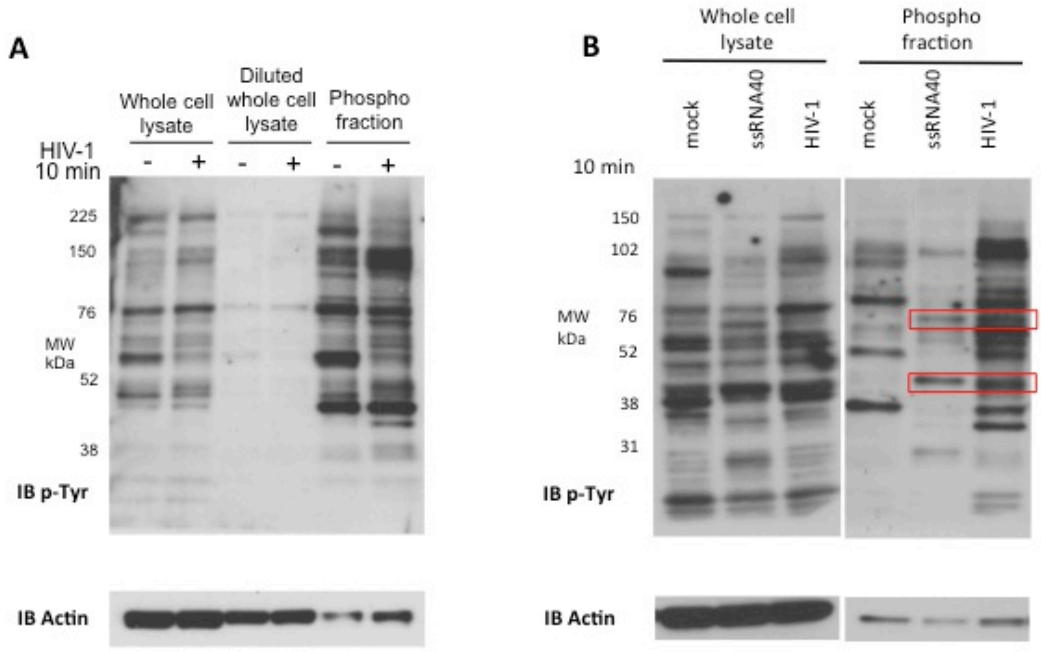

Figure 3.3. HIV-1 Induces Visible Changes of the Phosphoproteome within 10 minutes of Infection. A. MDDCs were infected with HIV-1 or mock for 10 minutes at 37°C. Cells were washed twice with cold HBS, lysed, and phosphoproteins enriched by phosphoprotein enrichment columns. Whole cell lysate, diluted whole cell lysate (0.1mg/ml) and phospho-enrichment column eluates were blotted for phosphotyrosine and beta actin. B. Comparison of the phosphoproteome of MDDCs activated by HIV-1 and ssRNA40 reveals interesting common changes (red boxes). MDDCs were stimulated with HIV-1 BaL, 10µg/ml ssRNA40 or mock for 10 minutes, lysed and enriched for phosphoproteins, which were detected by Western blot for P-Tyr.

according to their isoelectric point prior to separation by PAGE. In brief, phosphoprotein fractions are quantified after elution and concentration steps by Bradford assay and equalized across conditions. The latter step is crucial for a reliable interpretation of the results obtained, as classical loading controls such as actin and GAPDH will not be informative post fractionation of samples. Proteins are then mixed with ampholytes and loaded into sealed wells that overlie an immobilized pH-gradient gel strip. In this instance a 12-well low resolution strip over a pH range of 3-10 was used, as it had already yielded good results in the investigation of the NOD2 phosphoproteome (John Baker). An electric current is applied causing migration of proteins across the gel strip to the point where the pH of the strip matches their isoelectric point. Subsequently, samples (12 fractions per condition) are collected and cleared of salts with desalting columns. A silver stain of fractions obtained from such an experiment is shown in figure 3.4, where the efficacy of fractionation and the reduction

in complexity of the proteome are clearly observed. Changes in phosphorylation/levels of proteins between HIV-1 and mock treated samples that may have been too subtle to be detected by an immunoblot of phospho-eluates are clearly visible. This was encouraging indicating that the method may increase sensitivity for detection of previously unrecognized signaling molecules.

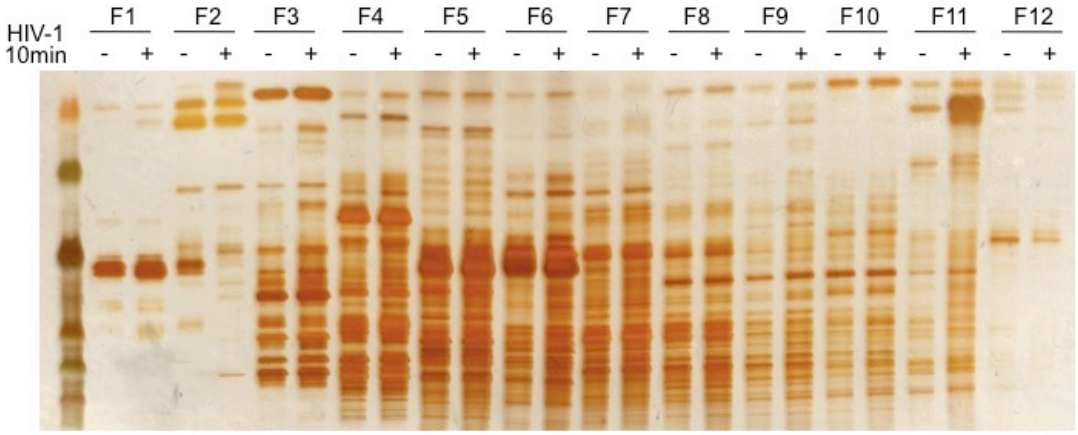

Figure 3.4. Offgel fractionation reduces the complexity of the phosphoproteome. Phosphoprotein-enriched samples of MDDCs infected with HIV-1 or mock for 10 min were separated into 12 fractions by isoelectric focusing, desalted and subjected to electrophoresis. Silverstain of fractions is shown.

3.3.4 Analysis of the HIV-1 phosphoproteome by mass spectrometry

Only 10% of the protein mass in a given cell is phosphorylated at a given time and about 1mg of protein are required for a successful LC-MS/MS run (on the machines that were available at the time of experimentation). Given that the cleaning and precipitation steps are associated with a certain degree of sample loss and each buffy coat yields approximately 30-50 mill MDDCs, a number of replicates were required to ensure sufficient amount of phosphoprotein for mass spectrometry. Therefore, I proceeded to collect nine biological replicates of DCs infected with NL4-3 BaL or mock for 10 min. Pooling multiple donors may also aid in detecting genuine signaling molecules that may otherwise have been too scarce to detect in a few donors. For each buffy coat, detectable

changes in the phosphoproteome were confirmed on PTyr immunoblots. Additionally, to ensure that these changes are associated with productive HIV-1 infection of DCs in each replicate, a small fraction of cells (1 mill DCs) were not included in the phosphoenrichment procedure, but infected with HIV-1 for 2 h and then kept in culture for collection of supernatants to measure HIV-1 infection p.i. (figure 3.6)

Preparation of the samples for LC-MS/MS analysis, involved pooling of phospho-eluate fractions of nine donors, concentration and quantification (figure 3.5). Equalized amounts of phosphoproteins were separated by IEF, fractions were cleaned by chloroform-methanol precipitation and then prepared for trypsin digestion and purification prior to loading on to the mass spectrometer according to standardized protocols.

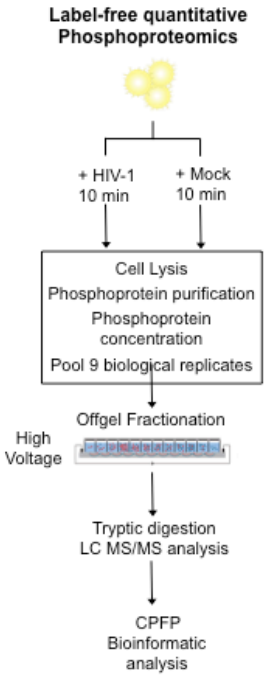

Figure 3.5. Multipronged approach to identify the early HIV-1 signalosome in dendritic cells. Workflow for first part of the screen is shown. MDDCs were infected with HIV-1 or mock for 10 min, lysed and enriched for phosphoproteins. Nine biological replicates were collected, pooled and quantified by Bradford dye assay. Equalized amounts of phosphoenriched lysates were separated by IEF and prepared for LC-MS/MS analysis before bioinformatics analysis by the CPFP proteomics pipeline.

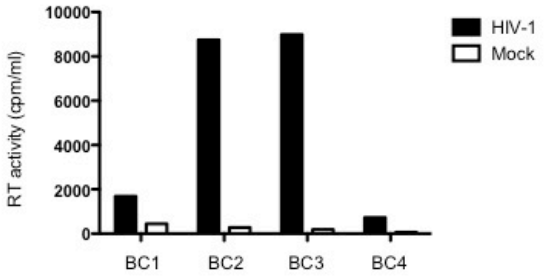

Figure 3.6. Confirmation of productive HIV-1 infection of DCs used for phosphoproteomics study. DCs infected for 2 h with HIV-1 BaL were kept in culture and supernatant taken every 2 days for measurement of HIV-1 reverse transcriptase activity in supernatant. The assay quantifies newly produced viral particles based on the ability of HIV-1 RT to reverse transcribe an artificial ssRNA primer leading to incorporation and hence quantification of H^3-labelled thymidine. Values obtained for 4 out of 9 donors on day 8 p.i. are shown.

All raw data obtained by LC-MS/MS was processed by the central proteomics facilities pipeline (CPFP) (Trudgian et al., 2010), which combines three different databases using Mascot (Matrix Science, London, UK), OMSSA (Geer et al., 2004) and X!TANDEM (Craig and Beavis, 2004) (figure 3.7). This analytic approach gives a higher number of peptide spectrum matches and unique peptide identifications, thus increasing both the number of protein identifications and the confidence in the data obtained. In this platform peptide identifications from each search engine are validated with PeptideProphet (Keller et al., 2005; Nesvizhskii et al., 2003), and further combined using iProphet. Finally, protein identifications are inferred using ProteinProphet (Nesvizhskii et al., 2003). To increase the confidence in the data obtained results were set at the 1% false discovery rate (Elias and Gygi, 2007). Since CPFP combines peptide identifications from multiple search engines it is not possible to use reported ion matches or intensities, such as Mascot Scores, as the different scoring schemes used by the search engines will introduce undesirable variability (Trudgian et al., 2011).

For illustration of the data analysis within the iProphet interface, the identification of LRRFIP1 as a protein identified in HIV-1 infected DCs is shown (figure 3.8). LRRFIP1 is a cytosolic nucleic acid sensor important in the antiviral type I interferon response (Yang et al., 2010). Peptides identified with highest confidence are assigned a weight (wt) of 1, those peptides unique to LRRFIP1 are marked by a star. LRRFIP1 is therefore

identified with a very high confidence, whereas LRRFIP2 is not. Importantly, at this high level of stringency threshold, even identification of a single peptide is considered as solid evidence of the presence of the protein in the sample. Preliminary analysis using CPFP identified a total of 64 and 157 phosphoproteins in mock- and HIV-1-infected DCs, respectively (Appendix Tables A1 and A2). For brevity purposes, the bulk of proteins identified by LC-MS/MS to be differentially phosphorylated will be referred to as the HIV-1 phosphoproteome or signalosome.

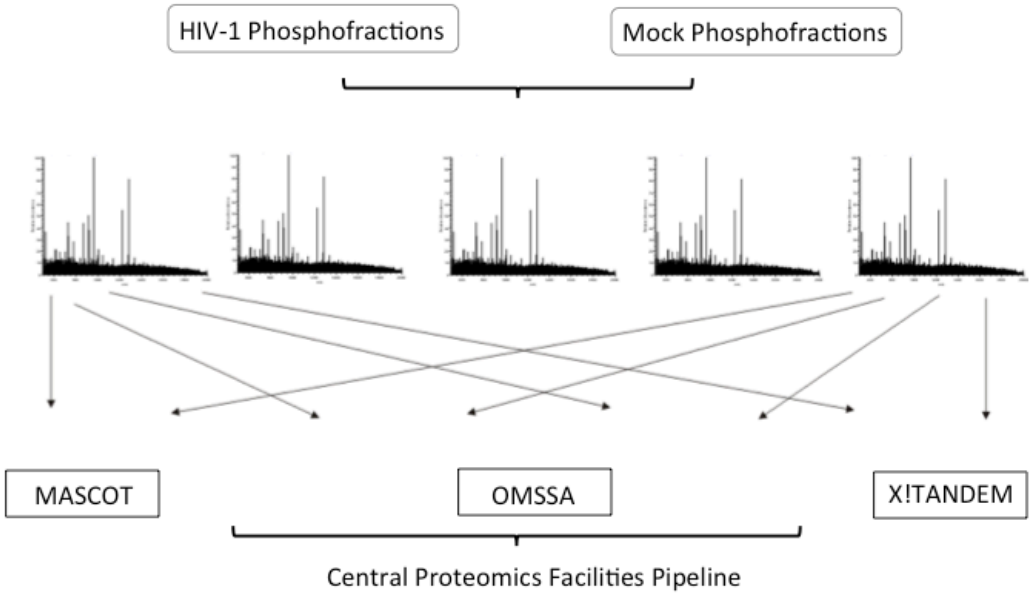

Figure 3.7. Identification of phosphoproteins with CPFP is based on three different search engines. CPFP is a proteomics analysis data platform that provides a web interface to a data analysis pipeline based on the tools from the trans-proteomics pipeline. Protein identification is based on Proteinprophet that uses data obtained from peptides that are identified via Peptideprophet.

Figure 3.8. Identification of LRRFIP1 to illustrate how phosphoproteins were identified within the iprophet interface. Peptides identified as unique within the sample are assigned a weight value of 1 and marked by a star.

3.3.5 Spectral index quantification aids in LC-MS/MS analysis

The value of proteomic data is significantly increased by the added information obtained from quantification of the proteins identified across conditions. Isotopic labeling protocols such as SILAC, that are usually employed in high-throughput proteomic screens, are not amenable to non-dividing primary cells such as DCs. Label-free quantification can be carried out with a variety of methods, one of them is based on spectral counting (SC) or normalized spectral index quantitation (SINQ). SC uses the number of spectra of a protein identified by a search engine to enumerate the relative abundance of the protein (Trudgian et al., 2011). Furthermore, it includes normalization and correction procedures that employ a normalized spectral index approach, which sums the intensities of identified peptide fragment ions to capture a measure of peptide abundance as well as presence/absence (Griffin et al., 2010). For instance, raw values for each protein are divided by the protein length to correct for the propensity of longer proteins to produce a greater number of peptides, and hence higher spectral index values, than shorter proteins (Trudgian et al., 2011). In addition, to correct for differences in protein loading between data sets, the calculated raw spectral index is normalized to all the sum of the spectral index across all proteins in the samples (Trudgian et al., 2011). A recent comparison of this approach to other label-free quantification methods by our collaborators showed the feasibility and good success rate of SC, although it is also less accurate than other more labour intensive quantification platforms (Trudgian et al., 2011).

Peptides identified in my mass spectrometry data in HIV-1 and mock-infected DCs were analyzed by SINQ (figure 3.9). This allowed a more accurate reflection of changes in phosphorylation, and showed that 172 proteins were exclusively phosphorylated and 134 proteins were differentially phosphorylated by HIV-1, respectively. More specifically 124 phosphoproteins were exclusively found within the HIV-1-infected fractions indicating that they were phosphorylated by HIV-1 (table 3.1), conversely 48 phosphoproteins were identified within the mock-infected fractions, indicating that they were likely to be dephosphorylated by HIV-1 (table 3.2). Based on SINQ analysis 68 proteins were upregulated by more than 1.25 fold, i.e. expressed at higher phosphorylation levels within the HIV-1-infected fraction (table 3.3). In comparison 66 proteins were downregulated by more than 0.75 fold within the HIV-1-infected fractions, indicating that they were differentially dephosphorylated by the virus (3.4).

It was now possible to correlate changes in phosphorylation of given proteins to known functions associated with these changes. For instance, p21-activated kinase 2 (PAK2) was found to be exclusively phosphorylated by HIV-1 within 10 min. PAK2 belongs to a family of serine/threonine kinases that serve as targets for the small GTP binding proteins, Cdc42 and RAC1 and are known to be phosphorylated by HIV-1 nef hereby enhancing HIV-1 replication (Van den Broeke et al., 2010). Conversely, eukaryotic translation initiation factor 4 gamma 1 (EIF4G1) was found to be dephosphorylated by HIV-1. EIF4G1 is involved in regulation of protein synthesis by facilitating the recruitment of mRNA to the ribosome and shown to be cleaved by the viral protease, leading to inhibition of cap- and poly(A)-dependent cellular protein synthesis while allowing viral genomic mRNA synthesis to proceed unhindered (Castello et al., 2009). EIF4G1 is phosphorylated by protein kinase C, a kinase with known interaction with HIV nef as well as member of the HIV-1 DCIR signaling cascade (Dobrikov et al., 2011; Lambert et al., 2011).

Collectively, characterization of HIV-1-induced changes in protein phosphorylation within 10 min of infection reveals dynamic changes in signaling of host molecules.

Tables 3.1 and 3.2. List of phosphoproteins identified by LC-MS/MS and spectral index quantification to be exclusively phosphorylated or dephosphorylated by HIV-1. Spectral and peptide numbers indicate the normal spectral index method, which basically uses the summed intensities of spectral peaks of identified peptide fragments ions to evaluate the abundance or presence/absence of the peptide.

Table 3.1. Proteins exclusively phosphorylated in HIV-1-infected fractions

Protein ID	Gene Symbol	Protein Name	Peptides Used	Spectra Used
IPI00382470	HSP90AA1	Isoform 1 of Heat shock protein HSP 90-alpha	30	606
IPI00010779	TPM4	Isoform 1 of Tropomyosin alpha-4	27	503
IPI00419258	HMGB1	HMGB1 High mobility group protein B1	15	149
IPI00008530	RPLP0	60S acidic ribosomal protein P0	9	35
IPI00021405	LMNA	LMNA Progerin	9	11
IPI00013894	STIP1	STIP1 protein	9	9
IPI00335168	MYL6B	Isoform Non-muscle of Myosin light polypeptide 6	8	86
IPI00470498	SERBP1	Isoform 3 of Plasminogen activator inhibitor 1 RNA-binding protein	7	20
IPI00003925	PDHB	PDHB 35 kDa protein	7	8
IPI00033494	MYL12B	Myosin regulatory light chain	5	13
IPI00059242	SYAP1	Synapse-associated protein 1	5	8
IPI00479722	PSME1	Proteasome activator complex subunit 1 isoform 2	5	7
IPI00215884	SFRS1	Isoform ASF-3 of Splicing factor, arginine/serine-rich 1	4	6
IPI00182938	AHCYL1	Adenosylhomocysteinase	4	5
IPI00291016	NDUFV3	Isoform 2 of NADH dehydrogenase [ubiquinone] flavoprotein 3, mitochondrial	4	5
IPI00106642	SDF2L1	Dihydropyrimidinase-like 2	4	5
IPI00218830	NMT1	Isoform Long of Glycylpeptide N-tetradecanoyltransferase 1	4	4
IPI00419979	PAK2	Serine/threonine-protein kinase PAK 2	4	4
IPI00015856	DNPEP	DNPEP 52 kDa protein	4	2
IPI00179330	UBB	Ubiquitin	3	9
IPI00300585	RRAGC	Ras-related GTP-binding protein C	3	6
IPI00012442	G3BP1	Ras GTPase-activating protein-binding protein 1	3	6
IPI00024971	OSBP	Isoform 1 of Oxysterol-binding protein 1	3	6
IPI00063234	PRKAR2A	cAMP-dependent protein kinase type II-alpha regulatory subunit	3	5
IPI00465028	TPI1	Isoform 1 of Triosephosphate isomerase	3	4
IPI00453476	PGAM1	Phosphoglycerate mutase 1	3	3
IPI00184670	AMPD2	Isoform Ex1B-2-3 of AMP deaminase 2	3	3
IPI00034319	CUTA	Isoform B of Protein CutA	3	2
IPI00465132	COPE	Coatomer subunit epsilon	2	12
IPI00101095	C20orf27	C20orf27 hypothetical protein LOC54976	2	11
IPI00009057	G3BP2	Isoform B of Ras GTPase-activating protein-binding protein 2	2	9
IPI00008527	RPLP1	60S acidic ribosomal protein P1	2	9
IPI00008994	NDRG2	Isoform 5 of Protein NDRG2	2	8
IPI00299033	KPNA3	Importin subunit alpha-3	2	7
IPI00023704	LPP	Lipoma-preferred partner	2	5
IPI00298558	PDCD10	Programmed cell death protein 10	2	4
IPI00643152	HSPA1L	HSPA1L 64 kDa protein Tax	2	4
IPI00021766	RTN4	Isoform 5 of Reticulon-4	2	4
IPI00105620	RRAGB	Isoform 2 of Ras-related GTP-binding protein B	2	4
IPI00384051	PSME2	Putative uncharacterized protein PSME2	2	4
IPI00473047	PRKAG1	5'-AMP-activated protein kinase subunit gamma-1 isoform 2	2	3
IPI00100160	CAND1	Isoform 2 of Cullin-associated NEDD8-dissociated protein 1	2	3
IPI00012535	DNAJA1	DnaJ homolog subfamily A member 1	2	3
IPI00002212	STK24	FLJ61383, highly similar to Serine/threonine-protein kinase 24	2	2
IPI00456359	ATXN2L	Ataxin-2-like protein isoform E	2	2
IPI00019927	PSMD7	26S proteasome non-ATPase regulatory subunit 7	2	2
IPI00215965	HNRNPA1	Isoform 2 of Heterogeneous nuclear ribonucleoprotein A1	2	2
IPI00867509	CORO1C	Coronin-1C	2	2
IPI00216917	C22orf9	Chromosome 22 open reading frame 9	2	2
IPI00472164	WASF2	Wiskott-Aldrich syndrome protein family member 2	2	2
IPI00221222	SUB1	Activated RNA polymerase II transcriptional coactivator p15	2	2
IPI00216393	CLTA	Isoform Non-brain of Clathrin light chain A	2	2
IPI00012578	KPNA4	Importin subunit alpha-4	2	2
IPI00012837	KIF5B	Kinesin-1 heavy chain	2	1
IPI00101987	C19orf62	Isoform 3 of BRCA1-A complex subunit MERIT40	2	1
IPI00027269	CBL	E3 ubiquitin-protein ligase CBL	2	1
IPI00031423	KRT33B	KRT33B 46 kDa protein	2	0
IPI00177716	HMGA1	HMGA1 protein	1	18
IPI00555621	PAK2	p21-activated kinase 2 variant (Fragment)	1	18
IPI00008219	RAD23A	UV excision repair protein RAD23 homolog A	1	5
IPI00011937	PRDX4	Putative uncharacterized protein PRDX4	1	4
IPI00289758	CAPN2	cDNA FLJ58224, highly similar to Calpain-2 catalytic subunit	1	4
IPI00027107	TUFM	Tu translation elongation factor, mitochondrial precursor	1	4
IPI00007426	ARL6IP5	cDNA FLJ52128, highly similar to PRA1 family protein 3	1	4
IPI00027253	GABARAP	Gamma-aminobutyric acid receptor-associated protein	1	3

Protein ID	Gene Symbol	Protein Name	Peptides Used	Spectra Used
IPI00022145	NUCKS1	Isoform 2 of Nuclear ubiquitous casein and cyclin-dependent kinases substrate	1	3
IPI00059764	ZNF428	Isoform 1 of Zinc finger protein 428	1	3
IPI00219678	EIF2S1	Eukaryotic translation initiation factor 2 subunit 1	1	3
IPI00304409	CARHSP1	Calcium-regulated heat stable protein 1	1	3
IPI00000675	CNPY3	Isoform 1 of Protein canopy homolog 3	1	2
IPI00019901	ADD1	Alpha-adducin isoform d	1	2
IPI00025974	CHMP4B	Charged multivesicular body protein 4b	1	2
IPI00000634	CCDC6	Coiled-coil domain-containing protein 6	1	2
IPI00010860	PSMD9	Isoform p27-L of 26S proteasome non- ATPase regulatory subunit 9	1	2
IPI00000792	CRYZ	crystallin, zeta (quinone reductase)	1	2
IPI00302592	FLNA	Filamin A, alpha	1	2
IPI00183526	NCL	NCL 32 kDa protein	1	2
IPI00005064	GPSM3	G-protein- signaling modulator 3	1	2
IPI00465439	ALDOA	Fructose-bisphosphate aldolase A	1	2
IPI00025084	CAPNS1	Calpain small subunit 1	1	2
IPI00018229	PLDN	Isoform1 of Pallidin	1	2
IPI00008575	KHDRBS1	cDNA FLJ54590, highly similar to KH domain-containing, RNA-binding, signaltransduction-associated protein 1	1	2
IPI00027272	BRCA1	BRCA1 25 kDa protein	1	2
IPI00431127	CCNK	Isoform 3 of Cyclin K	1	2
IPI00179700	HMGA1	Putative uncharacterized protein HMGA1	1	2
IPI00012503	PSAP	Isoform Sap-mu-6 of Proactivator polypeptide	1	2
IPI00003419	C11orf58	C11orf58 Small acidic protein	1	2
IPI00008289	BRCC3	BRCA1/BRCA2-containing complex, subunit 3	1	2
IPI00296485	MAP1S	Microtubule-associated protein 1S	1	2
IPI00302850	LOC100129492	Similar to small nuclear ribonucleoprotein D1 polypeptide 16kDa	1	2
IPI00007765	HSPA9	cDNA FLJ51903, highly similar to Stress-70 protein, mitochondrial	1	1
IPI00012833	PPP4C	Serine/threonine-protein phosphatase 4 catalytic subunit	1	1
IPI00396435	DHX15	Putative pre-mRNA-splicing factor ATP-dependent RNA helicase	1	1
IPI00003084	DRAP1	DR1-associated co-repressor	1	1
IPI00025807	SP3	Transcription factor Sp3 isoform 3	1	1
IPI00375380	PSMD13	Isoform 2 of 26S proteasome non- ATPase regulatory subunit 13	1	1
IPI00024740	YAF2	YY1 associated factor 2	1	1
IPI00295542	NUCB1	cDNA FLJ52898, highly similar to Nucleobindin-1	1	1
IPI00169383	PGK1	Phosphoglycerate kinase	1	1
IPI00216699	FERMT3	Isoform 1 of Fermitin family homolog 3	1	1
IPI00011107	IDH2	Isocitrate dehydrogenase	1	1
IPI00028059	NUMB	Isoform 3 of Protein numb homolog	1	1
IPI00023191	TOM1	cDNA FLJ54710, highly similar to Target of Myb protein 1	1	1
IPI00639863	MTM1	Myotubularin	1	1
IPI00784154	HSPD1	60 kDa heat shock protein, mitochondrial	1	1
IPI00291412	PPM1F	Protein phosphatase 1F	1	1
IPI00003527	SLC9A3R1	Na(+)/H (+) exchange regulatory cofactor NHE-RF1	1	1
IPI00301034	NADK	NAD kinase	1	1
IPI00020602	CSNK2A2	Casein kinase II subunit alpha	1	1
IPI00152695	WDR82	WD repeat-containing protein 82	1	1
IPI00020002	CNO	Protein cappuccino homolog	1	1
IPI00288941	NCOA5	Nuclear receptor coactivator 5	1	1
IPI00550821	CPSF7	Isoform 1 of Cleavage and polyadenylation specificity factor subunit 7	1	1
IPI00059292	MAGOHB	Protein mago nashi homolog 2	1	1
IPI00291175	VCL	cDNA FLJ53006, highly similar to Vinculin	1	1
IPI00171176	PANK2	Isoform 4 of Pantothenate kinase 2, mitochondrial	1	1
IPI00304692	RBMX	cDNA FLJ34201 fis, clone FCBBF3019714, highly similar to heterogenous nuclear ribonucleoprotein G	1	1
IPI00289601	HDAC2	Isoform 1 of Histone deacetylase 2	1	1
IPI00017964	SNRPD3	Small nuclear ribonucleoprotein Sm	1	1
IPI00021088	KCNAB1	cDNA FLJ59247, highly similar to Voltage-gated potassium channel subunit beta-1	1	1
IPI00018465	CCT7	T-complex protein 1 subunit eta isoform c	1	1
IPI00293857	ARRB1	Isoform 1A of Beta-arrestin-1	1	1
IPI00018398	PSMC3	26S protease regulatory subunit 6A	1	1
IPI00219483	SNRNP70	Isoform 1 of U1 small nuclear ribonucleoprotein 70 kDa	1	1

Table 3.2. Proteins exclusively phosphorylated in mock-infected fractions

Protein ID	Gene Symbol	Protein Name	Peptides Used	Spectra Used
IPI00414676	HSP90AB1	Heat shock protein HSP 90-beta	34	248
IPI00382894	TPM3	Tropomyosin 3, isoform CRA_b	18	194
IPI00007750	TUBA4A	TUBA4A cDNA FLJ58687, highly similar to Tubulin alpha-4 chain	10	35
IPI00789605	MYL6	Isoform Smooth muscle of Myosin light polypeptide 6	9	35
IPI00651653	DDX17	Isoform 3 of Probable ATP-dependent RNA helicase DDX17	5	11
IPI00396378	HNRNPA2B1	Isoform B1 of Heterogeneous nuclear ribonucleoproteins A2/B1	3	4
IPI00003865	HSPA8	Isoform 1 of Heat shock cognate 71 kDa protein	3	2
IPI00167419	ANKRD44	Isoform 1 of Serine/threonine-protein phosphatase 6 regulatory ankyrin repeat subunit B	2	3
IPI00011268	RALY	RNA binding protein, autoantigenic	2	3
IPI00183046	PTPN6	Isoform 3 of Tyrosine-protein phosphatase non-receptor type 6	2	3
IPI00031023	FLII	Protein flightless-1 homolog	2	2
IPI00304925	HSPA18	cDNA FLJ54408, highly similar to Heat shock 70 kDa protein 1	2	2
IPI00218993	HSPH1	Isoform Alpha of Heat shock protein 105 kDa	2	2
IPI00297169	LCP2	Lymphocyte cytosolic protein 2	2	1
IPI00010397	HLA-DRB1	HLA-DRB1	2	1
IPI00010320	CBX1	Chromob2x protein homolog 1	1	3
IPI00010133	CORO1A	Coronin-1 A	1	2
IPI00011454	GANAB	Isoform 3 of Neutral alpha-glucosidase AB	1	2
IPI00339277	SAMSN1	SAMSN1 Isoform 3 of SAM domain-containing protein SAMSN-1	1	2
IPI00012433	F8A1	Factor VIII intron 22 protein	1	2
IPI00171199	PSMA3	Isoform 1 of Proteasome subunit alpha type-3	1	1
IPI00009123	NUCB1	Isoform 2 of Nucleobindin-2	1	1
IPI00015973	EPB41L2	EPB41L2 band 4.1-like protein 2 isoform b	1	1
IPI00026670	TCEB2	Transcription elongation factor B (SIII), polypeptide 2 (18kDa, elongin B), isoform CRA_b	1	3
IPI00394804	RINL	Ras and Rab interactor-like protein	1	1
IPI00298994	TLN1	Talin 1	1	1
IPI00030355	PPP1R11	Protein phosphatase 1 regulatory subunit 11	1	1
IPI00027378	UBXN1	Isoform 2 of UBX domain-containing protein 1	1	1
IPI00166137	RALYL	RNA-binding Raly-like protein isoform 1	1	1
IPI00739464	LOC646821	LOC646821 similar to actin, gamma 1	1	1
IPI00296353	ARHGAP18	Isoform 2 of Rho GTPase-activating protein 18	1	1
IPI00183274	SNX1	cDNA FLJ46302, highly similar to Sortin nexin 1	1	1
IPI00064767	ARHGAP17	Isoform 1 of Rho GTPase-activating protein 17	1	1
IPI00220365	EIF4G1	EIF4G1 protein	1	1
IPI00647217	SKIV2L2	Superkiller viralicidic activity 2-like 2	1	1
IPI00013949	SGTA	Small glutamine-rich tetratricopeptiderepeat-containing protein A	1	1
IPI00332936	ZC3HAV1	Isoform 2 of Zinc finger CCCH-type antiviral protein 1	1	1
IPI00007244	MPO	Isoform H7 of Myeloperoxidase	1	1
IPI00012866	AKT1	RAC-alpha serine/threonine-protein kinase	1	1
IPI00009634	SQRDL	Sulfide:quinone oxidoreductase, mitochondrial	1	1
IPI00788612	LIMS1	LIM and senescent cell antigen-like-containing domain protein 1	1	1
IPI00005613	LOC441722	Similar to U2 small nuclear RNA auxillary factor 1	1	1
IPI00000816	YWHAE	14-3-3 protein epsilon	1	1
IPI00470477	ATG4B	Putative uncharacterized protein ATG4B	1	1
IPI00020319	BLOC1S1	Isoform 1 of Biogenesis of lysosome- related organelles complex 1 subunit 1	1	3
IPI00329338	PCYT1A	Choline-phosphate cytidylyltransferase A	1	1

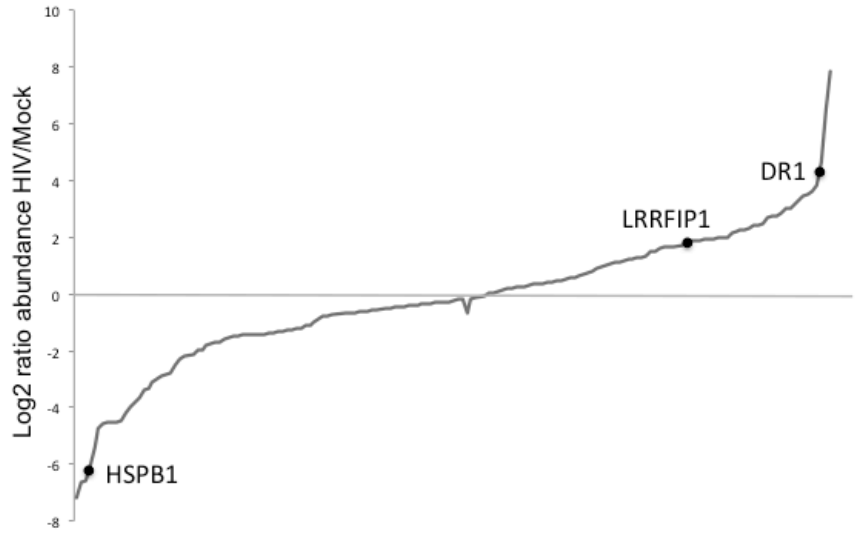

Figure 3.9. Distribution of fold changes in protein abundance between HIV-1 and mock-infected samples as determined by SINQ. The x axis represents proteins identified and the y axis the associated log2 fold change of the abundance of the protein in HIV-1-infected fractions compared to mock-infected fractions. The proteins DR1, LRRFIP1, HSBP1 are shown on the graph for illustration.

Tables 3.3 and 3.4. List of List of phosphoproteins identified by LC-MS/MS and spectral index quantification to be differentially phosphorylated, i.e phosphorylated or dephosphorylated by HIV-1. Spectral and peptide numbers indicate the normal spectral index method, which basically uses the summed intensities of spectral peaks of identified peptide fragments ions to evaluate the abundance or presence/absence of the peptide. These are normalized and the calculated ratio between their abundance in HIV-1 and mock-infested fractions indicates the difference in abundance of the phosphoprotein. Ratios>1.25 or <0.75 were considered to indicate differences between the two conditions.

Table 3.3. List of phosphoproteins identified by SINQ to be dephosphorylated in HIV-1-infected fractions compared to mock-infected fractions.

Gene	Length	Peptides	Spectra	HIV Norm	Mock Norm	Ratio	Log2
HSPB1	205	6	16	1.82E-05	2.77E-07	0.02	**-6.03**
ATP5A1	553	4	6	9.16E-07	3.88E-08	0.04	**-4.56**
EEF1D	281	5	10	1.22E-05	5.40E-07	0.04	**-4.5**
HNRNPU	806	7	37	5.20E-06	2.30E-07	0.04	**-4.5**
ST13	369	3	6	4.32E-06	1.92E-07	0.04	**-4.49**
PSMB7	277	1	1	1.36E-07	6.19E-09	0.05	**-4.46**
HNRNPC	293	5	13	8.00E-06	4.43E-07	0.06	**-4.17**
PEA15	130	2	9	1.99E-05	1.27E-06	0.06	**-3.97**
CANX	627	2	4	5.18E-07	3.75E-08	0.07	**-3.79**
EEF2	858	11	17	1.62E-06	1.29E-07	0.08	**-3.65**
MYH9	1960	10	12	7.11E-07	7.02E-08	0.1	**-3.34**
GAPDH	335	2	2	7.52E-07	1.01E-07	0.13	**-2.89**
OSTF1	214	3	5	9.09E-06	1.29E-06	0.14	**-2.82**
VASP	380	10	35	1.39E-05	2.00E-06	0.14	**-2.79**
PRKAR1A	381	4	8	9.86E-06	1.75E-06	0.18	**-2.49**
SNX5	404	3	5	2.03E-06	4.16E-07	0.2	**-2.29**
C6orf108	174	1	2	2.77E-06	5.98E-07	0.22	**-2.21**
EEF1B2	225	1	3	7.36E-06	1.62E-06	0.22	**-2.19**
HSD17B4	736	7	8	7.06E-07	1.62E-07	0.23	**-2.13**
FAM129B	733	15	66	1.44E-05	3.65E-06	0.25	**-1.98**
RCC2	522	9	22	6.82E-06	1.76E-06	0.26	**-1.95**
BSCL2	747	6	9	2.64E-06	7.44E-07	0.28	**-1.83**
AKAP12	1684	1	54	1.61E-05	4.73E-06	0.29	**-1.76**
RPS6	249	2	2	6.05E-07	1.84E-07	0.3	**-1.72**
EIF2S3	472	13	34	8.60E-06	2.85E-06	0.33	**-1.59**
SSR4	184	1	1	2.00E-07	6.99E-08	0.35	**-1.52**
ACLY	1101	9	12	1.10E-06	3.94E-07	0.36	**-1.49**
CTPS	591	1	2	2.53E-07	9.08E-08	0.36	**-1.48**
ENO3	434	1	2	3.64E-07	1.34E-07	0.37	**-1.45**
PSMA7	248	12	46	4.68E-05	1.74E-05	0.37	**-1.42**
PDIA4	645	9	21	4.29E-06	1.61E-06	0.37	**-1.42**
LOC64587	89	1	4	2.48E-05	9.33E-06	0.38	**-1.41**
ATG7	703	5	3	2.44E-07	9.20E-08	0.38	**-1.41**
PSMB4	264	5	19	8.72E-06	3.29E-06	0.38	**-1.41**
STK4	487	1	3	7.77E-07	2.97E-07	0.38	**-1.39**
PLEK	350	8	38	1.58E-05	6.08E-06	0.39	**-1.38**
PDAP1	181	1	1	5.30E-07	2.10E-07	0.4	**-1.33**
IRF2BP2	587	4	3	4.78E-07	1.93E-07	0.4	**-1.31**
HDGF	240	7	16	2.73E-05	1.12E-05	0.41	**-1.28**
ZYX	485	1	2	5.29E-07	2.22E-07	0.42	**-1.25**
S100A9	114	3	56	1.87E-04	8.07E-05	0.43	**-1.21**
BCKDK	382	7	22	8.49E-06	3.71E-06	0.44	**-1.2**
PSMB5	263	1	4	8.36E-07	3.83E-07	0.46	**-1.13**
AHNAK	5890	2	2	3.50E-08	1.61E-08	0.46	**-1.12**
CFL1	166	8	47	3.09E-05	1.57E-05	0.51	**-0.97**
KCTD12	325	4	4	2.59E-07	1.42E-07	0.55	**-0.87**
CALR	417	17	161	3.32E-04	1.95E-04	0.59	**-0.76**
ALOX15	684	4	3	3.37E-07	1.98E-07	0.59	**-0.76**
PSMA4	261	6	23	1.17E-05	7.18E-06	0.61	**-0.71**
EEF1G	487	5	5	8.94E-07	5.52E-07	0.62	**-0.69**
PDIA3	505	3	4	9.49E-07	5.90E-07	0.62	**-0.69**
HNRNPK	463	3	4	7.37E-07	4.60E-07	0.62	**-0.68**
CAP1	475	10	53	1.49E-05	9.45E-06	0.63	**-0.66**
HSPA5	655	14	23	1.77E-05	1.12E-05	0.64	**-0.65**
YBX1	324	4	1	1.49E-06	9.49E-07	0.64	**-0.65**
ACTB	375	6	13	2.06E-05	1.34E-05	0.65	**-0.63**
PPP1R7	360	4	11	5.86E-06	3.82E-06	0.65	**-0.62**
PSMB1	241	9	25	2.21E-05	1.44E-05	0.65	**-0.62**
NASP	788	4	5	4.26E-07	2.86E-07	0.67	**-0.57**
NPM1	265	4	10	1.54E-05	1.05E-05	0.68	**-0.55**
MIR1279	551	1	6	4.46E-07	3.05E-07	0.68	**-0.55**
F13A1	732	5	16	3.92E-06	2.72E-06	0.69	**-0.53**
NAP1L1	391	5	9	5.11E-06	3.61E-06	0.71	**-0.5**
LCP1	627	26	104	6.76E-05	4.84E-05	0.72	**-0.48**
SSB	408	6	7	1.44E-06	1.04E-06	0.72	**-0.47**
PALLD	672	3	4	4.97E-07	3.64E-07	0.73	**-0.45**

Table 3.4. List of phosphoproteins identified by SINQ to be phosphorylated in HIV-1 infected fractions compared to mock infected fractions.

Gene	Length	Peptides	Spectra	HIV Norm SI	Mock Norm SI	Ratio	Log2
PSMB6	239	2	1	1.83E-08	4.14E-06	226.37	**7.82**
RCSD1	416	1	1	2.70E-09	2.38E-07	87.92	**6.46**
DR1	176	2	2	7.63E-07	1.92E-05	25.20	**4.66**
PRMT5	620	1	1	1.51E-08	2.11E-07	14.04	**3.81**
PDHA1	428	1	1	3.26E-07	3.95E-06	12.12	**3.60**
PCNP	178	2	1	1.10E-07	1.23E-06	11.16	**3.48**
SFRS3	164	3	5	9.85E-07	1.09E-05	11.05	**3.47**
PA2G4	394	1	1	1.40E-07	1.39E-06	9.91	**3.31**
HCLS1	486	2	2	7.90E-08	6.96E-07	8.80	**3.14**
ZNF737	536	1	10	1.14E-07	9.37E-07	8.20	**3.04**
NT5C2	561	1	3	2.34E-07	1.91E-06	8.18	**3.03**
SH3BP1	701	1	1	1.28E-07	9.06E-07	7.08	**2.82**
DPYSL2	619	1	1	7.42E-08	5.03E-07	6.78	**2.76**
GFPT1	699	1	2	7.14E-08	4.71E-07	6.59	**2.72**
LASP1	261	2	10	3.35E-06	2.14E-05	6.38	**2.67**
PSMB3	205	3	4	1.21E-06	6.62E-06	5.45	**2.45**
BCL2L13	485	2	1	1.49E-07	7.85E-07	5.27	**2.40**
APOB48R	1088	13	26	5.86E-06	3.07E-05	5.25	**2.39**
TALDO1	337	5	18	3.14E-06	1.53E-05	4.86	**2.28**
PSMA1	263	6	7	3.16E-06	1.52E-05	4.81	**2.27**
YWHAZ	245	2	3	1.04E-06	4.95E-06	4.74	**2.24**
PYGB	843	9	7	1.30E-06	5.92E-06	4.56	**2.19**
SET	290	6	28	1.71E-05	7.53E-05	4.39	**2.13**
SEPT9	422	6	2	5.53E-07	2.17E-06	3.92	**1.97**
EIF2S2	333	3	3	2.81E-07	1.10E-06	3.92	**1.97**
BTF3L4	158	1	4	3.17E-06	1.24E-05	3.91	**1.97**
PSMB2	201	4	5	2.25E-06	8.65E-06	3.83	**1.94**
SAMHD1	626	25	86	1.12E-05	4.27E-05	3.83	**1.94**
LRRFIP1	784	8	13	3.78E-06	1.44E-05	3.80	**1.93**
VIM	466	4	6	4.84E-07	1.80E-06	3.72	**1.89**
NACA2	215	2	1	3.82E-06	1.42E-05	3.70	**1.89**
LIMA1	759	2	1	6.20E-08	2.24E-07	3.60	**1.85**
MAP2K1	393	3	4	4.31E-07	1.52E-06	3.52	**1.81**
PSMA6	246	7	22	5.84E-06	1.92E-05	3.28	**1.71**
CDC37	378	2	3	2.62E-07	8.41E-07	3.21	**1.68**
EIF4B	616	1	5	6.44E-07	2.04E-06	3.16	**1.66**
VCP	806	2	3	3.08E-07	9.59E-07	3.11	**1.64**
P4HB	508	11	19	5.56E-06	1.72E-05	3.10	**1.63**
SEPT2	361	7	14	6.41E-06	1.97E-05	3.07	**1.62**
B2M	119	1	2	1.27E-06	3.62E-06	2.86	**1.51**
VPS4B	444	3	3	6.45E-07	1.80E-06	2.79	**1.48**
PRKCSH	535	13	37	1.65E-05	4.12E-05	2.50	**1.32**
CD74	296	2	2	4.46E-07	1.09E-06	2.45	**1.29**
NACA	215	7	79	5.62E-05	1.36E-04	2.42	**1.27**
RNH1	461	6	5	8.34E-07	1.92E-06	2.30	**1.20**
RCN1	331	1	1	2.84E-07	6.53E-07	2.30	**1.20**
AP1B1	949	1	2	1.43E-07	3.25E-07	2.27	**1.18**
CSNK2A1	397	4	6	1.70E-06	3.73E-06	2.19	**1.13**
PSMB8	276	6	15	5.01E-06	1.07E-05	2.13	**1.09**
PKM2	531	3	6	6.48E-07	1.34E-06	2.07	**1.05**
HIST1H4F	103	1	1	1.42E-06	2.84E-06	2.00	**1.00**
S100A8	93	4	24	1.88E-05	3.59E-05	1.91	**0.94**
MARCKS	332	9	24	6.47E-05	1.20E-04	1.86	**0.89**
LSP1	339	15	141	1.87E-04	3.26E-04	1.74	**0.80**
TFG	400	1	1	2.94E-07	4.85E-07	1.65	**0.72**
ILF2	390	4	6	2.96E-06	4.70E-06	1.59	**0.67**
CORO1B	489	4	5	7.44E-07	1.14E-06	1.53	**0.61**
RPLP2	115	6	49	2.37E-04	3.50E-04	1.48	**0.56**
HMGB2	209	11	36	2.33E-05	3.43E-05	1.47	**0.55**
PTMS	102	1	2	2.27E-06	3.24E-06	1.43	**0.51**
BTF3	206	2	3	2.27E-06	3.16E-06	1.39	**0.48**
MSN	577	19	89	2.07E-05	2.86E-05	1.39	**0.47**
MVD	400	2	2	4.29E-07	5.65E-07	1.32	**0.40**
PSMA2	234	4	9	4.19E-06	5.49E-06	1.31	**0.39**
PURA	322	1	2	2.39E-07	3.06E-07	1.28	**0.35**
C1QBP	282	7	24	2.64E-05	3.35E-05	1.27	**0.35**
ILF3	690	7	13	1.51E-06	1.91E-06	1.26	**0.34**
DBNL	439	2	1	3.46E-07	4.33E-07	1.25	**0.33**

3.3.6 Bioinformatics analysis of the HIV-1 phosphoproteome

To obtain a better understanding of the HIV-1 phosphoproteome and the cellular subsystems recruited by HIV-1 in more detail, I carried out ingenuity pathway analysis (IPA) for canonical pathway and molecular and cellular function pathways of proteins identified within the HIV-1 phosphoproteome. Public annotation indicated that 64% of the detected proteins were cytosolic, whereas 22% were nuclear and 4% of the proteins were located in the plasma membrane. The remainder of the proteins were either of unknown location (7%) or extracellular (0.2%). IPA indicated that the HIV-1 phosphoproteome was with 134 proteins significantly biased towards proteins that control cellular trafficking (table 3.5). I further asked what key cellular functions and physiological systems may be associated with the molecules of the HIV-1 phosphoproteome. This is summarized in figure 3.10 and tables 3.5-3.6 and shows that HIV-1 induces PTM in proteins associated with diverse cellular functions, including functions affecting the cellular trafficking machinery such as cellular morphology, formation of cellular protrusions, immune cell trafficking and antigen presentation. Obviously, cytoskeletal components will be overrepresented in proteomic studies due to their higher abundance in cells, however bioinformatics in concert with manual analysis showed that the phosphoproteome contained a number of proteins involved in macro and microautophagy (such as RRAGA, RRAGC, GABARAP), neural synapse recycling (such as Pallidin, cappuccino) as well as exocytosis and secretory pathway (TOM1, SNX1, SNX5), most of these molecules had no previously characterized role in pathogen recognition. The over-representation of constituents of specific trafficking pathways (discussed further in the next chapter) indicates that HIV-1 signaling may induce rearrangement of these proteins to facilitate entry and trafficking of cargo in DCs. Conversely, only very few proteins belonging to pathways such as the MAPK and JAK-STAT signaling pathways were detected in the HIV-1 phosphoproteome, in keeping with the observation of HIV-1 inducing an immature phenotype in DCs (Hodges et al., 2007).

Table 3.5. Networks analysis of the HIV-1 phosphoproteome.

ID	Associated Network Functions	Score
1	Cellular assembly and organization, DNA replication, recombination and repair	53
2	Gene Expression and PTM	46
3	Cancer, carbohydrate metabolism, energy production	45
4	DNA replication, recombination and repair, RNA PTM, cellular assembly and organization	43
5	Cellular assembly and organization, cell morphology, cellular movement	34

All proteins identified as differentially phosphorylated were analyzed by Ingenuity pathway analysis and the top 5 cellular networks are shown with respective enrichment score associated with each category.

Table 3.6. System analysis of the HIV-1 phosphoproteome.

Physiological system	**Molecules**	**n**
Endocrine system development	DNAJA1, HSP90AB1, SERBP1, STIP1, HMGA1	5
Skeletal and muscle tissue development	ALDO1, FLII, LIMS1, MAP2K1, MYL12B, MYL6, MYL6B, MTM1, SRSF1, TLN1, TPM3, TPM4, VCL, AKT1, CAPN2, HMGB1, MYH9, NACA, PKM2, PAK2	20
Tissue morphology	FLNA, ALDOA, FLII, LIMS, MAP2K1, MYL12B, VASP, MYL6, MYL6B, VIM, VCL, HDAC2, TLN1, TPM3, SRSF1, TPM4	16
Immune cell trafficking	CD74, MPO, HMGB1, HSPD1, MAP2K1, PSMB8, PSME1, S100A9, PSME2, CBL, LCP2	11
Nervous system development	RTN4, MYH9, MYL12B, AKT1, BAIAP2, B2M, DPYSL2, VCL, LMNA, KIF5B, PSAP	11

All proteins identified as differentially phosphorylated were analyzed by Ingenuity pathway analysis and the top 5 physiological systems involved are shown.

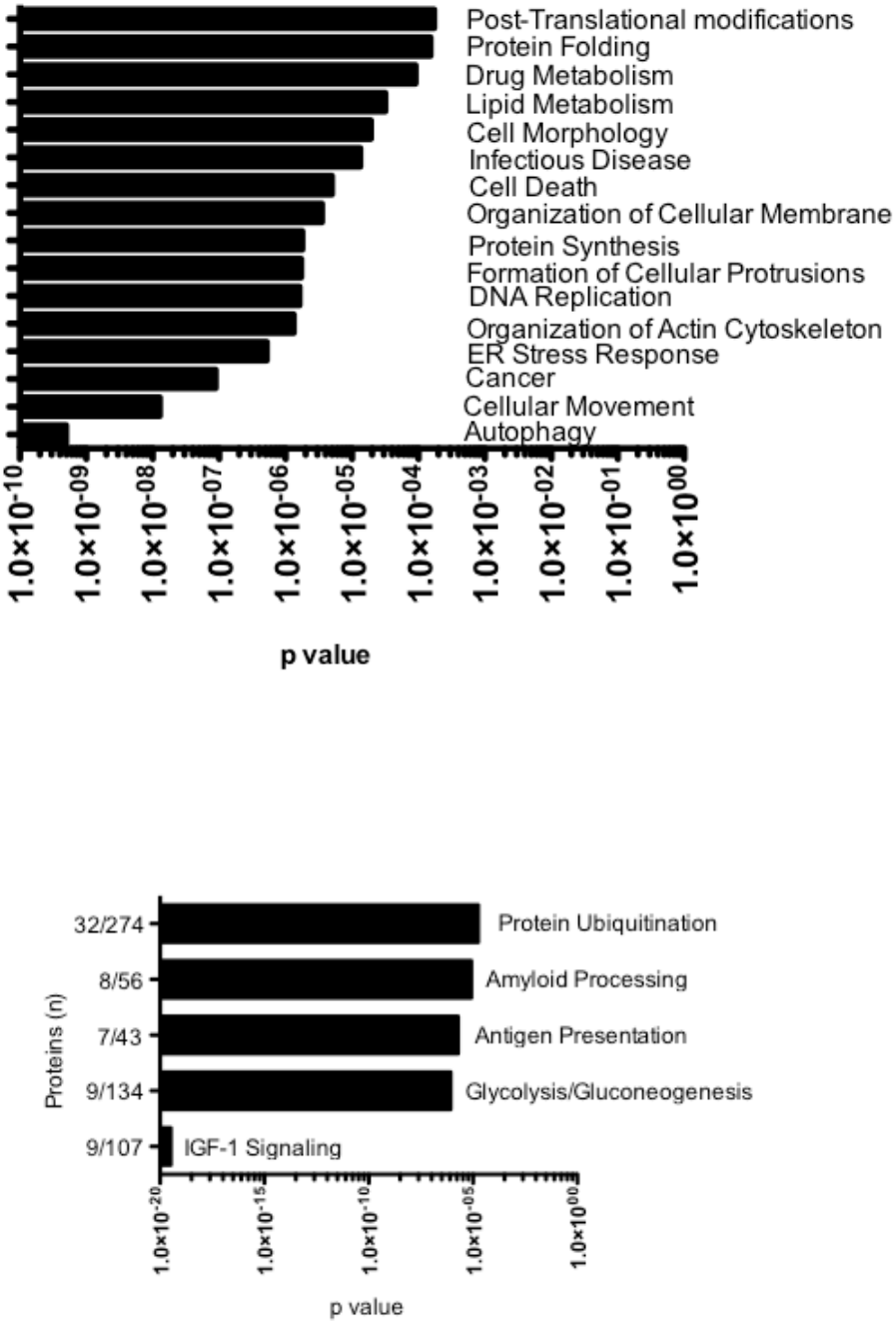

Figure 3.10. Ingenuity pathway analysis of the HIV-1 phosphoproteome. Molecular and cellular functions (top panel) and top five canonical pathways (lower panel) are shown. The p value for each category is shown on x axis with number of proteins (left panel) shown.

3.3.7 Correlation of the HIV-1 phosphoproteomics data to known HIV-1 interacting proteins

One measure to assess the accuracy and physiological relevance of a screening method is its comparability to other published peer-reviewed studies. Therefore, I compared my phosphoproteomics data to HIV-1 associated factors in the HIV interaction database (http://www.ncbi.nlm.nih.gov/RefSeq/HIVInteractions/), and found that 30% of the proteins of the HIV-1 signalosome have a known interaction with the virus (table 3.7). Remarkably a total of 2,393 human-protein coding genes, corresponding to 9.5% of all human genes, are listed as associated with HIV infection in the National Center for Biotechnology Information (NCBI) interaction database (Ptak et al., 2008). In simple terms this suggests that my approach was successful in enriching for HIV interacting proteins. However, some caution is required in interpreting the overlap between the HIV-1 signalosome data and the NCBI database. The vast majority of the NCBI database is based on studies of CD4+ T cells or cell lines, biasing the data towards non-innate cells where the expression of host factors and PRR signaling may differ to cells such as DCs. Furthermore, there is no single published study which examines such early changes in the signaling cascade induced upon HIV-1 infection. The earliest time point that I could find was a recent study which investigated the early host response in HIV-1-infected CD4+ T cells at 4, 8 and 20 hours p.i using quantitative proteomics (Navare et al., 2012). Given these caveats, it is perhaps surprising I was able to observe such strong enrichment for published HIV interacting proteins.

Interestingly, LARG, a protein previously shown by our group to be phosphorylated via the interaction of DC-SIGN with HIV-1, was not detected within the HIV-1 signalosome (Hodges et al., 2007). This may reflect differences in methodologies, both in the phosphoprotein enrichment procedure as well as the mass spectrometry platform. However, LASP1, a protein downstream of the HIV-1-DC-SIGN-LARG complex (Gringhuis et al., 2009), was found to be phosphorylated by HIV-1.

Table 3.7. Proteins identified in HIV-1 phosphoproteome with known interactions with HIV.

ACTB	HIST1H4F	PRKACA	RAD23A
AKT1	HLA-DRA	PRKAR1A	SGTA
ALOX15	HLA-DRB1	PRKAR2A	SNRPD1
AP1B1	HMGA1	PRKCD	SNRPD3
B2M	HNRNPA1	PSMA1	SP3
BANF1	HNRNPK	PSMA2	SSB
BRCA1	HSP90AA1	PSMA3	SUB1
C1QBP	HSPA5	PSMA4	TAF15
CALR	HSPA8	PSMA5	TCEB1
CANX	HSPA9	PSMA6	TCEB2
CAPN2	HSPD1	PSMA7	TLN1
CBL	KHDRBS1	PSMB1	TPM2
CFL1	KPNA3	PSMB10	TPM3
CHMP4B	KPNA4	PSMB2	TUBA4A
CSNK2A1	LCP1	PSMB3	TUBB
CSNK2A2	LMNA	PSMB5	TUBB6
DR1	MAP2K1	PSMB6	UBB
EEF1A1	MSN	PSMB7	VCL
EEF1D	MYH9	PSMB8	VIM
EIF2S1	NAP1L4	PSMB9	YBX1
EIF2S2	NCL	PSMC3	YWHAB
EIF2S3	NDRG2	PSMD13	YWHAE
EIF4G1	NMT1	PSMD7	YWHAG
EZR	NPM1	PSMD9	YWHAG
FLNA	PAK2	PSME1	YWHAZ
GANAB	PDIA4	PSME2	
HIST1H2AE	PPM1F	PTGES3	
HIST1H2BL	PPP1CA	PURA	

3.3.8 Confirmation of proteins differentially phosphorylated by HIV-1

Mass spectrometry is a powerful screening tool to identify novel components of a signaling cascade, however observations need to be validated by independent biochemical methods. A challenge of any screening experiment is how to choose targets for confirmation. The main objective of this work was to identify novel signaling molecules implicated in HIV-1-mediated immune evasion and given the significant proportion of trafficking proteins identified by the data set, it was tempting to focus on interesting signaling and trafficking proteins.

Initially, immunoblots of phosphoproteins following 10 min mock and HIV-1 infection were subjected to SDS PAGE and immunoblotted for multiple differentially phosphorylated proteins, as identified by mass spectrometry. However, for most proteins no detectable differences between conditions could be visualized. Changes in protein phosphorylation may only be present at a single site, thus being too subtle to be

detected on an immunoblot of phosphoeluates. Therefore, the immunoblots were repeated on mock and HIV-1-infected DCs post IEF fractionation. Figure 3.11 shows a representative example, where HIV-1-induced changes in phosphorylation of the cytoskeletal protein WAVE-2 are only visible on an immunoblot of fractionated phosphoeluates. Subsequently, I validated differential phosphorylation of the majority of candidate proteins tested (25 out of 30). Of note, 13 antibodies that were tested did not work on immunoblots. It was cost-prohibitive to perform biological replicates of confirmatory western blots post fractionation, therefore multiple different biological replicates were pooled prior to fractionation.

To obtain an unbiased interpretation of the visible differences on immunoblots, densitometry was performed and the ratio between HIV-1 and mock-infected conditions calculated. As mentioned earlier, a direct correlation to a loading control such as actin was not feasible for two reasons: (i) the phosphoenrichment procedure removes proteins such as beta-actin from the samples, (ii) the fractionation procedure will separate proteins according to their isoelectric point, so that proteins that are equal across conditions would still be detectable in selected fractions only. Therefore, I opted to use an indirect way to demonstrate that observed differences are due to differential phosphorylation rather than unequal loading onto IEF wells: I collected a small aliquot of samples pre-fractionation, subjected these to SDS PAGE and silver staining and used these as a surrogate for a loading control for each experiment (figure 3.11, controls). It is also noteworthy that samples are quantified by Bradford dye test before fractionation, so that altogether I am fairly confident that the differences I observe are triggered by HIV-1.

In summary, the data obtained by LC-MS/MS could be validated for the majority of proteins tested, underscoring the versatility of this approach for identification of novel signaling molecules downstream of HIV-1-DC interaction.

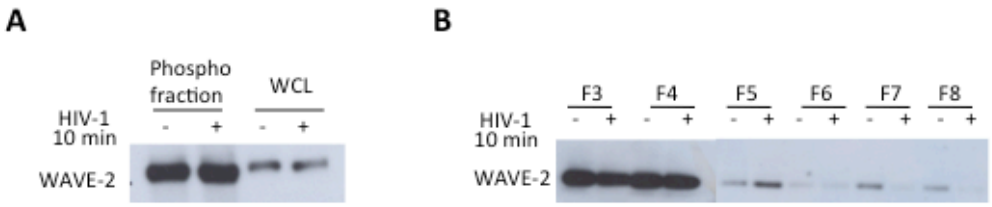

Figure 3.11. Confirmation of differentially phosphorylated proteins identified by LC-MS/MS requires immunoblot of samples post-fractionation. A. Western blot of whole cell lysate and phosphoenriched samples treated with HIV-1 or mock for 10 minutes is too insensitive to detect subtle post-translational modifications. B. Western blot of samples following fractionation by IEF allows visualization of HIV-1-induced differentially phosphorylated WAVE-2 (Wiskott-Aldrich syndrome protein-2). F denotes fraction.

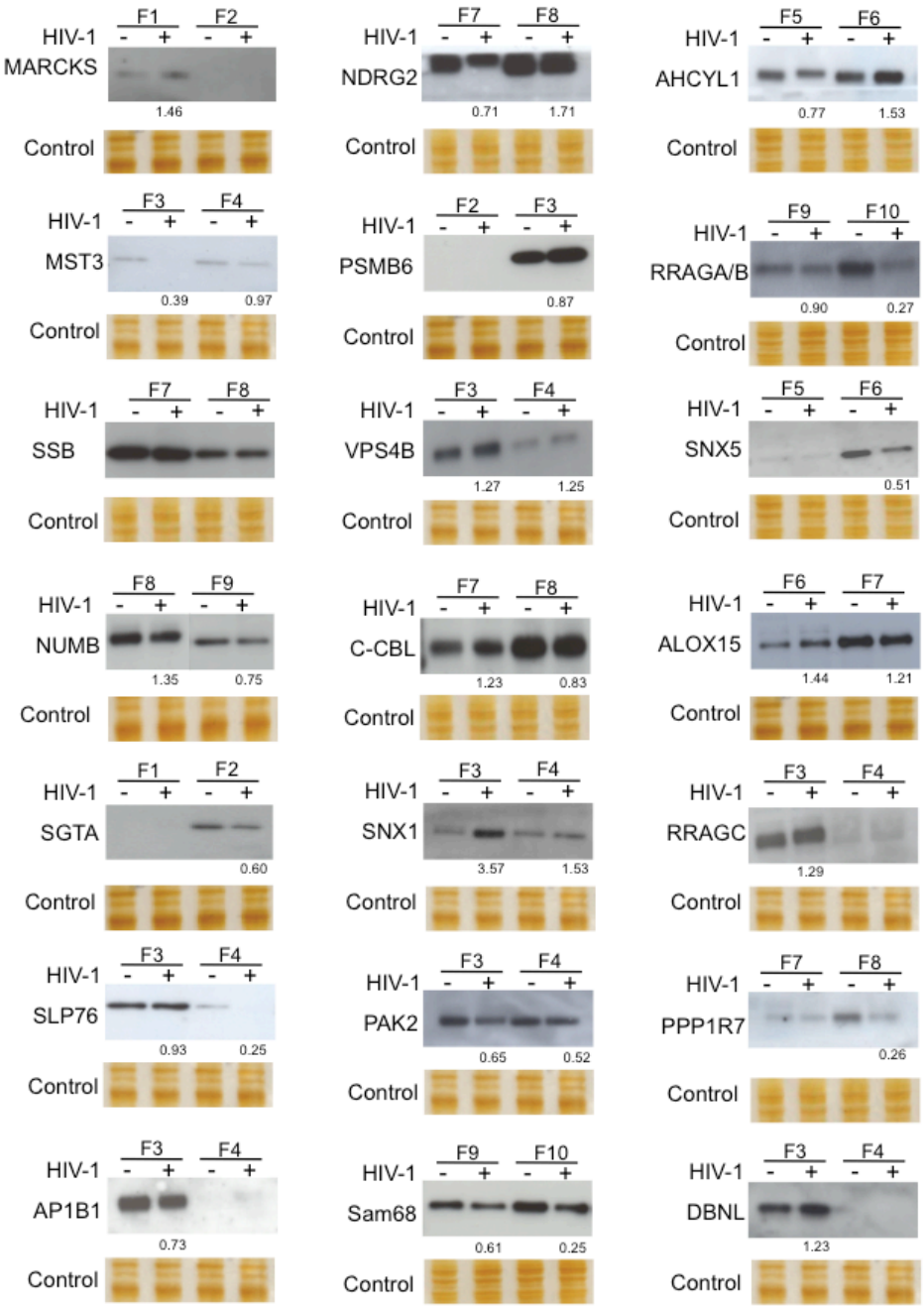

Figure 3.12. Validation of differential phosphorylation of proteins identified by LC-MS/MS of the HIV-1 phosphoproteome. Phosphoeluates of DCs infected with HIV-1 or mock for 10 min were subjected to IEF, desalted and subjected to immunoblotting for the proteins indicated. Two adjacent fractions where the proteins displayed the highest density are shown. Values represent the ratio between the densities calculated for the HIV-1 compared to the mock fraction by densitometry. Control represents a silverstain of phosphoeluates before IEF as discussed in 3.3.8. Representative sections shown to illustrate equal loading across conditions.

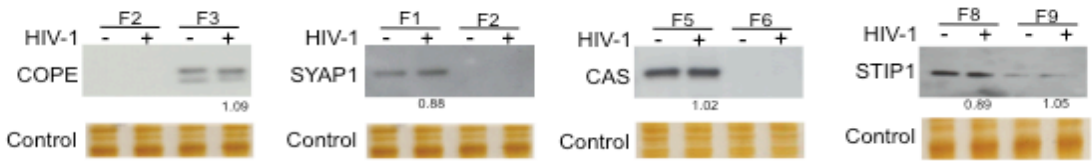

Figure 3.13. Proteins not validated as differentially phosphorylated by immunblot. Fractionated Phosphoeluates were immunoblotted for proteins identified as differentially phosphorylated by LC-MS/LC-MS/MS.

3.3.9 LC-MS/MS analysis of HIV-1 virions

HIV, like other enveloped and non-enveloped viruses, is known to incorporate multiple host proteins into the virion during the viral life cycle. It has been suggested that the producer cell type influences infectivity, presumably via expression of distinct host factors (Olinger et al., 2002; Santos et al., 2012). Given the high number of trafficking molecules identified within the HIV-1 phosphoproteome and the difficulties in distinguishing proteins specific to the signaling cascade elicited by HIV-1 relative to those that were part of the virion, it seemed pertinent to characterize the HIV-1 virion by proteomic analysis.

For proteomic analysis of HIV-1 viral particles, HEK293T cells were transfected with the proviral construct NL4-3 BaL via calcium phosphate precipitation. I chose to use the same cell line I had used to generate viral stocks for my phosphoproteomic study, and therefore expected the same host proteins to be incorporated in the virions. After 24 h viral supernatant was harvested, filtered and purified by sucrose gradient centrifugation. Viral preparation was then methanol-chloroform precipitated, resuspended in Urea buffer and prepared for LC-MS/MS analysis by the Orbitrap Velos Mass spectrometer. Data was processed using Mascot database against the human and pathogen databases with a Mascot score of 15 or above

Encouragingly, LC-MS/MS analysis identified the majority of HIV-1 encoded proteins, and a significant number of known HIV-1 associated host proteins (tables 3.8 and 3.9).

Viral encoded proteins identified included the abundant gag and pol, envelope, nef, tat, rev and even vif, an accessory protein usually associated with immature virions and displaying a complex, and yet unresolved formation with cellular factors. Host factors identified included Cyclophilin A, a protein known to be incorporated in the viral capsid to increase HIV-1 infectivity (Franke and Luban, 1996; Franke et al., 1994; Thali et al., 1994) as well as the cytoskeletal proteins Radixin-Moesin, which are part of the ERM family proteins known to attach actin filaments to the membrane during the entry process (Charrin and Alcover, 2006; Chertova et al., 2006). The ERM proteins were also detected within the HIV-1 phosphoproteome, indeed a total of 25 proteins were found to overlap between the HIV-1 phosphoproteome and the proteome of viral particles (table 3.9). However, only eight proteins were identified within the HIV-1-infected fractions (bold, table 3.10). It is difficult to draw any conclusion from this overlap, given that two distinct experimental approaches as well as two quite different LC-MS/MS instruments provided the basis for these datasets.

Remarkably, a high proportion of proteins identified were novel proteins not previously described in HIV-1 virions. These proteins belong to a wide variety of cellular processes, including actin cytoskeleton, ubiquitin, proteasomes, metabolism and intracellular organelles (table 3.11 and figure 3.14). The acquisition of cellular proteins into virions may be a bystander process, merely by being fortuitously present at the site of viral budding. Alternatively, proteins such as Tsg101 and Chmp4b, that are associated with the ESCRT machinery may preferentially get incorporated into the virion by an active mechanism to aid in the viral life cycle (Diaz et al., 2010; Morita et al., 2011). This is an established process for proteins such as integrins and the aforementioned Cyclophilin that are actively recruited to increase viral infectivity and hence pathogenesis (Franke and Luban, 1996).

Altogether, the characterization of the HIV-1-associated proteins provided a useful insight into the biology of the virus. However, the number of HIV-1-incorporated proteins that were identified by LC-MS/MS is fairly large, and caveats should be considered when interpreting these data. Importantly, a negative control consisting of LC-MS/MS analysis of cellular proteins derived from the supernatant of non-transfected HEK 293T cells was lacking, and although I attempted to produce highly purified virus contamination of the samples with soluble proteins and vesicle particles cannot be excluded. Some of the proteins identified here may simply be adherent rather than truly

incorporated into the viral particles. For instance, it cannot distinguish between cellular exosomes derived from HEK293T cells and cellular proteins incorporated into virions or even viral exosomes In addition, the proteins characterize a population of virions rather than a single virion. It is noteworthy that a recent large-scale proteomic analysis of *M. tuberculosis* by the Orbitrap instrument, which has considerably higher sensitivity than other LC-MS/MS platforms, yielded improved gene annotations in Sanger and The Institute for Genomic Research databases (de Souza et al., 2008). It would therefore be very interesting to repeat this experiment with the appropriate controls.

Collectively, this data supports the notion that HIV-1 interacts with a multitude of host proteins during its replication cycle. Further biological studies will be needed to define the relevance of these host proteins to viral pathogenesis.

Table 3.8. HIV-1 proteins identified by LC-MS/MS of NL4-3 BaL.

Accession Number	Protein Name	Mascot
P12497	Gag-Pol polyprotein; Pr160Gag-Pol	13569
P12493	Gag-Pol polyprotein; Pr55Gag	12180
P03407	Protein Nef	373
P35961	Envelope glycoprotein gp160	285
O89942	Protein Vpr	81
P12490	Truncated surface protein; Glycoprotein 120	65
P04616	Protein Rev	44
P04610	Protein Tat	29
P12504	Virion infectivity factor	20

Table 3.9. Known HIV-associated host proteins identified in viral LC-MS/MS

Cyclophilin A	Tsg101
Elongation factor-1 alpha	Annexin A5
Ubiquitin	Chloride intracellular channel protein 1
Glyceraldehyde-3-phosphate	Annexin A2
Heat shock 70kDa	Vps35
Histone H2B	2~,3~-cyclic-nucleotide 3~-phosphodiesterase
Beta-globin	Phosphoglycerate kinase 1
CD63	Complement C4-B
Signal recognition particle 14 kDa protein	Rab GDP dissociation inhibitor beta
Protein S100-A10	Alpha-2-HS-glycoprotein
Syndecan-2	Annexin A11
Cofilin-1	Adenylyl cyclase-associated protein 1
Clathrin light chain A	Coronin-1A
ADP-ribosylation factor 1	Alpha-enolase
CD9 antigen	Monocyte differentiation antigen CD14
Syntenin-1; MDA-9	ATP synthase subunit beta
Triosephosphate isomerase	Tubulin alpha-1A chain
Glutathione S-transferase P	Pigment epithelium-derived factor
GTP-binding nuclear protein GSP1/Ran	Radixin
Tetraspanin-14	Filamin-A
Transforming protein RhoA	Heat shock 70 kDa protein 1
Heat shock 70 kDa protein 2	Heat shock 70 kDa protein 1-like
Heat shock 70 kDa protein	

Table 3.10. Common proteins identified by LC-MS/MS of HIV-1 BaL and phosphoproteomic screen of HIV-1-infected DCs.

Accession	Protein Name	Mascot
Q9Y490	Talin-1	851
P02554	Tubulin beta chain	723
Q5XIF6	Tubulin alpha-4A chain	598
Q92122	Pyruvate kinase muscle isozyme	312
Q2HJ81	Tubulin beta-6 chain	296
Q5NVI9	DnaJ homolog subfamily A member 1	209
P21333	**Filamin-A**	**200**
Q258K2	Myosin-9	189
Q2HJ49	Moesin	155
P35241	**Radixin**	**133**
P23528	**Cofilin-1**	**128**
Q99JW4	LIM and senescent cell antigen-like-containing domain protein 1	107
P06748	**Nucleophosmin**	**99**
Q32LP0	Fermitin family homolog 3	96
P15311	**Ezrin**	**89**
Q9D8B3	Charged multivesicular body protein 4b	74
Q0VBZ9	MARCKS-related protein	54
Q756H2	Enolase	47
P09496	**Clathrin light chain A**	**45**
Q4R4J2	Coronin-1A	42
Q5R8S2	Proteasome subunit beta type-5	40
Q5R440	Calnexin	31
P18206	**Vinculin**	**30**
Q2NKY7	Septin-2	27
Q9ULV4	**Coronin-1C**	**24**

Mascot values refer to the score of mass spectrometry analysis of virions.
Proteins in bold were identified in HIV-1-infected DCs only.

Table 3.11. Host factors identified by viral LC-MS/MS involved in trafficking

Cellular function	Proteins
Clathrin-mediated endocytosis signaling	ACTG1, ALB, APOA2, APOD, APOE, CLTA, CLTB, CLTC, CLU, CSNK2A1, F2, HSPA8, ITGB1, ITGB3, RAB11A, RAB4B, RAB5C, RAC1, TF, TFRC, TSG101
Caveolar-mediated endocytosis signaling	ACTG1, ALB, COPA, COPB1, EGFR, FLNA, FLNB, FLNC, HLA-A, ITGB1, ITGB3, RAB5C
Actin cytoskeleton signaling	ACTG1, ACTN4, CD14, CFL1, EZR, F2, FN1, GSN, ITGB1, MSN, MYH9, MYH10, PFN1, PPP1CB, RAC1, RDX, ROCK2, VCL
Virus entry via endocytic pathways	ACTG1, ACTN4, CD14, CFL1, EZR, F2, FN1, GSN, ITGB1, MSN, MYH9, MYH10, PFN1, PPP1CB, RAC1, RDX, ROCK2, VCL
Mechanism of viral exit from host cells	ACTG1, CHMP2A, CHMP4B, PDCD6IP, TSG101

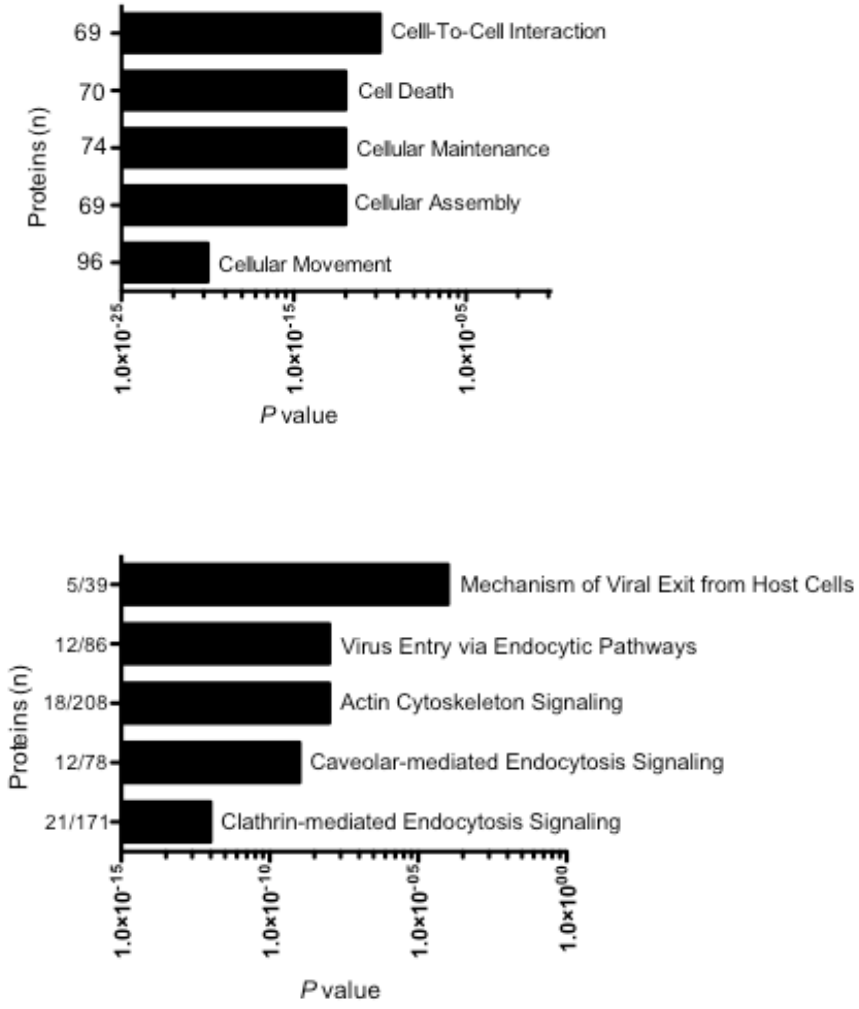

Figure 3.14. Ingenuity pathway analysis of host proteins identified by LC-MS/MS analysis of HIV-1 virions. Top five cellular pathways (upper graph) and trafficking cellular functions (lower graph) shown. The p value (x axis) and number of proteins (left panel) for each category are shown.

3.3.10 Investigation of changes in the transcriptome of HIV-1-infected DCs

So far, I have shown that HIV-1 is capable to induce remarkable changes in the phosphoproteome of MDDCs within 10 min of infection. In order to further dissect the signaling cascade following early HIV-1 infection, I carried out an Affymetrix gene expression assay of HIV-1-infected DCs. Briefly, 4 mill DCs from four donors were infected with NL4-3 BaL (MOI of 1) or mock, after 2 h cells were washed twice, total RNA was extracted, quantified using the Nanodrop UV spectrophotometer and frozen at -80°C. Successful productive infection of DCs was tested by measurement of HIV-1 RT activity in supernatant of 1 mill DCs that had been kept in culture for each respective donor. RNA was prepared for microarray studies after initial checking of the RNA integrity on the Agilent 3100 Bioanalyzer platform. RNA with an integrity value of more than 8 was included for preparation of samples for analysis on the Affymetrix Genechip Human Gene 1.0 Set Array, which includes 28,869 gene probes. I prepared RNA samples for hybridization using the GeneChip WT Terminal Labeling Kit (Affymetrix). In brief, RNA was reverse transcribed into cDNA, amplified by in vitro transcription, cRNA was synthesized using a random primer pool. cRNA was reverse transcribed back into cDNA and fragmented into shorter cDNA oligonucleotides. Effective fragmentation was confirmed on the Bioanalyzer. Subsequently, samples were labeled and hybridized to the Genechip by our collaborator Dr. Dilair Baban (Wellcome Trust Centre of Human Genetics, Oxford). On chip normalization was performed to provide raw signal intensities and global scaling was used to compare genes from chip to chip. All data quality controls passed the initial quality guideline set by Affymetrix. Data was analyzed using Genespring GX software and differentially expressed genes between infected and non-infected cells were considered significant if they passed a 2-way ANOVA test at $p < 0.01$ and a change of greater than 2-fold. In a parallel experiment (originally carried out for a separate project) DCs of the same donors were activated with LPS for 24 h and treated as described above for analysis by microarray.
Intriguingly, HIV-1 failed to induce any changes in gene expression above the cut-off value of 2. To illustrate this point I compiled a list of the top 25 up- and downregulated genes in HIV-1-infected DCs (table 3.12): IL1 β and early growth response 1 are the

only genes that were upregulated by more than 1.5 fold. In contrast, LPS triggered significant differentially regulated changes in gene expression (table 3.13), which excludes technical problems with sample preparation or array platform used. As mentioned earlier, changes observed in large-scale screens should be validated by a second method. Therefore, I chose some of the mostly regulated transcripts with known functions in the innate immune response for validation by real-time PCR. There was a good correlation between the fold changes observed by real-time PCR and microarray, confirming that HIV-1 fails to induce significant changes in the DC transcriptome within 2 h of infection (figure 3.15). An interesting finding emerging from these experiments was the upregulation of IL1β mRNA in response to HIV-1 infection both in the array (1.67 fold change) and by real-time PCR (2.99 fold change). IL1β is an inflammatory cytokine involved in the NALP3 inflammasome signaling cascade. A recent study has shown that HIV-1 induces IL1β in DCs from healthy individuals, whereas DCs from HIV-1-infected subjects showed no changes in IL1β expression following in vitro HIV-1 infection (Pontillo et al., 2012), indicating that HIV-1 infection may induce dysregulation of the inflammasome signaling cascade.

Two hours may be too early to detect changes in gene expression upon HIV-1 infection and arguably not all phosphorylation-induced signaling may not necessarily be accompanied by transcriptional changes. However, our group has carried out multiple microarray studies of DCs activated with different PRR ligands for 2 h and showed differential regulation in gene expression in all these studies: DC-SIGN activation (Ashleigh Hodges), NOD2 activation (John Baker), TLR8 activation (Al Leslie). To address this issue, I looked at the expression of DCs that had been infected with Influenza for 2 h in comparison to DCs infected with HIV-1 and concentrated on genes involved in the interferon response. Figure 3.16 demonstrates that influenza, another enveloped ssRNA virus that enters cells via endocytosis, induces upregulation of IL6, IFNβ1 and the interferon stimulated exonuclease ISG20 transcripts within 2 h of infection. Furthermore, I compared expression of IRF7 and STAT1 in DCs infected with HIV-1 6 h post infection in comparison to DCs activated with the HIV-1-derived TLR8 ligand ssRNA40, and again could easily detect upregulation of the interferon response in TLR8-activated DCs, whereas HIV-1 failed to induce such a response even 6 h post infection. A number of different groups have analyzed the transcriptional

profile of DCs infected with HIV-1, VSV-HIV-1 and SIV *in vitro* and generally two divergent views have emerged from these studies. While some investigators showed enhanced expression of genes implicated in signal transduction, cell proliferation and cell cycle, transcription and immune response related-genes at different times post *in vitro* infection (Harman et al., 2009; Mehla and Ayyavoo, 2012), others have found a remarkable lack of changes in gene expression profiles in ex vivo infected DCs up to 36 h post infection (Manel et al., 2010). Conflicting results that most likely arise from differences in experimental conditions. Hamann et al performed a time course experiment comparing the changes induced by viable as well as chemically inactivated virus (both using a high MOI of 10) and gp120 on MDDCs (Harman et al., 2009). Their rationale behind using such high titre virus was that due to the low efficiency of viral infection in DCs, they may otherwise miss effects of the virus on DCs. They compared gene expression of DCs infected for 6, 24 and 48 h and showed that the effect of HIV on the cellular transcriptome was biphasic: an initial phase within the first 12 hours due to binding and entry and signaling from the endosome of the virus and a second phase after 24 h due to *de novo* viral replication. However, other investigators showed that changes in transcriptional profile of HIV-1-infected DCs only occurred after a delay of 24-36 h p. i. (Manel et al., 2010). Concurring with the opinion of the latter group, I could not detect any changes in gene expression of interferon and inflammatory genes in DCs that were infected with a higher MOI of 10 (figure 3.13).

In summary, despite the ability of HIV-1 to trigger significant and widespread changes in phosphorylation of host proteins within 10 min of infection, it does not appear to induce changes in the transcriptome of DCs infected with HIV-1 following 2 h of infection.

Table 3.12. Differentially regulated genes following 2 h HIV-1 infection

Top 25 upregulated genes following 2 h HIV-1 infection			
p value	**Fold change**	**Description**	**Gene ID**
0.001171874	1.67	interleukin 1, beta	IL1B
4.97E-06	1.65	early growth response 1	EGR1
0.00877332	1.40	eukaryotic translation initiation factor 4B	EIF4B
1.70E-04	1.35	similar to Zinc finger, RNA-binding motif and serine/arginine rich 2	LOC100129391
1.70E-04	1.35	claudin 1	CLDN1
4.13E-06	1.32	chromosome 13 open reading frame 15	C13orf15
0.021553166	1.29	oncostatin M	OSM
0.022203838	1.27	matrix metallopeptidase 12 (macrophage elastase)	MMP12
4.26E-08	1.26	early growth response 2 (Krox-20 homolog, Drosophila)	EGR2
4.39E-07	1.26	inhibin, beta A	INHBA
1.95E-04	1.26	plasminogen activator, urokinase	PLAU
0.004614992	1.24	cholesterol 25-hydroxylase	CH25H
8.81E-04	1.24	heat shock 70kDa protein 6 (HSP70B')	HSPA6
0.040088598	1.24	chemokine (C-C motif) ligand 8	CCL8
0.003044526	1.24	thrombomodulin	THBD
0.015809977	1.23	ribosomal protein L26	RPL26
0.038325205	1.23	matrix metallopeptidase 19	MMP19
0.041530196	1.22	heat shock 70kDa protein 6 (HSP70B')	HSPA6
1.08E-05	1.22	chromosome 15 open reading frame 48	C15orf48
9.26E-07	1.22	interleukin 27	IL27
5.25E-04	1.21	activating transcription factor 3	ATF3
0.011510745	1.20	G protein-coupled receptor 77	GPR77
7.92E-06	1.20	tubulin, beta 2A	TUBB2A
0.001421809	1.20	metallothionein 1X	MT1X
0.002276117	1.20	peptidylprolyl isomerase A (cyclophilin A)	PPIA
Top 25 downregulated genes following 2 h HIV-1 infection			
	Fold change	**Description**	**Gene ID**
1.2448239	1.24	glycophorin C (Gerbich blood group)	GYPC
0.012615548	1.21	zinc finger, X-linked, duplicated B	ZXDB
1.18E-05	1.21	suppressor of tumorigenicity 20	ST20
0.008053494	1.21	similar to Zinc finger protein 626	LOC100128975
3.76E-05	1.20	interferon stimulated exonuclease gene 20kDa	ISG20
0.005056289	1.20	ankyrin repeat domain 20B	ANKRD20B
0.031824227	1.19	pyridoxal-dependent decarboxylase domain containing 2	PDXDC2
8.98E-04	1.19	tumor protein p63 regulated 1	TPRG1
4.22E-04	1.18	insulinoma-associated 1	INSM1
0.031824227	1.17	ribosomal protein L18a	RPL18A
1.70E-07	1.17	regulator of G-protein signaling 1	RGS1
0.006834392	1.17	SMT3 suppressor of mif two 3 homolog 4 (S. cerevisiae)	SUMO4
1.46E-06	1.17	zinc finger protein 331	ZNF331
7.06E-04	1.17	spastic ataxia of Charlevoix-Saguenay (sacsin)	SACS
0.002011435	1.17	endothelin 1	EDN1
5.85E-06	1.17	activin A receptor, type IC	ACVR1C
1.41E-05	1.17	immunoglobulin superfamily, member 3	IGSF3
2.98E-05	1.17	neurogranin (protein kinase C substrate, RC3)	NRGN
0.008439591	1.16	aldehyde dehydrogenase 7 family, member A1	ALDH7A1
4.70E-06	1.16	solute carrier family 2 (facilitated glucose transporter), member 14	SLC2A14
3.07E-06	1.16	interferon regulatory factor 2	IRF2
4.85E-05	1.16	SPECC1-like | adenosine A2a receptor	SPECC1L
3.20E-04	1.16	nuclear factor of activated T-cells 5, tonicity-responsive	NFAT5
0.026685957	1.16	F-box protein 5	FBXO5
0.012962321	1.15	nuclear receptor coactivator 2	NCOA2

Table 3.13. Differentially regulated genes following 24 h LPS activation

Top 10 upregulated genes following 24 h LPS activation			
P value	**Fold change**	**Description**	**Gene ID**
1.50E-11	83.46	cytokine receptor-like factor 2	CRLF2
3.29E-11	74.24	chemokine (C-C motif) ligand 5	CCL5
8.88E-11	70.49	interleukin 2 receptor, alpha	Il2RA
2.66E-11	67.76	tumor necrosis factor, alpha-induced protein 6	TNFAIP6
5.85E-12	67.65	claudin 1	CCL19
4.37E-10	56.03	chromosome 13 open reading frame 15	CCR7
1.92E-11	55.41	oncostatin M	EBI3
2.61E-12	45.61	matrix metallopeptidase 12 (macrophage elastase)	RSAD2
2.33E-12	45.09	early growth response 2 (Krox-20 homolog, Drosophila)	USP18
1.92E-11	43.73	inhibin, beta A	TNFRSF9

Top 10 downregulated genes following 24 h LPS activation			
P value	**Fold change**	**Description**	**Gene ID**
2.04E-06	104.03	coagulation factor XIII, A1 polypeptide	F13A1
3.29E-11	74.42	CD1a molecule	CD1a
2.46E-06	45.58	mannose receptor, C type 1	MRC1
5.53E-09	41.93	CD1c molecule	CD1C
5.36E-10	34.71	C-type lectin domain family 10, member A	CLEC10A
4.35E-10	30.17	chromosome 1 open reading frame 162	C1orf162
6.57E-08	30.01	Rho GDP dissociation inhibitor (GDI) beta	ARHGDIB
6.03E-08	26.96	CD36	CD36
5.88E-09	25.66	GLI pathogenesis-related 1 (glioma)	GLIPR1
4.82E-07	25.36	membrane-spanning 4-domains, subfamily	MS4A6A

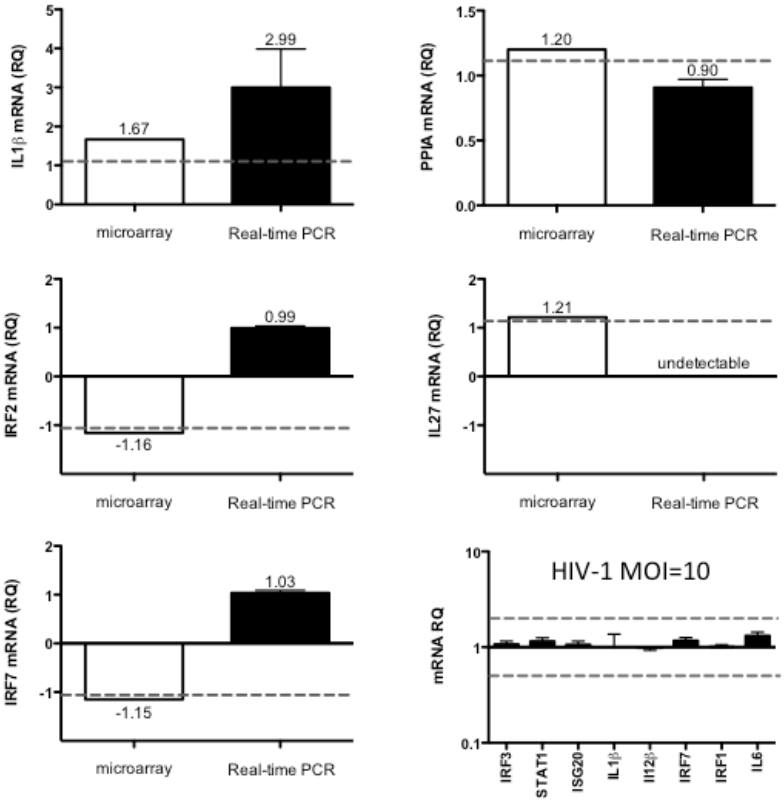

Figure 3.15. Validation of differential expression of a selected set of genes from the microarray by real time PCR. Measuring the mRNA expression of indicated genes by real-time PCR using the same mRNA that was used for the array analysis. Expression is normalized against GAPDH and mock control. Data is from four donors and presented as means ± SEM. For each gene the value obtained by micro array analysis is also shown. The last graph shows changes in interferon and inflammatory genes in HIV-1-infected DCs infected with a higher MOI of 10, values are obtained by real-time PCR in three different donors.

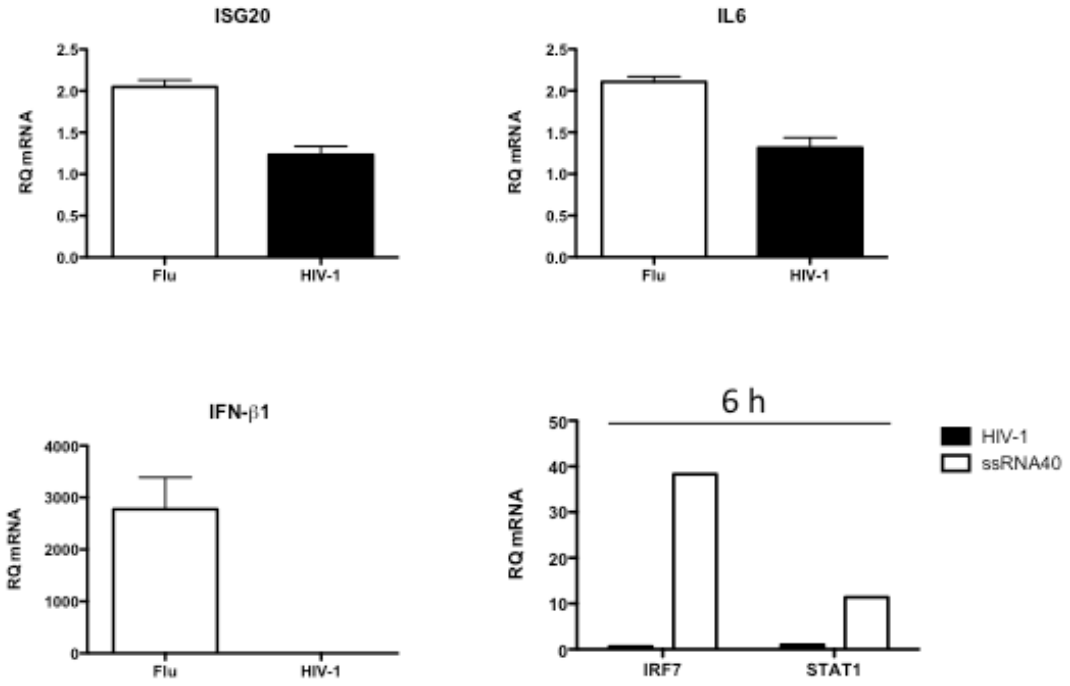

Figure 3.16. Comparison of interferon genes in DCs infected with HIV-1, Influenza and HIV-1 derived TLR8 ligand. DCs were infected with HIV-1 or Influenza PR8 or mock for 2 h and processed for real-time PCR analysis. Relative expression of ISG20, IL6 and IL1β was calculated normalized to GAPDH and mock control. Values for Flu are three technical replicates from one donor and representative of values obtained for two donors. For TLR8 activation DCs were activated with 2.5μg/ml ssRNA40 and lyovec control for 2 h, washed and incubated for another 4 h before real-time PCR analysis. HIV-1-infected DCs harvested 6 h p.i. were analyzed in comparison.

3.4 Discussion

To summarise, the work described in this chapter attempts to carry out a comprehensive characterization of the early HIV-1 signalsome in DCs. It used a novel phosphoproteomics protocol combining phosphoprotein affinity-column enrichment, off-gel IEF and LC-MS/MS to identify differentially phosphorylated proteins in primary MDDCs following HIV-1 infection. Furthermore, a novel bioinformatics analysis consisting of rigorous identification criteria as well as spectral index quantification was employed to characterize the number of candidate targets for phosphorylation and dephosphorylation downstream of HIV-1 infection with high confidence. To complement the characterization of the HIV-1 proteome, purified HIV-1 virus was

analyzed for the expression of host proteins by LC-MS/MS and the transcriptional profile of HIV-1-infected DCs was analyzed by microarray. Altogether, the results of these three screens strongly indicate that the virus orchestrates a remarkable interaction with the host cell without alerting the cell's innate immune defences of its own presence.

Rather surprisingly, it was found that HIV-1 induces a robust signalosome within only 10 minutes of infection. This is intriguing for a number of reasons, all indicating that this signalosome may be part of an immune evasive strategy of the virus: 1. HIV-1 fails to induce maturation of DCs (Hodges et al., 2007). 2. HIV-1 does not induce a rapid antiviral or inflammatory response one would expect from the recognition of a ssRNA virus ((Manel et al., 2010), and the microarray study presented here). 3. In contrast to other cell types such as activated CD4+ T cells, HIV-1 infection of DCs and macrophages is poorly efficient, a process recently recognized to be at least in part due to the myeloid specific restriction factor SAMHD1 and its ability to control cellular dNTPs and hence viral transcription (Goldstone et al., 2011; Laguette et al., 2011). 4. HIV-1 is readily detectable within DCs within an hour of infection and known to survive in a non-lysosomal compartment (Garcia et al., 2005; Piguet and Steinman, 2007). The general impression therefore is of a virus that succeeds in using a vast array of different cellular host factors to remain undetected allowing it to promote dissemination. This is supported by the abundance of molecules involved in macro and microautophagy, neural synapse formation and vesicular trafficking within the HIV-1 phosphoproteome and the paucity of signaling molecules downstream of PAMP recognition and upstream of interferon and inflammatory cytokine signaling. The virus may actively hijack vesicular trafficking pathways to bypass lysosomal degradation and hereby antigen presentation, and traffic via a non-lysosomal compartment to the virological synapse to infect target cells. The following chapter will provide further supporting evidence for this model.

In this phosphoproteomic study, I combined several technical approaches to characterize the HIV-1 phosphoproteome with high confidence, evident by the high proportion of validated differentially phosphorylated proteins on immunoblots of targets tested. Additionally, the relative ease, reproducibility and feasibility of carrying out this protocol in primary cells, underscores the versatility of this approach for the identification of further signaling pathways. Indeed, this method has since been used in

our group to characterize novel signalosomes, one of which has focused on the TLR8 signalosome to dissect the HIV-1 signalosome (Al Leslie). Technically there have been great advances since this work was carried out, e.g. the recent introduction of isobaric peptide tags for relative and absolute quantification (iTRAQ) technology, which represents a major breakthrough in quantitative proteomics by facilitating accurate quantitation of peptides and proteins across conditions in primary, non-dividing cells (Jones and Nuhse, 2011). It would be interesting to repeat this experiment using iTRAQ technology and compare the phosphoproteome of DCs infected with VSV-pseudotyped HIV-1 for instance that may pinpoint the changes induces by the interaction of the viral envelope with the cell. Furthermore, a timecourse experiment starting from as early as 1 min p.i. may aid in discerning the route the virus takes within the cell.

As mentioned in the introduction earlier, most HIV-1 proteomic studies are based on affinity tagging and purification mass spectrometry, whereby the interaction of singular viral proteins with host proteins are mapped with high confidence and then the relevance of these proteins in the viral life cycle are inferred from biological studies. While these studies are highly informative, a major drawback is that they are mostly carried out in cell lines that are not the natural target cells of the virus. Further, the interaction of whole virion with the host cell may differ from the effect that single viral proteins may exert. For instance, microarray studies of DCs expressing HIV-1 tat via adenovirus-mediated gene transfer delivery show expression of interferon-response genes (Izmailova et al., 2003), a finding that has not been confirmed in DCs infected with HIV-1 (Manel et al., 2010).

To my knowledge, this is the first phosphoproteomic study of HIV-1-infected cells. A further great advantage is that this study focused on primary MDDCs that have such important role in HIV-1 pathogenesis. Given the high proportion of trafficking molecules in the HIV-1 signalosome, it would be informative to carry out a comparable study of DCs exposed to phagocytic beads (Handley et al., 2005) to map the physiological endocytic route in DCs and identify pathways actively recruited by HIV-1 to enter DCs without being recognized as a danger "non-self" signal.

A fairly recent discovery within the signaling field is the close interplay between signaling mediators and trafficking molecules, whereby trafficking molecules directly influence the localization of PRR or other signaling intermediates, thereby controlling the outcome of the signaling cascade via compartmentalization of members of the

signaling complex (McGettrick and O'Neill, 2010; Sasai et al., 2010). Interestingly, PRAT4A, a transport protein implicated in chaperoning TLR4 and endosomal TLR trafficking (Takahashi et al., 2007), was found to be differentially phosphorylated by HIV-1, indicating that it may play a role in HIV-1 recognition, either as part of TLR8-mediated recognition or an unknown sensor.

Another interesting finding from this work is the assessment of the total protein composition of HIV-1 viral particles by LC-MS/MS and the sheer number of identified proteins. HIV-1 (Chertova et al., 2006), like some other viruses such as Influenza and Filovirus (Shaw et al., 2008; Spurgers et al., 2010), is known to incorporate host proteins during its life cycle. The high number of identified proteins is most likely due to the high sensitivity of the LC-MS/MS platform used, however it is difficult to differentiate between proteins truly incorporated into viral particles from viral and cellular exosomes or impurities in the sample. Over-representation of cellular functions involved in cell maintenance and assembly as well as endocytic pathways as assessed by IPA are strongly suggestive of a predominant non-random incorporation of host proteins into virions. It would be fascinating to repeat this experiment with the Orbitrap machine with virions produced in primary cells, such as MDDCs as well as virions transferring across the VS via *trans*-infection and complement these studies with functional experiments to assess the role of these proteins in viral life cycle.

Altogether the work presented here is the fist phosphoproteomic study of HIV-1-infected DCs and demonstrates that HIV-1 triggers a remarkable signalosome within 10 min of infection without inducing an antiviral interferon response. The remaining two chapters will assess the role of some of these proteins in HIV-1-mediated immune evasion and DC biology.

Chapter 4

Characterization of Host Factors required for HIV-1 *trans*-infection

4.1 Introduction

Phosphoproteomic analysis of the HIV signaling complex showed an abundance of proteins involved in trafficking and cytoskeletal pathways. Over 30% of the proteins encoded by the human genome deliver to secretory and endocytic pathways (Wang et al., 2010b). Tight control of the convergence between organelle trafficking, maturation of intracellular compartments and signaling pathways ultimately controls the homeostasis and the execution of regulatory mechanisms (Blander and Medzhitov, 2004). Viruses such as HIV-1 have developed intricate strategies to exploit the host cell's endocytosis and secretory pathways to facilitate their release in a temporally and spatially coordinated manner to target cells. Here, the process of *trans*-infection mediated by DCs across virological synapses provides a novel mechanism of viral transmission. DCs that have captured and sequestered HIV-1 in an infectious form hereby act as "Trojan horses" for incoming virions to reach target CD4 T cells (Greene and Peterlin, 2002; Piguet and Blauvelt, 2002). The precise molecular machinery underlying the actual transfer of virus from DCs to CD4+ T cells via the protective *trans*-compartment is still unknown.

Characterization of a virological synapse between DCs pulsed with fluorescent virions and uninfected CD4+ T cells demonstrated polarization of virions to the DC-T cell contact zone with enrichment of CD4 and chemokine coreceptors on the T cell side (McDonald et al., 2003). Early immunofluorescence studies of the trans-compartment demonstrated transient colocalization of HIV-1 with the transferrin receptor (a marker for recycling endosomes), suggesting a role for the endocytic pathway in HIV-1 transfer

(Kwon et al., 2002). A fraction of internalized virions were trapped inside DCs for at least 4 hours without entering lysosomal degradative compartments (Garcia et al., 2005; Kwon et al., 2002; Turville et al., 2004). Classical markers of the endosomal pathway were shown to be not useful for delineating this compartment, based on lack of colocalization between HIV-1 particles and markers for early endosomes, recycling endosomes, classical late endosomes, lysosomes, the trans-golgi network and the MHC class II compartments (Garcia et al., 2005). In LPS-matured MDDCs HIV-1 was internalized into a distinct vesicular compartment characterized by a mildly acidic pH of 6.2, similar to that of early endosomes but distinct from late endosomes and lysosomes (Garcia et al., 2005). Virus retained at this pH was more infectious than virus incubated at more acidic or neutral/alkaline conditions, suggesting that correct trafficking of HIV-1 though the endosomal compartments is important for viral transmission (Garcia et al., 2005; Kwon et al., 2002).

The compartment was further characterized by the presence of the tetraspanins CD81, CD82 and CD9 (Garcia et al., 2005), which upon contact with uninfected CD4 target cells relocated along with intracellular pools of virus quickly to the VS, supporting the notion that HIV-1 may follow a similar trafficking pathway that CD81 uses to traffic to the immunological synapse. Moreover, this compartment was also present in LPS-activated MDDCs in the absence of HIV-1 (Garcia et al., 2005; Kwon et al., 2002), indicating that HIV-1 may target a pre-existing vesicular compartment in DCs. Given the unique antigen-processing function of DCs (Mellman and Steinman, 2001), this compartment may contribute to protection of HIV-1 from degradation and allow sufficient time for virus to disseminate via *trans*-infection pathway in mucosal tissues. In CD34-derived DCs the phagocytic pathway controls antigen degradation during cross presentation by maintaining alkalinization of the phagosomal lumen through the recruitment of the NADPH oxidase NOX2, hence preventing acidification and untimely antigen degradation (Savina et al., 2006). Acidification of intracellular organelles can also be prevented by preventing the recruitment of proton pump vacuolar ATPases to the compartment, a process that has been described for budding and accumulation of HIV-1 in viral assembly compartments in macrophages (Jouve et al., 2007). Altogether the unique features of the *trans*-infection pathway remain to be dissected in greater detail.

The essential role of DC-SIGN in the interaction of HIV-1 with myeloid DCs (addressed in chapter 1) cannot be reiterated enough, although recent data indicates that it may not be unique to HIV-1. Measles virus appears to coopt DC-SIGN expressing DCs as Trojan horses for viral transfer in a similar fashion to HIV-1 (de Witte et al., 2008), although viral transfer across the VS to CD150+ target cells is more efficient via the *cis* infection pathway (Koethe et al., 2012). Clinically the important role of DC-SIGN in HIV-1 recognition is supported by work showing that DC-SIGN variants are associated with increased mother-to-child transmission of HIV-1 due to the expression of DC-SIGN on CD163+ placental macrophages (Boily-Larouche et al., 2012).

4.2 Aims

The aims of this chapter are

- To investigate the biological relevance of proteins of the HIV-1 phosphoproteome in HIV-1 infection using a targeted RNAi screen
- To perform a molecular characterization of the *trans* compartment
- To identify novel host vesicular trafficking pathways used by the virus to promote its dissemination

4.3 Results

4.3.1 Set up of an RNAi screen to assess the role of the HIV-1 signalosome in HIV-1 infection

Differential phosphorylation of a protein per se does not allow conclusions about the role of this protein in the signaling pathway, in particular, if it is part of a pathogen-specific evasion strategy, a physiological immune response, a restriction factor or a simple bystander phenomenon. The HIV-1 phosphoproteome contained proteins belonging to various cellular functions, for the vast majority though the functional consequences of differential phosphorylation were unknown. To take the results of my phosphoproteomics data further, I decided to conduct a secondary screening assay based on the list of proteins that were differentially phosphorylated by the virus. I used a combination of bioinformatics and literature analysis and compiled a list of 120 proteins belonging to the HIV-1 phosphoproteome and implicated in either trafficking, ubiquitination, signaling, autophagy or neural synapse formation. Proteins with well-described HIV-1 interactions were excluded. RNA interference (RNAi) was used to study the loss-of-function phenotype of these proteins for investigation of their role in HIV-1 replication. For the reasons outlined earlier, HIV-1 *trans*-infection in a DC-CD4 co-culture system was used as a measure for viral infection. Figure 4.1 demonstrates the kinetics of *in vitro* HIV-1 infection of MDDCs and corroborates the role of the *trans* compartment in viral dissemination. DCs were transfected with Dharmacon smartpool siRNAs, known to deliver high knockdown results with minimal off target effects, using the Neon™ transfection system, a novel electroporation device that achieves satisfying levels of knockdown with minimal reduction of cell viability. Experience from our group had established the poor transfection efficiencies achieved with lipid-based transfection reagents in MDDCs. Nucleofection with the Amaxa™ system, a well established technique for transfection of DCs, is associated with high levels of cell toxicity, therefore precluding any standardization in cell numbers required for such a screen. A lentiviral based approach, although the most attractive, was not possible due

to time and manpower constraints. A lentiviral-based system would also have allowed to carry out an over-expression screen.

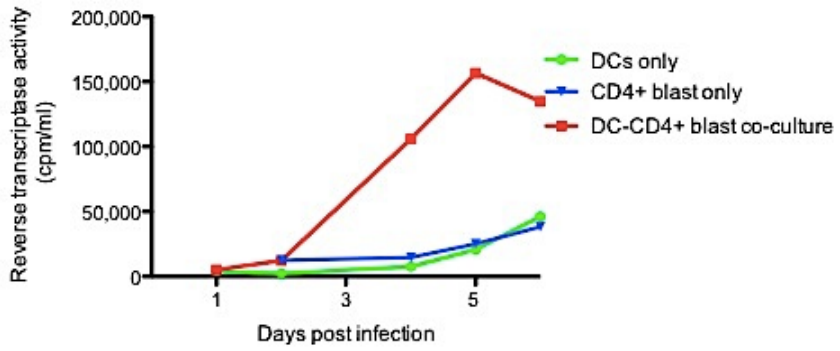

Figure 4.1: Kinetics of in vitro HIV-1 infection of MDDCs illustrates that HIV-1 replication is enhanced in a DC-CD4 co-culture system. Immature DCs were infected with NL4-3 BaL for 2 hours at an MOI of 0.1 followed by two wash steps to remove any unbound virus. Subsequently, they were either cultured alone in R10 or co-cultured with autologous PHA-activated CD4+ T cells at a ratio of 1:3 (DC:CD4). Supernatant was collected at indicated days and analysed for newly produced HIV-1 particles using a Quanti-RT kit, which detects HIV-1 Reverse transcriptase activity. For comparison, CD4+ PHA blasts were infected with HIV-1 and analysed for levels of productive infection (note, that the levels are lower than expected as NL4-3 BaL is a M-tropic strain). Addition of CD4+ blasts greatly accelerates and increases the levels of HIV-1 replication compared to DCs or CD4+ blasts infected with HIV-1 alone. One representative donor out of two is shown.

Due to the difficulties in performing such a screen in an automated platform in a BSL-3 facility, initial set up experiments were carried out to optimize and streamline conditions. The experimental workflow illustrated in figure 4.2 was the most reproducible and feasible approach. It allowed me to (i) employ a fluorescent-based and technically feasible readout in a non-automated format, (ii) achieve good levels of gene knockdown with minimal off target effects and no interferon induction, (iii) monitor for cell viability, (iv) work with small cell numbers and carry out technical and biological replicates.

Time course experiments were done to determine suitable times for efficient gene knockdown and robust flow cytometric detection of HIV-1 transfer to CD4 cells. Reproducible results were obtained in DCs that were infected 48 h after electroporation and harvested for measurement of viral transfer to CD4+ PHA blasts 72 h after infection. As already demonstrated contribution of de novo viral production by DCs is

negligible at this timepoint (figure 4.1). In brief, $75x10^3$ DCs were transfected with smartpool siRNA in triplicates in a 96 well plate, usually 24-48 genes were examined at each given experiment. 48 h later plates were washed and infected with NL4-3 BaL (MOI 0.1) in a final volume of 50 μl for 2 h, washed twice and co-cultured with $22.5x10^4$ autologous CD4+ T cell blasts before flow cytometry staining 72 h later. Levels of intracellular p24 gag in CD4+ cells for each siRNA were compared to levels obtained for non-silencing scrambled siRNA (Figure 4.3). To ensure target gene silencing a variety of commercially available fluorescently labeled non-targeting controls can be used, however experience in our group has shown that electroporation of DCs may result in unspecific uptake of these fluorescently-labeled siRNAs without any concomitant knockdown of the target gene. Therefore, downregulation of DC-SIGN was used as a positive control for knockdown efficiency (figure 4.3c). For each gene 3-4 independent experiments were done and the p24 gag+ population was calculated after gating on the live CD3+ T cell population relative to the p24+ population obtained for non-silencing siRNA.

A reduction in HIV-1 infection may be due to increased cell death, therefore in a secondary validation step a random selection of the genes modulating HIV-1 *trans*-infection were examined in a FACS based cell viability assay. I could not detect any significant increase in cell death 48 h following knockdown of the genes tested (table 4.4).

Obviously RNAi screens are fraught with inherent limitations (reviewed in (Bushman et al., 2009)). A number of criteria should be met for a gene to be recognized as important for HIV-1 replication: the level of reduction in mRNA and protein levels achieved with the RNAi technology used must be biologically possible; the protein must be sufficiently unstable to allow functionally significant reduction over the time period tested; the knockdown should not induce cellular toxicity; the function targeted should not be induced by multiple redundant genes or off target activities of the siRNA. The choice of smartpool siRNAs and the neon™ transfection methodology may have minimized, but certainly not completely resolved, some of these caveats and figure 4.4 demonstrates reasonable knockdown on a protein level for a selection of siRNAs tested. It was cost-prohibitive to test efficient knockdown for all 120 genes.

In summary, the data presented so far show the feasibility of performing a targeted RNAi screen to elucidate the role of host factors in HIV-1 *trans*-infection. Notably, this screen was carried out in primary cells.

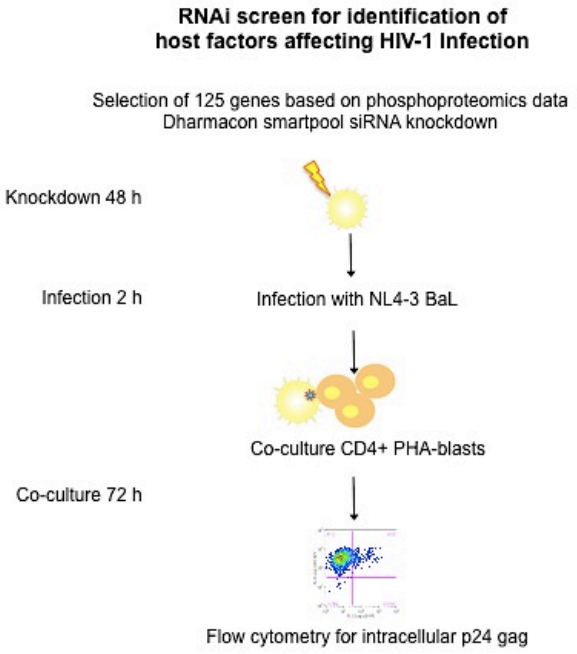

Figure 4.2. Multipronged approach to identify the early HIV-1 signalosome in dendritic cells. Workflow for the second part of the screen is shown. In brief, $75x10^3$ DCs were transfected in triplicates with Smartpool siRNAs and incubated in 96-well plates for 48 h, cells were washed and infected with NL4-3 BaL (MOI of 0.1) for 2 h. Cells were washed twice with media to remove any non-internalized virus. Finally, autologous CD4+ PHA blasts (blasted for 72 hrs) were added to each well at a ratio of 1:3 (DC:CD4). Three days later cells were stained for live dead and surface markers and intracellular p24 and analyzed by flow cytometry for intracellular p24 gag in CD4+ T cells.

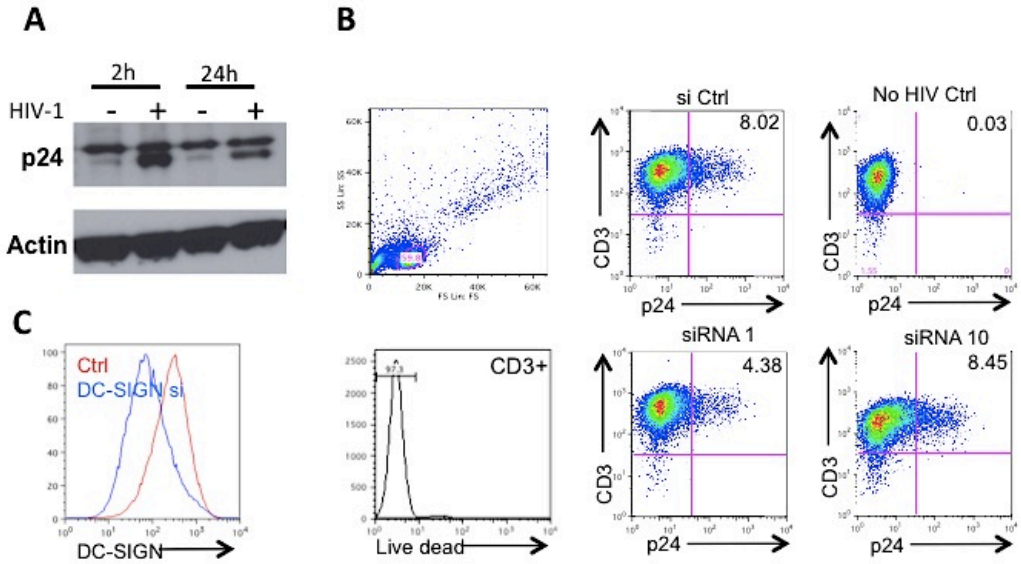

Figure 4.3. FACS-based screen for effect of genes on HIV-1 *trans*-infection in DC-CD4+ T cell co-culture. A. Western blot for p24 confirms detection of HIV-1 p24 gag in DCs 2 and 24 h post infection. **B.** Representative FACS plots of siRNAs with effect (siRNA 1) and no effect (siRNA 10) compared to control (si Ctrl) on HIV-1 *trans*-infection. **C.** Neon™ based transfection achieves reasonable levels of knockdown. DC-SIGN MFI values are 258 for Ctrl and 83 for DC-SIGN siRNA, respectively.

Table 4.1. List of genes tested in RNAi screen for effect on HIV-1 *trans*-infection.

Gene ID	>100%	76-100%	50-75%	25-49%
ADD1				**0.45 (0.11)**
ADD3			**0.59 (0.10)**	
AHCYL1	1.08 (0.10)			
AHNAK			**0.64 (0.08)**	
AKAP12		0.90 (0.20)		
AKT1			**0.69 (0.22)**	
ALOX15		0.88 (0.01)		
AP1B1			**0.58 (0.21)**	
ARL6AP5		0.83 (0.16)		
ARRB1		0.92 (0.23)		
ATG4B		0.90 (0.11)		
ATG7		0.76 (0.04)		
BAIAP2		0.97 (0.15)		
BLOC1S1		0.81 (0.13)		
BRCA1		0.92 (0.29)		
BRCC3			**0.60 (0.14)**	
CAND1				**0.44 (0.18)**
CAPNS1		0.82 (0.19)		
CARHSP1				**0.49 (0.01)**
CBL20		0.93 (0.26)		
CD74			**0.56 (0.19)**	
CHMP4B			**0.65 (0.16)**	
CLTA			**0.75 (0.15)**	
CNO		0.94 (0.15)		
CNPY3			**0.74 (0.15)**	
COPE	1.12 (0.30)			
CORO1B			**0.70 (0.18)**	
CTPS		0.77 (0.12)		
DBNL	1.04 (0.15)			
DPYSL		0.93 (0.12)		
DR1			**0.62 (0.10)**	
EIF2S1		0.83 (0.11)		
EIF4B		0.82 (0.19)		
EIF4G1			**0.74 (0.17)**	
ENO2			**0.73 (0.05)**	
EPB41L2	1.08 (0.05)			
EVL	1.1 (0.12)			
EZR		0.85 (0.03)		
FERMT3		0.80 (0.21)		
FLII		0.87 (0.04)		
FLNA			**0.75 (0.12)**	
G3BP1			**0.61 (0.18)**	
G3BP2			**0.72 (0.22)**	
GABARAP			**0.68 (0.1)**	
GC1QR		0.78 (0.21)		
GFPT1			**0.75 (0.04)**	
HCLS1		0.98 (0.23)		
HSD17B4		0.94 (0.25)		
HSPA8		0.90 (0.12)		
HSPB1			**0.66 (0.11)**	
KIAA1949		0.76 (0.07)		
KIF5B	1.04 (0.27)			
KPNA4			**0.70 (0.19)**	
LASP1			**0.60 (0.06)**	
LCP2	1.26 (0.25)			
LIMA1		0.79 (0.16)		
LIMS1			**0.54 (0.14)**	
LPP			**0.74 (0.17)**	
LRRFIP1			**0.63 (0.06)**	
MAP1S			**0.72 (0.07)**	
MAP2K1			**0.75 (0.03)**	

Gene ID	>100%	76-100%	50-75%	25-49%
MARCKS			**0.63 (0.12)**	
MSN			**0.61 (0.03)**	
MST		0.85 (0.10)		
MVD	1.48 (0.25)			
NCL			**0.61 (0.17)**	
NDRG2			**0.63 (0.08)**	
NPM1			**0.62 (0.16)**	
NUCB1			**0.73 (0.20)**	
NUMB	1.26 (0.28)			
OSBP			**0.70 (0.07)**	
OSTF1		0.94 (0.08)		
PA2G4	1.25 (0.30)			
PALLD		0.84 (0.16)		
PASP			**0.71 (0.24)**	
PCNP			**0.56 (0.21)**	
PEA15		0.90 (0.20)		
PEX19		0.95 (0.41)		
PLDN		0.94 (0.08)		
PLEK			**0.65 (0.03)**	
PPP1R7	1.05 (0.17)			
PPP4C		0.98 (0.06)		
PRKAR2A		0.85 (0.06)		
PRMT5		0.92 (0.18)		
PSAP			**0.71 (0.24)**	
PSMB6			**0.75 (0.2)**	
RAD23A		0.78 (0.20)		
RCC2	1.05 (0.16)			
RCN1		0.84 (0.03)		
RCSD1	1.07 (0.16)			
RINL		0.87 (0.22)		
RPS6		0.83 (0.14)		
RRAGA*			**0.68 (0.06)**	
RRAGC*	1.18 (0.25)			
S100A8		0.95 (0.05)		
S100A9	1.02 (0.32)			
SAMHD1	1.11 (0.21)			
SAMSN1			**0.72 (0.05)**	
SFRS3			**0.66 (0.06)**	
SHP-1	1.15 (0.25)			
SLC9A3R1	1.10 (0.20)			
SNRNP70	1.17 (0.13)			
SNX1		0.96 (0.05)		
SNX5			**0.75 (0.24)**	
SSB			**0.65 (0.12)**	
SSR4		0.92 (0.11)		
TCEB2		0.96 (0.12)		
TFG		0.98 (0.15)		
TLN1			**0.64 (0.06)**	
TOM1			**0.63 (0.04)**	
TUBA4A		0.81 (0.18)		
VASP			**0.70 (0.15)**	
VCL		0.82 (0.06)		
VCP			**0.70 (0.03)**	
VIM		0.95 (0.14)		
VPS4B				**0.40(0.07)**
WAVE2		0.82 (0.01)		
YBX1			**0.71 (0.17)**	
ZC3HAV1			**0.66 (0.18)**	
ZYX			**0.69 (0.09)**	

DCs were transfected with Smartpool siRNAs for indicated genes and control non-silencing siRNA, harvested 48hrs later and infected with NL4-3 BaL for 2 h, subsequently co-cultures with CD4+ PHA-blasts for 72 hours before analysis for intracellular p24 gag in CD4+ T cells. Values represent *trans*-infection as measured by intracellular p24 gag in CD4+ T cells relative to siRNA control. Values represent mean of 3-4 biological replicates $\pm$ SEM. * denotes double knockdown of RRagA+RRagB and RRagC+RRagD, respectively

Table 4.2. List of genes tested in RNAi screen causing more than 25% reduction in HIV-1 *trans-infection* with functional annotations.

Gene ID	Name	Function	Ref
ADD1	Adducin 1	Actin binding protein of membrane skeleton involved in synaptic remodelling. Phosphorylated by Protein kinase C.	(Stevens and Littleton, 2011)
ADD3	Adducin 3	Actin binding protein of membrane skeleton involved in synaptic remodelling. Bound by Calmodulin.	(Stevens and Littleton, 2011)
AHNAK	AHNAK nucleoprotein	Scaffold protein involved in Ca2+ signalling and phosphorylated by Protein kinase B.	(Matza et al., 2009)
AKT1	v-akt murine thymoma viral oncogene homolog 1	Serine-threonine protein kinase with anti-apoptotic function. Activated by tat, inhibited by vpr, dephosphorylated by env. Phosphorylated by mTOR.	(Hers et al., 2011)
AP1B1	Adaptor-related protein complex 1, beta 1 subunit	Part of cytoplasmatic coat of endosomal vesicles, mediates recruitment of clathrin to the membrane and recognition of sorting signals. Stabilized on endosomal membranes by nef by ARF1-dependent attachment.	(Coleman et al., 2006)
BRCC3	BRCA1/ BRCA2-containing complex, subunit 3	E3 ubiquitin ligase with role in the DNA damage response. Interacts with CAND1. Effector of Raf-1 (DC-SIGN signalosome) and implicated in positive regulation of p-Erk.	(Boudreau et al., 2007; Sowa et al., 2009)
CAND1	Cullin-associated and neddylation-dissociated 1	Positive regulator of CUL1-containing Cullin-RING ligases. Member of the *in vitro* nuclear interactome of tat.	(Gautier et al., 2009; Sowa et al., 2009)
CARHSP1	Calcium regulated heat stable protein 1, 24kDa	Cold shock domain containing protein binding RNA, dsDNA and ssDNA. Phosphorylated by AKT and mTOR	(Hou et al., 2011)
CD74	CD74 molecule, MHC, class II invariant chain	Part of MHC class II and important chaperone regulating antigen presentation. Upregulated by nef.	(Keppler et al., 2006)
CHMP4B	Charged multivesicular body protein 4B	Member of ESCRT III complex functioning in the sorting of endocytosed receptors into endosomes. Involved in budding of HIV-1 via interaction of ALIX1.	(Morita et al., 2011)
CLTA	Clathrin, light chain A	Main structural component of the cytoplasmic face of coated pits and vesicles, which entrap specific macromolecules during receptor-mediated endocytosis.	(McMahon and Boucrot, 2011)
CNPY3	Canopy 3 homolog	Chaperone with role in TLR localization. Associates with the immature form of TLR4 regulating its expression.	(Wakabayashi et al., 2006)

CORO1B	Coronin, actin binding protein, 1B	WD repeat-containing actin-binding protein that regulates cell motility and lamellopodia formation in concert with Arp2/3 complex and Cofilin. Phosphorylated by AKT1.	(Cai et al., 2005)
DR1	Down-regulator of transcription 1, TBP-binding	TATA box binding phosphoprotein inhibiting the assembly of the preinitiation complex and controlling the rate of RNA polymerase II transcription.	(Gilfillan et al., 2005)
EIF4G1	eukaryotic translation initiation factor 4 gamma, 1	Facilitates recruitment of mRNA to ribosome facilitating translation. Cleaved by poliovirus and HIV-1 protease.	(Alvarez et al., 2003)
ENO2	Enolase 2	Neuron-specific isoenzyme of metalloenzyme responsible for the catalysis of the penultimative step of glycolysis.	(Guo et al., 2005)
FLNA	Filamin A, alpha	Regulates actin linked caveloae dynamics and crosslinks actin filaments to membrane glycoproteins. Interacts with gag to regulate assembly	(Cooper et al., 2011)
G3BP1	GTPase activating protein (SH3 domain) binding protein 1	Nuclear RNA-binding protein and member of the Ras signal transduction pathways. Involved in stress granule assembly. Co-opted by HCV for viral replication	(Yi et al., 2011)
G3BP2	GTPase activating protein (SH3 domain) binding protein 2	May control NF-κB signaling by retaining IκB/NF-κB complexes in the cytoplasm. Involved in stress granule assembly.	(Cristea et al., 2010)
GFPT1	glutamine-fructose-6-phosphate transaminase1	Rate-limiting enzyme in the hexoamine biosynthetic pathway with a potential role in autophagy.	(Behrends et al., 2010)
HSPB1	heat shock 27kDa protein 1	Small heat shock protein involved in multitude stress related of cellular processes, including ubiquitination, autophagy, actin reorganization and signalling.	(Arrigo et al., 2007)
KPNA4	karyopherin alpha 4 (importin alpha 3)	Cytoplasmic proteins that recognize nuclear localization signals docking them to the nuclear pore complex. Interacts with integrase contributing to nuclear import and viral replication.	(Ao et al., 2010)
LASP1	LIM and SH3 protein 1	Actin binding protein involved in cytoskeletal organization and CXCR2-mediated chemotaxis.	(Raman et al., 2010)
LIMS1	LIM and senescent cell antigen-like domains 1	Adaptor protein involved in integrin signalling and integrin mediated cell adhesion. Found in focal adhesion plaques.	(Ito et al., 2010)
LPP	LIM domain containing preferred translocation partner in lipoma	Actin cytoskeleton protein related to zyxin Localizes in focal adhesions as well as in cell-to-cell contacts. Binds VASP, a protein implicated in the control of actin organization.	(Petit et al., 2000)

LRRFIP1	leucine rich repeat (in FLII) interacting protein 1	Cytosolic nucleic acid-binding protein mediating type I interferon production via beta-catenin activation. Phosphorylated in response to immunologic stimuli and directed to lysosomal structures.	(Yang et al., 2010)
MAP1S	microtubule-associated protein 1S	Positive regulator of autophagosomal biogenesis and degradation.	(Xie et al., 2011)
MARCKS	myristoylated alanine-rich protein kinase C substrate	Actin filament crosslinking protein involved in cell motility, phagocytosis, and membrane trafficking. Phosphorylation by protein kinase C or binding to calcium-calmodulin inhibits its association with actin.	(Yamaguchi et al., 2009)
MSN	Moesin	Member of ERM family, which includes ezrin and radixin and is phosphorylated by env. Localizes to filopodia and other membranous protrusion important for cell-cell recognition and movement.	(Kubo et al., 2008)
NCL	Nucleolin	A nuclear phosphoprotein involved in ribosome synthesis. Recently identified as an entry receptor for RSV and Crimean-congo hemorrhagic fever virus.	(Tayyari et al., 2011)
NDRG2	NDRG family member 2	Member of the N-myc downregulated gene family, which belongs to the alpha/beta hydrolase superfamily. Downregulated during LPS-induced DC maturation and may modulate p38 MAPK phosphorylation and IL10 production.	(Choi et al., 2010)
NPM1	Nucleophosmin	Nuclear phosphoprotein interacting with tat and rev to promote their nuclear localization. In macrophages negative regulator of inflammatory cytokine production.	(Guery et al., 2011)
NUCB1	Nucleobindin 1	Member of a small calcium-binding EF-hand protein family. May have a key role in Golgi calcium homeostasis and Ca(2+)-regulated signal transduction events.	(Kapoor et al., 2010)
OSBP	oxysterol binding protein	Cholesterol binding scaffolding protein involved in vesicle transport.	(Xu et al., 2001)
PSAP	Prosaposin	Lysosomal highly conserved glycoprotein, which is a precursor for saposin A-D and localizes to lysosomes-maturing phagosomes May be part of nef mediated lipid raft recruitment.	(Krautkramer et al., 2004)
PCNP	PEST proteolytic signal containing nuclear protein	Novel PEST-containing nuclear protein with unknown function.	(Mori et al., 2004)
PLEK	Pleckstrin	A major substrate of protein kinase C in platelets and leukocytes. Appears to play an important role in exocytosis through a currently unknown mechanism.	(Ji et al., 2003)
SAMSN1	SAM domain, SH3 domain and nuclear localization signals 1	Immunoinhibitory signal inducing Rac1-dependent membrane ruffle formation and regulating cell spreading and polarization.	(von Holleben et al., 2011)
SSB	Sjogren syndrome antigen B (autoantigen La)	Involved in diverse aspects of RNA metabolism. Induced by HBV and HCV. Shields RSV ssRNA from RIG-I, abrogating early type I interferon response. May be involved in RISC-mediated mRNA cleavage. May be involved in viral release via lipid rafts in MuLV and HIV.	(Bitko et al., 2008; Liu et al., 2011; Shirasaki et al., 2010)

TLN1	Talin 1	Cytoskeletal protein and integral part of part of focal adhesion complexes. May be involved in tyrosine phosphorylation of paxillin and act with vinculin during retroviral infection	(Brown et al., 2011)
TOM1	target of myb1	Forms complex with Tollip and regulates endosomal trafficking of ubiquinated proteins. Recruits clathrin to endosomes. Regulates post-golgi trafficking and signalling, binds Tsg101.	(Katoh et al., 2004)
VASP	vasodilator-stimulated phosphoprotein	Member of the ENA-VASP family Associates with filamentous actin formation and filopodia formation.	(Vaggi et al., 2011)
VCP	valosin containing protein	ATP binding protein involved in vesicle transport and fusion, 26S proteasome function and assembly of peroxisomes. Essential for maturation of ubiquitin-containing autophagosomes.	(Meerang et al., 2011; Tresse et al., 2010)
VPS4B	vacuolar protein sorting 4 homolog B	ATPase associating with the endosomal compartment and involved in intracellular trafficking. Interacts with CHMP substrates to facilitate viral (HBV, HTLV1) egress and budding and release of endosomal vesicles. Recognizes ESCTR-III assemblies.	(Lambert et al., 2007; Stuchell-Brereton et al., 2007)
ZC3HAV1	zinc finger CCCH-type, antiviral 1	CCCH-type zinc finger protein that may inhibit infection by retroviruses and induce an innate immune response. Is an interferon-stimulated gene that is direct target of IRF. Inhibits HIV-1 infection by targeting spliced mRNA for degradation.	(MacDonald et al., 2007; Wang et al., 2010a; Zhu et al., 2011)
ZYX	Zyxin	Zinc-binding phosphoprotein concentrating at focal adhesions and modulating cytoskeletal organization of actin bundles. Interacts with LASP1.	(Li et al., 2004a)

Table. 4. 3. Cell viability assay excludes significant increase in cell death associated with the RNAi knockdown. MDDCs were electroporated with dharmacon smartpool siRNAs and ctrl siRNA with the neon™ electroporation system and assayed for cell viability 48 hours later with the Invitrogen live/dead stain kit. Values represent alive DCs relative to non-silencing siRNA and mean ± SEM of three independent experiments, * only one donor done.

Gene	Alive DCs (Relative to Ctrl)
Ctrl	1
ADD1	0.92 (0.03)
Ahnak1	1.02 (0.04)
AKT1	0.97 (0.03)
AP1B1	0.92 (0.06)
CAND1	0.99 (0.03)
CARHSP1	0.96 (0.03)
CHMP4B	0.94 (0.04)
DTNBP1	0.98 (0.01)
G3BP1	0.91 (0.02)
GABARAP	0.93 (0.03)
LASP1	0.98 (0.01)
LRRFIP1	0.95 (0.02)
RRAGA+RRAGB	0.91 (0.02)
SNAPIN	0.99 (0.01)
SNX5	0.96 (0.02)
SSB	0.91 (0.02)
TOM1	0.91*
VPS4B	0.99 (0.03)

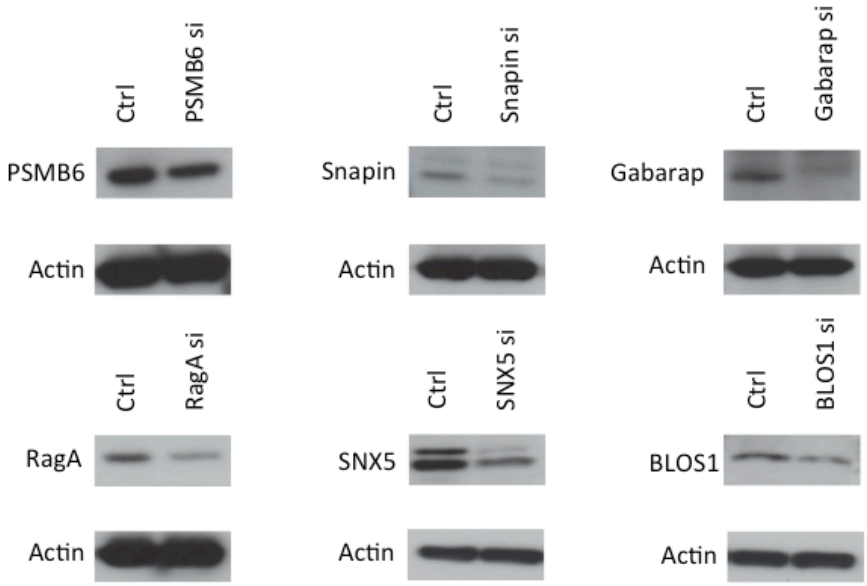

Figure 4.4. Testing knockdown efficiency following electroporation with selected siRNAs. DCs were electroporated with scrambled and specific siRNA using Neon transfection system and harvested 48 h later for immunoblot of proteins as indicated.

4.3.2 RNAi screen identifies multiple host factors reducing HIV-1 trans-infection by more than 25%

Of 125 genes tested, four genes reduced HIV-1 trans-infection by more than 50%, while another 51 displayed reproducible, but moderate activities with a reduction in HIV-1 *trans*-infection between 50-75% (figure 4.5). Tables 4.1 and 4.2 show results of the screen with relative frequencies and functional annotations, respectively.

Due to the non-automated, small scale nature of the screen an integrative statistical analysis based on z scores could not be performed. Given the difficulties in achieving complete knockdowns in DCs and potential donor-specific variabilities, low level but consistent reduction in HIV-1 transfer identified here were considered to be suggestive of an effect mediated by the gene. As each candidate host factor identified here was also differentially phosphorylated by HIV-1, I was fairly confident that my approach was correct.

ADD1, CAND1, VPS4 and CARHSP1 resulted in a reduction in HIV-1 *trans*-infection by more than 50%. Adducin 1 is a heterodimer consisting of related subunits that plays a role in actin-based cytoskeletal organization. Recent elegant work in the drosophila model suggests that phosphorylation-dependent regulation of adducins controls their level, localization and activity, hereby influencing actin-based synapse elaboration and spectrin-based synapse stabilization at the neuromuscular junction (Babic and Zinsmaier, 2011; Bednarek and Caroni, 2011). LC-MS/LC analysis had shown that HIV-1 triggered phosphorylation of ADD1 (table 3.1). The effect on HIV-1 *trans*-infection may therefore indicate a mechanism whereby the interaction of HIV-1 with ADD1 regulates stability and dynamics at the virological synapse.

But for instance the mechanism accounting for CAND1 mediated effect on HIV-1 *trans*-infection is less clear. CAND1 is a cullin binding protein that interacts with unneddylated cullins. In humans 7 cullin homologues form cullin ring ligases (CRL). Current models suggest that CRL complexes are controlled by cycles of CRL denyddelation and CAND1 binding (Bennett et al., 2010) and that these are instrumental for the control of most regulated protein turnover in eukaryotic cells, including protein degradation, cell signaling, transcriptional regulation, vesicle trafficking and immune response (Bosu and Kipreos, 2008). Although the interaction of CAND1 with cullin

proteins has been well characterized in structural and *in vitro* studies, the exact role of CAND1 in regulating E3 ligase activity *in vivo* is still unknown (Goldenberg et al., 2004; Petroski and Deshaies, 2005). CAND1 may have a role in diverting incoming virions from an ubiquitination pathway to the *trans* compartment. An alternative explanation may come from observations that suggest a role for CAND1 in inflammasome activation (Dr. Tom Monie, personal communication). LC-MS/MS showed phosphorylation of CAND1 by HIV-1.

Taken together using targeted RNAi for knocking down host factors within the HIV-1 signalosome, identifies multiple novel host proteins important in HIV-1 *trans*-infection from DCs to CD4 target cells.

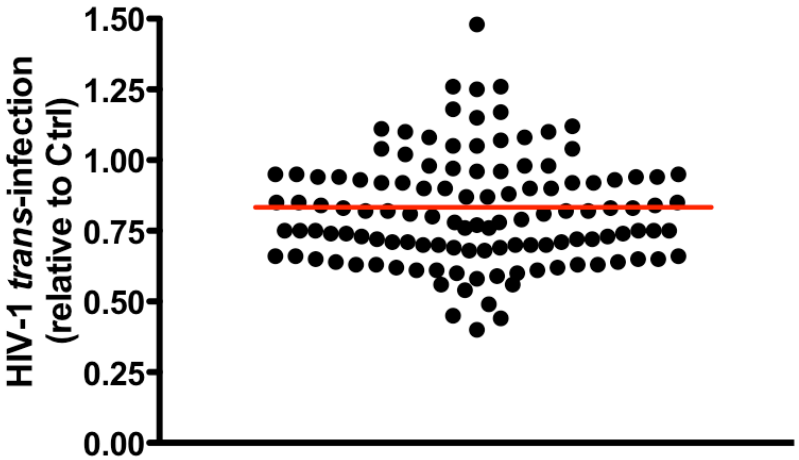

Figure 4.5. Dot-plot of RNAi screen for identification of genes affecting HIV-1 *trans*-infection. Each dot represents a single gene. Values are mean of 3-4 independent experiments. The red line indicates the population mean.

4.3.3 Bioinformatics analysis of host factors involved in HIV-1 *trans*-infection

To establish a system-level understanding of the host factors identified in the RNAi screen, I carried out bioinformatics analysis of all genes reducing HIV-1 *trans*-infection by more than 25% using ingenuity pathway analysis. Obviously, the screen is biased

towards cellular functions that formed the basis for the selection of the 120 genes. For example, unsurprisingly, 26 out of 55 genes affecting *trans*-infection were involved in trafficking (table 4.2) and more specifically in pathways such as integrin signaling, endocytosis and FAK signaling (figure 4.7a). Further, I curated network analysis with subcellular localization of these host factors. It became evident that HIV-1 recruits host proteins within 10 min of infection that fell into classes spanning multiple aspects of cell biology from RNA processing, DNA repair to neural synapse recycling and the exocytosis and secretory pathway (figures 4.6-4.8).

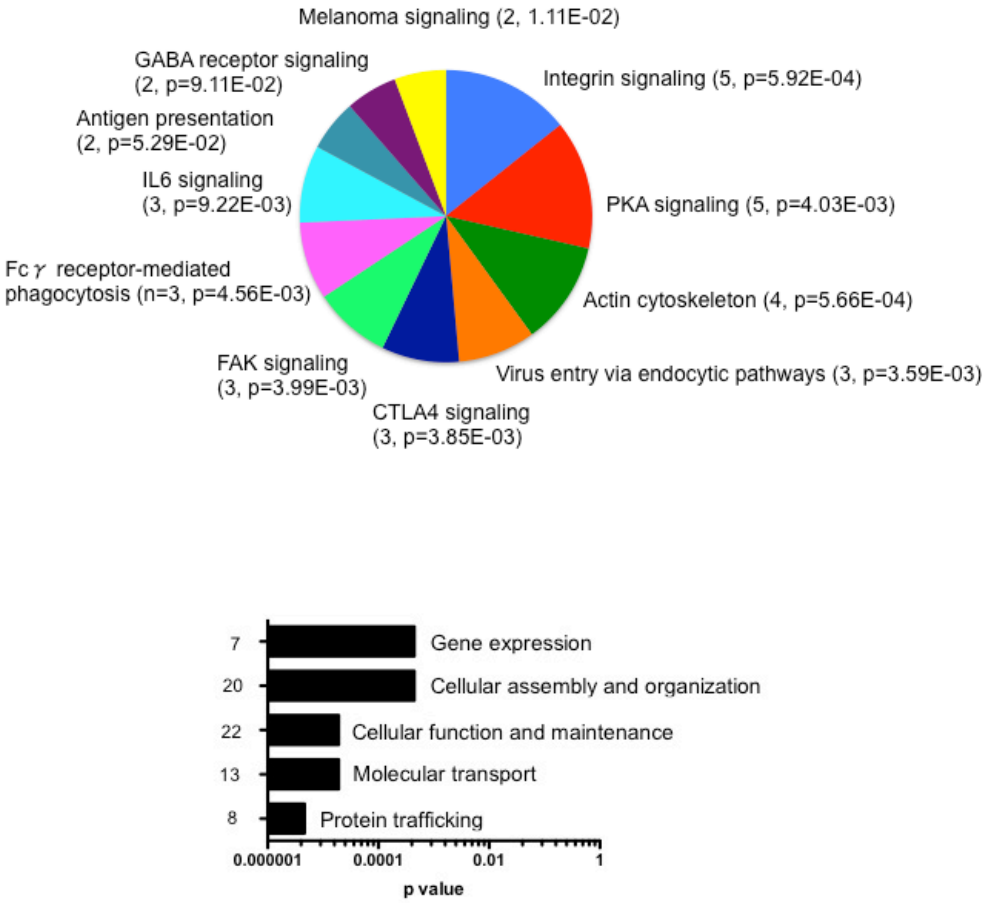

Figure 4.6. IPA classifying host factors affecting HIV-1 *trans*-infection by molecular function (top panel) and canonical pathways (lower panel).

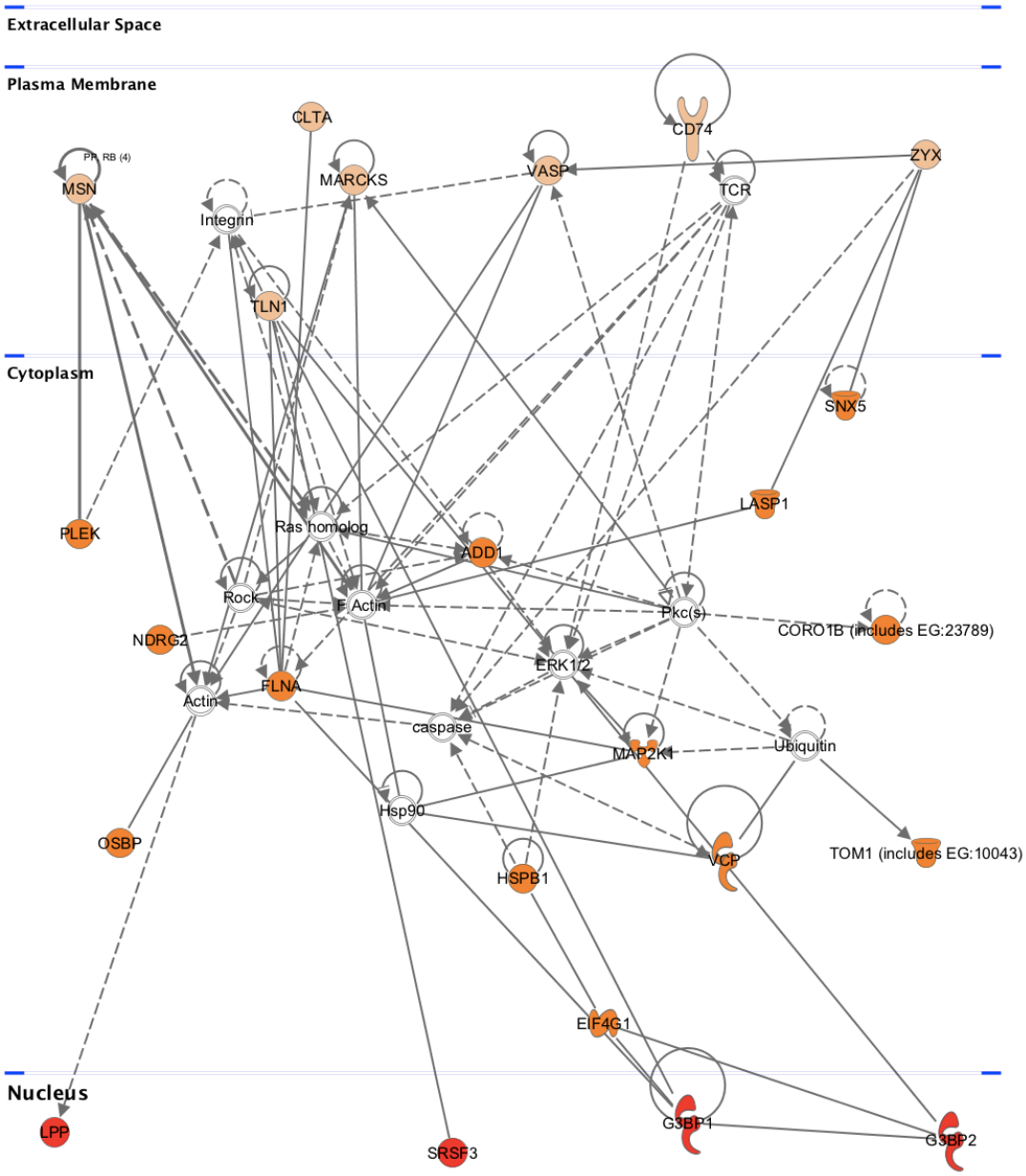

Figure 4.7. Top Network derived from functional analysis of the RNAi screen in IPA showing connections among proteins. Top network involving tissue and cell morphology, cellular assembly and organization is illustrated with a topological view clarifying the subcellular localization of the proteins. Coloured nodes are genes affecting HIV-1 *trans*-infection as identified by RNAi screen. Dashed lines are indirect interactions, others are direct interactions.

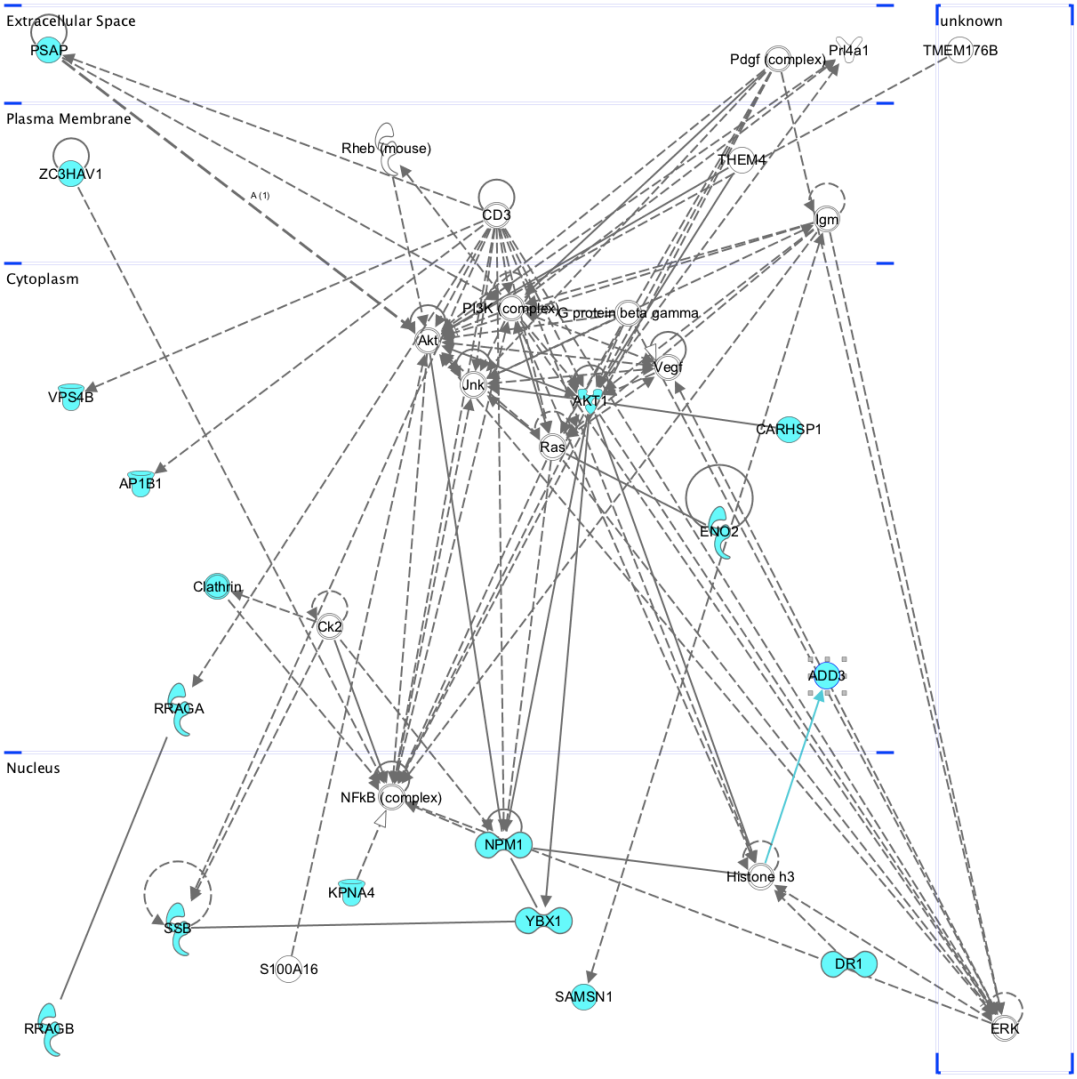

Figure 4.8. Second top network derived from functional analysis of the RNAi screen in IPA showing network involving connections among proteins. Network involving gene expression, infectious disease and organismal development is illustrated with a topological view clarifying the subcellular localization of the proteins. Coloured nodes are genes affecting HIV-1 *trans*-infection as identified by RNAi screen. Dashed lines are indirect interactions, others are direct interactions.

4.3.4 HIV-1 entry assay to elucidate the role of host factors involved in HIV-1 *trans*-infection

To investigate whether the reduction in *trans*-infection is due to an inhibition of HIV-1 entry into DCs, I set up a technically simple entry assay. I labeled purified NL4-3 BaL with a fluorescent dye that I could easily detect by flow cytometry. Confocal microscopy of fluorescent HIV-1-infected DCs confirmed that labeled virions had efficiently entered DCs two hours post infection (figure 4.9a). I chose some of the genes that had an effect on *trans*-infection and performed knockdown experiments. 48 hours post transfection DCs were infected with labeled HIV-1 for 2 hours, washed twice and incubated with trypsin to remove any surface bound virus before analysis by flow cytometry for expression of ATTO488 fluorescent HIV-1 staining. Figure 4.10b illustrates a representative example of results obtained. Knockdown of DC-SIGN was used as a positive control and led to a reduction in viral entry only between 50-80% of control. This may be due to inefficient knockdown of DC-SIGN, which is highly expressed on MDDCs (figure 4.9b). It may also be in keeping with the notion that DC-SIGN is not the sole mediator of HIV-1 attachment to DCs. Based on the results obtained with DC-SIGN, I set a cut-off of 25% control as an indicator of the gene playing a possible role in viral entry (figure 4.9c). Two genes reached the cut-off set: GABARAP and G3BP1.

Gamma-aminobutyric acid receptor-associated protein, GABARAP, a protein that belongs to the group of ATG8 related proteins with a crucial role in the autophagic process in yeast, possibly by facilitating hemi-fusion via elongation of the phagophore membrane (Abeliovich et al., 2000; Nakatogawa et al., 2007). It acts at a late stage of autophagosome formation possibly by sealing the autophagosomes (Weidberg et al., 2010). How GABARAP may selectively act on viral entry can only remain speculative at this point and certainly merits further investigation. It may be part of the machinery that mediates viral entry via endocytosis and endosomal fusion (Miyauchi et al., 2009). Altogether, RNAi mediated knockdown of GABARAP reduced HIV-1 *trans*-infection (table 4.1) and HIV-1 triggered phosphorylation of GABARAP (table 3.1). It would be interesting to study the co-localization of HIV-1 in DCs deficient of GABARAP with

other endo-lysosomal markers to define the role of this protein in viral fusion as well as formation of the *trans* compartment.

GTPase activating protein-binding protein 1 (G3BP1) is a recognized component of stress granules and involved in replication of Arenaviruses and HCV (Baird et al., 2012; Yi et al., 2011). It binds RNA/RNA duplexes and RNA/DNA duplexes, and specifically binds the SH3 domain of Ras-GTPase-activating proteins and is part of the Ras signal transduction pathway. Interestingly the Ras-PI3K signaling pathway has been implicated in clathrin-independent endocytosis and the internalization of influenza (Fujioka et al., 2011). Additionally, G3BP1 is recruited to sites of integrin ligation, where it potentially plays a role in cytoskeletal organization (Meng et al., 2004). Hence, G3BP1 may act on several steps of the HIV-1 entry process. Altogether this screening assay demonstrates that out of a selection of 16 genes tested only 2 had an effect on HIV-1 entry to DCs. Although the effect observed was modest, it is nevertheless interesting and reveals an unexpected role for these proteins in viral entry. It is noteworthy that the exact mode of HIV-1 entry to DCs is still unresolved (chapter 1). Given the known function and intracellular localization of these proteins it is likely that they exert their function during entry into the endosomal compartment. A further, and better strategy to specifically address the role of these proteins in viral entry would be a fusion assay using a β-lactamase dye assay, where β-lactamase-vpr chimeric proteins are incorporated into HIV-1 virions and their delivery into the cytoplasm is measured by the enzymatic cleavage of a fluorescent dye (Cavrois et al., 2002).

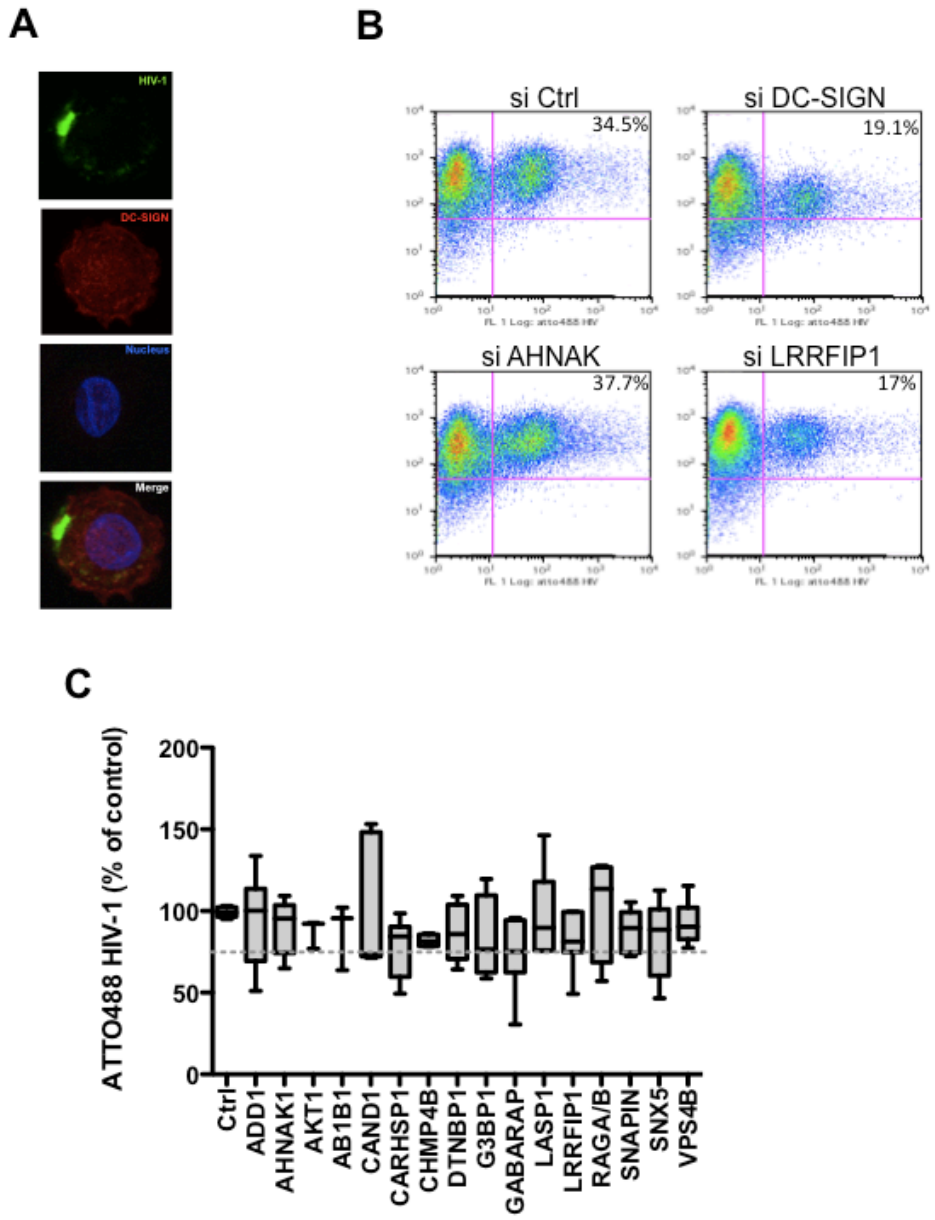

Figure 4.9. Identification of genes that reduce HIV-1 entry to MDDCs. (A) (A) Entry of Atto488 labeled HIV-1 was confirmed by immunofluorescence. **(B)** MDDCs were transfected with siRNAs of genes identified in siRNA library screen to reduce HIV-1 infection, 48 h post transfection cells were infected with ATTO488 labeled HIV-1 for 2 h and analyzed by flow cytometry. Representative FACS plots shown. **(C)** Summary of all genes tested for entry relative to control. Data are depicted as box and whisker plots. Data are from 3 independent experiments.

4.3.5 Identification of novel members of the autophagy machinery in HIV-1 signaling

The HIV-1 phosphoproteome contained multiple components of the autophagy machinery. These were included in the RNAi screen to elucidate their role in HIV-1 infection. The screen revealed that knockdown of 12 out of 24 autophagy proteins tested reduced HIV-1 *trans*-infection (table 4.4). As such this was not surprising, HIV-1 is known to inhibit autophagy to regulate innate and adaptive immunity in DCs (Blanchet et al., 2010). However, firstly most of the proteins identified had not previously been described in viral infection, suggesting a complex interaction of HIV-1 with the autophagy machinery. A notion, which was supported by bioinformatic analysis of these proteins (figure 4.10). Secondly, their selective recruitment by the virus so early upon exposure supported the notion that the entering virus usurps members of the autophagy machinery to divert virions away from degradation into the *trans* compartment.

Noteworthy among these proteins are target of myb1, TOM1, a cytosolic protein with yet unknown function, that forms a complex with Tollip, a ubiquitin-binding protein known to interact with several TLRs and IL1R signaling. It recruits clathrin to the endosomal membrane resulting in lysosomal targeting of ubiquitin-conjugated proteins (Katoh et al., 2006). HIV-1 phosphorylated TOM1 within 10 min of infection (figure 3.11) and TOM1 knockdown reduced *trans*-infection (table 4.1).

Furthermore, valosin-containing protein (VCP) is an ATPase with described roles in the proteasomal and ER-associated degradation pathway (ERAP), assembly of peroxisomes as well as vesicle transport and fusion (Bug and Meyer, 2012). Its identification as a regulator of the *trans*-infection pathway may be quite fascinating and certainly warrants further investigation. It associates with clathrin and interestingly is required for poliovirus replication to interfere with cellular protein secretion (Arita et al., 2012). In HIV-1 infection down-regulation of CD4 partially occurs via VCP-mediated ERAP (Magadan et al., 2010). However, its interaction with HIV-1 may be more complex given recent work, which sheds light on a number of crucial cellular functions of VCP. Firstly, two groups established an important role for VCP in the endocytic pathway. Ritz

et al showed an interaction between VCP or its partner UBXD1[1] and Caveolin, with ubiquitination of Caveolin, accumulation of enlarged endosomes and a defect in ILV formation upon VPS inhibition or knockdown (Ritz et al., 2011). Ramanathan and Ye demonstrated that the early endosomal antigen 1 (EEA1) was a substrate for VCP, whereby VCP knockdown results in enlargement of the early endosome and perturbation in endocytic cargo trafficking (Ramanathan and Ye, 2012). Despite distinct mechanisms emanating from these two studies, both establish VCP as a key player in endosomal trafficking and ILV formation. Generally VCP appears to be a player at the intersection between autophagy, ubiquitination and the DNA damage response (Ju and Weihl, 2010; Meerang et al., 2011).

Table 4.4 Effect of proteins belonging to the autophagy machinery on HIV-1 *trans*-infection

Autophagy proteins with NO effect on HIV *trans*-infection	Autophagy proteins with effect on HIV *trans*-infection
ATF4B	AKT1
ATG7	BLOC1 complex (Snapin)*
BAIAP2	BLOC1 complex (DTNBP1)*
CAPNS1	BRCA1
EIF2S1	EIF4G1
EIF4B	GABARAP
HSPA8	RRAGA/B
KIF5B	TOM1
RPS6	VCP
RRAGC/D	YBX1
S100A8	MAP1S
S100A9	MAP2K1

* see 4.3.7

A further interesting set of proteins that were differentially phosphorylated by HIV-1 are the Ras-related GTP-binding proteins RRAGB and RRAGC, whereby HIV-1 differentially phosphorylated both RagB and RagC (figure 3.11). These Rag GTPases are essential in mTORC1 activation by mediating translocation of mTORC1 to the lysosomal surface in response to amino acid signaling (figure 4.11) (Sancak et al., 2010). Mammals express four Rag proteins —RagA, RagB, RagC, and RagD— that form heterodimers consisting of RagA or RagB with RagC or RagD. RagA and RagB, like RagC and RagD, are highly similar to each other and are functionally redundant

[1] UBXD1 – UBX-domain containing protein, VCP co-factor with two VCP binding domains, involved in substrate recruitment and hence activity regulation of VCP

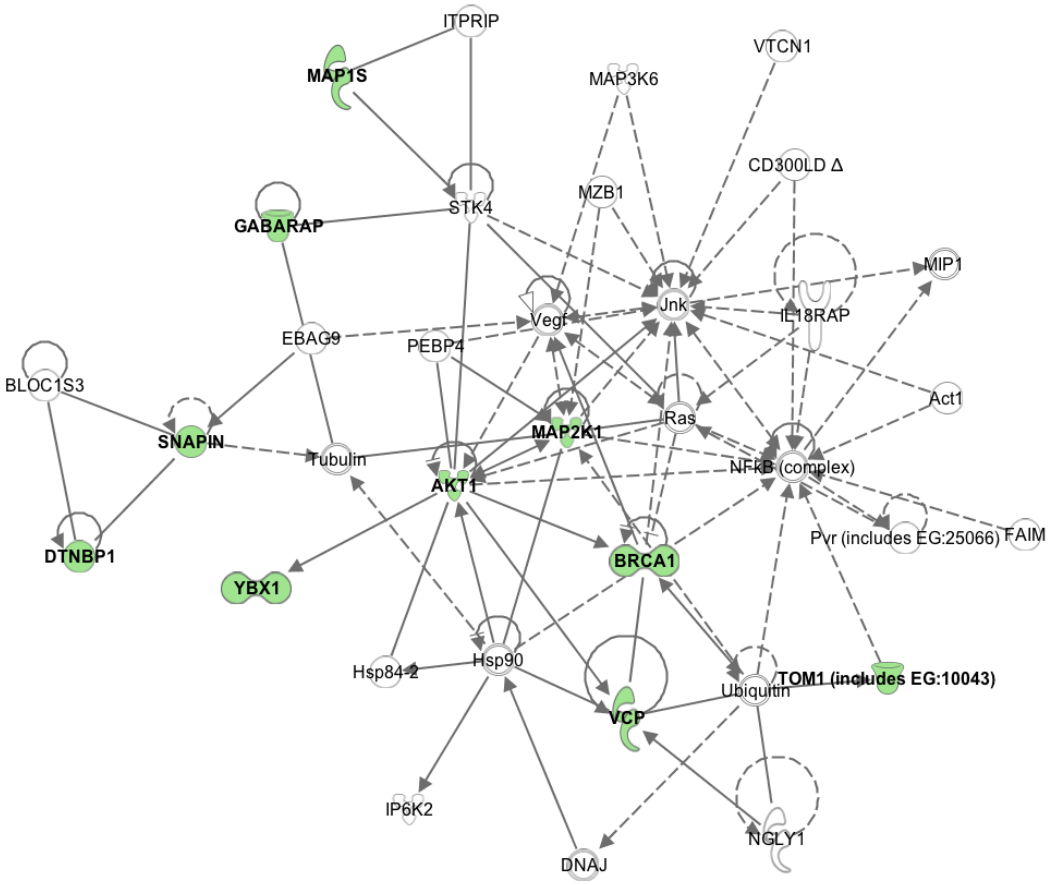

Figure 4.10. Top network of autophagy proteins affecting HIV-1 trans-infection involving cell cycle and tissue development. Score of 25 with 10 molecules. Coloured molecules are from screen.

(Sancak et al., 2008). Amino acids promote the loading of RagB with GTP, which enables interaction with mTORC1. It is unknown how phosphorylation of Rag proteins affects their activity. To investigate this, I transfected expression plasmids containing cDNAs encoding wild-type RagA, inactive RagA (T21L) and constitutionally active RagA (Q66L) and performed an immunoblot for RagA after enrichment for phosphoproteins from the whole cell lysate (figure 4.11b). Active RagA (Q66L) displayed higher levels of phosphorylation in comparison to wild type and inactive RagA (T21L), indicating that phosphorylation of RagA by HIV-1 induces its activation and hence activation of mTORC1. This may be part of the signaling pathway leading to inhibition of autophagy by HIV. However an *in vitro* GTPase assay would be necessary to conclusively demonstrate HIV-1-mediated activation of RagA.

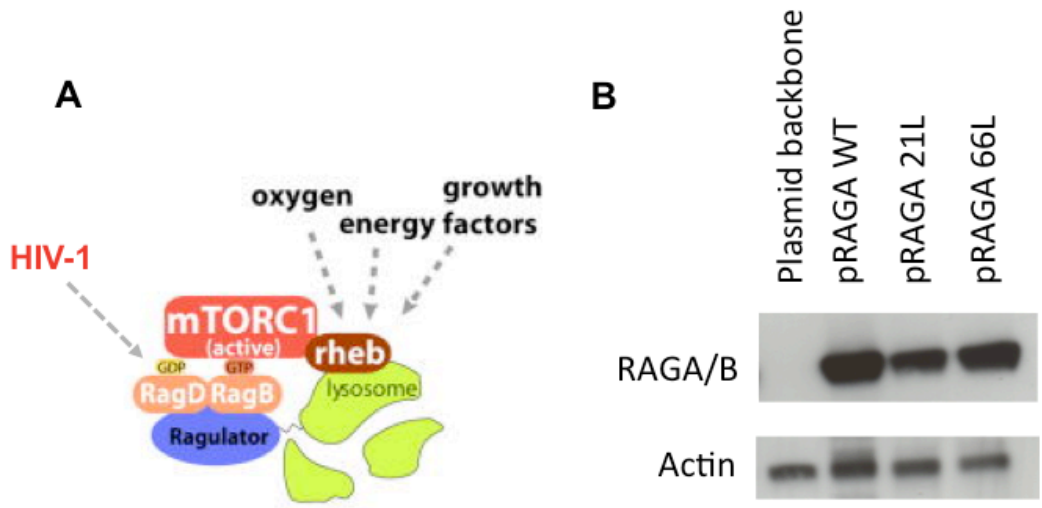

Figure 4.11. Activation of Rags. A. Model of Rag GTPase signalling and mTOR activation. Adapted from (Sancak et al., 2008) **B.** Assessment of the phosphorylation status of RAGA. HEK 293T cells were transfected with the indicated cDNAs in expression plasmids, lysed and enriched for phosphoproteins and analyzed by immunoblotting for expression of RAGA and loading control. The increased density of the band for pRAGA WT most likely represents increased loading.

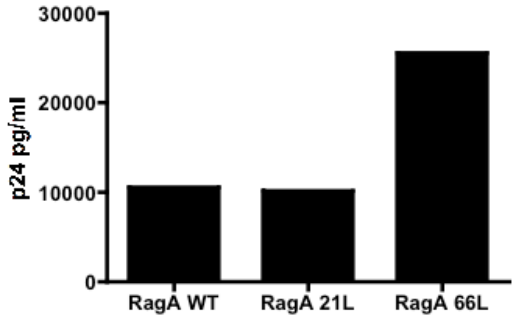

Figure 4.12. Upregulation of constitutionally active RagA which inhibits autophagy and activates mTORC1, may lead to increased viral *trans*-infection. DCs were transfected with vectors encoding indicated cDNAs and infected with NL4-3 BaL for 2 h, washed, counted and then co-cultured with PHA-activated CD4 blasts. Supernatant was harvested every 2 days for p24 measurement by ELISA (shown are values obtained on day 2 p.i.). Graph shows one representative donor out of 2 donors.

To elucidate the functional consequences of RagA phosphorylation on HIV-1 infection, I first looked at siRNA-mediated knockdown of RagA and RagB as well as RagC and RagD (simultaneous knockdown was necessary given that each partner is functionally redundant) and its effect on HIV-1 *trans*-infection. Loss of RagA/B reduced *trans*-infection, whereas loss of RagC/D had no effect (table 4.1). Similarly, overexpression of constitutionally active RagA/B increased HIV-1 *trans*-infection (figure 4.12). Definitely, more work is merited to elucidate the role of Rag proteins in differential trafficking of intraluminal vesicles upon HIV-1 infection.

Altogether, the selective recruitment of members of the autophagy machinery identified by combined phosphoproteomics and RNAi screen aids in characterizing the molecular machinery of the *trans* compartment.

4.3.6 Identification of the BLOC1 complex in HIV-1 mediated immune evasion

Phosphoproteomic analysis had identified three components of the BLOC1 (biogenesis of lysosome-related organelles complex 1) complex to be differentially phosphorylated by HIV-1 within 10 min. These were BLOC1 subunit 1 (BLOC1S1), that was dephosphorylated, and cappuccino homolog (CNO) as well as pallidin homolog (PLDN) that were phosphorylated by HIV-1 (tables 3.3 and 3.4). BLOS1 has two predicted phosphorylation sites at T135 and Y142 and CNO three sites at T165, Y196 and Y207 respectively, whereas there are no predicted sites within the pallidin sequence[2]. I was unable to confirm HIV-1-induced differential phosphorylation of these three proteins due to lack of specific antibodies working on a western blot (not shown). It is not clear from the literature how these sites are phosphorylated and what functional implications differential phosphorylation of these subunits may have. Previous work has shown how differential phosphorylation of proteins involved in vesicular trafficking and exocytosis, such as SNAREs (soluble N-ethylmaleimide-sensitive fusion factor attachment protein receptors), by specific kinases regulates assembly and function of these proteins (Foster

[2] Scansite.mit.edu phosphosite.org

et al., 1998; Snyder et al., 2006). It is conceivable that differential phosphorylation of BLOC1 subunits may mediate similar effects.

As I was unable to blot for the three aforementioned subunits of BLOC1, I used a BLOC1S1 specific immunofluorescent antibody to examine the spatial relationship to HIV-1. Confocal experiments showed that BLOC1S1 co-localized with HIV-1 in a LAMP2 positive lysosomal compartment within two hours of infection (figure 4.13).

Knockdown of either three genes by RNAi had no effect on HIV-1 *trans*-infection (table 3.1). It was nevertheless compelling to find three subunits of a single complex within the HIV-1 phosphoproteome, therefore I decided to pursue this further and investigate its role in HIV-1 infection.

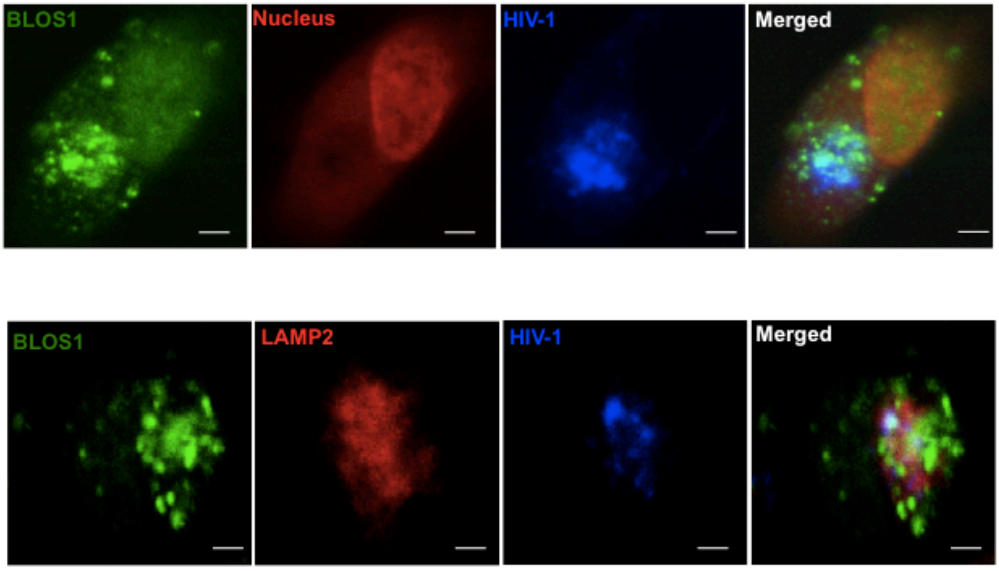

Figure 4.13. HIV-1 co-localizes with BLOS1 in a lysosomal compartment. DCs were infected with ATTO 647N-labelled HIV-1 for 2 hrs and stained for BLOS1, SYTO orange nuclear dye (upper panel) and LAMP2 (lower panel).

4.3.7 A short introduction to BLOC1 complex

BLOC-1 complex belongs to the endosomal protein sorting machinery and was first identified through its association with the Hermansky-Pudlak-syndrome (HPS), a group of heterogenous autosomal recessive disorders due to mutations in genes affecting the biogenesis of lysosomal related organelles (LROs) (reviewed in (Di Pietro and Dell'Angelica, 2005; Wei, 2006). LROs are intracellular organelles found in specialized

secretory cells such as platelets, pigments cells (melanocytes, pigment epithelial cells), neutrophils, T cells and lung type II epithelial cells. They share with lysosomes an acidic pH and at least one integral membrane protein. So far, 8 human and 15 murine HPS genes have been identified, all accounting for distinct clinical phenotypes. These may range from mild albinism and bleeding diathesis to more severe syndromes characterized by pulmonary fibrosis, granulomatous colitis or immunodeficiency.

BLOC-1 is an octameric complex (figure 4.16) and each subunit forms a linear complex containing eight flexibly connected globular domains such that the linear chain can bend by as much as 45° (Lee et al., 2012). It is relatively large with a Stokes radius of 95 Å and a native molecular size of 200 $\pm$ 30 kDa (Lee et al., 2012). Two stable subcomplexes have been identified, pallidin-Cappuccino-BLOS1 and dysbindin-Snapin-BLOS2 (Lee et al., 2012). These heterotrimers appear to be flexible within the longer BLOC-1 chain allowing simultaneous interaction between the subunits during endosome biogenesis and sorting.

HPS genes belong to five distinct cytosolic complexes BLOC-1, BLOC-2, BLOC-3, the clathrin adaptor protein-3 (AP-3) complex and the homotypic fusion and vacuole protein sorting (HOPS) complex (Dell'Angelica, 2009; Di Pietro and Dell'Angelica, 2005; Li et al., 2004b; Wei, 2006). Yeast two hybrid systems have identified a number of molecules interacting with BLOC-1 subunits, e.g. AP-3 and BLOC-2, the SNARE's syntaxin-13 and SNAP25 (Buxton et al., 2003; Starcevic and Dell'Angelica, 2004). Despite these known interactions its exact mechanism of action remains obscure. Interestingly, BLOC components in general are widely conserved throughout evolution (Hayes et al., 2011). Whereas many investigators have focused on single subunits in isolation, other investigators, based on evolutionary conservation from drosophila to mammals both in structure as well as molecular interactions, advocate that all eight subunits only work in concert with the whole complex (Mullin et al., 2011). The latter view is further supported by findings showing that deficiency of one subunit triggers downregulation of other subunits (Mullin et al., 2011).

Mutations in BLOC1 subunits, namely dysbindin and pallidin have been described in HPS7 and HPS9, respectively (table 4.5). Interestingly, multiple GWAS studies have identified dysbindin as a susceptibility gene for the development of schizophrenia (Mullin et al., 2011). AP-3 and BLOC-1 subunits localize to nerve terminals and axons

altering the composition of synaptic vesicles and the expression of neurotransmitter receptors (Newell-Litwa et al., 2009; Talbot et al., 2006). Further, members of the BLOC1 family have been shown to affect melanosomal biogenesis by acting at an early step of melanosome formation at the trans golgi network with accumulation of melanin deficient pre-melanosomes, explaining why BLOC1 deficient mice display the most severe form of pigmentation defect among the HPS mouse models (Raposo and Marks, 2007).

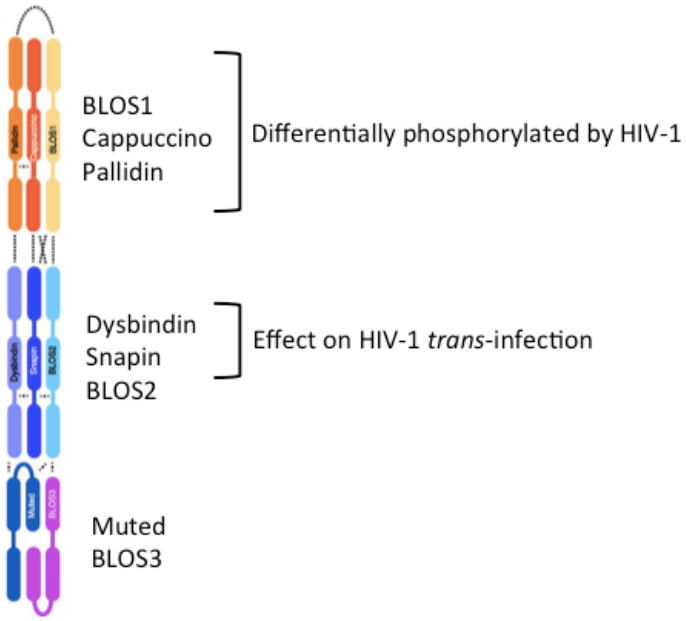

Figure 4.14. Schematic model of BLOC-1 complex based on yeast two-hybrid mapping and coiled-coil predictions. BLOC-1 is an elongated octameric complex with two stable heterotrimeric subcomplexes that appear to form the structural core. Indicated in figure are the proteins identified within the HIV-1 signalosome and the RNAi screen. Adapted from (Lee et al., 2012).

Table 4.5. BLOC-1 complex subunits

Subunits	Human subtype	Mouse strain
Pallidin	HPS-9	Pallid
Cappuccino		Cappuccino
BLOS3	HPS-8	
Muted		Muted
Dysbindin	HPS-7	Sandy
Snapin		
BLOS1		
BLOS2		

To recapitulate, in mammalian cells, endocytosed cargo that is internalized through clathrin-coated pits passes through early endosomes that undergo stepwise maturation to late endosomes (also referred to as MVBs), before delivery to lysosomes for degradation by proteases and acid hydrolases (Schelhaas, 2010). BLOC1 resides on endosomes and is required for cargo sorting in early endosomes.

4.3.8 BLOC-1 subunits snapin and dysbindin affect HIV-1 *trans*-infection

To assess the role of BLOC-1 in HIV-1 infection further, I looked at levels of *trans*-infection after knockdown of each BLOC-1 subunit. Intriguingly, snapin and dysbindin displayed a strong effect on HIV-1 *trans*-infection with the former reducing infection by 50% upon knockdown (figure 4.15), whereas snapin knockdown had no effect on early HIV-1 transcription (figure 4.16). So far, these findings indicate that HIV-1 recruits BLOC-1 upon entry by differentially phosphorylating members of the first sub-complex and using two members of the second sub-complex for passage to the *trans*-compartment.

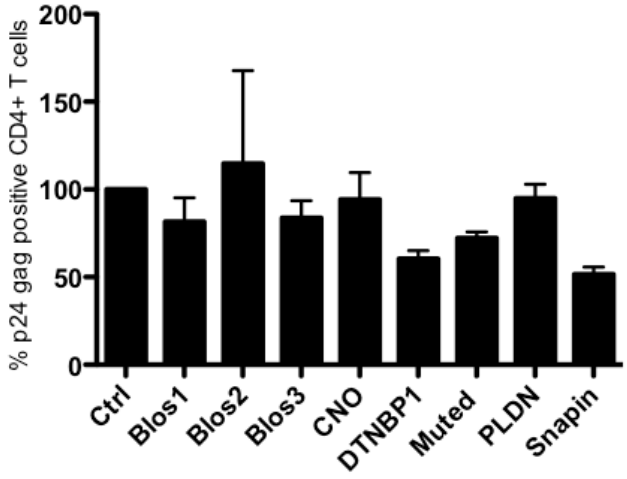

Figure 4.15 Effect of knockdown of BLOC1 complex subunits on HIV-1 *trans*-infection. DCs were transfected with siRNAs targeting BLOC1 genes, 48hrs post transfection infected with HIV-1 BaL for 2 hours and co-cultured with CD4+ PHA blasts for 72 hours. Intracellular p24 gag was quantified by flow cytometry. Data are representative of 3-4 independent experiments.

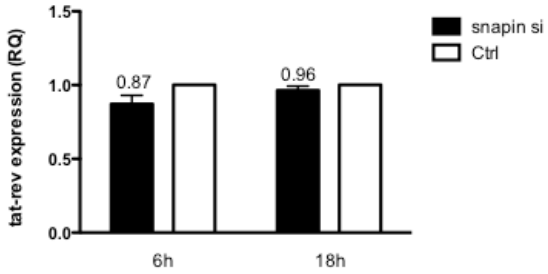

Figure 4.16. Snapin knockdown has no effect on early HIV-1 transcription. DCs were transfected with snapin and non-silencing control siRNA, infected 2 days later with HIV-1 for 2 h and harvested 6 and 18 h later. mRNA was isolated and analysed for expression of HIV-1 tat-rev by real-time PCR. Values were normalized against GAPDH control. Bars are mean ± SEM of three technical replicates. One representative donor out of two is shown.

4.3.9 Identification of the role of BLOC-1 subunit snapin in PRR signaling

Given the role of BLOC-1 complex in the endo-lysosomal system, I postulated that the reduction in *trans*-infection mediated by snapin, and to a lesser extent dysbindin knockdown, may either be due to "mis"trafficking of virions away from the trans compartment to the lysosomal system or due to induction of an antiviral response.

Work by B. Beutler's group using a genetic screen to identify proteins required for murine pDC function, identified the proteins AP-3, BLOC-1 and BLOC-2 as essential for murine pDC signaling through TLR7 and TLR9 (Blasius et al., 2010). Interestingly, these proteins were dispensible for signaling in conventional DCs and the authors inferred that a LRO-like organelle is required for TLR response in pDCs.

To investigate the effect of BLOC-1 subunits in MDDCs, I looked at levels of type I interferons and cytokines following HIV-1 infection and ssRNA40 stimulation in cells transfected with control, BLOC1S1, snapin and dysbindin siRNAs, respectively. Surprisingly, TLR8 activation resulted in a strongly enhanced up-regulation of anti-viral and -inflammatory cytokines in cells deficient of snapin, whereas knockdown of BLOC1S1 or dysbindin had no effect (figure 4.17). Efficient down-regulation of snapin with snapin siRNA was routinely observed both on mRNA and protein level (figure

4.18). To see if the effect of snapin on TLR signaling is restricted to TLR8, I compared the levels of cytokine and chemokine mRNA in snapin deficient DCs following activation with ligands for TLR8, TLR3 and TLR4. Preliminary experiments show that snapin may regulate the TLR response differentially, whereby it exerts the most pronounced effect on TLR8 mediated recognition of ssRNA40 (figure 4.19). It would be interesting to carry out comprehensive studies of the PRR response in snapin deficient cells comparing different PRR ligands, and *in vivo*, using snapin knockout mice. These findings identify a novel role for snapin in control of TLR recognition, something that definitely merits further investigation.

Next, I decided to investigate the effect of snapin on the cytokine and type I interferon response to HIV-1. Intriguingly, knockdown of snapin resulted in induction of IFN β 1, IL6 and MIP1 α on mRNA level upon HIV-1 infection (figure 4.20). These results need to be confirmed on more donors and on a protein level, but certainly appear to suggest a role for snapin in HIV-1 sensing.

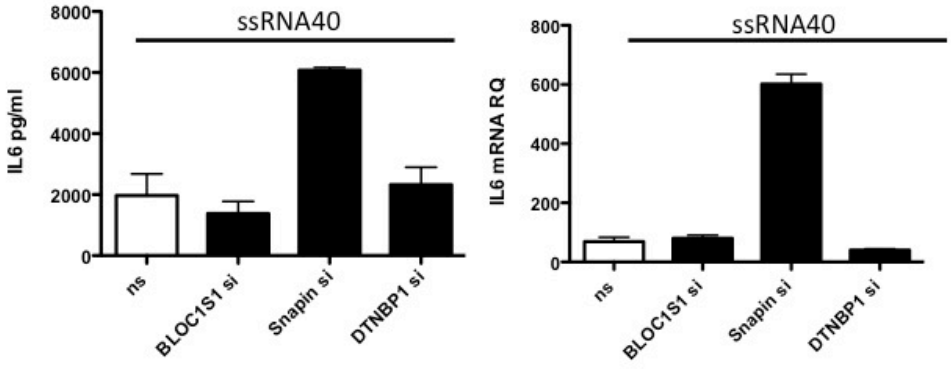

Figure 4.17. Snapin knockdown strongly upregulates the cytokine response following TLR8 activation. DCs were transfected with indicated siRNAs and scrambled (Ctrl) siRNA and incubated with 1µg/ml ssRNA40, lyovec control, HIV-1 NL4-3 BaL or media control for 18 hours for RNA isolation and 24 hours for supernatant collection. cDNA was prepared for qRT-PCR and relative gene expression was normalized to GAPDH. Values shown are relative to unstimulated control and representative of 4 independent experiments.

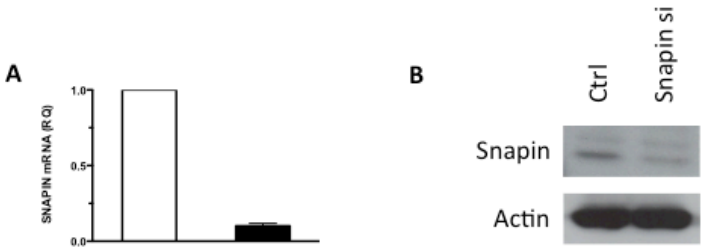

Figure 4.18 Validation of snapin knockdown by qRT-PCR and immunoblot. DCs were transfected with snapin and scrambled siRNA respectively and harvested 48 hours later for qRT-PCR analysis and immunoblot for expression of snapin. **A.** cDNA was prepared from mRNA for qRT-PCR and normalized to GAPDH. Values are 5 independent experiments and are mean ± SEM. **B.** Expression of snapin and actin assessed by immunoblot.

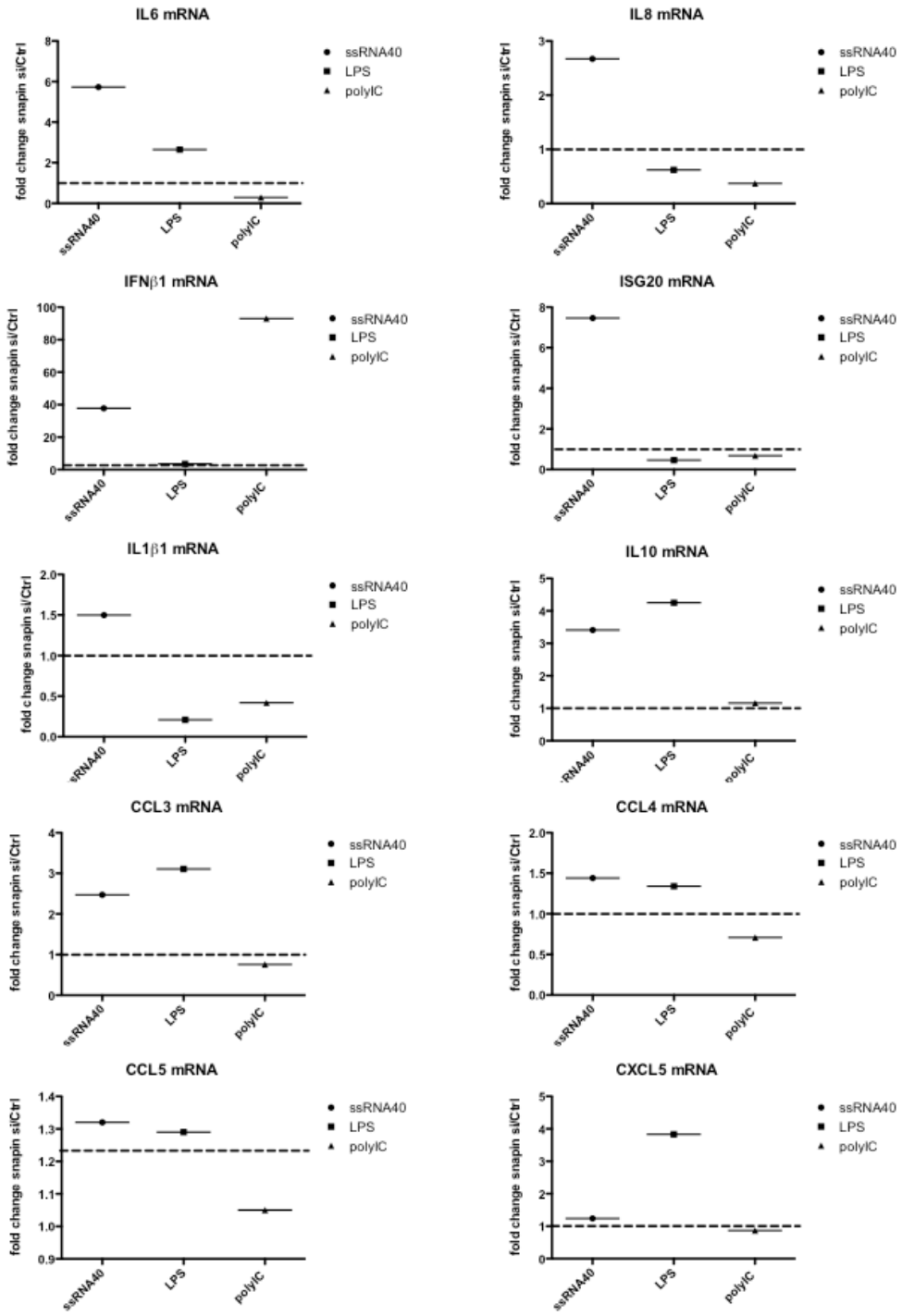

Figure 4.19. Snapin knockdown may have the strongest effect on the response to TLR8 activation. DCs were transfected with snapin and scrambled siRNA and incubated with 1µg/ml ssRNA40 (TLR8), 100ng/ml LPS (TLR4) and 1µg/ml polyIC (TLR3) for 18 hours before qRT-PCR analysis for different cytokines (IL6, IL8, IL10, IL1β), interferons (IFNβ1) and interferon genes (IRF3, ISG20) and chemokines (CCL3, CCL4, CCL5, CXCL5). Values were normalized to GAPDH as well as unstimulated control. For better illustration dots with line are representative of snapin relative to control siRNA. Data are one from one experiment.

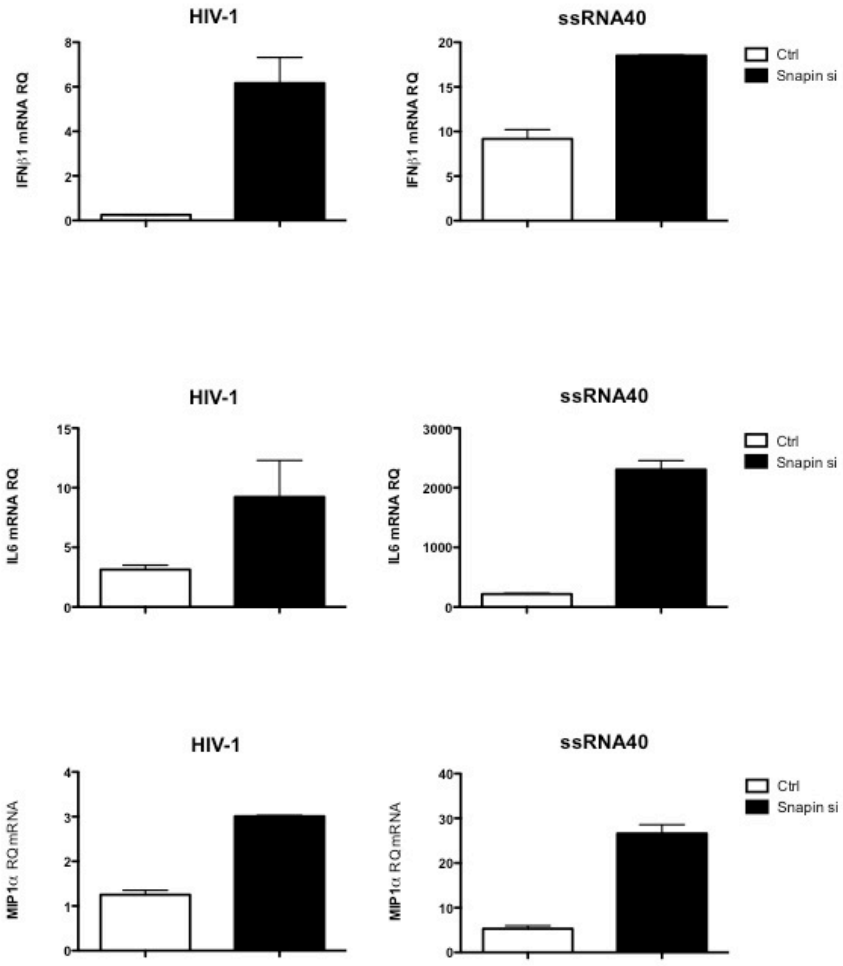

Figure 4.20. Investigation of snapin knockdown on the interferon, cytokine and chemokine response to HIV-1 infection. DCs were transfected with snapin and scrambled siRNA and incubated with 1μg/ml ssRNA40, HIV-1 NL4-3 BaL and control media for 2 h, washed and harvested 18 hours later for real-time PCR analysis for IFNβ1, IL6 and MIP1α (CCL3). Values were normalized to GAPDH control. Values are mean ± SEM of three technical replicates. One representative example from two experiments is shown.

4.3.10 Identification of snapin as a key player in formation of the TOR-autophagy spatial coupling compartment (TASCC)

A further explanation for the role of snapin in both *trans*-infection as well as PRR signaling stems from a more recent concept of autophagy mediated protein degradation, that states that senescent cells are not as quiescent as one may expect, but incorporate an active protein secretion program (Narita et al., 2011). Narita et al showed that in oncogene induced cellular senescence a profound reorganization of the endomembrane system occurs, resulting in the formation of a membrane compartment responsible for secretion of inflammatory cytokines, growth factors and modulators of the extracellular matrix. This compartment – named TASCC – carries out the secretory program and is constituted of autophagosomes and the mammalian target of rapamycin (mTOR) complex 1 kinase (mTORC1). Degradation of proteins by autophagosomes generates an amino acid rich environment that is used by mTORC1 to synthesize secretory proteins. The authors showed the close link between autophagy and mTORC1 by co-localization of mTORC1-studded LAMP2 positive lysosomes together with autophagosomes in a perinuclear region that led to synthesis and secretion of cytokines such as IL6 and IL8 (Zoncu and Sabatini, 2011). Ultrastructurally, TASCC is in close proximity to the ER, golgi apparatus and the trans-golgi network (figure 4.21). Essentially, TASCC explains how mTOR may function in both autophagy and protein synthesis simultaneously, e.g. during senescence or xenophagy: mTOR is switched off to induce autophagy, but is then recruited by Rag GTPases (RagA/b and RagC/D) to lysosomal compartments ready to meet the degraded material (Sancak et al., 2010; Zoncu and Sabatini, 2011). Here, increased amino acid concentrations activate mTOR again to facilitate protein synthesis, i.e. cytokine induction and secretion.

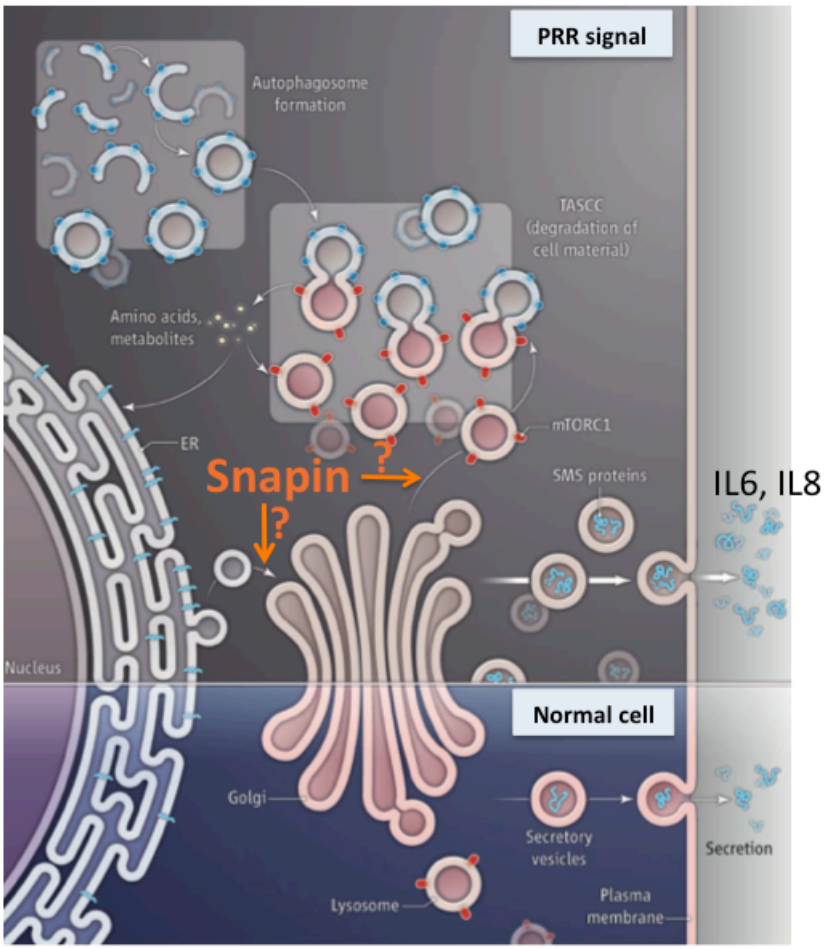

Figure 4.21. The model for TASCC formation. In a normal cell autophagy is repressed and there is tight regulation of the secretory pathway. In oncogene induced senescence and potentially following PRR signaling, autophagosomes form outside the TASCC (negatively regulated by mTORC1). Following maturation they fuse with lysosomes that contain mTORC1. This results in TASCC formation where amino acids that are released by autophagosomes recruit mTORC1 to the TASCC via Rag GTPases. The same amino acids are presumably used for protein synthesis and secretion. Hence, protein degradation and synthesis occur in closely spatial location, exemplified by the expression of the transgolgi marker TGN46, lysosomal markers LAMP2 and LC3 as well as mTORC1. Snapin acts as a negative regulator of TASCC by preventing the activation of the secretory pathway. Adapted from (Zoncu and Sabatini, 2011)

Given the role of snapin in the endolysosomal system and control of TLR8 signaling, I asked whether snapin has a role in the TASCC signaling pathway. I performed immunofluorescence analysis of snapin siRNA transfected cells following HIV-1 infection and ssRNA40 stimulation by staining for TASCC markers TGN46, LAMP, mTOR1 and LC3. Due to lack of a working snapin antibody, I used BLOS1 as a surrogate marker for the localization of the whole BLOC-1 complex and hence snapin. I could see that TLR8 activation induced formation of TASCC with increased co-localization of mTOR1 with LAMP1, LC3 and TGN46 (figure 4.22-23). Conversely, HIV-1 infection resulted in a block to formation of the TASCC complex upon HIV-1 infection (figure 4.24). Intriguingly, knockdown of snapin removed the block for formation of TASCC in HIV-1-infected DCs (figure 4.25-6). To summarize, snapin appears to be a negative regulator of TASCC accumulation and its knockdown reverses the block to TASCC formation upon HIV-1 infection. Given the inhibitory effect of brefeldin A on TASCC formation that Narita et al observed and the known function of snapin in late endosomal trafficking it is conceivable that snapin may interfere with either late endosomal or even de novo lysosome biogenesis, a critical step in TASCC nucleation (Narita et al., 2011). Further, HIV-1-mediated changes in RagA/B and RagC/D may interfere with translocation of mTORC1 to TASCC. Other proteins such as the sorting nexins SNX1 and SNX5 could be other players in this process given that they are differentially phosphorylated by HIV-1 and (iii) associate with BLOC-1 in arabidopsis (Cui et al., 2010). Sorting nexins are trafficking proteins involved in early endosome to golgi transport (Worby and Dixon, 2002). It would be interesting to re-address their effect on *trans*-infection with over-expression vectors, given their lack of a convincing effect in the RNAi screen (table 4.1).

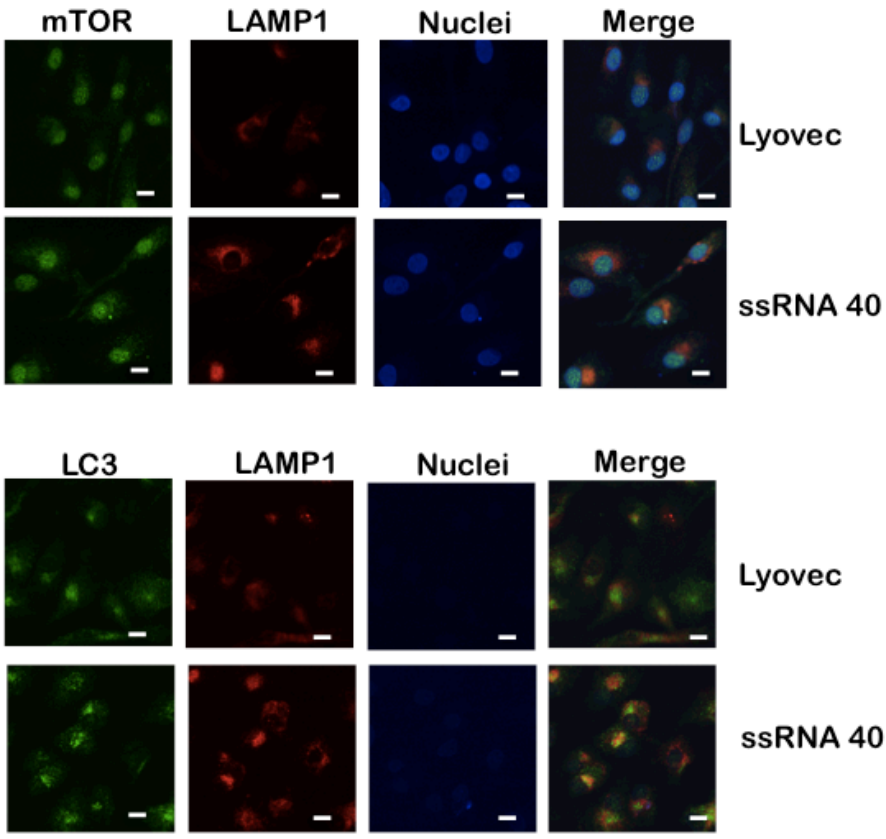

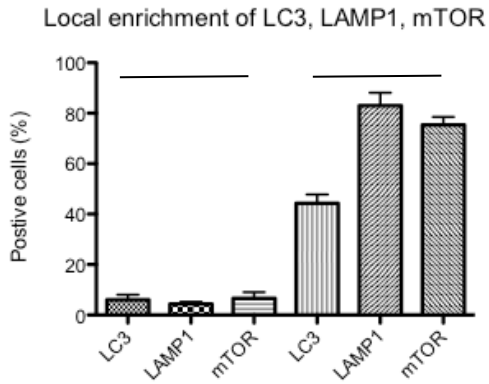

Figure 4.22. TLR8 activation induces formation of TASCC in DCs. DCs were incubated in the presence of 1μg/ml ssRNA40 and lyovec control for 2 h, washed and transferred to slides and stained for mTORC1, LC3, LAMP1 and TO-PRO3 nuclear stain 16 h later. Representative images shown. Scale bar 10μm. Data are means ± SD of one replicate counting of 100 DCs and identifying those with TASCC structures. The three left bars are lyovec control, the remainder are ssRNA40-activated DCs.

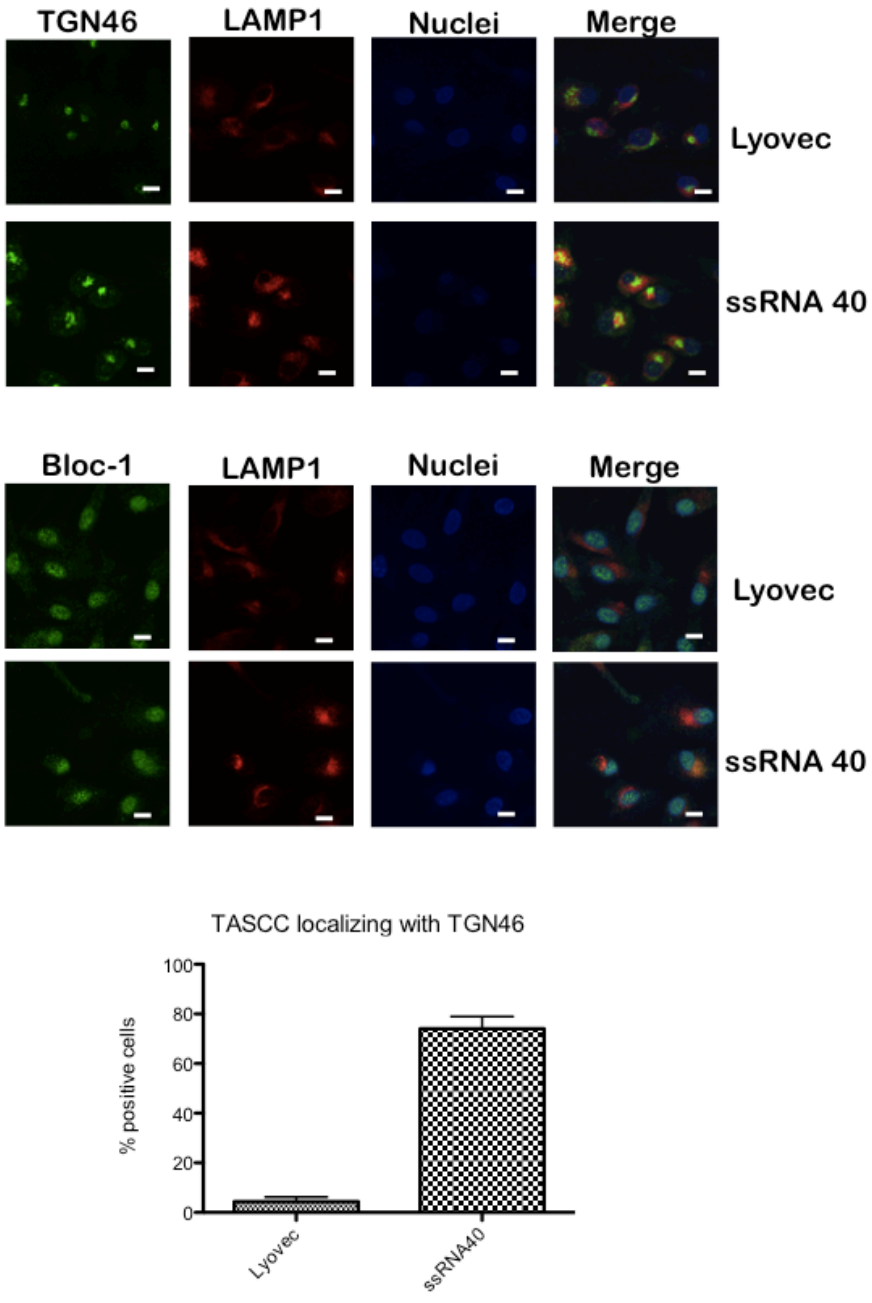

Figure 4.23 A. Spatial association between TASCC and secretory apparatus on ssRNA40/TLR8 triggering. B. Localization of BLOC1S1 with TASCC on TLR8 triggering. DCs were incubated in the presence of 1µg/ml ssRNA40 and lyovec control for 2 h, washed and transferred to slides and stained for TGN46, LAMP1, BLOC1S1 and TO-PRO3 nuclear stain 16 h later. Representative images shown. Scale bar 10µm. Data are means ± SD of one replicate counting of 100 DCs and identifying those with TASCC structures.

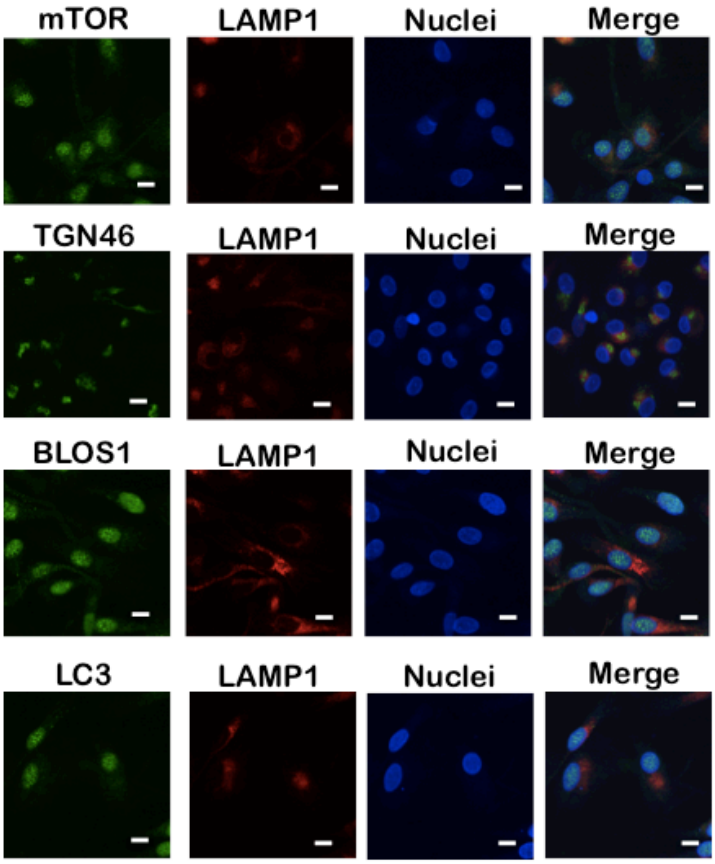

Figure 4.24. HIV-1 infection leads to failure of TASCC formation in DCs. DCs were infected with HIV-1 and mock for 2 h, washed and transferred to slides and stained for TGN46, LAMP1, BLOC1S1, mTOR, LC3 and TO-PRO3 nuclear stain 16 h later. Representative images shown. Scale bar 10μm.

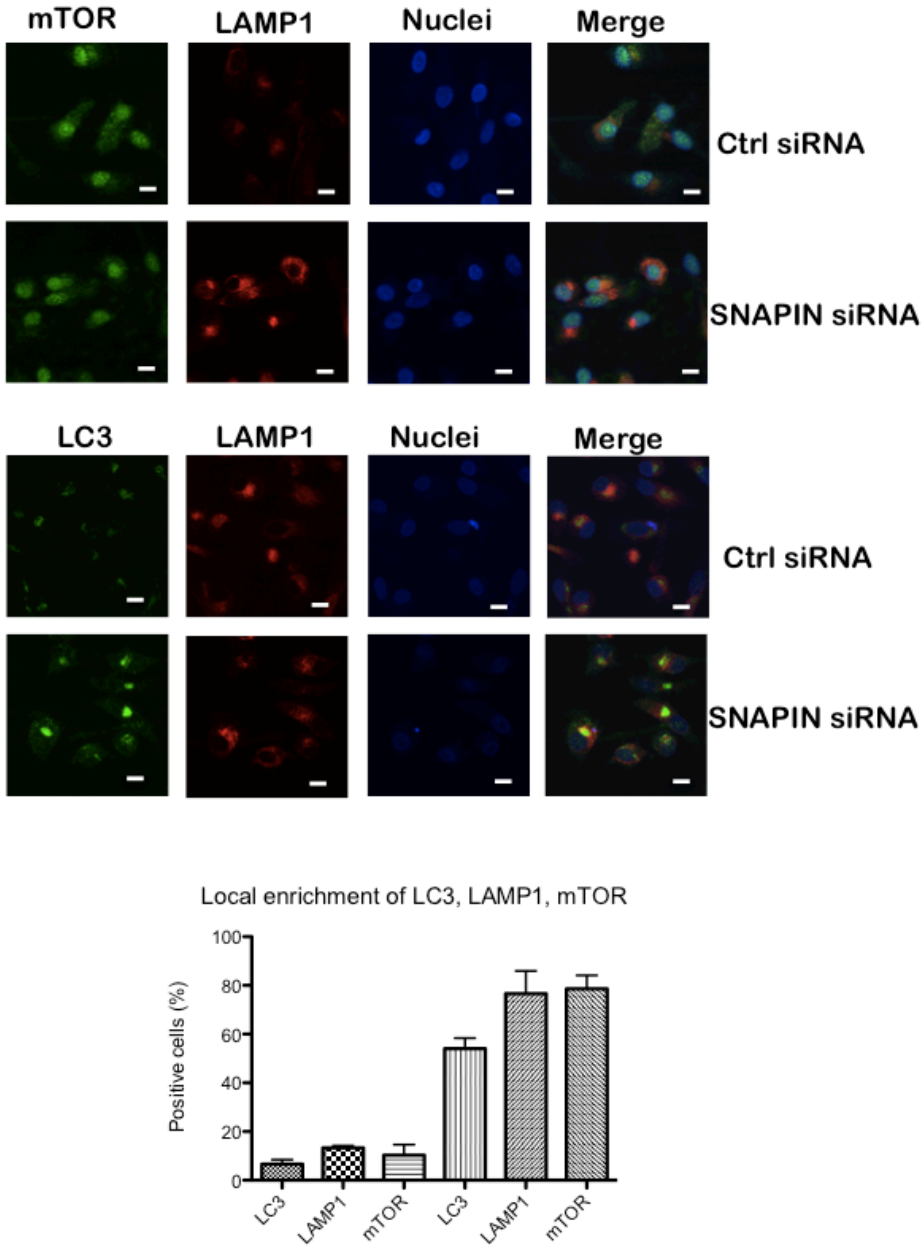

Figure 4.25. Snapin knockdown removes block for formation of TASCC in HIV-1 infected DCs. DCs were transfected with snapin and control siRNA and infected with NL4-3 BaL for 2 h, washed and transferred to slides and stained for mTORC1, LC3, LAMP1, TGN46, and TO-PRO3 nuclear stain 16 h later. Representative images shown. Scale bar 10μm. Data are means ± SD of one replicate counting of 100 DCs and identifying those with TASCC structures. The three left bars are DCs transfected with siRNA control, the remainder are DCs transfected with snapin siRNA.

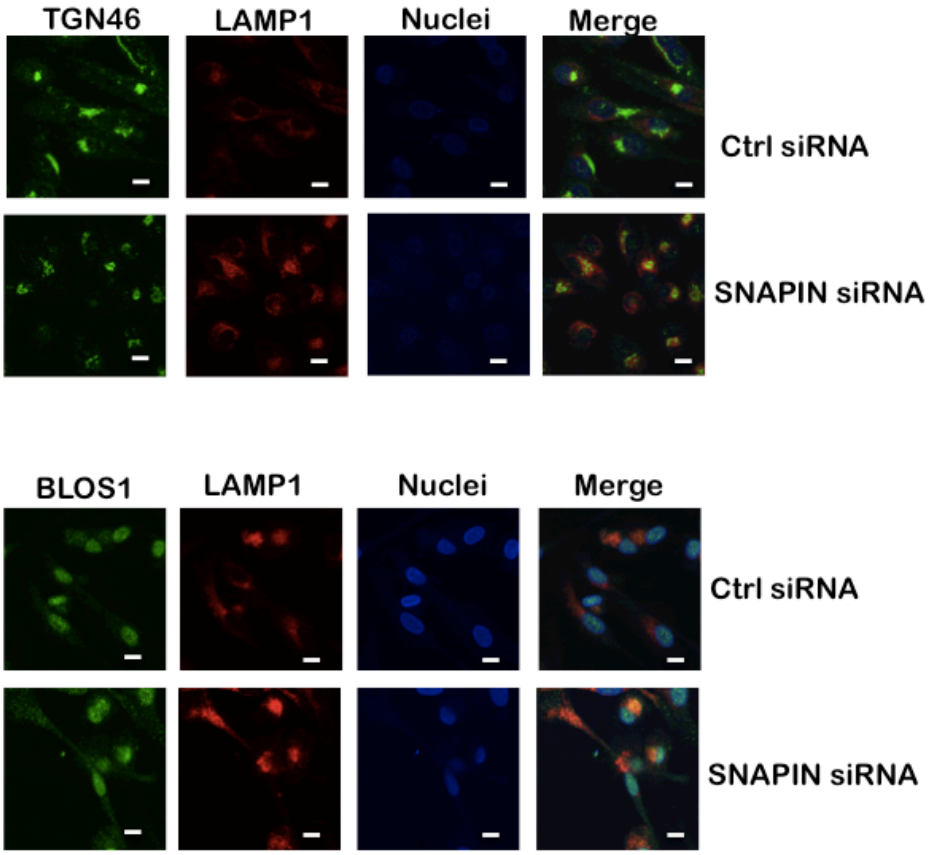

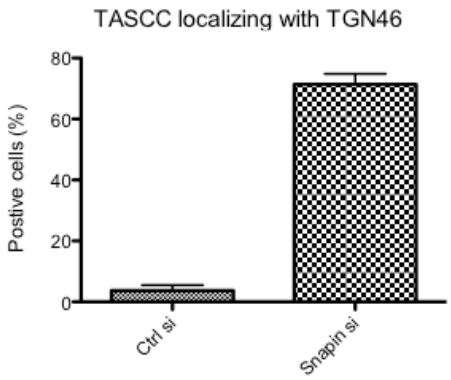

Figure 4.26. Snapin knockdown removes block for formation of TASCC in HIV-1 infected DCs. DCs were transfected with snapin and control siRNA and infected with NL4-3 BaL for 2 h, washed and transferred to slides and stained for BLOS1, LAMP1, TGN46, and TO-PRO3 nuclear stain 16 h later. Representative images shown. Scale bar 10μm. Data are means ± SD of one replicate counting of 100 DCs and identifying those with TASCC structures.

Altogether, TASCC is reminiscent of the intracellular LC3 containing structures that Blanchet et al called immunoamphisomes, compartments between endosome and autophagosome formation, that were capable of intercepting engulfed virions targeting them towards lysosomal degradation (Blanchet et al., 2010). Snapin seems to be acting as a decision maker for the formation of these compartments, whether termed immunoamphisome or TASCC. This provides direct evidence that HIV-1 uses components of the regulated secretory pathway to facilitate its own propagation, it is rather remarkable that these components are recruited so early during infection.

4.4 Discussion

In this chapter I conduct a secondary targeted screen based on the results of the HIV-1 phosphoproteomic data for the identification of novel host factors affecting *trans*-infection. I identify 54 new proteins required for HIV-1 *trans*-infection, and previously described in cellular functions, such as the secretory pathway, autophagy process and DNA repair machinery. Furthermore, the data establishes a role for snapin as a new player in both innate sensing by TLRs as well as HIV-1 *trans*-infection.

Conducting this RNAi screen was associated with a number of advantages: Firstly, it was conducted in primary MDDCs, whereas published genome-wide RNAi screens have been based on studies of host factors in Hela and HEK 293T cells (Konig et al., 2008; Zhou et al., 2008). Secondly, it focused on HIV-1 *trans*-infection rather than markers of early or late viral replication, to elucidate the potential role of mucosal DCs in the early events of HIV-1 infection and viral dissemination. Thirdly, the 54 host factors identified as important for HIV-1 trans-infection, were already shown to be differentially phosphorylated by HIV-1 within 10 min, which considerably increases the confidence in the data and the biological relevance of these host factors. However, there were also a number of problems associated with the screen, all owing to the fact of conducting this screen in a non-automated format in primary cells. This resulted in obtaining relative modest reductions in HIV-1 *trans*-infection with large variability between donors and hence difficulty in carrying out statistical analysis of the data.

Generally, the reduction in *trans*-infection could be due to interference with a multitude of steps, starting with efficiency of viral uptake to fusion in a possibly endosomal compartment, trafficking of virions from the endosomal compartment to the *trans* compartment and finally formation and viral transfer via the virological synapse.

The interaction of HIV-1 with BLOC-1 complex, and in particular snapin, is intriguing. The role of snapin in *trans*-infection, PRR (and potentially HIV-1) sensing as well as formation of TASCC strongly suggest that snapin may act as a decision maker in the formation or signaling of ILVs. In neurons snapin is essential in endosome-lysosomal fusion by linking late endosomal transport and the retrograde transport motor dynein (Cai et al., 2010; Yuzaki, 2010) and snapin knockout neurons display an accumulation of immature lysosomes. Given the known importance of dynein in mediating snapin function, snapin may in concert with dynein determine the rate by which HIV-1 traverses through the endo-lysosomal system to reach the *trans* compartment or bypass it altogether. In addition, dynein-mediated transport has been shown to be essential in IS formation in T cells (Hashimoto-Tane et al., 2011) and it is conceivable that it may also play a role in VS formation in DCs. Using an over-expression system with snapin mutants in the dynein-binding region would aid in characterizing the trafficking defect associated with snapin knockdown in this setting.

A very important function of snapin is to regulate the association of the calcium sensor synaptogamin with the synaptic snare complex. Absence of snapin reduces calcium-regulated exocytosis (Dickman et al., 2012). This could explain how snapin and dysbindin may regulate formation of the viral synapse or viral delivery to the synapse. Live cell microscopy and comprehensive studies of the synapse would be fascinating. In *Drosophila* both snapin and dysbindin presynaptically determine the homeostatic modulation of vesicle release and calcium dependency of vesicle release (Pan et al., 2009). This would suggest that specialized vesicle pools or variations in the coupling of calcium sensors and the fusion machinery may be regulated by the BLOC-1 complex (Mullin et al., 2011).

Further, two more proteins are worth mentioning as potential up-stream regulators of snapin function during HIV-1 signaling: the protein kinase PKA as well as A kinase anchor protein 12, AKAP12, which are both differentially phosphorylated by HIV-1. In neurons, PKA regulates snapin by phosphorylating it and modulating vesicle exocytosis

and synaptic plasticity (Thakur et al., 2004). AKAP12 is a scaffold protein for PKA and PKC and controls actin-cytoskeleton dynamics (Akakura and Gelman, 2012). Calcium may be a key factor in this process and certainly warrants further investigation. A question that has not been addressed is how HIV-1 recruits BLOC-1 complex to manipulate the host trafficking machinery to its own advantage. DC-SIGN mediated signaling may play an important role, given the known function of DC-SIGN in subversion of the immune response and increasing viral synapse formation. Studies using VSV-pseudotyped HIV-1 and THP-1 cells expressing different DC-SIGN cytoplasmic tail mutants will be helpful in investigating the role of DC-SIGN in this context.

The exact physiological relevance of snapin as a regulator of TLR8 signaling is not as yet clear. A recent study using a yeast two-hybrid cDNA library identified snapin as a novel endogenous TLR2 ligand in rheumatoid arthritis RA (Shi et al., 2012), suggesting a role for persistent TLR2 signaling in the pathogenesis of the disease. Mechanistically, snapin may control access to the compartment where cleavage of ectodomain of TLR8 occurs, similar to the regulation of TLR9 by adaptor protein 3 (Sasai et al., 2010). Furthermore, snapin may, by virtue of its function as a motor of LRO biogenesis, cause arrest of LROs between early endosome to late endosomes and hence accumulation of early endosomes, where the interaction between TLR8 and its ligand is prolonged. Along similar lines, the hyperinflammatory immune response in cystic fibrosis has been linked to abnormal retention of TLR4 in the early endosome and reduced TLR4 translocation into the lysosomal-degradative compartment, triggering inflammatory signaling pathways (Bruscia et al., 2011). One of the unresolved issues in HIV-TLR8 interaction is how the virus signals via TLR8 to promote transcriptional elongation, but at the same time evades the induction of a type I interferon response that should ensue upon recognition of viral ssRNA (Gringhuis et al., 2010). It is tempting to speculate that host molecules, such as snapin/BLOC-1, may be actively usurped by HIV-1 to regulate TLR8 trafficking and signaling. This is supported by the observations presented here, whereby snapin knockdown had no effect on HIV-1 transcription, but induced an exaggerated inflammatory TLR8 response.

It would be valuable to expand the BLOC-1 related findings obtained in MDDCs to DCs from patients with BLOC1 mutations. However, to date only two of the eight genes

encoding BLOC-1 subunits are known to cause HPS disease in humans, namely HPS-7 and HPS-8, of which in the literature only one HPS-7 patient and six HPS-8 patients from a single family have been described (Cullinane et al., 2012; Li et al., 2003; Morgan et al., 2006). Patients with HPS-2, caused by a mutation in the gene encoding for the β3A subunit of the AP-3 complex, display defects in HIV-1 assembly at the late stage of infection (Liu et al., 2012). Conclusively, these findings suggest that snapin connects the innate immune response to the machinery responsible for formation and trafficking of intraluminal vesicles.

Intriguingly proteins implicated in the DNA damage response (DDR) were identified within the RNAi screen. These include the aforementioned VCP as well as BRCA1/BRCA2-containing complex, subunit 3, BRCC3, and breast cancer 1 early onset, BRCA1. Why should the DDR affect HIV-1 *trans*-infection? BRCC3 is a E3 ubiquitin ligase with role in the DDR. It also recently has been identified to regulate Raf-1 and phosphorylation of Erk1 (Boudreau et al., 2007). Raf-1 on the other hand is part of the DC-SIGN signalosome (Gringhuis et al., 2009). Hence, the identification of BRCC3 as a novel HIV-1 host factor may reflect its involvement in the DC-SIGN signaling complex. BRCA1 forms a complex called the BRCA1-associated genome surveillance complex with other proteins including BRCC3 to regulate the DDR (Wu et al., 2010). It is possible that the DDR senses HIV nucleic acids in the cytosol, and triggers transport of HIV-1-containing intraluminal vesicles via the *trans* compartment in an equivalent way to melanosome release to protect skin from UV DNA damage response, i.e. a pathway conservation between DCs and melanocytes.

Further analysis of the RNAi screen revealed a set of genes that regulate the stress granule (SG) machinery, were differentially phosphorylated by HIV-1 and had a modest effect on *trans*-infection. These were G3BP1, G3BP2, EIF4G1 and CarHSP1. Stress granules are dense cytosolic aggregates of translationally silent mRNA that regulate mRNA storage and triage it either into the degradative or back into the translational pathway (Thomas et al., 2011). There has recently been some indication that the pathways regulating SG and autophagosome formation may be interlinked by novel regulatory pathways via temporary recruitment of sub-population of protein aggregates away from SGs and autophagic vacuoles. This would represent a clever mechanism whereby proteins are reversibly sequestered away from their functionally important site

in the cell (Christian et al., 2010). For instance, stress caused by heat triggers translocation of TORC1 into SGs and hence spatiotemporal inhibition of TORC1 activity (Takahara and Maeda, 2012), most likely via induction of the small GTPase Rho1 (Yan et al., 2012). Moreover, TORC1 reactivation is directed through SG disassembly. Interestingly, SG mediated TORC1 inhibition decreases the frequency of heat stress-induced DNA mutations protecting the cells from DNA damage (Takahara and Maeda, 2012). Furthermore, the dynamics of SG formation depend on dynein and microtubule dynamics (Loschi et al., 2009; Tsai et al., 2009).

This chapter demonstrates that HIV-1 usurps members of the vesicular trafficking and autophagy, DNA repair and SG machinery within 10 min of infection to facilitate *trans*-infection. Elucidation of the intricate pathways that a pathogen like HIV-1 uses, unravels novel mechanisms important for DC biology.

Chapter 5

Identification of SHP-1 in HIV-1-mediated immune evasion

5.1 Introduction

Characterization of the HIV-1 phosphoproteome revealed multiple novel signaling proteins not previously known to be associated with HIV-1 infection. One such protein was the Src-homology 2 (SH2)-domain containing phosphatase SHP-1, that on phosphoproteomic analysis was absent in HIV-1-infected DCs compared to non-infected DCs. Recent data has highlighted the role of SHP-1 as a key regulator of a homeostatic innate immune response (O'Neill, 2008). This chapter will focus on the interaction of HIV-1 with SHP-1 as a possible immune evasive mechanism.

5.1.1 SHP-1 structure and regulation

At the steady state the balance between phosphorylation and dephosphorylation is determined by the opposing action of protein kinases and phosphatases (Hunter, 1995). At least 107 genes have been identified as coding for protein tyrosine phosphatases (PTP), and they have been divided into four distinct classes (Alonso et al., 2004). SHP-1 – and its functionally distinct homologue SHP-2 – belong to the first class, the non-receptor tyrosine phosphatases (Lorenz, 2009). SHP-1 is a cytosolic phosphatase with a central catalytic PTP domain flanked by two tandem N-terminal SH2 domains and a C-terminal tail with potential tyrosine phosphorylation sites (Figure 5.1) (Lorenz, 2009; Poole and Jones, 2005). The SH2 domains are important for both regulating the localization as well as the activity of SHP-1 (Tsui et al., 2006). In the absence of ligands, the N-terminal SH2-domain folds onto the catalytic domain to block substrate

access by insertion of a loop into the catalytic pocket of the PTP domain, thereby repressing its activity (Hof et al., 1998). Upon engagement, SHP-1, via its SH2 domains, is recruited to the tyrosine-phosphorylated ITIM motif within the cytoplasmic domain of a receptor (Yang et al., 2003). This leads to a conformational change of the N-terminal SH2 domains unblocking the catalytic domain. Subsequently, SHP-1 binds to tyrosine-phosphorylated sites of downstream molecules, thereby turning off the signal cascade. The C-terminal SH2 domain is not required for this activation, but is indispensible for SHP-1 signaling and may even aid in recruiting binding partners to give an inhibitory signal independent of the phosphatase domain (Minoo et al., 2004; Poole and Jones, 2005).

Multiple studies have described SHP-1 as a negative regulator of signaling downstream of cytokine receptors, receptor tyrosine kinases and immune receptor complexes. In T-cell receptor (TCR) signaling, SHP-1 inactivates Src-family kinases and may bind to Lck (Lankester et al., 1995), ZAP-70 (Plas et al., 1996) or Vav (Kon-Kozlowski et al., 1996), although no clear binding partner has been identified so far. The role of SHP-1 in signaling is not restricted to T cells but extends to all cells of the haematopoetic system. Altogether SHP-1-mediated dephosphorylation of signaling molecules has to occur in a correct and timely manner to allow for both efficient and controlled signaling. This is determined by precise regulation of its activity and cellular localization (Lorenz, 2009).

Generally, whereas the initiation of signaling cascades is well described, the mechanisms by which signaling is negatively controlled or terminated are less well known. Evaluation of the precise role and regulation of phosphorylation sites on SHP-1 itself has been technically difficult, since these sites, by providing excellent substrates for the phosphatase themselves, can undergo autodephosphorylation (Bouchard et al., 1994). Further difficulties have arisen from the intrinsic instability of the intramolecular interactions within the phosphatase. SHP-1 has multiple potential phosphorylation sites[1] and three – Tyr536, Tyr564, Ser591 - have been characterized in functional studies. Phosphorylation of the Tyr536 residue, either by insulin or Lck, or the Tyr564 residue, by Lyn, increases the activity of SHP-1 (Bennett et al., 1994; Lorenz et al., 1994; Uchida et al., 1994). Zhang et al used an elegant in vitro model of protein ligation with incorporation of phosphonate analogues and demonstrated that phosphorylation of

[1] Scansite.mit.edu

Tyr536 increases SHP-1 activity about 4–8-fold, whereas phosphorylation of Tyr564 causes at the most a 1.6-fold increase (Zhang et al., 2003). A further study showed that Ser591 close to the very end of the C tail of SHP-1 is within a cluster of basophilic motifs important for membrane binding motifs and nuclear localization signals. Phosphorylation, by neutralizing the net charge of positively charged residues around Ser591, seems to be responsible for regulating these functions (Craggs and Kellie, 2001). Further, Ser591 was shown to be phosphorylated within one minute following TCR stimulation, an effect not mediated by PKC and associated with transient inhibition of its phosphatase activity (Craggs and Kellie, 2001). In neutrophils, however, Ser591 was found to be phosphorylated by purified PKC in vitro, concomitant with a reduction in the phosphatase activity (Brumell et al., 1997).

As mentioned above, SHP-1 has also been shown to mediate its inhibitory effect via mechanisms independent of its central catalytic domain. Following ligand binding, SHP-1 is recruited to the receptor/Janus kinase (Jak) complex, which leads to its phosphorylation on the C-terminal tyrosine residues. This results in recruitment of the growth-factor receptor-bound protein GrB/SOCS-1 complex with subsequent targeting of SOCS-1 to the Jak2 kinase and inhibition of cytokine signaling (Minoo et al., 2004).

The C-terminus of SHP-1 fulfills a dual regulatory role in SHP-1 biology, it affects its enzymatic activity as well as its localization to distinct membrane microdomains. The most terminal end of the C-terminus contains a tightly regulated nuclear localization signal that, in T cells at least, mediates its constitutive localization to lipid rafts, or ordered lipid-protein nanodomains (Eggeling et al., 2009; Fawcett and Lorenz, 2005). This is of relevance, given that recent data indicates that protein-protein complexes work in concert with lipid rafts to critically regulate early T-cell signaling and the proper formation of the immunological synapse (Douglass and Vale, 2005; Gaus et al., 2005). Phosphorylation of Ser591 impairs localization of SHP-1 to lipid rafts. Importantly, there is some evidence for the role of lipid rafts in HIV entry via CD4 and CCR5 (Popik et al., 2002). Further, there is direct evidence for the presence of DC-SIGN microdomains as docking sites for HIV entry to DCs (Cambi et al., 2004) or even DC-SIGN and CD4-independent entry of HIV via unidentified receptors located in lipid rafts (Gummuluru et al., 2003).

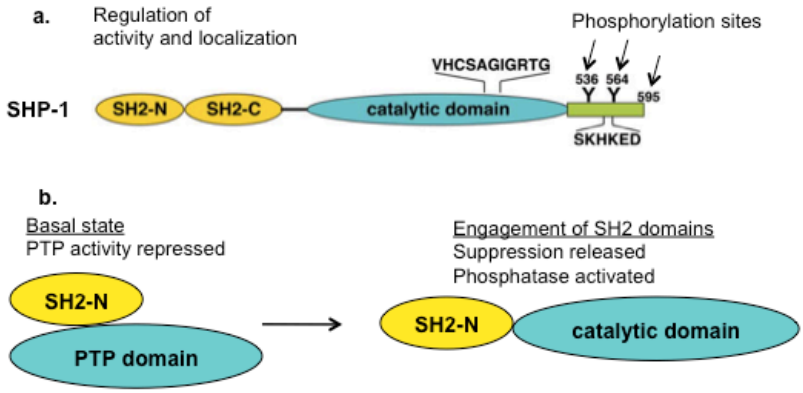

Figure 5.1. Schematic structure of SHP-1. a. SHP-1 contains a central catalytic domain containing the characteristic PTP signature motif VHCSAGIGRTG, two SH2 domains at their N-termini, and a C-terminus with potential tyrosine phosphorylation sites. The SH2 domains have been shown to be important for localization as well as for activity regulation. b. At the basal state, the N-terminal SH2-domain is intramolecularly associated with the PTP domain, thereby repressing its activity . Upon engagement of the SH2 domains, this suppression is released leading to activation of the phosphatase. Adapted from (Lorenz, 2009).

5.1.2 Role of SHP-1 in innate immunity

SHP-1 is predominantly expressed in haematopoetic and endothelial cells. Its homologue SHP-2 on the other hand is expressed ubiquitously and serves a positive regulatory role in signaling pathways (Lorenz, 2009). There is a substantial body of evidence for the role of SHP-1 in T and B cell differentiation and signaling, which is beyond the scope of this chapter (Tamir et al., 2000). For example, CEACAM1 associates with and recruits SHP-1 to the TCR/CD3 complex leading to dephosphorylation of CD3-zeta and ZAP-70 and consequently decreased activation of the elements downstream of ZAP-70 (Chen et al., 2008). The physiological consequence is termination of the cytolytic function initiated by the TCR/CD3 complex. However, many other aspects of SHP-1 biology, such as the specific substrates targeted by SHP-1, how SHP-1 is incorporated into the signaling complex and its role in innate immunity are still poorly understood.

The majority of work on SHP-1 function is based on the genetic model of SHP-1 deficiency, the motheaten mouse *me*/*me* model (Zhang et al., 2000). The motheaten mice either express no SHP-1 (me^{-}/me^{-}) or catalytically inactive SHP-1 (me^{viable}/me^{viable})

due to splice mutations in the gene (Tsui et al., 2006). Phenotypically they display patchy defects in skin pigmentation due to displacement of hair follicles by neutrophils, hence their name. Motheaten mice develop symptoms reminiscent of systemic lupus erythematodes with severe hyperinflammation as well as immunodeficiency (Lorenz, 2009). Characteristic findings are overproduction and accumulation of macrophages and neutrophils in several organs and increased production of autoantibodies and immunoglobulins, leading to glomerulonephritis and a haemorrhagic interstitial pneumonitis that ultimately causes death at about 3-6 weeks of age (Nakayama et al., 1997; Shultz and Green, 1976). Studies of me^{-}/me^{-} mice bred into *nude* or *rag* knockout backgrounds suggest that defects of the myeloid cell lineage are crucial for the development of the inflammatory syndrome, whereas lymphoid cells appear to be dispensable (Yu et al., 1996). This underscores the role of SHP-1 in the innate immune system. Although studies of the me^{-}/me^{-} model have been invaluable in understanding the biological function of SHP-1, it has been difficult to discriminate between primary, cell autonomous defects caused by direct loss of SHP-1 and secondary defects caused by dysregulation of affected cell populations. However, the recent description of a conditional knockout of SHP-1 may be helpful in clarifying this (Fowler et al., 2010). Interestingly a mutation in the gene encoding for SHP-1 has been linked to Sezary syndrome, a T-cell cutaneous lymphoma with chronic inflammation (Ma et al., 2003).

An important study by Cao and coworkers identified the mechanism whereby SHP-1 acts as a master switch in the homeostatic regulation of TLR signaling (An et al., 2008). Examining PRR signaling in me^{-}/me^{-} mice Cao and colleagues demonstrate that in response to TLR4, TLR3 and RIG-I stimulation SHP-1 deficiency leads to increased induction of a proinflammatory response with production of TNFα, IL6 and IL1β, while simultaneously reducing an anti-inflammatory response with impaired production of type I interferons. Mice infected with vesicular stomatitis virus fail to induce an IFN-β response in the absence of SHP-1. They further find that SHP-1 signaling leads to basal activation of the kinase IRAK1 and then to its rapid degradation, mediated by direct binding of SHP-1 to the ITIM motif within IRAK1. This in turn is responsible for the inhibition of proinflammatory cytokines and simultaneous induction of type I IFN production. Of note, this effect was independent of the phosphatase activity of SHP-1. In summary, this study identifies SHP-1 as a key regulator of IRAK1 and the induction

of an appropriate anti-viral immune response by skewing the balance from proinflammatory cytokines to anti-inflammatory type I interferons.

Given these findings, it is tempting to speculate that manipulation of SHP-1 by HIV-1 may create a favourable environment for the virus with a dampened antiviral interferon response towards a proinflammatory response. This may (i) increase viral transcription via NF-kB mediated activation of the LTR (Fortin et al., 2001) and (ii) attract more susceptible target cells, reminiscent of the findings of the acute SIV NPH model described in the introduction (Li et al., 2009). Indeed, studies by M. Olivier and co-workers provided more insights into the role of SHP-1 in evasion of the immune response towards a pathogen (Shio et al., 2012). They showed that the intracellular parasite Leishmania activates SHP-1 in macrophages, thereby inactivating JAK2 and Erk1/2 and hence critical macrophage functions such as production of nitric oxide, IL12 and TNF-α (Abu-Dayyeh et al., 2008). Furthermore, corroborating the findings by Cao et al, the same group demonstrated that SHP-1 also inhibited TLR-induced macrophage activation via binding of SHP-1 to a conserved motif within IRAK-1, leading to deactivation of IRAK1 (Abu-Dayyeh et al., 2008).

These publications do not completely concur with studies showing that defective production of IFNα in IRAK1-deficient cells is due to the fact that IRAK1 is an essential kinase for IRF7 (Uematsu et al., 2005), and more work is required to clarify these findings. Despite conflicting literature into the mechanism of SHP-1 in regulation of the innate immune response, a large body of evidence supports the integral role of SHP-1 in terminating or inhibiting activation signaling cascades to modulate the immune response. The correct balance between activation and inhibition is critical to an appropriate immune response, if a defect in negative regulation occurs, immunopathology may ensue (O'Neill, 2008). Chronic HIV-1 infection is characterized by systemic immune activation due to dysregulated immune responses to the virus itself, microbial products, co-infections and homeostatic signals (Douek et al., 2009). Hence, I hypothesized that the complete dephosphorylation of SHP-1 mediated by HIV-1 may be part of an immune evasive strategy of the virus to induce a favourable inflammatory environment in DCs upon encounter in mucosal tissues.

5.2 Aims

- to confirm dephosphorylation of SHP-1 by HIV-1
- to identify the trigger for HIV-1-mediated dephosphorylation of SHP-1
- elucidate the role of SHP-1 in the immune response to HIV-1
- identify novel HIV-1 mediated evasion pathway in DCs.

5.3 Results

5.3.1 Identification and confirmation of HIV-1-mediated dephosphorylation of SHP-1

LC-MS/MS analysis of HIV-1-infected phosphoprotein fractions revealed absence of the usually abundant cytosolic phosphatase SHP-1. In contrast, it was detected in fraction 9 of mock-infected DCs with an Ions score of 63 (figure 5.2a), identifying SHP-1 as a protein dephosphorylated by HIV-1 within 10 minutes. Rigorous bioinformatic analysis (see chapter 3) set at a false discovery rate of 1% showed a robust score with identification of three unique peptides to SHP-1 (figure 5.2b).

Strikingly, in a parallel phosphoproteomic screen carried out within our group (John Baker) characterizing the NOD-2 signalosome, we had made the opposite observation: Activation of DCs with muramyl dipeptide (MDP) - the ligand for NOD2 – induced phosphorylation of SHP-1 (John Baker). In addition, there are no reports on dephosphorylation of SHP-1 following PRR signaling, whereas investigations have ascribed phosphorylation of SHP-1 as a mechanism for regulation of its phosphatase activity. This suggested a unique HIV-1-triggered phenomenon.

Initially, I confirmed the preliminary observation made by LC-MS/MS analysis by immunoblotting phosphofractions of DCs infected with HIV-1 or mock for SHP-1. SHP-1 was completely absent in HIV-1-infected phosphofractions in multiple biological replicates tested (Figure 5.3a).

Figure 5.2. Identification of SHP-1 (PTPN-6) in Fraction 9 of mock-infected samples by LC-MS/MS. A. Mascot analysis identifies SHP-1 with a Mascot score of 63. In bold red are peptides identified by LC-MS/MS matching the protein sequence of SHP-1. **B.** Analysis of LC-MS/MS data by Proteomics Pipeline identified SHP-1 with a high confidence. Shown are peptide sequences identified with their respective weight (wt). A wt of 1 depicts recognition of a unique peptide sequence to the protein sequence of SHP-1. SHP-1 was completely absent from HIV-1-infected fractions 1-12.

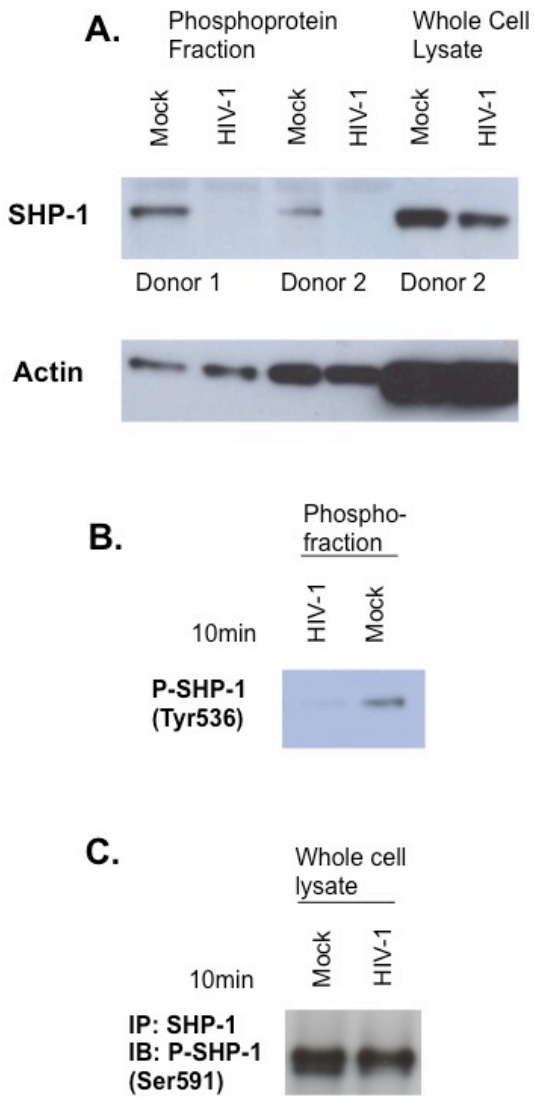

Figure 5.3. Confirmation of SHP-1 dephosphorylation. A. SHP-1 is dephosphorylated by HIV-1 within 10 min. Immunoblot of phosphofractions and whole cell lysates of DCs infected with mock or HIV-1 for 10 min. Western blot of SHP-1 and Actin is shown. **B.** SHP-1 is dephosphorylated at Tyr536 residue following HIV-1 infection. Phosphoenriched fractions were blotted with an antibody specific for the Tyr536 residue of SHP-1. **C.** SHP-1 may be dephosphorylated at Ser591 residue. DCs were infected with HIV-1 or mock for 10 min, lysed and immunoprecipitated with an antibody to SHP-1, and immunoblotted with an antibody specific for the Ser591 residue of SHP-1.

SHP-1 has potentially three phosphorylation sites. Blotting with a commercial phospho-specific antibody against the Tyr536 residue shows dephosphorylation of SHP-1 at this residue following 10 min of HIV-1 infection (Figure 5.3b). There is no commercially available antibody for the Tyr564 residue. Further, using a commercial antibody specific for the Ser591 residue, I could not detect any differences between HIV-1 and mock infection following phosphoenrichment of whole cell lysates. To exclude poor phosphoenrichment efficiency by the columns, I immunoprecipitated SHP-1 following 10 min HIV-1 and mock infection and blotted for Ser591, and could observe lower density in the HIV-1-infected sample indicating dephosphorylation of SHP-1 at the Ser591 site. The lack of complete dephosphorylation observed may be due to non-specific cross-reactivity, a recognized technical problem of phosphoserine-specific antibodies.

In summary, HIV-1 dephosphorylates SHP-1 within 10 min of infection. This work is the first to show dephosphorylation of this important phosphatase by a pathogen. Furthermore, HIV-1 induces dephosphorylation at the Tyr536 residue, a residue with a known role in regulating the phosphatase activity of the protein (Zhang et al., 2003).

5.3.2 Investigation of the effect of HIV-1 on the phosphatase activity and intracellular localization of SHP-1

To determine whether HIV-1-mediated dephosphorylation of SHP-1 affects the phosphatase activity of SHP-1, DCs were infected with HIV-1 over a time course of 3, 10 and 30 min, lysed and equalized for protein concentration by a Bradford dye assay. Following immunoprecipitation of SHP-1 with SHP-1 antibody-conjugated agarose beads over 3 hours, a synthetic phosphopeptide substrate was added that is dephosphorylated by active SHP-1 to generate free phosphate and unphosphorylated peptide. The amount of free phosphate, that is the phosphatase activity, was determined by a sensitive dye binding assay. Figure 5.4 demonstrates consistent and rapid changes in the phosphatase activity induced by HIV-1 in comparison to mock, the activity is decreased by ~20% at early time points returning to normal levels after 30 minutes. This indicates that the changes in SHP-1 are induced fairly early during infection and may be mediated at the entry step of the virus into DCs, possibly via a cell surface protein.

In T cells, activation of the TCR with CD3/CD28 antibodies is associated with a temporal regulation of the SHP-1 phosphatase activity due to sequential phosphorylation of distinct residues. The activity is reduced by 30% within one minute concomitant with the phosphorylation of the Ser591 residue, subsequently the activity increases over time with a peak at 30 min secondary to phosphorylation of the Tyr536 residue (Liu et al., 2007a; Zhang et al., 2003).

Further mechanisms that may regulate SHP-1 function are changes in cellular localization, e.g. by altering the distribution of SHP-1 in and out of lipid rafts or its nuclear translocation. Phosphorylation of Ser591 has been shown to decrease membrane localization and prevent nuclear localization of SHP-1 (Liu et al., 2007a). In order to investigate whether HIV-1 alters the distribution of SHP-1 within DCs, DCs were infected with HIV-1 or mock for 2 hours, seeded at $2x10^5$ cells per well onto poly-L-lysine tissue culture slides. Cells were allowed to adhere for 1 hour prior to fixation, permeabilization and staining with antibodies to SHP-1, DC-SIGN and a nuclear To-Pro stain and analyzed by confocal microscopy. As illustrated in figure 5.5, infection of DCs with HIV-1 did not led to visible changes in the diffuse cytoplasmic localization of SHP-1 in DCs or an increase in co-localization of SHP-1 with DC-SIGN. These experiments, however, do not address differential HIV-1-induced localization to lipid rafts.

Altogether the data I have presented so far, indicate that HIV-1 dephosphorylates SHP-1 at the Tyr536 – and possibly the Ser591 – residue leading to rapid reduction of the phosphatase activity. This is in accord with experimental data documenting that phosphorylation of Tyr536 activates the catalytic activity of SHP-1 (Zhang et al., 2003). Further, HIV-1 does not induce dramatic changes in localization of SHP-1 in DCs.

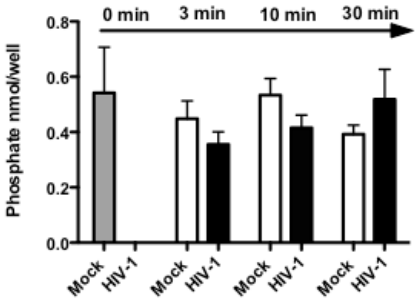

Figure 5.4. HIV-1 leads to a small but consistent reduction of SHP-1 phosphatase activity. DCs were infected with HIV-1 or mock for the indicated timepoints and lysed. Equal amount of protein (determined by Bradford dye assay) were immunoprecipitated with a SHP-1 antibody conjugated to agarose beads. A synthetic phosphopetide that is dephosphorylated by active SHP-1 was added. The amount of free phosphate in nmol/well was determined by a dye binding assay. Shown are three biological replicates as a mean ± SEM.

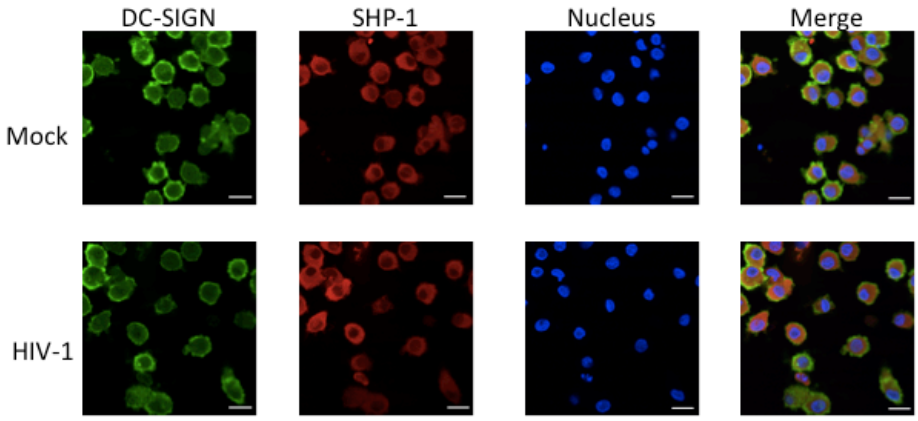

Figure 5.5. HIV-1 infection does not induce visible changes in SHP-1 localization. DCs were infected with HIV-1 or mock for 2 h, washed and left to adhere on slides for 1 hour. Following fixation and permeabilization they were stained for DC-SIGN, SHP-1 and nucleus and visualized by confocal microscopy. One representative donor is shown.

5.3.3 Exploring potential HIV-1 ligands triggering dephosphorylation of SHP-1

As mentioned in the introduction, studies of the regulation of SHP-1 itself have been hampered by technical difficulties explaining why there is no published work on phosphatases specifically dephosphorylating SHP-1.

Given the observation that dephosphorylation and deactivation of the phosphatase is induced early upon HIV-1 exposure, I hypothesized that this may be mediated by membrane receptor mediated signaling. The most obvious receptor in this setting is DC-SIGN, given that is highly expressed on DCs and binds the highly glycosylated envelope protein of HIV-1 upon entry to DCs. To test this, I used H200, a DC-SIGN specific antibody, that previous work in our group had shown to specifically bind and signal via DC-SIGN (Hodges et al., 2007). DCs were activated with plate-bound H200 at a concentration of 10μg/ml for 10 minutes, enriched for phosphoproteins as per usual protocol and immunoblotted for SHP-1. Figure 5.6 demonstrates that DC-SIGN signaling does not dephosphorylate SHP-1.

HIV-1-mediated dephosphorylation of SHP-1 may be due to a combinatorial interaction of the viral glycoprotein with DC-SIGN in concert with other possible receptors, a process that may not be reproducible with H200 activation on its own. To explore this possibility, I activated DCs with recombinant gp120 (rgp120) for 15 min and immunoblotted for phosphotyrosines at first to ensure that rgp120 is able to elicit a signaling cascade in DCs. I could not detect any visible changes in tyrosine phosphorylation upon activation with rgp120 monomers (figure 5.7), an observation that was in keeping with previous experience in our group (A. Hodges). It is conceivable that rgp120 do not display the three-dimensional conformation of N-linked glycans required to aggregate or tetramerize DC-SIGN and initiate a signaling cascade (Hong et al., 2007). In order to investigate the role of DC-SIGN in the dephosphorylation of SHP-1 cell lines such as THP-1 stably transfected with various DC-SIGN tail mutants would be more valuable.

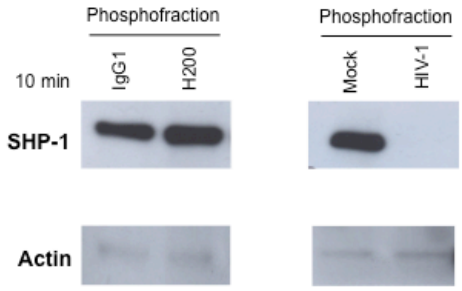

Figure 5.6. HIV-1-induced dephosphorylation of SHP-1 is not mediated via DC-SIGN. MDDCs were activated with 10µg/ml H200, an isotype control, mock and HIV-1 for 10 min, lysed and enriched for phosphoproteins. Immunoblots for SHP-1 and Actin are shown.

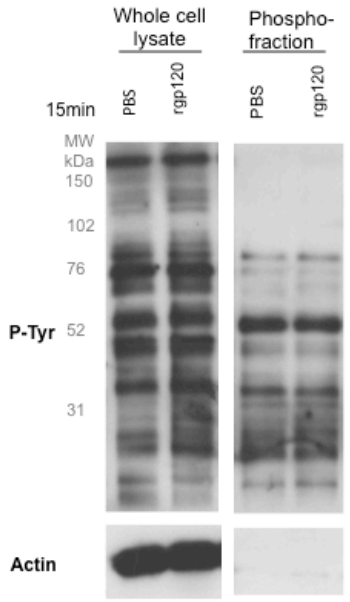

Figure 5.7. Recombinant gp120 fails to elicit visible changes in tyrosine phosphorylation in DCs. DCs were incubated with 10µg/ml rgp120, lysed, enriched for phosphoproteins and immunobloted for phosphotyrosines and Actin.

Next, I assessed the role of other PRRs in HIV-1 triggered dephosphorylation, given the evidence for SHP-1 in TLR and RLR signaling (An et al., 2008). HIV-1 can potentially express multiple PAMPs (discussed in 1.3.1): HIV-1 ssRNA can be recognized by TLR8 in endosomes and signal through the adaptor protein MyD88; short and long dsRNA replication intermediates that have gained access to the cytosol can bind to the retinoic acid-inducible gene-like receptors, RIG-I, MDA5 and LGP2, and signal through CARD-CARD interactions with MAVS, resulting in inflammatory cytokine and type I IFN production; however, it is unlikely that ssRNA viral genomes containing 5'-triphosphates – the natural ligands for RIG-I - are produced in the course of HIV-1 replication. In order to explore the possibility that SHP-1 dephosphorylation may be triggered via the recognition of TLR8 or RIG-I, DCs were activated with 10μg/ml ssRNA40, a TLR8-specific ligand derived from the HIV-1 LTR genome and 1μg/ml poly-IC-LMW, a RLR-specific ligand consisting of synthetic dsRNA polymer complexed with lyovec. Activation with neither of these ligands did result in dephosphorylation of SHP-1 (figure 5.8). This is unlikely to be due to a lack of signaling per se, as I have already shown that ssRNA40 is able to elicit a signaling cascade (figure 3.2).

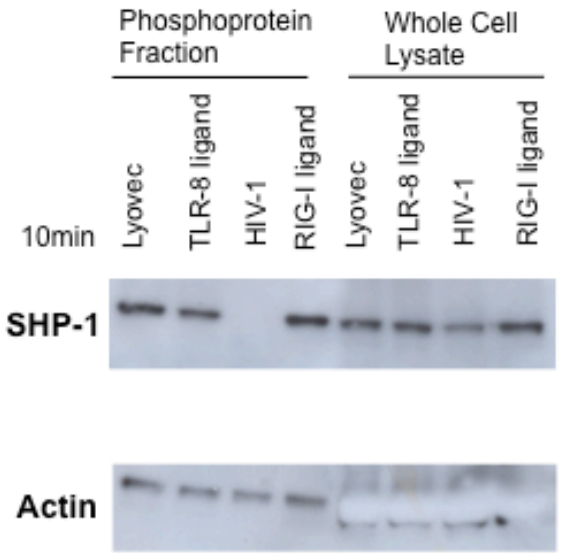

Figure 5.8. HIV-1-induced dephosphorylation of SHP-1 is not mediated via the PRRs TLR8 or RIG-I. DCs were activated with 10µg/ml ssRNA40, 1µg/ml polyIC-LMW, lyovec control and HIV-1 BaL for 10 min, lysed, enriched for phosphoproteins and immunoblotted for SHP-1 and Actin.

Recent work by M. Tremblay and co-workers has elucidated the role of DCIR as a member of a novel group of C-type lectin receptors (CLR) that include a single carbohydrate recognition domain at the COOH terminal (Lambert et al., 2008). DCIR is the only CLR that expresses an ITIM motif in its transmembrane region (Kanazawa et al., 2004). A recent study, published while the work described in this chapter was in progress, showed that engagement of DCIR by HIV-1 leads to phosphorylation of key residues in the ITIM region of DCIR and recruitment of a signaling complex consisting of the kinase Syk and Src family kinases and activation of SHP-1 and SHP-2 (Lambert et al., 2011). Activation of DCs with a DCIR signaling antibody did not induce visible changes in SHP-1 phosphorylation (work carried out by Al Leslie, data not shown).

Further potential receptors, that may be involved in dephosphorylation of SHP-1, but not explored in this work are: (i) CCR5, binding of MIP1-ß beta to CCR5 induces tyrosine phosphorylation of SHP-1 (Ganju et al., 2000), despite generally low levels of CCR5 expression on DCs (only 5-11%) compared to CD4 T cells (Dong et al., 2007); (ii) CD33-related subset of sialic-acid-binding Ig-like lectins (Siglecs), a family of transmembrane proteins that recognize glycans with poorly conserved binding specificities. CD33 is expressed both on immature and mature myeloid cells and has a conserved intracellular proximal ITIM and distal ITIM-like motif (Walter et al., 2008). Upon engagement of the receptor, these motifs become tyrosine phosphorylated, transmitting inhibitory signals by binding and activating SHP-1 (and SHP- 2). It would be interesting to investigate CD33 as a potential HIV-1 receptor mediating SHP-1 dephosphorylation, e.g. by using siRNA knockdown or CD33 activating ligands. (iii) SHP-1 dephosphorylation may also be part of a "normal" process of viral endocytosis mediated by actin and a caveolin scaffolding complex (see below), for instance upon recruitment of SHP-1 to the plasma membrane.

In summary, I could exclude a role for DC-SIGN, TLR8 or RIG-I in HIV-1-mediated dephosphorylation of SHP-1. Further work should explore the role of other potential PRRs such as DCIR and CD33 in SHP-1 and HIV-1 signaling.

5.3.4 Manipulation of SHP-1 and its effect on HIV-1 replication and type I interferon induction

So far I have established that SHP-1, a phosphatase with an important immune regulatory function, was dephosphorylated and diminished in activity by HIV-1 early during infection. The next question is whether this is part of an immune evasion strategy of the virus? Two approaches for manipulation of SHP-1 were chosen: knockdown of SHP-1 by RNAi transfection as well as upregulation of a catalytically inactive mutant and a wild type SHP-1 plasmid by electroporation. Transfection efficiencies were good as determined by immunoblot and qPCR, respectively (figure 5.9). At first, the effect of SHP-1 on HIV-1 replication was assessed. Knockdown of SHP-1 had no effect on HIV-1 *trans*-infection, although there was a small trend towards an increase in *trans*-infection in some donors (for details of methodology see siRNA library screen in Chapter 4). To determine the effect of SHP-1 on early HIV-1 infection of DCs, I examined a different aspect of HIV-1 infection by measuring the levels of successful integration and viral gene transcription. Although DCs show low or rather delayed HIV-1 replication, Gringhuis et al had demonstrated that HIV-1 transcription is ongoing as early as 6 h following infection (Gringhuis et al., 2010). Therefore, DCs transfected with SHP-1 siRNA were infected with HIV-1 48 h post transfection for 2 h and RNA was harvested 6 or 24 h later. Genomic DNA was removed prior to SYBR-green based qPCR for tat-rev genes. As seen in figure 5.11b, SHP-1 knockdown leads to reduction of HIV-1 transcription, whereas knockdown of IRAK-1 doesn't.

In summary, SHP-1 knockdown has no effect on HIV-1 *trans*-infection but reduces successful viral transcription. These results may appear contradictory at first, however they address two distinct aspects of HIV-1 infection; the *trans*-infection assay is a measure for virions that succeed in evading lysosomal degradation to traffic to the *trans*-compartment. The qPCR assay is a measure for successful uncoating, reverse transcription and integration of virus into the host genome for subsequent assembly and de novo virus production.

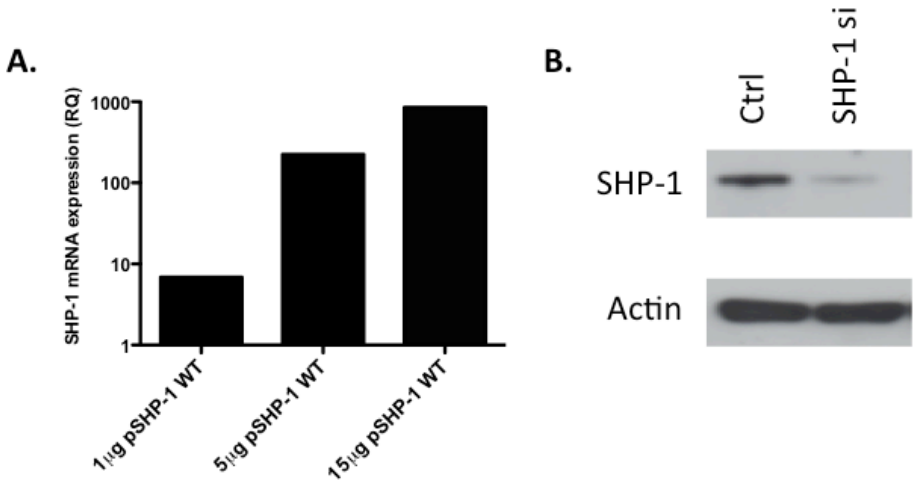

Figure 5.9. Confirmation of efficient upregulation and knockdown of SHP-1 by electroporation. **A.** Electroporation of DCs with different concentrations of SHP-1 plasmid induces upregulation of SHP-1 as measured by qPCR 24 h post transfection. **B.** Electroporation of DCs with a SHP-1 siRNA leads to downregulation of SHP-1 expression as measured by immunoblot of DCs harvested 48 h post transfection.

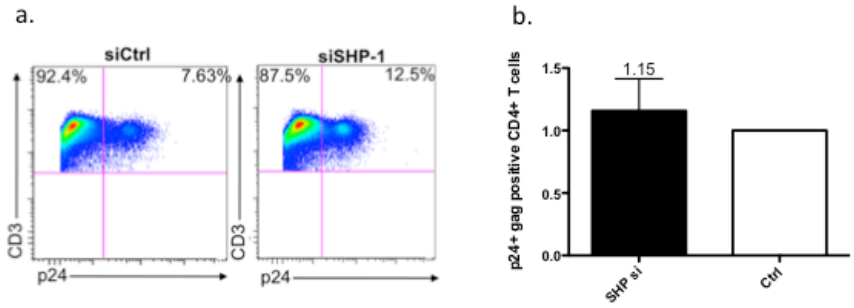

Figure 5.10. Effect of SHP-1 knockdown on HIV-1 *trans*-infection. DCs were electroporated with SHP-1 and control siRNA and infected with HIV-1 48h post transfection for 2h. CD4+ PHA blasts were added at ratio 1:3 and cells were co-cultured for 72h prior to intracellular staining for p24 gag and flow cytometry. a. Representative FACS plot shown. b. Relative frequency of p24 gag + T cells in SHP-1 knockdown to control siRNA. Data represents mean ± SEM of 4 biological replicates.

Whereas SHP-1 knockdown is a valuable tool to investigate the overall effect of SHP-1 as such, a more elegant method is based on overexpression of the catalytically inactive mutant form of the protein. This allows direct examination of functional effects dependent on the phosphatase activity of SHP-1, although as mentioned before SHP-1 may also exert phosphatase-independent effects.

For overexpression of wild type and catalytically inactive SHP-1, I used two plasmids, pJ3SHP-1 WT and pJ3SHP-1CS, which has a C→ S mutation at position 453, rendering it catalytically inactive (Plas et al., 1999). Plasmids were transformed into competent bacteria and DNA isolated with an endotoxin free kit according to standardized protocols. Insertion of correct DNA was verified by restriction enzyme digest and sequencing. DNA was transfected into DCs using the Amaxa nucleofector kit, and although I could detect efficient upregulation of SHP-1 along different DNA concentrations by real time PCR (figure 5.9), there was considerable amount of cell death associated with the transfection (figure 5.12). Using other electroporation devices such as the Neon system was associated with even lower cell viability. Efforts to optimize culture and transfection conditions did not lead to a reduction in cell death. It is conceivable that primary DCs are particularly susceptible to the effects of electroporation with a DNA that encodes a gene with such an important role in immune regulation. SHP-1 has also been shown to be involved in cell death pathways controlling the internalization of a death-inducing complex via vav dephosphorylation (Koncz et al., 2008).

Whereas quantification of *trans*-infection heavily relies on comparable numbers of viable DCs, the HIV-1 transcription assay, due to the inherent GAPDH control in all conditions, allows normalization across conditions. Overexpression of wild type and inactive SHP-1 in DCs both may result in an increase in early viral transcription compared to a control plasmid (figure 5.11a), however given the experimental flaws just mentioned, it is difficult to infer any direct effect of SHP-1 from these results.

Next the question was addressed if SHP-1 may be involved in the evasion of an interferon response to HIV-1. Inferring from Cao and co-workers' paper HIV-1 mediated manipulation of SHP-1 could lead to following scenario: HIV-1 dephosphorylates and therefore inactivates SHP-1, which results in an increase in the inflammatory response via upregulation of NF-kB, while downmodulating the

interferon response via IRFs. However, knockdown of SHP-1 failed to show any difference in the induction of the type I interferon IFN-ß1 or IRF3 or the inflammatory cytokines IL6 and IL8 following HIV-1 infection (figure 5.13).

In conclusion, knockdown of SHP-1 leads to a reduction in viral transcription but has no effect on HIV-1 DC-CD4 *trans*-infection or the induction of inflammatory cytokines.

Given the difficulties of SHP-1 DNA electroporation in DCs, I decided to develop a lentiviral system of transgene overexpression to circumvent this problem, allowing me to investigate the effect of SHP-1 on interferon and cytokine production more thoroughly.

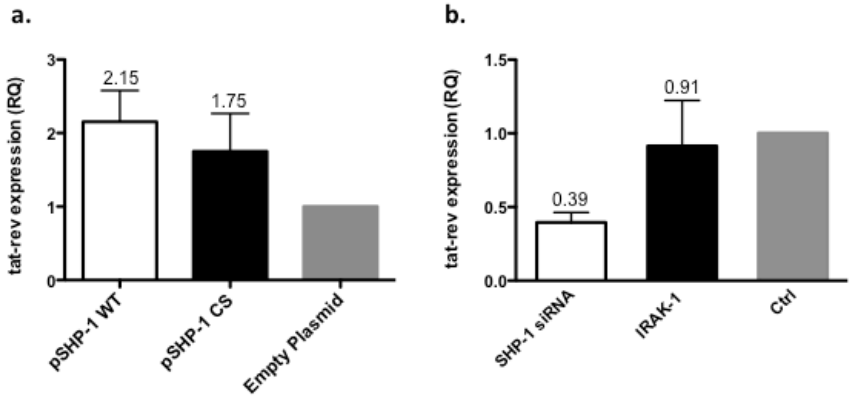

Figure 5.11. Investigation of the role of SHP-1 in early HIV-1 transcription. QPCR analysis of tat-rev mRNA expression in DCs infected with HIV-1 for 24 h. a. DCs transfected with wild type and C453S catalytically inactive SHP-1 plasmids were infected 24h post transfection with HIV-1 and harvested for qPCR 24h p.i. b. DCs transfected with SHP-1, IRAK-1 and control siRNA were infected 24h post transfection with HIV-1 and harvested for qPCR 24h p.i. Tat-rev expression was determined relative to GAPDH expression and expressed relative to empty plasmid or scrambled siRNA control. Data are represented as mean ± SEM of 6 (for a) and 5 (for b SHP-1 siRNA) and 2 (for IRAK-1 siRNA).

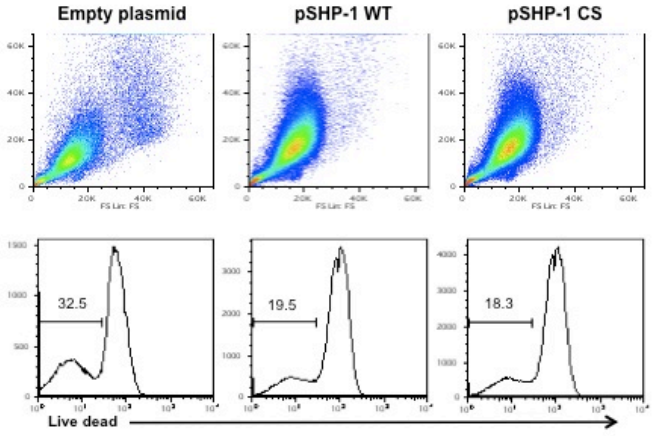

Figure 5.12. Electroporation of DCs with SHP-1 DNA causes significant cell death. DCs were electropolated with 1µg/ml of DNA using the amaxa nucleofector kit set at optimized conditions. 24 h post transfections DCs were harvested and stained with a fixable live dead stain. Shown are representative FACS plots of numerous replicates.

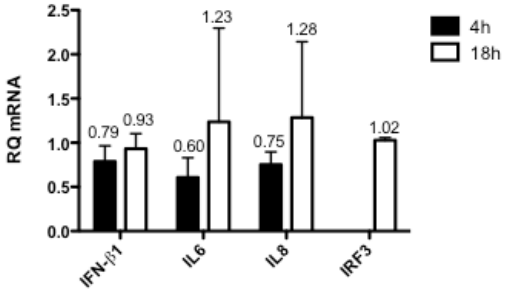

Figure 5.13. Investigation of the effect of SHP-1 knockdown on IFNβ 1, IL6, IL8 and IRF3 induction following HIV-1 infection. DCs were transfected with SHP-1 siRNA and scrambled siRNA, harvested 48h post-transfection and infected with HIV-1 or mock for 2h. Cells were harvested at 4 and 18h post Infection and analyzed by qPCR for indicated genes and GAPDH. Expression levels were normalized against mock and GAPDH. Data are representative of 3 independent experiments ± SEM.

5.3.5 Setting up a successful lentiviral system for transduction of primary DCs

Efficient genetic modification of primary cells for both ectopic gene expression as well as genetic knockdown can be difficult and DCs are known to be a particularly difficult cell type to transfect. In addition, successful genetic modification has been shown to be associated with cellular cytotoxicity and unspecific activation. Methods such as liposome-mediated transfection are ineffective due to inherent resistance of DCs. Further, electroporation, despite achieving satisfactory levels of transfection, is not without its caveats. Our group has been using two different electroporation devices – Amaxa® and Neon™ - with optimized protocols that have enabled us to achieve high transfection efficiencies, however Amaxa® nucleofection can be associated with variable levels of cytotoxicity and/or activation of DCs and we have not been able to establish a working protocol for efficient transfection of DNA using the Neon™ system yet. Therefore, I decided to set up a working protocol for efficient transduction of DCs with lentiviral vectors (LV).

A number of recent reports have described successful LV-mediated transduction of DCs (Berger et al., 2011; Manel et al., 2010). DCs are known to display an inherent restriction to lentiviral infection and productive infection can only be achieved by using unphysiologically high MOIs. To relieve the resistance in DCs to LV transduction, LV infection can be carried out in the presence of noninfectious viral like particles containing SIV vpx, which overcomes the restriction, therefore allowing the transgene coding the HIV-1 LV to achieve high transduction efficiency. The outline of the protocol is described in figure 5.14.

To make lentiviruses encoding wild type and catalytically inactive SHP-1, I started by designing primers to amplify the SHP-1 insert in the above mentioned SHP-1 plasmids (pJ3SHP-1 WT and C453S). The insert was cut out, amplified by PCR with SHP-1 primers and ligated into a plasmid encoding HIV-1 genes and Emerald. Successful and correct insert was examined by restriction digest and sequencing. At a second step, I made lentiviruses by transfecting HEK 293T cells with a mixture consisting of (i) the

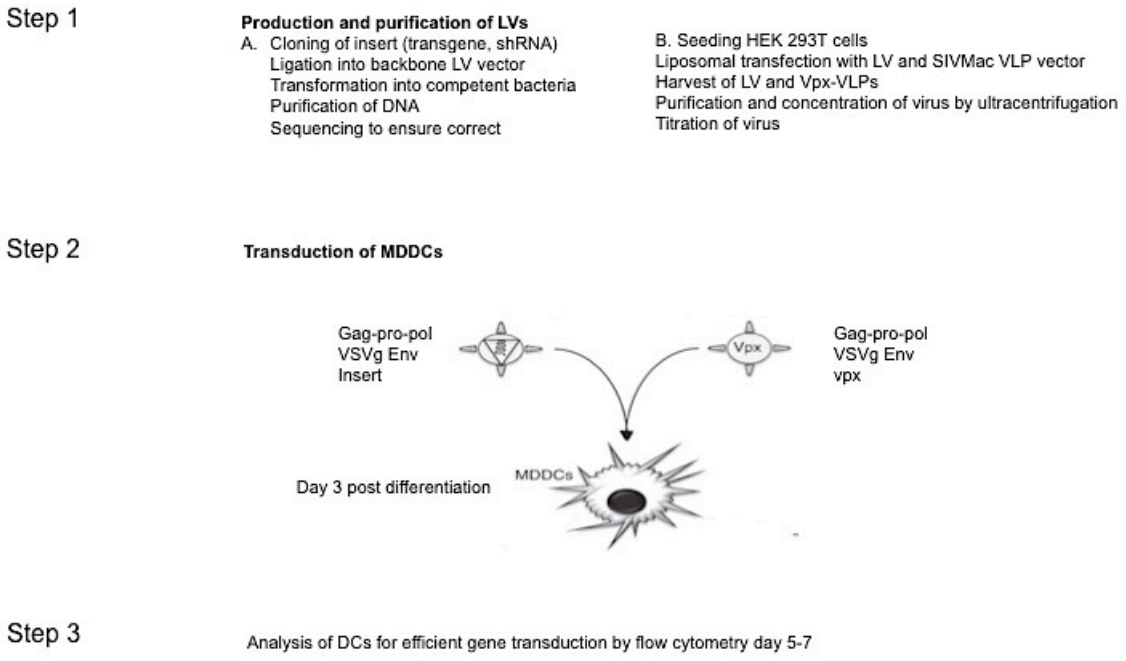

Figure 5.14. **Experimental workflow for lentiviral transduction of DCs**. Adapted from (Berger et al., 2011).

SHP-1 expression plasmid, (ii) a packaging plasmid consisting of gag and pol and (iii) a VSV-G viral envelope plasmid. In parallel, lentivirus was made containing Vpx-VLPs. The third step, that is still undergoing optimization, included simultaneous infection of DCs with both lentivirus and VLPs to induce expression of SHP-1. As demonstrated in figure 5.15, I could achieve reasonable levels of infection measured by upregulation of SHP-1 and detection of a population of cells double positive for SHP-1 and Emerald. This was possible by infecting DCs on day 3 post differentiation and measuring for transfection efficiency 4 days later, i.e. at day 7 post differentiation. Higher transduction efficiencies are desirable and there are still multiple modifications that can be attempted, e.g. using higher MOI or changing timings of infection and harvesting. As a first step, however, cloning of the transgene into a different lentiviral vector should be attempted. Here an HIV vector construct with IRES-Emerald was used and in retrospect the IRES sequence may have impaired upstream gene expression in DCs (Palmowski et al., 2004). It may also be difficult to overexpress a protein with such inherently high levels of expression and there are no established protocols for LV induced overexpression in DCs. As I'll show later, knockdown of a gene by this method has been more successful.

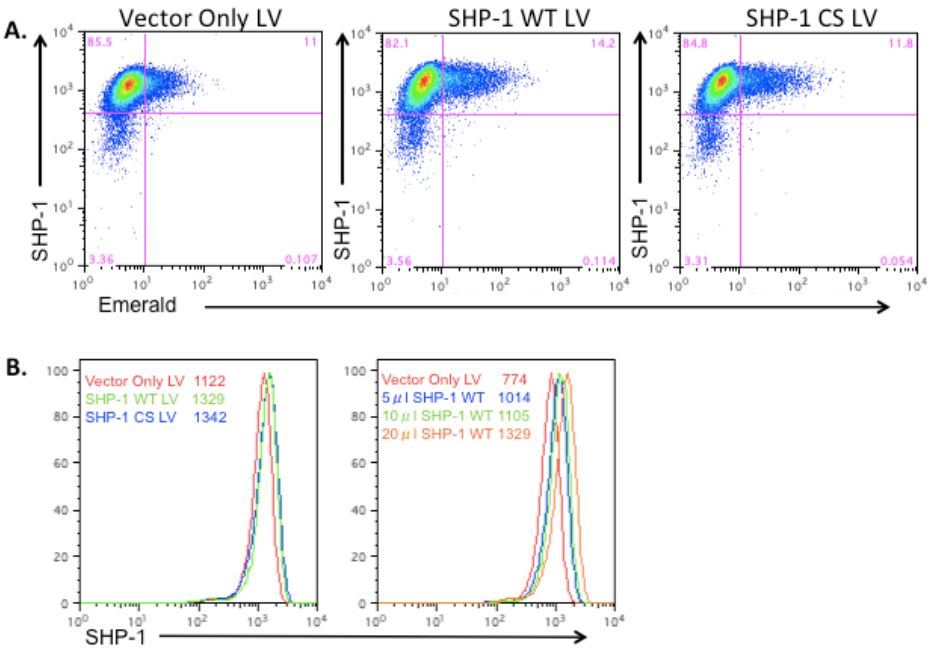

Figure 5.15. Lentiviral transduction of DCs with SHP-1 expressing vectors. DCs harvested on day 3 post differentiation were co-infected with vpx VLPs and SHP-1 containing lentiviruses for 2 h and analysed for levels of SHP-1 and Emerald by flow cytometry 4 days later**. A.** Lentiviral infection induces expression of SHP-1 in a small population of DCs as assessed by co-expression of SHP-1 and Emerald. **B.** Increasing concentrations of SHP-1 LV vector increases transduction efficiency (MFI of SHP-1 expression shown).

5.3.6 Analysis of the SHP-1 signaling complex within the HIV-1 signalosome

SHP-1 is present in distinct cytosolic pools in complex with other signaling molecules, and the finely balanced interplay between these molecules determines the net outcome of the signaling cascade (Paling and Welham, 2005; Perez-Villar et al., 1999; Stefanova et al., 2003). The bulk of published work on SHP-1 signaling is derived from studies of T and B cell receptor signaling and may not be applicable to innate signaling in DCs. Therefore to obtain a better understanding of the SHP-1 induced signaling complex (herein referred as the SHP-1 signalosome), I performed bioinformatics analysis of the HIV-1 signalosome with the aim to identify phosphoproteins clustering with SHP-1. I found 17 proteins that, according to my LC-MS/MS analysis, were differentially phosphorylated by HIV-1 within 10 min and had a known interaction with SHP-1

(Figure 5.16). Seven of these proteins had an effect on HIV-1 *trans*-infection, as determined by the siRNA library screen (table 4.1). Immunoblot analysis of chosen phosphoproteins confirmed differential phosphorylation of these proteins by HIV-1 across different fractions (figure 5.17).

Interestingly, the majority of these molecules are involved in actin-mediated reorganization, in particular as actin binding proteins, focal adhesion proteins and adaptor proteins, specifically filopodia and lamellopodia formation and integrin activation. This may not be surprising given that actin itself has been shown to be a direct substrate of SHP-1 (Lin et al., 2004).

Src associated in mitosis, 68 kDa (Sam68) has been ascribed important regulatory functions at two distinct steps of HIV-1 gene expression: 1. Nuclear exploitation of HIV-1 unspliced or singly spliced RNA with HIV-1 rev. 2. Translational regulation of HIV-1 RNA (He et al., 2009; Henao-Mejia et al., 2009). Additionally, Sam68 has also been implicated as an adaptor molecule associating with members of the Src family kinases and shown to be constitutively tyrosine-phosphorylated and co-immunoprecipitated with other molecules such as Cbl, SHP-1 and the growth factor receptor bound protein 2 (Fusaki et al., 1997). Hence, it would be interesting to study the functional significance of Sam68 in the entry to DCs.

The tyrosine kinase Abl and WAVE-2 have recently been shown to be essential for HIV-1 hemifusion, consisting of pore formation, pore enlargement and content mixing in CD4+ T cells (Harmon et al., 2010). Of note, WAVE-2 is phosphorylated and hereby activated by Abl. LIMS1 is involved in integrin signaling and found in focal adhesion plaques. Following TCR activation a signaling cascade involving WAVE-2 and an ARP2/3-vinculin-talin complex leads to integrin clustering, a process linking receptor mediated actin polymerization to integrin activation (Nolz et al., 2007). Talin-1 and vinculin, two proteins localizing to focal adhesions complexes have been implicated in endocytosis or fusion of retroviruses (Brown et al., 2011). While these represent well-characterized pathways in T cells, the relevance of these findings in DCs is still unknown.

Interestingly, in macrophages following Fc-receptor mediated phagocytosis a large complex including SLP-76, Ena/VASP proteins, WAVE-2, Nck and the Fyn binding/SLP-76 associated proteins (Fyb/SLAP), is formed and recruited to the

phagocytic cup. The complex then induces remodeling of the actin cytoskeleton allowing extension of pseudopodia and efficient particle internalization (Krause et al., 2000). ITIM motif containing receptors utilizing SHP-1 negatively regulate Src and Syk family PTK-dependent activation pathways in a variety of haematopoetic cells. One common target within these pathways is the SH2 domain containing leucocyte protein SLP76, which in T and NK cells is specifically dephosphorylated by SHP-1 (Binstadt et al., 1998). Phosphoproteomic analysis showed that HIV-1 induced dephosphorylation of SLP-76 (figure 5.17). SLP-76 is a binding partner of vav, a guanine nucleotide exchange factor for Rho family GTPases, that is a critical signaling molecule downstream of the TCR (Clements et al., 1998; Crespo et al., 1997). In DCs vav is an important component of a signaling pathway involving focal adhesion kinase, phospholipase C-γ2, and ERK1/2 following integrin ligation, resulting in cytoskeletal rearrangements and DC migration (Spurrell et al., 2009). A recent study demonstrated an association of SLP-76 with HIV nef and F-actin that facilitated viral release from T cells (Nagaraja et al., 2012).

The role of actin and actin remodeling in HIV-1 entry is undisputed and HIV-1 has evolved elaborate strategies to manipulate the actin and cytoskeleton machinery to its own advantage (Stolp and Fackler, 2011). Bioinformatics analysis of the SHP-1 signalosome is suggestive of SHP-1 playing a role in regulation of the DC cytoarchitecture, possibly in concert with other cytoskeletal proteins to facilitate HIV-1 entry/endocytosis. Live cell imaging of HIV-1 infected DCs to accurately assess the role of the SHP-1 signalosome in terms of kinetics and location during the earliest stage of viral infection may aid in characterizing the functional significance of SHP-1 in HIV-1 signaling. The remainder of this chapter will deal with how the finding of SHP-1 as part of the signalsome led to the discovery of another intricate mechanism in HIV-1 pathogenesis.

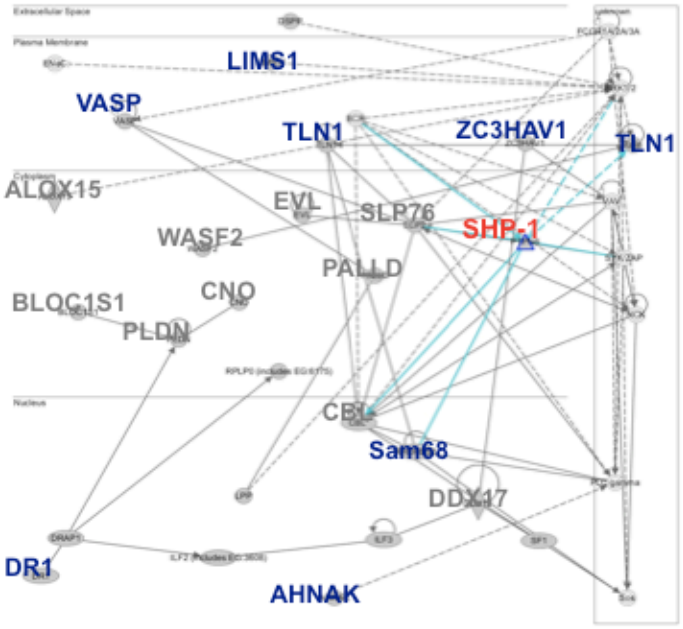

Figure 5.16. Ingenuity pathway analysis of the HIV-1 phosphoproteome identifies a signaling complex of proteins interacting with SHP-1. Phosphoproteins identified by LC-MS/MS and clustering with SHP-1 are depicted. Blue coloured proteins are proteins with an effect on HIV-1 trans infection, grey coloured proteins had no significant effect on *trans*-infection.

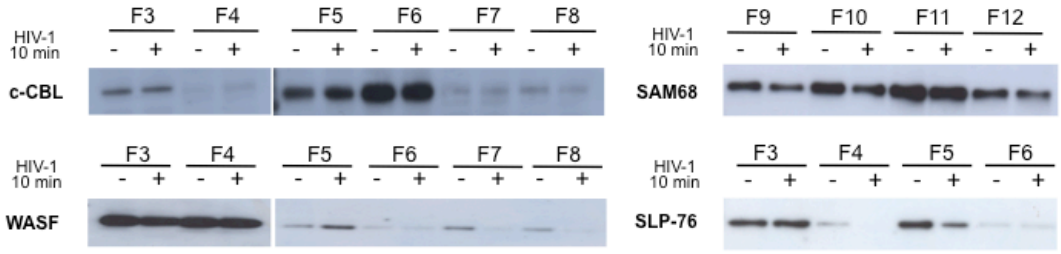

Figure 5.17. HIV-1 induces differential phosphorylation of proteins involved in the SHP-1 signalosome. DCs were infected with HIV-1 and mock for 10 min, lysed and enriched for phosphoproteins. Phosphoproteins were equalized among conditions, desalted and separated by isoelectric focussing. Immunoblots of single fractions were immunoblotted for proteins as indicated. c-CBL: Cbl proto-oncogene, E3 ubiquitin protein ligase. WASF: WAS protein family, member 1 (also called WAVE-2). SLP76: SH2 domain containing leukocyte protein of 76kDa (also called LCP2). Sam68: KH domain containing, RNA binding, signal transduction associated 1.

5.3.7 Rationale for exploring another putative receptor mediating dephosphorylation of SHP-1

As mentioned earlier SHP-1 binds to the cytosolic ITIM domain of membrane receptors. In myeloid cells and neurons, SHP-1 (and SHP-2) is known to associate with signal regulatory protein SIRPα, a transmembrane receptor known to participate in integrin-mediated adhesion (Matozaki et al., 2009). SIRPα contains two cytosolic ITIM domains with four tyrosine residues that are phosphorylated in response to a variety of stimuli, the two C-terminal sites providing the binding sites for SHP-1, that either is actively recruited, or according to some studies constitutively associated with SIRPα (Kong et al., 2007; Murai-Takebe et al., 2004). SIRPα has three immunoglobulin like domains in its extracellular region, which is heavily glycosylated, binding either soluble proteins such as surfactant A and D, that are present at high levels in the lung to prevent inflammation, or CD47 (Barclay and Brown, 2006). The latter interaction has recently attracted a lot of attention due to its potential as a therapeutic target in haematological conditions (Chao et al., 2012).

CD47, a marker of self on immune and nonimmune cells, is implicated in the generation of immune responses (van den Berg and van der Schoot, 2008). It is expressed ubiquitously on most cell types and was originally identified in association with $\alpha_v\beta_3$ integrin, hence its alternative name integrin-associated protein IAP (Lindberg et al., 1996). CD47 is a member of the immunoglobulin superfamily with a V-type Ig-like segment expressed extracellularly, five putative membrane-spanning domains and a short cytoplasmic tail (Matozaki et al., 2009). The interaction between the N-terminal IgV domain of SIRPα and the extracellular Ig-domain of CD47 has been resolved by X-ray crystallography showing that the interface between SIRPα and CD47 is reminiscent of antigen-antibody complexes (Hatherley et al., 2008; Liu et al., 2007b; Nakaishi et al., 2008). In addition, the lateral surface of the IgV domain of SIRPα has been suggested to be important for CD47 binding (Lee et al., 2007). In addition to its ability to associate with integrins, CD47 serves as a receptor for Thrombospondin 1, a multifunctional protein shown to be involved in angiogenesis and cell adhesion among others (Sarfati et al., 2008). Given the diversity of interacting partners, CD47, not surprisingly, plays an important role in a wide variety of cellular processes, such as leucocyte motility, migration and adhesion as well as phagocytosis.

Ligation of SIRPα with CD47 induces tyrosine phosphorylation in the cytoplasmic region of the former protein in macrophages (Tsuda et al., 1998), an effect that is not generalized among all cell types. The expression of CD47 on red blood cells or platelets prevents phagocytosis by splenic red pulp macrophages via SIRPα, a physiological mechanism to prevent conditions such as haemolytic anemia (Oldenborg et al., 2000). Generally the SIRPα-CD47 interaction allows discrimination of "non-self" from "self" or an "eat me" from a "do not eat me" signal, therefore controlling (xeno) transplant rejection and hematopoietic stem cell engraftment (van den Berg and van der Schoot, 2008). Weissman and Majeti have recently demonstrated in a number of studies, that CD47 is upregulated on myeloid leukemic cells and circulating hematopoietic stem cells during inflammation-mediated mobilization, enabling them to evade phagocytosis by macrophages (Majeti et al., 2009). They further showed that CD47 expression on leukemia cells in acute lymphoblastic leukemia (ALL) and acute myeloid leukemia (AML) is an independent poor prognostic factor (Majeti et al., 2009). By using a blocking CD47 antibody in a human xenograft mouse model they depleted leukemic cells through phagocytosis of malignant cells (Chao et al., 2010). The combination with the therapeutic anti-CD20 antibody rituximab increased this effect by promoting synergy between the Fc receptor dependent (mediated by Rituximab) and Fc receptor independent (mediated by anti-CD47) stimulation of phagocytosis (Spaargaren, 2011). Further work by the same groups have extended these observations to other haematological malignancies including Non-Hodgkin lymphoma showing that blocking of CD47 inhibited dissemination of lymphoma via impairment of migration of cells toward CXCL12 and CXCL13-mediated signals (Chao et al., 2011). Of note, motheaten mice, which have reduced activity of SHP-1 compared to wild type mice, have enhanced phagocytic response (Dong et al., 1999).

Domain 1 of human SIRPα is highly polymorphic, however these polymorphism are unlikely to affect the binding site to CD47 (Takenaka et al., 2007). The notion is that these avoid binding of pathogens to the receptors and hence downregulation through the inhibitory receptor (Barclay, 2009; Barclay and Hatherley, 2008). Further, they may be important as genetic determinants for hematopoietic stem cell engraftment (van den Berg and van der Schoot, 2008).

In terms of PRR signaling, SIRPα is a negative regulator of both polyIC-RIG-I-MDA5 and TLR3/TRIF dependent signaling pathways. It has been suggested that SIRPα serves as a scaffold to capture important regulatory proteins and assemble adhesion-regulated multimeric complexes, therefore sequestering them away from their targets resulting in inhibition of the signaling pathway (Dong et al., 2008).

Furthermore, SIRPα has been implicated as a positive regulator for the development of Th17-cell related autoimmune conditions (Matozaki et al., 2009) as well as for homeostatic regulation of dendritic cell subsets in lymphoid tissues (Naik et al., 2005; Saito et al., 2010).

As described in chapter 3, HIV-1 hijacks multiple host proteins during its life cycle. I hypothesized that during the budding process HIV-1 may acquire the ubiquitously expressed CD47 during budding from the surface of host cells, and that the interaction between host CD47 on the viral membrane and SIRPα on MDDCs may be involved in formation of the SHP-1 signalosome upon viral encounter.

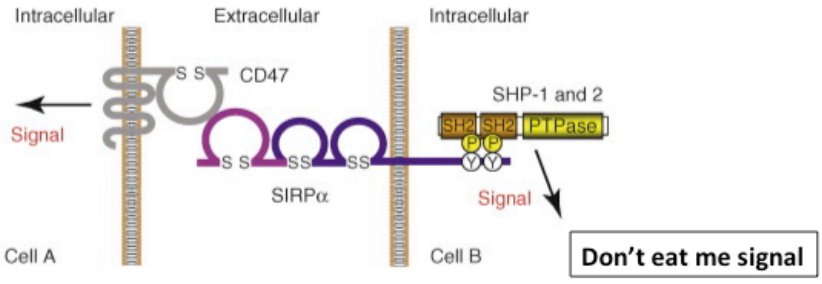

Figure 5.18. The CD47-SIRPα signaling complex. SIRPα is a transmembrane protein that contains three Ig-like domains in its extracellular region and two tyrosine phosphorylation sites in its cytoplasmic region. The tyrosine-phosphorylated sites of SIRPα bind to the protein tyrosine phosphatases, SHP-1 and SHP-2, and thereby activate these phosphatases. SIRPα ligand CD47 is also a member of the Ig superfamily, possessing a V-type Ig-like extracellular domain, five membrane-spanning segments and a short cytoplasmic tail. The N-terminal IgV-like domain of SIRPα binds to the Ig-like domain of CD47. The *trans*-interaction of the two proteins could mediate intercellular signalling in a bidirectional manner. Adapted from (Matozaki et al., 2009).

5.3.8 Investigation of SIRP α expression in myeloid cells

To explore the possibility that SIRPα may be involved in HIV-1-induced dephosphorylation of SHP-1, I first ascertained that SIRPα is expressed in MDDCs (figure 5.19). In addition, I also looked at its expression on myeloid DCs isolated ex vivo from healthy colonic tissue and show that it is highly co-expressed with DC-SIGN on myeloid DCs, delineated by the expression of CD11c and HLA-DR and lack of expression of the lineage marker. This is important, as mucosal DCs are one of the first cells to encounter HIV during infection and this is the first time human mucosal DCs are examined for the expression of SIRPα. It also validates our approach of using MDDCs as a model for mucosal DCs to study HIV pathogenesis.

Fortin et al, investigating DC subsets in a murine colitis model showed that CD103+ DCs in the lamina propria and mesenteric lymph nodes preferentially expressed SIRPα. Furthermore, the mobilization of CD103+SIRPα+ DCs in response to inflammation was mediated by CD47, induced a Th17 skewed response and played a major role in the development of experimental colitis (Fortin et al., 2009). This suggests an opposite role of this subset to the more tolerogenic CD103+ ($SIRP\alpha^-$) subset (Scott et al., 2011).

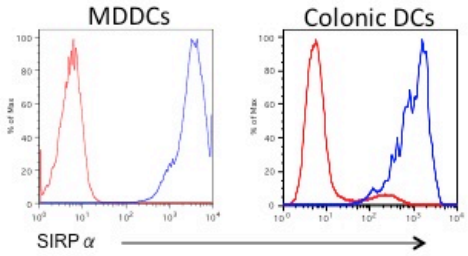

Figure 5.19. SIRP is expressed on MDDCs and mucosal gut DCs. For MDDCs cells were gated on CD11c+ DCs (blue line), red depicts isotype control. For gut DCs, mucosal mononuclear cells were isolated from healthy colonic mucosa and gated on lineage-HLA DR+CD11c+DC-SIGN+ cells, which were all SIRPα positive (blue line). Red line depicts CD11c- non-myeloid mucosal mononuclear cells.

5.3.9 Investigation of phosphorylation of SIRPα following HIV-1 infection

Ligand binding has been shown to induce phosphorylation of SIRP-α, followed by recruitment of SHP-1 to its ITIM motif (Matozaki et al., 2009). Given that SHP-1 is

dephosphorylated by HIV-1, it was tempting to speculate that HIV-1 could also induce changes in phosphorylation of SIRPα. However, according to the LC-MS/MS analysis SIRP-α was not differentially phosphorylated within 10 minutes of HIV-1 infection. This was further confirmed by western blot analysis of SIRP-α on phosphoenriched samples (figure 5.20). These findings do not exclude differential phosphorylation of SIRPα at an earlier timepoint with normalization of SIRPα at 10 min or changes in SIRPα after 10 min.

In summary, so far I have shown that SIRPα is highly expressed on MDDCs and mucosal DCs, but is not differentially phosphorylated by HIV-1 10 min p.i.

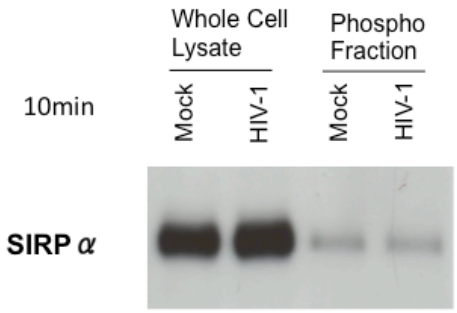

Figure 5.20. HIV-1 does not induce changes in SIRPα phosphorylation. DCs were infected with HIV-1 or mock for 10 min, lysed and enriched for phosphoproteins. Immunoblot of whole cell lysate and phosphoenriched samples for SIRPα shown.

5.3.10 Investigating the expression of CD47 – the ligand for SIRPα - in HIV-1 virions

In order to confirm that HIV virions are capable of incorporating CD47 during budding, I examined the expression of CD47 on HEK 293T cells, the cells I use for generation of viral stocks. To also address this question in a more physiological setting, I looked at CD47 expression in primary CD4+ T cells and Jurkat cells. As expected, CD47 is highly expressed on all cell subsets examined (figure 5.21).

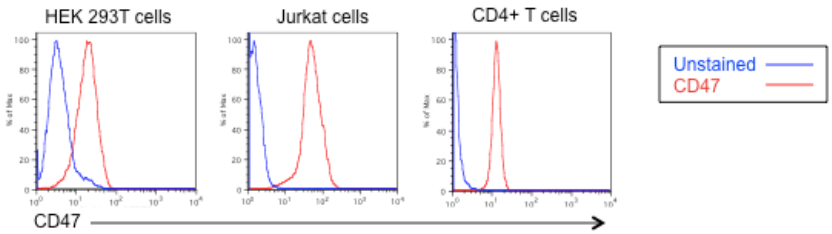

Figure 5.21. CD47 is expressed on cells commonly used for generation of HIV-1. Surface expression of CD47 was analyzed by FACS staining.

To investigate the presence of CD47 in HIV-1 virions, I started by immunoblotting for CD47 in my HIV-1 stocks. Briefly, viral supernatans were boiled with SDS PAGE buffer and analyzed by western blot for CD47 using a CD47 antibody shown to be functional in western blots (Broom et al., 2009). Although, I could visualize a band corresponding to the predicted size of CD47 of 47 to 52 kDa by western blot (figure 5.22a), there were multiple other bands present, which may indicate abundance of impurities and components such as FCS in preparations derived from viral supernatants. Of note, staining with other CD47 antibodies (not shown) yielded identical findings.

To reduce contaminations in viral preparation, I took advantage of a well-established technique involving isolation of HIV-1 virions with commercially available beads against CD44. This is based on the observation that CD44 is incorporated into viral particles derived from CD4+ cells, CEM174 and SupT1 cells and that CD44 microbeads can be used to capture intact HIV-1 virions. Isolating intact virions would allow me to exclude other cellular contaminants in the viral supernatant. HEK 293T cells, however, do not express CD44, therefore I induced expression of CD44 by transfecting HEK 293T cells with a CD44 plasmid (pRcCMV CD44). Subsequently, HIV-1 was produced as per usual protocol by transfection of pWolf NL4-3 BaL in CD44+ HEK 293T cells. Viral supernatants were harvested after 24 hours and titrated. Subsequently, I isolated CD44+ HIV-1 virions with CD44+ microbeads and magnetic column separation as per manufacturer's instructions and immunoblotted the CD44+ viral eluates for CD47. Isolation of CD44+ HIV-1 virion clearly reduces background and detection of unspecific bands (figure 5.22b). Encouragingly, the band previously detected at around

40-50kDa was still present. To assess if this band could represent CD47, I used two different CD47 blocking peptides shown to inhibit CD47 binding, S19 specific for the N-terminal and C18 specific for the C-terminal region of CD47. Viral supernatants of CD44+ NL4-3 BaL collected after CD44+ bead isolation were run on a NUPAGE gel as before. Immunoblotting with CD47 antibody was preceded by an hour incubation of the membranes with blocking peptides, either used individually and in combination. However, there was no detectable change in intensity of the band in question (figure 5.23a). Finally, I compared the expression of CD44+ NL4-3 BaL after CD44 isolation and my usual viral stock (made in HEK 293T cells that don't express CD44) using a

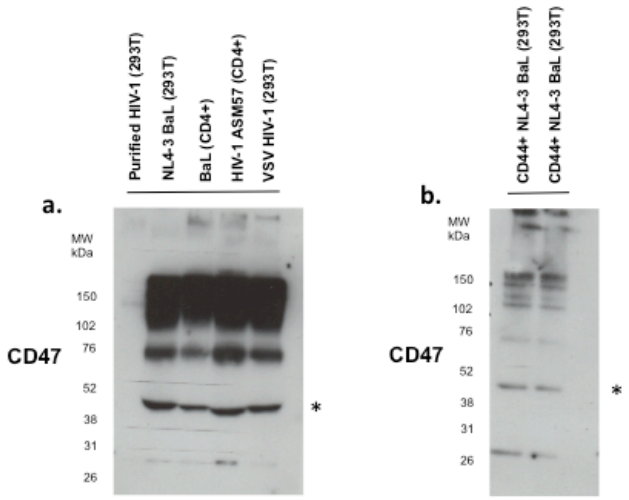

Figure 5.22. Western blot for CD47 in different HIV-1 stocks fails to detect CD47 expression. A. Viral supernatants were boiled with SDS PAGE and immunoblotted for the expression of CD47 using a commercially available antibody, known to be specific for CD47 with a predicted size of 47-52 kDa. **B**. NL4-3 BaL generated in CD44+ HEK 293T cells and separated with CD44+ microbeads was immunoblotted for CD47.

Details of viral stocks used: 1. Purified HIV-1: NL4-3 BaL generated in HEK 293T cells after ultracentrifugation and sucrose gradient purification. 2. NL4-3 BaL (normal viral stock) generated in HEK 293T cells. 3. BaL, primary BaL generated after infection of primary PHA activated CD4+ T cell blasts. 4. HIV-1 ASM57, primary M tropic HIV-1 strain from a LTNP generated after infection of primary PHA activated CD4 T cell blasts. 5. VSV-pseudotyped NL4-3 BaL generated in HEK 293T cells.

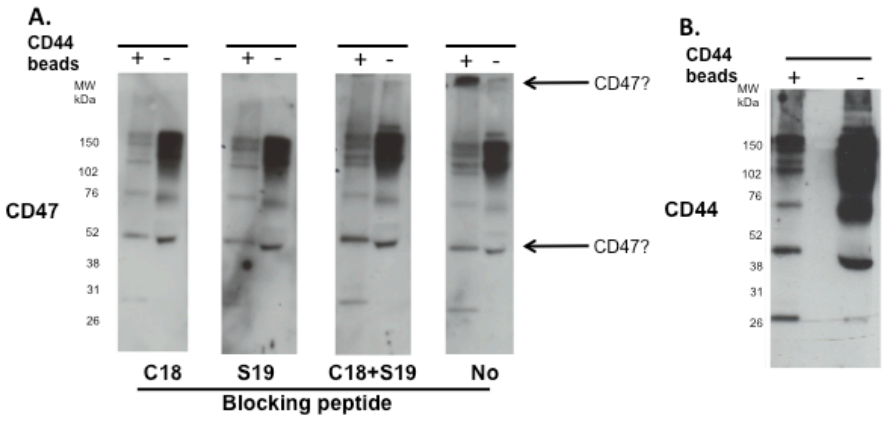

Figure 5.23. A. CD47 blocking peptides do not improve identification of CD47 by WB of viral isolates. CD44+ NL4-3 BaL was isolated with CD44 microbeads and analyzed by western blot for CD47 expression following pre-incubation of membranes with CD47 specific blocking peptides. **B.** Immunoblotting may not be the right technique to detect surface proteins incorporated in HIV-1 virions. NL4-3 BaL made in CD44+ HEK 293T cells and CD44- HEK 293 T cells was immunoblotted for CD44. CD44 usually creates a smear at a predicted size of 80 kDa.

commercially available CD44 antibody. There was no detectable band corresponding to CD44, which usually creates a smear at around 80kDa (figure 5.23b).

Taken together, these experiments suggest that immunoblotting may not be the optimal technique to detect proteins such as CD47 expressed on the HIV-1 membrane. It may be due to low abundance of these proteins, masking of epitopes/configuration because of their incorporation in the viral membrane, post-translational modifications such as glycosylation or sumolyation or changes associated with preparation of the samples, e.g. denaturation due to boiling with SDS PAGE. A native gel could have excluded the latter possibility, however this was not possible due to safety concerns. Moreover, CD47 may be present in a different isoform, and indeed a recent study demonstrated that CD47 is a proteoglycan that is only present (or detectable by various biochemical methods) in a high molecular weight isoform of ~250 kDa due to heparin sulfate modifications in Jurkat T cells (Kaur et al., 2011). In retrospect, the high molecular weight band in figure 5.23a may be indicative of the presence of CD47, however more specific biochemical assays are required to confirm this.

In-gel digestion is a long established and reliable approach for identification of proteins by MALDI mass spectrometry (Shevchenko et al., 1996). Therefore, CD44+ isolated

virions were subjected to electrophoresis, stained by Coomassie staining, multiple protein bands of different molecular weights that could represent different post-translationally modified isoforms of CD47 were excised, prepared according to standardized protocols for tryptic digestion and protein identification by MALDI mass spectrometry. Subsequent, mascot analysis identified multiple viral and cellular proteins as well as contaminants, but did not detect CD47 in any of the excised bands (not shown).

To increase the sensitivity of my analysis I analyzed highly purified and concentrated HIV-1 on the LTQ Orbitrap mass spectrometer. The list of proteins identified has already been presented in chapter 3. Again, CD47 was not among the proteins identified by mass spectrometry of purified virus (and also not in a web-based database[2]), either because it is not incorporated into virions, or at such low levels that are below the sensitivity of the Orbitrap. CD47 may show inherent insolubility with conventional methods due to the presence of its five transmembrane segments embedded within the lipid membrane (Rebres et al., 2001). Cellular surface proteins incorporated into viral membrane may require an additional separation step to allow reliable identification. This notion is further supported by a study of Sapphire et al that identified CD48 as a virally incorporated host protein only after a combination of LC-MS/MS and affinity chromatography isolation of heparin bound sulfated proteoglycans (Saphire et al., 2006). Technical advances in membrane proteomics could be attempted to establish the presence of CD47 in NL4-3 BaL by LC-MS/MS (Barrera and Robinson, 2011).

Various proteomic methods failed to identify CD47 within HIV-1 virions, therefore I chose immunolabeling as an alternative approach. Given that I could isolate intact virions reliably with CD44 microbeads, I explored the possibility of detecting CD47-labeled virions by flow cytometry. Purified CD44+ virions were stained with HLA-DR, a host protein known to be incorporated in the viral membrane and CD47 and analyzed by flow cytometry. Virions displayed slightly increased expression of HLA-DR. Additionally, virions had increased expression of CD47 compared to isotype control, albeit at very low levels indicating that flow cytometry is not the correct technique to identify host proteins incorporated in viral membrane.

[2] Database of host proteins in HIV-1 http://web.ncifcrf.gov/research/avp/protein_db.

Finally, immunoelectron microscopy was used to examine the expression of CD47 on virions. This was carried out with kind help of Dr David Ferguson (Department of Pathology, Oxford). Initially, purified virions were fixed with a mixture of 4% paraformaldehyde/0.2%glutaraldehyde and processed for immunoelectron microscopy. Single immunolabeling was carried out for CD47 as well as gp120 (using 2g12) followed by gold labeling. Images were promising, both envelope as well as CD47 were detected on the surface of virions, with very little background staining (figure 5.25a/b). To take these observations further, we performed similar stainings on HEK 293T cells transfected with pWolf NL4-3 BaL to visualize budding virions from the parental cells. Budding virions clearly acquire CD47 from the host cell membrane (5.25c/d). The density of CD47 (and also 2G12) staining was generally low considering the high expression of CD47 on HEK 293T cells, which may indicate that the staining requires further optimization. This is also supported by work that has shown that HIV-1 and SIV virions produced from various T-cell lines contain between 7 and 14 Env trimers per virion (Zhu et al., 2006). However, it may also suggest that expression of CD47 on the cellular membrane is rather clustered than diffuse. It is also unclear if the acquisition of CD47 by the virus is an active process initiated by the viral budding machinery with CD47 assembling at sites of viral budding or a random process.

In summary, multiple different approaches were used to demonstrate the incorporation of CD47 in HIV-1 virions. Immunoelectron microscopy showed the expression of CD47 on both purified virions as well as budding HIV-1.

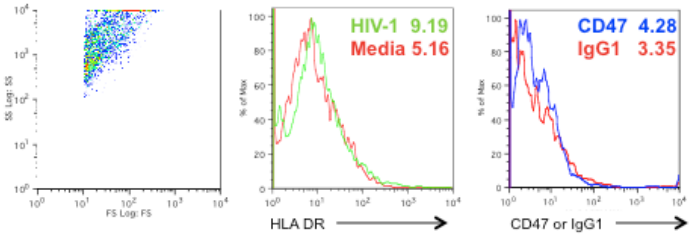

Figure 5.24. Detection of cellular proteins HLA-DR and CD47 in HIV-1 virions by flow cytometry. Intact virions isolated with CD44 microbeads were stained with fluorochrome labelled HLA-DR, CD47 and isotype control antibodies and analyzed by flow cytometry.

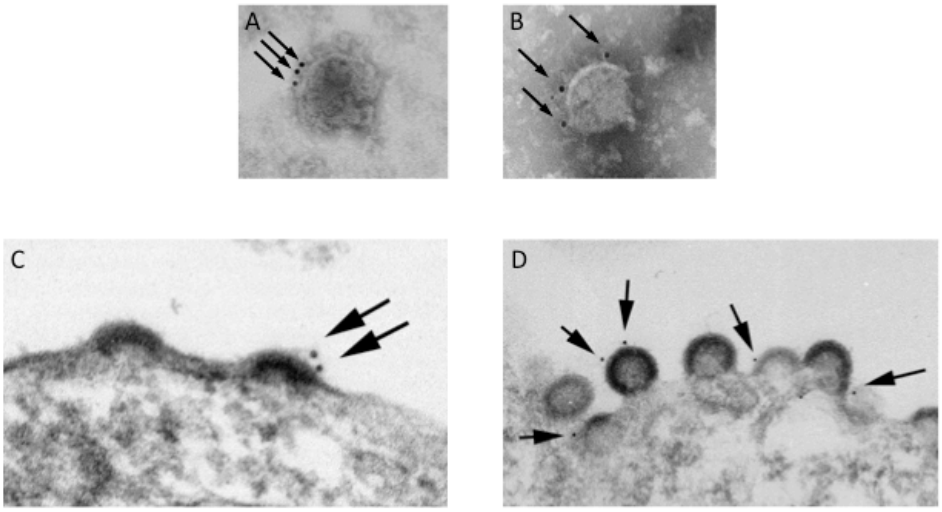

Figure 5.25. CD47 is incorporated into virions. Purified NL4-3 BaL HIV-1 were prepared for immunoelectron microscopy and labelled with (A) anti-CD47 and (B) anti-envelope antibody followed by 10nm gold. 293T cells were transfected with pWolf NL4-3 BaL and fixed 24 hrs post transfection.Fixed cells were prepared for immunoelectron microscopy and labeled with (C) anti-CD47 and (D) anti-envelope respectively followed by 10nm gold (Arrowheads). Images show representative budding virions.

5.3.11 Blocking the interaction between SIRPα and CD47 and the effect on viral replication

Given that SIRPα is expressed on MDDCs and CD47 seems to be incorporated into the HIV-1 viral envelope, I sought to investigate the effect of inhibition of the interaction between CD47 and SIRPα. As mentioned above, recent work by Weissman and coworkers had established that human solid tumor, leucaemia and lymphoma cells require CD47 expression to suppress phagocytic innate immune surveillance and that the CD47 blocking antibody BRIC126 leads to tumor cell phagocytosis and elimination (Chao et al., 2010).

In order to examine the effect of CD47 blockade on HIV-1 infection, I pre-incubated NL4-3 BaL with 10μg/ml anti-CD47 antibody (BRIC126) and IgG2a isotype control respectively for 1 hour. Subsequently DCs were infected with antibody-coated HIV-1 for 2 h and harvested 24 h later for RNA isolation and evaluation of tat-rev transcription by qPCR. Anti-CD47 led to a dramatic reduction in viral transcription in DCs (figure 5.26a). Reports have shown that immobilized or crosslinked antibodies against CD47 may induce apoptosis of several malignant lymphoid lines (Kikuchi et al., 2004; Uno et al., 2007). Therefore, to ensure that the observed reduction in HIV-1 infection was not due to cellular toxicity, DCs incubated with antibody coated HIV-1 were examined for cell death by simple trypan blue staining. There was no difference in number of dead cells between anti-CD47 and isotype control treated DCs (figure 5.26b).

Further, to investigate if the same blocking effect could be observed for HIV-1 *trans*-infection, DCs were infected with anti-CD47 and isotype control-coated NL4-3 BaL for 2 h and subsequently co-cultured with CD4+ T cell blasts for assessment of HIV-1 infection by p24 ELISA. Again, CD47 antibody inhibited *trans*-infection and this effect was concentration dependent with anti-CD47 used at 0.1-5 μg/ml having only minimal-moderate inhibitory effects (5.26c/d).

Having established that I could reduce HIV-1 transcription and *trans*-infection with a CD47 blocking antibody, I next sought to ensure that this was a specific effect mediated by inhibition of CD47 binding rather than by unspecific binding to the FcR. Using another CD47 antibody (2D3), that has no blocking activity, I could not observe any reduction in HIV-1 transcription (figure 5.27a). Further, looking at another cellular host protein known to be incorporated into the viral envelope, the aforementioned CD44, pre-incubation of CD44+ NL4-3 BaL with a CD44 antibody and infection of DCs with this virus did not change levels of HIV-1 transcription (figure 5.27b). These findings support the notion that the observed reduction in HIV-1 infection may not be FcR mediated and would be in keeping with the work by Weissman and colleagues, that showed the phagocytosis of anti-CD47 treated tumor cells to be FcR independent (Chao et al., 2010). To investigate this further, I used a SIRPα Fc that binds the FcR, hypothesizing that binding to the potential receptor – SIRPα - for virally incorporated CD47 should lead to an increase in HIV-1 infection. Infection of DCs with NL4-3 BaL in the presence of SIRPα Fc did not change viral transcription (figure 5.27c).

Generation of CD47 F(ab')$_2$ fragments and repeat of these set of experiment would aid in clarifying if the inhibitory effect is FcR mediated.

In conclusion, blocking of CD47 with anti-CD47 (BRIC126) antibody reduces both viral transcription in DCs and DC-CD4 *trans*-infection.

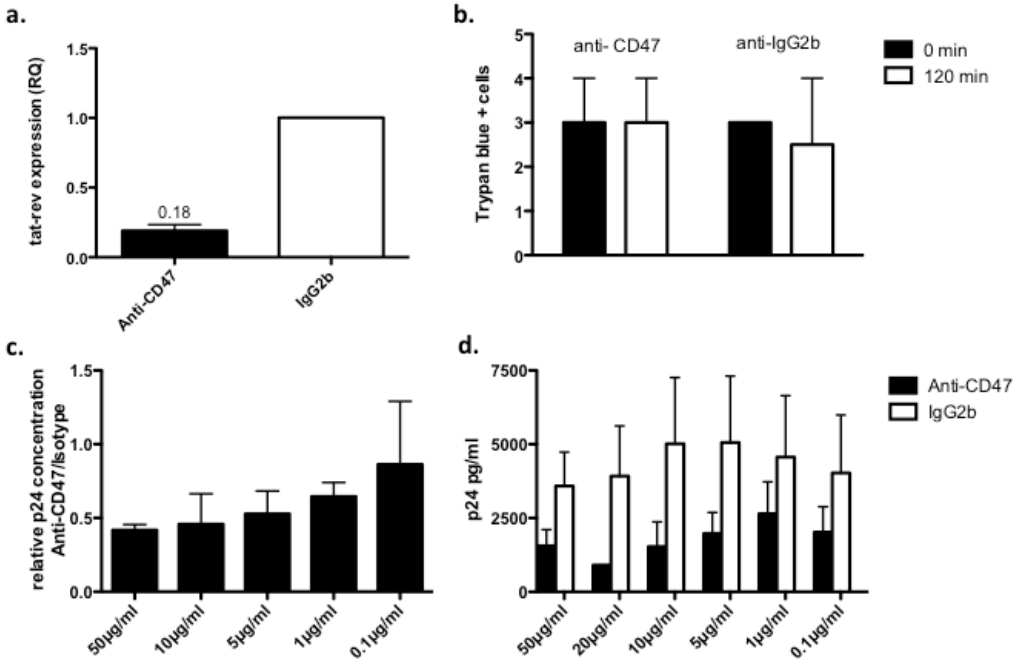

Figure 5.26. Anti-CD47 antibody inhibits HIV-1 transcription and *trans*-infection. a. DCs were infected with anti-CD47 and isotype control coated HIV-1 for 2 h and harvested 24 h p.i. for qPCR. HIV-1 tat-rev mRNA was calculated relative to GAPDH. Shown are 4 biological replicates ± SEM. b. anti-CD47 antibody does not induce cell death in DCs. Data are three biological replicates mean ± SEM. c. CD47 mediated inhibition of HIV-1 infection is concentration dependent. d. Anti-CD47 Ab reduces HIV-1 transinfection in a DC-CD4 coculture. For c+d: HIV-1 BaL was preincubated with anti-CD47 or isotype control for 1 h. DCs were infected with antibody-coated HIV-1 for 2 h, virus was washed off, DCs were co-cultured with PHA-activated CD4+ T cells at a ratio of 1:3 (DC:CD4). Supernatant was analyzed on days 2, 4, 6 and 8 p.i for p24 by ELISA. Results of day 2 are shown. Data are three biological replicates mean ± SEM.

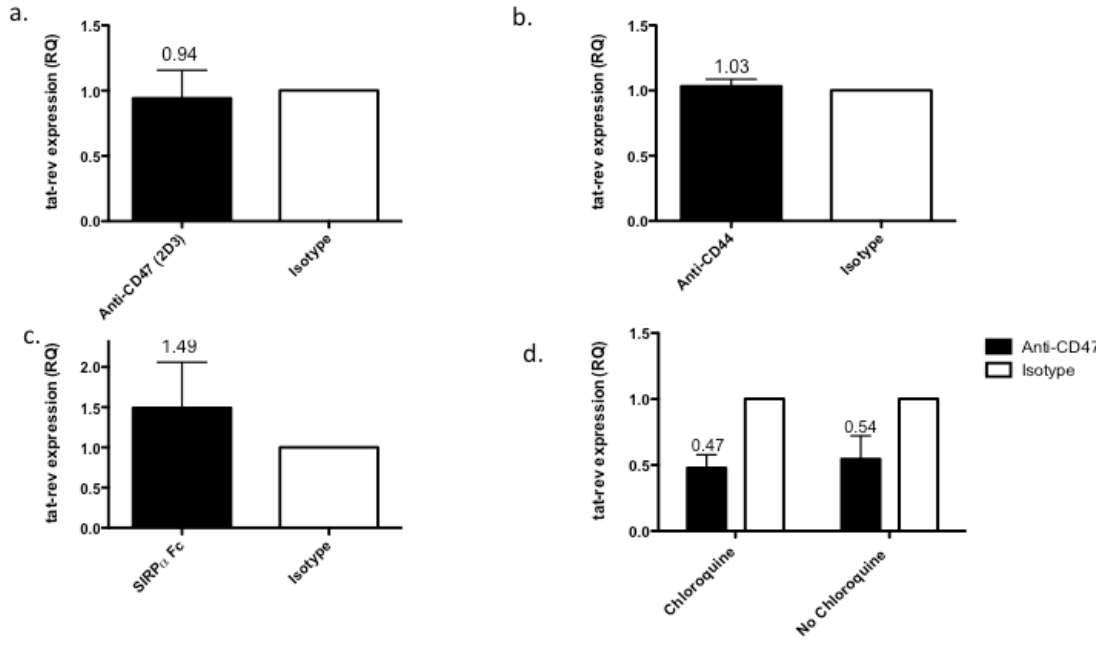

Figure 5.27. Investigations into the inhibitory activity of anti-CD47 antibody on viral transcription. a. The 2D3 clone of anti-CD47 has no effect on viral transcription. **b.** Infection with anti-CD44 coated CD44+ NL4-3 BaL has no effect on viral transcription. c. The inhibitory activity of anti-CD47 Ab may not be Fc mediated, as recombinant SIRPα had no effect on HIV-1 transcription. d. Chloroquine has no effect on CD47 antibody mediated HIV-1 inhibition. DCs were preincubated with 50 (50nm) chloroquine for 30 min before infection with anti-CD47 or isotype coated HIV-1 for 2 h. Cells were harvested for qPCR 24h p.i. Expression is normalized for GAPDH expression and expressed relative to isotype control condition. Data are mean ± SEM of three independent experiments.

5.3.12 Investigation of the mechanism of CD47-mediated reduction in HIV-1 infection

Multiple mechanisms may account for the reduction in HIV-1 infection mediated by CD47 blocking. They may be a consequence of restricted viral entry and/or endocytosis, increased trafficking to lysosomal compartments or changes in HIV-1-mediated signaling pathways, to name only a few.

In terms of entry, it is highly likely that SIRPα will play a prominent role in CD47 binding and maybe even endocytosis, given its high surface expression in DCs and the ample evidence for CD47-SIRPα interaction in the literature. In order to investigate this, I examined the consequence of SIRPα knockdown on HIV-1 infection. Surprisingly, transfection of DCs with a commercially available SIRPα siRNA did not

result in changes in HIV-1 infection (figure 5.28a), however this was found to be due to inadequate knockdown of SIRPα as assessed by western blot of DCs post transfection with SIRPα and control siRNA (figure 5.28b). To investigate this further, I designed a shRNA targeting SIRPα mRNA and introduced it into a lentivirus. Preliminary work shows that using increasing MOI of the LV result in up to almost 60% reduction in SIRPα expression (figure 5.28c). Further optimization of the lentiviral mediated delivery system in DCs should lead to even higher knockdown efficiencies with the aim of re-addressing the question whether down-regulation of SIRPα expression will affect HIV-1 infection.

A simple method of assessing viral entry is to look at the localization of virions in infected DCs by immunofluorescence. However, it has so far proven difficult to reliably stain for CD47-antibody coated virions with an antibody that is made in a host other than mouse (data not shown).

The data presented so far suggests that host CD47 may be part of an immune evasion strategy whereby HIV-1 actively uses CD47 to support viral infection. Viral CD47 may trigger a favourable signaling cascade. As an initial quick screening experiment, I used Chloroquine to block signaling from the endosomal compartment. Chloroquine is a lysosomotropic agent that prevents endosomal acidification and hence blocks signaling of endosomal TLRs by masking the PAMP of nucleic acids. Pre-treatment of DCs with chloroquine had no effect on anti-CD47-mediated reduction of HIV-1 transcription (figure 5.27d). Further extensive comparison of the signaling cascade induced by anti-CD47 coated HIV-1 to control virus, e.g. by phosphoproteomic and/or gene expression studies may provide more cues to the mechanism of CD47 in HIV-1 signaling.

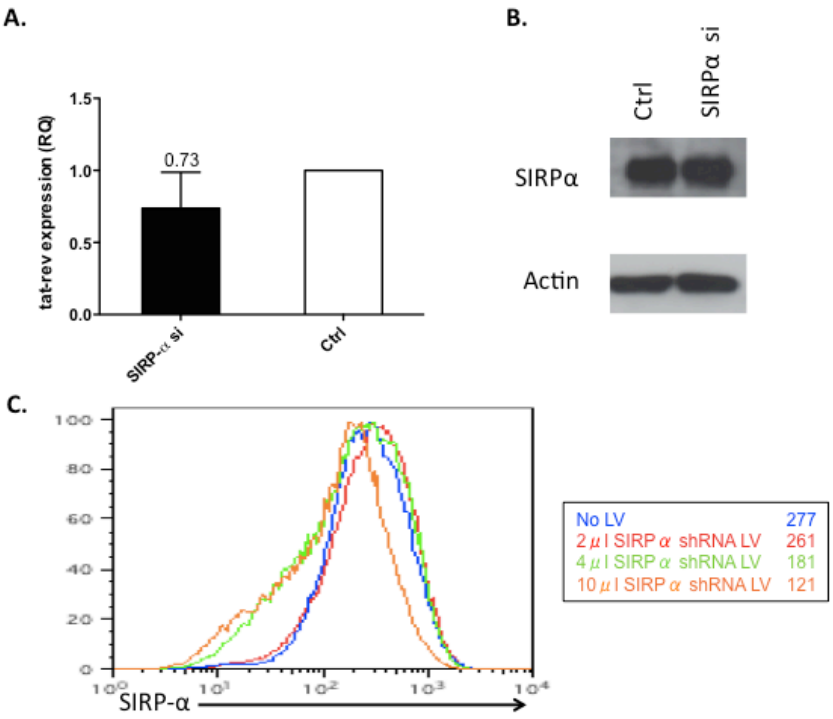

Figure 5.28. Investigation of the effect of SIRP-α knockdown on HIV-1 infection. **A.** DCs were transfected with SIRP-α and control siRNA and infected 24h post transfection with HIV-1 and harvested for qPCR 24h p.i. Tat-rev expression was determined relative to GAPDH expression and expressed relative to scrambled siRNA control. Data are represented as mean ± SEM of 5 independent experiments. **B**. Electroporation of DCs with a commercially available SIRP-α siRNA does not result in detectable knockdown of SIRPα. **C.** infection of DCs with increasing amounts of a lentivirus encoding SIRPα shRNA leads to detectable reductions in levels of SIRPα expression. Numbers represent MFI expression.

5.3.13 Generation of CD47 negative HIV-1 BaL by lentiviral transduction

The effect mediated by coating of NL4-3 BaL with monoclonal anti-CD47 antibody strongly suggests that the observed reduction in HIV-1 infection is due to the blockage of virally expressed CD47 interaction with DC. To provide further conclusive evidence to support this, I decided to generate CD47 negative NL4-3 BaL using a cell line that lacked CD47. Given the ubiquitous expression of CD47 among different cell types, I designed a CD47 shRNA targeting CD47 mRNA that was introduced into a lentiviral vector and used for infection of HEK 293T cells. After two rounds of infection and

several cell passages CD47 expression was reduced by 70% as assessed by flow cytometry (figure 5.31). This cell line can now be used to generate viral stocks of NL4-3 BaL that lack CD47 to compare CD47+ and CD47- HIV-1 and hence used for more detailed investigation of the role of host acquired CD47 in HIV-1 infection.

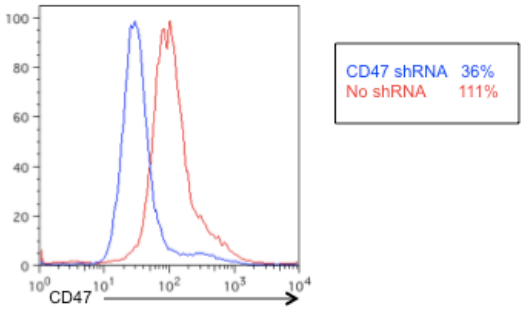

Figure 5.29. Generation of CD47 negative HEK 293T cells via lentiviral mediated transduction with a shRNA targeting CD47. HEK 293T cells were infected with a lentivirus encoding a shRNA specific for CD47 mRNA and after several rounds of passages reinfected and assessed by flow cytometry for CD47 expression.

5.4 Discussion

The data presented in this chapter demonstrate for the first time dephosphorylation of SHP-1, a major cellular phosphatase, by a pathogen. Given the important role of SHP-1 as a negative regulator in multiple signaling pathways, it seemed pertinent to study the function of SHP-1 in HIV-1 infection of DCs.

Despite ample evidence for the role of SHP-1 as a signal-aborting phosphatase in the adaptive immune system, its role in innate signaling pathways remains to be fully characterized. The previously mentioned study by Cao and co-workers (An et al., 2008) was supported by a more recent study that established SHP-1 as an important negative regulator of DC signaling in mouse bone-marrow derived DCs (Ramachandran et al., 2011). SHP-1 inhibited LPS-mediated NF-kB and AP-1 activation and hence the

induction of a proinflammatory cytokine response. Additionally, it inhibited DC survival via activation of AKT1. Despite these findings, SHP-1 knockdown had no effect on induction of inflammatory and type 1 interferon response following HIV-1 infection (figure 5.13). It is noteworthy that generally my attempts to manipulate SHP-1 were hampered with significant technical difficulties. It would be therefore worthwhile to re-address the role of SHP-1 in HIV-1 signaling with DCs overexpressing wild type and inactive SHP-1 by LV mediated transduction, where cell toxicity and activation do not cause any major concerns.

Although HIV-1-mediated manipulation of SHP-1 would provide a mechanistic explanation for HIV-1 and the evasion of an innate antiviral response, there is more evidence for a role of SHP-1 in HIV-1-induced changes of the cytoskeleton. This is based on the predominance of trafficking and cytoskeletal molecules in the HIV-1 (chapter 3) and the SHP-1 signalosome (figure 5.16) and the relative lack of signaling proteins. HIV-1 may target SHP-1 to induce cytoskeletal changes during multiple steps of HIV-1 replication, but given the very early (3 min) reduction in the SHP-1 phosphatase activity induced by the virus, the phases of entry and endocytosis of the virus are most likely candidates. SHP-1 may be a component of an entry complex – either at the cell membrane or the endosome - involving the actin cytoskeleton and molecules such as talin and focal adhesions proteins (Stolp and Fackler, 2011). It would be interesting to perform live cell imaging with labeled virus to recapitulate early HIV-1 infection in DCs following SHP-1 manipulation. Moreover, the role of each protein of the SHP-1 signalosome for its effect on HIV-1 fusion can be assessed using the vpr-BLAM assay (Cavrois et al., 2002).

Technically it may be challenging to ascertain the exact molecular mechanism triggering dephosphorylation of SHP-1. SHP-1 may undergo auto-dephosphorylation itself, an observation that has been made in previous *in vitro* studies (You and Zhao, 1997) and also described for other cellular phosphatases such as PP2A (Mao et al., 2005). This will be technically difficult to show in HIV-1 infected DCs, because it requires presence of EDTA in the assay, which on the other hand may inhibit other important steps in HIV-1 recognition such as CLR signaling.

I had anticipated that identification of the host molecule mediating SHP-1 dephosphorylation, may provide cues as to the viral component involved in this process.

A separate line of enquiry that I haven't explored in this work would be lipids of the viral envelope. HIV contains a lipid bilayer and lipids may modulate the activity of SHP-1. Low micromolar concentrations of phosphatidic acid can increase the activity up to 25 fold, whereas negatively charged lipids may reduce the activity (Frank et al., 1999).

To complicate matters recent work has questioned the simplified notion that SHP-1 only binds to phosphorylated ITIM motifs of receptors, hereby impeding ITAM initiated signaling (Blank et al., 2009; Pfirsch-Maisonnas et al., 2011). Inhibitory ITAMs (ITAMi) have been shown to propagate inhibitory signals by formation of microcluster compartments that actively recruit and trap inhibitory signaling effectors such as SHP-1. These so called "inhibisomes" were initiated by the accumulation of both activating and inhibitory effectors with depolymerization of actin-trapping activating receptors into lipid rafts.

During the earliest stages of infection HIV-1 succeeds in inducing an almost tolerogenic state in DCs. The Wnt-beta-catenin signaling pathway has recently been shown to induce a tolerogenic anti-inflammatory DC response in the gut mucosa (Manicassamy et al., 2010). Interestingly, SHP-1 dephosphorylates and inhibits beta-catenin function by inducing its degradation via a GSK3b-dependent mechanism (Simoneau et al., 2011). It would be fascinating to study the role of SHP-1 in HIV-1 infection in light of these findings.

While exploring possible receptors mediating dephosphorylation of SHP-1, I identified the CD47-SIRPα interaction as a possible mechanism to explain how HIV-1 may succeed in being recognized as self (Medzhitov and Janeway, 2000). HIV-1 has been described to be a notorious mimic of host cells, most prominently exemplified by the difficulties in inducing neutralizing antibody responses to host sugars coating the viral envelope (Pashov et al., 2009). The incorporation of host cellular proteins into the virion have been shown to play a role in the early stages of HIV-1 replication by enhancement of attachment leading to efficient fusion of virion and cell membranes, entry of virions into the cell cytoplasm, as well as modulation of signal transduction pathways essential for diverse biological functions (Clapham and McKnight, 2001; Ott, 2002; Stauber et al., 1999). For instance, incorporation of ICAM-1 into viral particles enhances attachment to cells expressing its ligand LFA-1 (lymphocyte function-associated

antigen-1) (Fortin et al., 1999; Paquette et al., 1998). Therapeutic efforts to disrupt the interaction of HIV-1 with cell surface receptors have resulted in the development of Maraviroc, a CCR5 antagonist that is currently in clinical use as a in 2nd line antiretroviral treatment. Interestingly, a screen for cell surface targets for HIV-1 therapy using genetic suppressor element technology identified CD47 as a cognate gene suppressing viral replication (Dunn et al., 2004). The consistent reduction of HIV-1 infection in the presence of anti-CD47 antibodies is therefore fairly exciting. Clinical trials into the potential application of anti-CD47 as a treatment for lymphoma and leukemia are already in progress. It is noteworthy that despite the ubiquitous expression of CD47, CD47-deficient mice have a rather mild phenotype, and the blocking anti–mouse CD47 antibody does not exert toxicity in mice, and a blocking anti–human CD47 does not affect phagocytosis of normal human PB cells and $CD34^+$ BM cells in vitro (Spaargaren, 2011).

The comparison of HIV-1 BaL generated in CD47 negative and CD47 positive host cells will be very interesting. If CD47 negative HIV displays lower infectivity, then further studies are warranted to look at the mechanism of virally incorporated CD47 recognition: Is the inhibitory effect specific for DCs due to their expression of SIRPα? Does CD47 lead to opsonization and hence divergent trafficking into phagolysosomes of virions? Is a different signaling cascade induced? Is the incorporation of CD47 by HIV-1 an active recruitment or a random sampling of the protein during the budding process? And, most interesting of all, can it provide new insights into the recognition of self versus non-self?

To summarise, the work described in this chapter characterizes the role of SHP-1 dephosphorylation in the HIV-1 phosphoproteome. Although, no conclusive mechanistic explanation as to how SHP-1 is dephosphorylated and the functional consequences for infection could be provided, further studies should address these issues in a robust cellular system. Further, it describes the SIRPα-CD47 pathway as a possible novel part of HIV pathogenesis and the blockage of this pathway as a possible means of manipulation HIV-1 infection, at least for studies in to the biology of HIV-1 infection and self and non-self recognition. Some aspects of this work are subject of ongoing work in the laboratory, and may yield significant insights into the role of these molecules in HIV-1 pathogenesis.

Chapter 6

General Discussion

6.1 Introduction

The work described in this thesis uses a multi-pronged approach to understand the interaction of HIV-1 with DCs during the early stage of infection. First, in chapter 3, I employed a phosphoproteomic screen to identify novel differentially phosphorylated signaling molecules downstream of HIV-1, the results of this screen provide the basis for most of the work that will follow. In addition, I carry out a proteomic screen of HIV-1 virions to identify host molecules incorporated into the virus. Lastly, I carry out a microarray study of DCs infected with HIV-1 to obtain a transcriptional profile of the response of DCs to HIV-1 infection. In chapter 4, I carry out a smaller more targeted screen based on the results of the phosphoproteomic study to identify host targets that are differentially phosphorylated by the virus and required for efficient *trans*-infection from DCs to CD4+ T cells. In the remainder of the chapter, I focus on the role of BLOC-1 complex, and in particular snapin, in HIV-1 and TLR8 sensing. The final results chapter elucidates the role of SHP-1 in HIV-1 signaling and identifies tentatively a role for CD47 in HIV-1 recognition.

6.2 The HIV-1 signalosome

I used a novel established protocol in our lab, based on affinity-column purification, off-gel IEF and LC-MS/MS analysis to identify proteins differentially phosphorylated by HIV-1 within 10 minutes. I combined this analysis with a novel bioinformatics method to obtain a quantitative assessment for the relative abundance of phosphorylated proteins between conditions. I selected about 10% of these proteins for validation of the LC-MS/MS data using an alternative traditional biochemical method, an immunoblot in

this instance. Bioinformatics analysis revealed an abundance of proteins involved in cellular assembly and organization in general, and particularly involved in functions such as vesicular trafficking, actin and lamellopodia formation, neural synapse formation and ubiquitination and a relative scarcity of signaling mediators such as MAPK and JAK-STAT signaling pathways, concurring with proteomic profiling of HIV-1-infected CD4+ T cells, which also lack any type I interferon and inflammatory induction pathways (Chan et al., 2007). Proteomic analysis of HIV-1 virions confirmed the notion that HIV-1 has a close interaction with host proteins and hijacks them during viral replication. Based on the results of the phophoproteomic study, I decided to carry out a further screen to investigate the transcriptional profile of HIV-1-infected DCs and intriguingly did not detect any significant differentially regulated genes by HIV-1.

The phosphoproteomic analysis of HIV-1-infected DCs describes, to the best of my knowledge, the first comprehensive proteomic screen of phosphorylated proteins in response to HIV-1, the first proteomic screen of DCs in response to HIV-1 and the first proteomic screen of any cell in response to HIV-1 within such an early timepoint. The recent developments in label-free proteomics approaches have allowed more extensive studies of the proteome profile of HIV-1-infected CD4+ T cells at different time points and as early as 4 h p.i., and have revealed a dynamic interaction between host and virus (Chan et al., 2007; Navare et al., 2012; Ringrose et al., 2008) with up to 3,255 host proteins differentially expressed in response to HIV-1 (Chan et al., 2007). It is difficult to compare the result of this work to these datasets due to major differences in experimental settings, including time-point, viral isolate and especially host cell type. These aforementioned studies have provided novel insights into the interaction of the virus with T cells showing overrepresentation of cellular pathways including protein synthesis, cell proliferation and T-cell activation (Navare et al., 2012). The work presented here however greatly benefits from focusing on identification of phosphoproteins in response to HIV-1 and the added step of separation by IEF to aid in identifying novel low abundant proteins. Further work is ongoing to characterize the functional significance of some of these host factors in HIV-1 recognition and in PRR signaling in general.

The absence of any significant changes in mRNA levels in response to high titre HIV-1 was initially surprising and confirmed in a second microarray study (first array data not

shown). It does not contradict the studies of Harman et al showing induction of up to 100 genes 6 h p.i. (Harman et al., 2009), which are indicative of a response to efficient viral transcription of a small fraction of virions that have avoided lysosomal degradation and trafficking to the *trans*-compartment (Gringhuis et al., 2010). It concurs with the general notion that early innate immune responses are disabled by the virus or the host (e.g. SAMHD1) and that HIV-1 behaves distinct to other ssRNA viruses, such as influenza (van 't Wout et al., 2003) or HCV (Arnaud et al., 2011; Basu et al., 2006). Altogether the first chapter demonstrate that HIV-1 induces a robust signalosome on entry to DCs, that contrasts with its ability to activate general innate defences, which implies that it makes an effort to remain immunologically silent.

6.3 RNAi screen identifies novel host factors required for *trans*-infection

In chapter 4 I investigated the role of host factors differentially phosphorylated by HIV-1 for their role in facilitating *trans*-infection. I set up an experimental protocol in DCs that allowed me to carry out a custom RNAi screen in a larger than usual format. The result of the screen indicated that HIV-1 recruits host factors involved in a range of cellular processes such as autophagy, the DNA damage response, cytoskeletal organization and vesicular trafficking to enable enhanced *trans*-infection.

Transfer of virus occurs predominantly across virological synapses between infected DCs (or T cells) and T cells. At the the CD4-CD4 VS this is preceded with clustering of secretory organelles, in particular lysosomes, mitochondria, lipid bodies and the MTOC at the contact zone suggesting major rearrangement of the cytoskeleton in this process (Jolly et al., 2011). Recent work has demonstrated the direct involvement of the regulated secretory pathway in viral transfer between T cells. CD4+ T cells from individuals with Chediak-Higashi syndrome, a condition characterized by defects in in the regulated secretory pathway, display reduced cell-to-cell spread across the T-cell-T-cell VS (Jolly et al., 2011). Generally the nature of the secretory pathway in DCs is less well described, although it is likely that the general principle mechanisms pertaining to other immune cells such as T cells may also apply to DCs. The results of the RNAi screen were not specifically investigated for their role in synapse formation, however the identification of trafficking molecules such as SNX1 and SNX5 as well as BLOC-1

complex within the HIV-1 signalosome may indicate their involvement in viral transfer across the VS. It would be interesting to study the role of these proteins in synapse formation in the context of DC-T cell VS as well as T cell-T cell VS.

HIV-1-infected DCs that have been productively infected in the presence of vpx inhibit *trans*-infection through secretion of type I interferons, presumably induced via recognition of an unknown DNA sensor (Manel et al., 2010). The apparent SAMHD-1-mediated fitness cost of virus in failing to productively infect DCs may hereby serve the virus well by disabling DCs from stimulating CD4 cells and enabling them for enhanced *trans*-infection (Manel and Littman, 2011). Therefore, it is conceivable that the observed reduction in *trans*-infection in the RNAi screen by a given host factor may indicate a role for the protein in the recognition of HIV nucleic acids. A question that should be fairly easy to be addressed in future studies by investigating the type I interferon response in a similar experimental setting as the RNAi screen. Interestingly a recent study of *M. tuberculosis* revealed a novel link between DNA sensing and autophagy. Recognition of *M. tuberculosis* DNA by the STING-dependent cytosolic pathway was required for ubiquitin-mediated delivery of bacteria to autophagosomes (Watson et al., 2012). Work by Akira and colleagues further showed Atg9a-dependent trafficking regulated the assembly of STING and TBK1 and hence dsDNA response (Saitoh et al., 2010). It is possible that members of the endo-lysosomal and autophagy machinery that were identified within the RNAi screen may be implicated in the avoidance of the DNA sensor upon HIV-1 infection, for instance by shielding away potential HIV-derived ligands in a non-immunological compartment.

The discovery of snapin as an important molecule in the formation of ILVs and hence regulation of DC biology in general, also supports the notion how the study of HIV-1-host interactions as a model system have greatly expanded our knowledge of cell biology and how pathogens and host interact. Although it was not the primary aim of this study to identify host restriction factors, it would be interesting to study the function of candidate proteins of the HIV-1 phosphoproteome in host restriction of HIV-1, for instance by using the lentiviral overexpression system once it is optimized at a satisfactory level. I would even speculate that other host factors involved in SAMHD1-mediated interaction with the virus will be within the HIV-1 phosphoproteome and one

could use bioinformatics prediction analysis of likely candidates by finding partner-binding motifs in the SAM domain of SAMHD1.

Differential phosphorylation of three BLOC-1 subunits by HIV-1 was strongly suggestive of a direct recruitment of this complex by HIV-1. Snapin, and to a lesser extent dysbindin, were shown to be required for *trans*-infection. Further investigations demonstrated a multifunctional role for snapin in TLR and HIV-1 sensing supporting a role for snapin in HIV-1-mediated immune evasion.

6.4 Potential model explaining the interaction between HIV-1 and BLOC-1

While the exact structure of BLOC-1 complex is still unresolved, as mentioned in 4.3.7 BLOC-1 is an octameric complex that consists of two subcomplexes (figure 4.14) formed by three proteins each, with the first one consisting of BLOS1, pallidin and cappuccino and the second one consisting of BLOS2, snapin and dysbindin (Lee et al., 2012). The subcomplexes are quite stable, and the interaction within each subcomplex may even be more stable than the entire complex together. This could suggest a scenario whereby the interaction between the virus and one subcomplex may either limit the access or induce the interaction of the other subcomplex to target proteins. BLOS1 and pallidin are responsible for correct assembly of the entire complex (Falcon-Perez et al., 2002; Lee et al., 2012). Hence, HIV-1-induced differential phosphorylation of the first subcomplex may affect the function or localization of the other subcomplex and the formation of the complex altogether. This may allow interaction of the components of the second subcomplex with potential candidate proteins such as actin and dynein, which will be further discussed in the next section.

The next question arises as to the mechanism whereby HIV-1 is interacting with members of BLOC-1, or more specifically with the first subcomplex. BLOC-1 subunits contain coiled coil domains (Lee et al., 2012) and proteins containing coiled coils are known to interact with other proteins containing coiled coils (Mason and Arndt, 2004). In addition, both snapin (2^{nd} subcomplex) and pallidin (1^{st} subcomplex) bind to SNAREs and fusion between cellular membranes is mediated by the interaction between t-SNARE and v-SNARE protein complexes involving helical structures apposing two membranes for fusion, analogous to gp41-mediated membrane fusion (Chan and Kim,

1998). Furthermore, the heptad-repeat domains of gp41 form trimeric coiled coils to eventually form the six-helix bundle required for membrane fusion (Chan and Kim, 1998). Therefore, it is possible that either pallidin or snapin interact with HIV-1 gp41, and given the results of the HIV-1 phosphoproteomics data pallidin seems a more likely candidate. Future work is required to elucidate the interaction between HIV-1 and BLOC-1 subunits in greater detail.

6.5 Potential model explaining the effect of snapin in HIV-1 trafficking

The second BLOC-1 subcomplex has at least two described interactions with the cellular motor machinery. Monfregola et al using co-IP and over-expression experiments showed that the actin nucleation-promoting factor named WASH (Wiskott-Aldrich syndrome protein and SCAR homologue) was co-expressed with BLOS2, the exact nature of this interaction in terms of stability and transient nature remains to be confirmed in future studies (Monfregola et al., 2010). Although neither of the proteins involved in WASH were identified within the HIV-1 phosphoproteome, a role for WASH and its associated downstream molecule Arp2/3, a known protein involved in HIV-1 entry at the post-hemifusion step (Harmon et al., 2010), cannot be excluded at this point and should be addressed in future studies.

Moreover, binding of snapin to the dynein intermediate chain is essential for dynein-mediated transport of late endosomes (Cai et al., 2010). Snapin in neurons acts as a dynein motor adaptor and coordinates late endosome-lysosomal trafficking, hence maintaining efficient autophagy function in neurons. Snapin deficiency results in impaired retrograde transport and clustering of late endosomes and aberrant accumulation of immature lysosomes.

Intriguingly, studies of CMV have shown that mTOR is transported by dynein to a perinuclear area termed the viral cytoplasmic assembly compartment (Clippinger and Alwine, 2012). CMV, like HIV-1, also inhibits autophagy by activating mTOR to regulate early, but not late translational control of viral proteins (Clippinger et al., 2011). Several viruses use the microtubule system to either move their nucleic acid/protein cores to intracellular replication sites immediately after entering the cell and/or transport newly assembled viral progeny to the plasma membrane to facilitate their dissemination. In the case of HIV-1, inhibition of dynein activity abrogates viral

transport towards the nucleus during the early stages of infection (McDonald et al., 2002).

6.6 HIV-1-mediated interaction with snapin may activate mTOR

As mentioned in the introduction HIV-1 induces a rapid inhibition of autophagy via activation of mTOR (Blanchet et al., 2010), although the exact molecular mechanism for this phenomenon remains to be elucidated. Inhibition of autophagy in DCs, due to their sentinel role as APC and regulators of innate and adaptive immune response, appears to serve the virus well in many regards: it counteracts lysosome-mediated viral degradation and increases *trans*-infection, inhibits TLR responsiveness and impairs antigen-presentation. Snapin knockdown reduced *trans*-infection, increased TLR responsiveness to TLR8 activation, allowed induction of an anti-HIV-1 interferon and inflammatory response and released HIV-1-induced inhibition of TASCC formation. Therefore, HIV-1-mediated activation of mTOR may be mediated via the action of snapin. In this model HIV-1-mediated inhibition of TASCC formation would inhibit the secretory pathway and hence the synthesis and secretion of immune mediators such as IFNβ1, IL6 and CCL5. Further, increased TLR8 activation observed upon snapin knockdown could be explained by the role of snapin in TLR ligand delivery to an endosomal signaling compartment. Studies in ATG5 or LC3 deficient DCs suggest that TLR signaling is regulated by control of TLR ligand delivery to immunoamphisomes (Blanchet et al., 2010). Similar findings were reported in ATG5 deficient murine pDCs (Lee et al., 2007), in contrast mice deficient in ATG16L displayed no defects in TLR signaling (Saitoh et al., 2008). Moreover there is increasing evidence for a control of TLR signaling though compartmentalization and regulation of access of TLRs and their adaptor molecules to PAMPs (Barton and Kagan, 2009). Future studies should aid in clarifying the complex interaction of TLR signaling and intracellular trafficking.

mTOR is an evolutionary conserved serine/threonine kinase that has emerged as a critical signal integrator of various cellular pathways due to its ability to sense and integrate cues from the cellular microenvironment (Zoncu et al., 2011). Under steady state conditions its activity is tightly regulated by multiple inhibitory mechanisms to enforce normal homeostasis in the cell. Activation of mTOR by snapin would also explain the elusive prenatal lethality of snapin-null mice (Yuzaki, 2010).

Accumulating evidence, not necessarily from immunological studies, suggest that membrane trafficking and subcellular targeting control mTOR signaling (Zoncu et al., 2011). Hence, snapin (and BLOC-1) by its virtue of regulating ILV trafficking and fusion of endosomal compartments may activate mTOR by recruiting it to an endo-lysosomal membrane via dynein-mediated transport to a location away from TASCC. Future studies using LV-mediated overexpression of snapin with mutations in the dynein binding regions should address the localization of mTOR and TASCC upon HIV-1 and TLR signaling. The role of snapin in HIV-1 antigen presentation should also be included in these experiments. The functional significance of the Rag GTPases in changing mTOR activity upon HIV-1 infection should be elucidated in these studies as well. Moreover, the recent description of the mTOR phosphoproteome should allow a systematic comparative analysis of the HIV-1 and mTOR phosphoproteome to identify common downstream pathways that could help in clarifying the complexity of the molecular machinery set in motion by HIV-1 (Hsu et al., 2011; Yu et al., 2011). Altogether, these findings place snapin at a unique position at the interface between the innate immune response to the machinery regulating vesicular trafficking and the translational response.

6.7 HIV-1-mediated dephosphorylation of SHP-1 and the interaction of HIV-1 with CD47

In chapter 5 I focused on characterizing the role of SHP-1 in HIV-1 signaling, based on the observation that it was dephosphorylated by HIV-1 and is an important negative regulator of the immune response. My hypothesis was that dephosphorylation of SHP-1 may provide a mechanism for how HIV-1 manipulates the innate immune response. I confirmed dephosphorylation of SHP-1 and showed rapid deactivation of the phosphatase activity of SHP-1 by the virus. Using different PRR ligands I could not identify a particular ligand triggering dephosphorylation of SHP-1. Based on bioinformatics analysis and literature review I concluded with a putative model, whereby SHP-1 dephosphorylation is mediated by recruitment of the protein together with other signaling and trafficking molecules into a signalosome on entry of the virus, to either the DC plasma membrane or the endosomal membrane. An elegant way to further explore this could be to design a library of SH2 target peptides derived from

protein sequence databases to identify candidate proteins interacting with the SH2 domain of SHP-1.

Investigating downstream effects of SHP-1 dephoshorylation was associated with some experimental challenges, hence I decided to set up a lentiviral based overexpression system in DCs, which should provide a valuable tool to re-address this issue in future studies. Interestingly, recent work has demonstrated a previously unappreciated role for SHP-1 in phagolysosome biogenesis (Gomez et al., 2012). SHP-1 is recruited early to phagosomes and is required for the acquisition of lysosomal features and acidification. In light of the work presented in chapter 4, it would be interesting to investigate the role of SHP-1 in HIV-1 endocytosis and trafficking to endo-lysosomal compartments.

Studies of HIV-1-mediated dephosphorylation of SHP-1 highlighted another intricate aspect of the interaction between HIV-1 and the host cell. Incorporation of host CD47 within viral particles was shown to enhance HIV-1 infectivity and anti-CD47 antibody-mediated inhibition of the interaction between DCs and CD47 resulted in a reduction of HIV-1 replication, both transcription of early HIV-1 genes as well as HIV-1 *trans*-infection. LV shRNA mediated downregulation of SIRPα expression should help to clarify if this effect is mediated via SIRPα, which would indicate a mechanism unique to phagocytic cell subsets. More work is required to elucidate the mechanism of CD47-mediated HIV-1 infection.

The concept of host proteins being incorporated into HIV-1 particles – and indeed viruses in general – as an immune evasive strategy is, as such, not new. Acquisition of CD28 into the viral envelope increases infectivity (Giguere et al., 2002) and similarly antigen-presenting particle technology to generate surface engineered non-infectious viral particles can induce strong immune responses (Mosca et al., 2007). Further work is required to look into the potential of targeted CD47 manipulation as a clinical tool, and it may prove difficult to translate *in vitro* findings to the clinical setting. The excellent results that were achieved with anti-CD47 antibody treatment in solid tumors, Hodgkin and Non-Hodgin Lymphomas can in part be explained by the high expression of CD47 (up to 3-fold) on cancer cells compared to non-malignant cells (Majeti et al., 2009). Future studies should investigate the level of CD47 expression on HIV-1 viral particles, in particular viral isolates from HIV-1-infected patients rather than viral preparations generated *in vitro*. This could be achieved with the development of more advanced

techniques to isolate highly purified virions and access to highly sensitive LC-MS/MS instruments, which only require minute amount of material. Given the high abundance of host proteins ((Chertova et al., 2006) and chapter 3) and host sugars (Scanlan et al., 2007) in HIV-1 virions, a simplified notion would be that the viral membrane may essentially be regarded as host membrane with a few viral glycoproteins dispersed in. Better characterization of the role of these host proteins in the viral life cycle could potentially allow to unpick viral reservoirs *in vivo*, for instance by pinpointing latent reservoirs based on certain host protein content. Altogether, the acquisition of CD47 by the virus illustrates another strategy of HIV-1 co-opting the missing-self strategy of immune recognition to protect itself from detection by the host (Medzhitov and Janeway, 2002).

6.8 Concluding thoughts

As discussed many times in this thesis, DCs play a crucial role in the early mucosal events of infection, and the propagation of virus to target resting CD4+ T cells residing in lymphoid tissue. The interaction of HIV-1 with DCs was considered to have three distinct outcomes (Piguet and Steinman, 2007): (i) degradation of the majority of incoming virions via the lysosomal pathway, a process we now know is due to the action of SAMHD1; (ii) a small fraction (1-3%) evading degradation and completing reverse transcription for production of *de novo* virus, a process that can now be explained by the crosstalk between TLR8 and DC-SIGN (Gringhuis et al., 2010); and lastly (iii) a significant amount of virus traversing into the *trans*-compartment to infect CD4+ T cells via the VS (Geijtenbeek et al., 2000), a process, which appears to be fairly unique to HIV-1 and is still poorly understood.

Since the work on this thesis commenced, our understanding of the innate interaction of HIV-1 with the host has advanced considerably (Iwasaki, 2012). We now appreciate the role of host factors, such as TREX1 that digest HIV-1 DNA to avoid induction of the type I interferon response, and SAMHD1 that removes essential building blocks for the virus to complete replication. Further, we learned of the still slightly elusive and selective interplay between TLR8 and DC-SIGN and efforts in finding the putative cytosolic DNA sensor that HIV-1 actively hides from. Altogether these data draw a fascinating image of a virus that seems to have mastered the art of immune evasion in

every single aspect. Initially it seemed rather remarkable that the recruitment of host factors involved in *trans*-infection occurs as early as ten minutes upon infection, however given that the virus is so efficiently restricted by SAMHD1, this may represent an alarmed survival strategy for the virus to quickly traffic to the *trans*-compartment to hide and disseminate. The question arises, if interventional strategies such as microbicides or vaccine adjuvants need to take these factors into account.

It is obviously difficult to assess the relevance of *in vitro* findings to the actual events occurring during HIV-1 infection in mucosal tissues, although *in vitro* studies of the interactions between HIV-1 and DC, mostly MDDCs, are crucial in making those first steps towards understanding a complex process. It would be important to confirm the observations obtained here, in DC subsets of mucosal tissues in the NPH model, and in primary mucosal myeloid DC subsets infected *ex vivo*. While these cells may not be amenable to large scale screens owing to their comparative rarity, now that specific candidate host factors have been identified, these can be followed up in targeted experiments such as real-time PCR or immunofluorescence studies, which should be amenable to smaller cell numbers.

One novel concept, which was recently introduced by R. Medzhitov, adds another layer of complexity to innate immune sensing (Medzhitov, 2011). Hereby, innate sensing is not only based on a receptor or a set of receptors recognizing a PAMP, but rather sensing alterations in the cellular microenvironment induced by some stereotypic function of a pathogen or a virulence factor, for instance set in place by disruptions of the cytoskeleton or the endocytic machinery. Similar areas have been identified in the area of plant immunology (Dangl and Jones, 2001). It would be interesting to know if such mechanisms could also account for HIV-1 sensing, as the results presented in this thesis indicate that HIV-1 may coopt common cellular pathways – LRO biosynthesis, DNA damage response, mTOR - to exert specialized membrane regulatory functions – *trans*-infection, endosomal TLR signaling, TASCC formation – to create a favourable cellular environment. This would be an extremely difficult, but also fascinating area to study.

Chapter 7

References

Abeliovich, H., Dunn, W.A., Jr., Kim, J., and Klionsky, D.J. (2000). Dissection of autophagosome biogenesis into distinct nucleation and expansion steps. The Journal of cell biology *151*, 1025-1034.

Abu-Dayyeh, I., Shio, M.T., Sato, S., Akira, S., Cousineau, B., and Olivier, M. (2008). Leishmania-induced IRAK-1 inactivation is mediated by SHP-1 interacting with an evolutionarily conserved KTIM motif. PLoS neglected tropical diseases *2*, e305.

Akakura, S., and Gelman, I.H. (2012). Pivotal Role of AKAP12 in the Regulation of Cellular Adhesion Dynamics: Control of Cytoskeletal Architecture, Cell Migration, and Mitogenic Signaling. Journal of signal transduction *2012*, 529179.

Alonso, A., Sasin, J., Bottini, N., Friedberg, I., Osterman, A., Godzik, A., Hunter, T., Dixon, J., and Mustelin, T. (2004). Protein tyrosine phosphatases in the human genome. Cell *117*, 699-711.

Alvarez, E., Menendez-Arias, L., and Carrasco, L. (2003). The eukaryotic translation initiation factor 4GI is cleaved by different retroviral proteases. Journal of virology *77*, 12392-12400.

An, H., Hou, J., Zhou, J., Zhao, W., Xu, H., Zheng, Y., Yu, Y., Liu, S., and Cao, X. (2008). Phosphatase SHP-1 promotes TLR- and RIG-I-activated production of type I interferon by inhibiting the kinase IRAK1. Nature immunology *9*, 542-550.

Ao, Z., Danappa Jayappa, K., Wang, B., Zheng, Y., Kung, S., Rassart, E., Depping, R., Kohler, M., Cohen, E.A., and Yao, X. (2010). Importin alpha3 interacts with HIV-1 integrase and contributes to HIV-1 nuclear import and replication. Journal of virology *84*, 8650-8663.

Arita, M., Wakita, T., and Shimizu, H. (2012). Valosin-containing protein (VCP/p97) is required for poliovirus replication and is involved in cellular protein secretion pathway in poliovirus infection. Journal of virology *86*, 5541-5553.

Arnaud, N., Dabo, S., Akazawa, D., Fukasawa, M., Shinkai-Ouchi, F., Hugon, J., Wakita, T., and Meurs, E.F. (2011). Hepatitis C virus reveals a novel early control in acute immune response. PLoS pathogens *7*, e1002289.

Arrigo, A.P., Simon, S., Gibert, B., Kretz-Remy, C., Nivon, M., Czekalla, A., Guillet, D., Moulin, M., Diaz-Latoud, C., and Vicart, P. (2007). Hsp27 (HspB1) and alphaB-crystallin (HspB5) as therapeutic targets. FEBS letters *581*, 3665-3674.

Babic, M., and Zinsmaier, K.E. (2011). Memory, synapse stability, and beta-adducin. Neuron *69*, 1039-1041.

Bainbridge, J.W., Stephens, C., Parsley, K., Demaison, C., Halfyard, A., Thrasher, A.J., and Ali, R.R. (2001). In vivo gene transfer to the mouse eye using an HIV-based lentiviral vector; efficient long-term transduction of corneal endothelium and retinal pigment epithelium. Gene therapy *8*, 1665-1668.

Baird, N.L., York, J., and Nunberg, J.H. (2012). Arenavirus infection induces discrete cytosolic structures for RNA replication. Journal of virology *86*, 11301-11310.

Barclay, A.N. (2009). Signal regulatory protein alpha (SIRPalpha)/CD47 interaction and function. Current opinion in immunology *21*, 47-52.

Barclay, A.N., and Brown, M.H. (2006). The SIRP family of receptors and immune regulation. Nature reviews Immunology *6*, 457-464.

Barclay, A.N., and Hatherley, D. (2008). The counterbalance theory for evolution and function of paired receptors. Immunity *29*, 675-678.

Barrera, N.P., and Robinson, C.V. (2011). Advances in the mass spectrometry of membrane proteins: from individual proteins to intact complexes. Annual review of biochemistry *80*, 247-271.

Barton, G.M., and Kagan, J.C. (2009). A cell biological view of Toll-like receptor function: regulation through compartmentalization. Nature reviews Immunology *9*, 535-542.

Basu, A., Meyer, K., Lai, K.K., Saito, K., Di Bisceglie, A.M., Grosso, L.E., Ray, R.B., and Ray, R. (2006). Microarray analyses and molecular profiling of Stat3 signaling pathway induced by hepatitis C virus core protein in human hepatocytes. Virology *349*, 347-358.

Bednarek, E., and Caroni, P. (2011). beta-Adducin is required for stable assembly of new synapses and improved memory upon environmental enrichment. Neuron *69*, 1132-1146.

Behrends, C., Sowa, M.E., Gygi, S.P., and Harper, J.W. (2010). Network organization of the human autophagy system. Nature *466*, 68-76.

Bennett, A.M., Tang, T.L., Sugimoto, S., Walsh, C.T., and Neel, B.G. (1994). Protein-tyrosine-phosphatase SHPTP2 couples platelet-derived growth factor receptor beta to Ras. Proceedings of the National Academy of Sciences of the United States of America *91*, 7335-7339.

Bennett, E.J., Rush, J., Gygi, S.P., and Harper, J.W. (2010). Dynamics of cullin-RING ubiquitin ligase network revealed by systematic quantitative proteomics. Cell *143*, 951-965.

Berger, G., Durand, S., Goujon, C., Nguyen, X.N., Cordeil, S., Darlix, J.L., and Cimarelli, A. (2011). A simple, versatile and efficient method to genetically modify human monocyte-derived dendritic cells with HIV-1-derived lentiviral vectors. Nature protocols *6*, 806-816.

Binstadt, B.A., Billadeau, D.D., Jevremovic, D., Williams, B.L., Fang, N., Yi, T., Koretzky, G.A., Abraham, R.T., and Leibson, P.J. (1998). SLP-76 is a direct substrate of SHP-1 recruited to killer cell inhibitory receptors. The Journal of biological chemistry *273*, 27518-27523.

Bitko, V., Musiyenko, A., Bayfield, M.A., Maraia, R.J., and Barik, S. (2008). Cellular La protein shields nonsegmented negative-strand RNA viral leader RNA from RIG-I and enhances virus growth by diverse mechanisms. Journal of virology *82*, 7977-7987.

Blanchet, F., Moris, A., Mitchell, J.P., and Piguet, V. (2011). A look at HIV journey: from dendritic cells to infection spread in CD4(+) T cells. Current opinion in HIV and AIDS *6*, 391-397.

Blanchet, F.P., Moris, A., Nikolic, D.S., Lehmann, M., Cardinaud, S., Stalder, R., Garcia, E., Dinkins, C., Leuba, F., Wu, L., *et al*. (2010). Human immunodeficiency virus-1 inhibition of immunoamphisomes in dendritic cells impairs early innate and adaptive immune responses. Immunity *32*, 654-669.

Blander, J.M., and Medzhitov, R. (2004). Regulation of phagosome maturation by signals from toll-like receptors. Science *304*, 1014-1018.

Blank, U., Launay, P., Benhamou, M., and Monteiro, R.C. (2009). Inhibitory ITAMs as novel regulators of immunity. Immunological reviews *232*, 59-71.

Blasius, A.L., Arnold, C.N., Georgel, P., Rutschmann, S., Xia, Y., Lin, P., Ross, C., Li, X., Smart, N.G., and Beutler, B. (2010). Slc15a4, AP-3, and Hermansky-Pudlak syndrome proteins are required for Toll-like receptor signaling in plasmacytoid dendritic cells. Proceedings of the National Academy of Sciences of the United States of America *107*, 19973-19978.

Boily-Larouche, G., Milev, M.P., Zijenah, L.S., Labbe, A.C., Zannou, D.M., Humphrey, J.H., Ward, B.J., Poudrier, J., Mouland, A.J., Cohen, E.A., *et al*. (2012). Naturally-occurring genetic variants in human DC-SIGN increase HIV-1 capture, cell-transfer and risk of mother-to-child transmission. PloS one *7*, e40706.

Bosu, D.R., and Kipreos, E.T. (2008). Cullin-RING ubiquitin ligases: global regulation and activation cycles. Cell division *3*, 7.

Bouchard, P., Zhao, Z., Banville, D., Dumas, F., Fischer, E.H., and Shen, S.H. (1994). Phosphorylation and identification of a major tyrosine phosphorylation site in protein tyrosine phosphatase 1C. The Journal of biological chemistry *269*, 19585-19589.

Boudreau, H.E., Broustas, C.G., Gokhale, P.C., Kumar, D., Mewani, R.R., Rone, J.D., Haddad, B.R., and Kasid, U. (2007). Expression of BRCC3, a novel cell cycle regulated molecule, is associated with increased phospho-ERK and cell proliferation. International journal of molecular medicine *19*, 29-39.

Brass, A.L., Dykxhoorn, D.M., Benita, Y., Yan, N., Engelman, A., Xavier, R.J., Lieberman, J., and Elledge, S.J. (2008). Identification of host proteins required for HIV infection through a functional genomic screen. Science *319*, 921-926.

Broom, O.J., Zhang, Y., Oldenborg, P.A., Massoumi, R., and Sjolander, A. (2009). CD47 regulates collagen I-induced cyclooxygenase-2 expression and intestinal epithelial cell migration. PloS one *4*, e6371.

Brown, C., Morham, S.G., Walsh, D., and Naghavi, M.H. (2011). Focal adhesion proteins talin-1 and vinculin negatively affect paxillin phosphorylation and limit retroviral infection. Journal of molecular biology *410*, 761-777.

Brumell, J.H., Chan, C.K., Butler, J., Borregaard, N., Siminovitch, K.A., Grinstein, S., and Downey, G.P. (1997). Regulation of Src homology 2-containing tyrosine phosphatase 1 during activation of human neutrophils. Role of protein kinase C. The Journal of biological chemistry *272*, 875-882.

Bruscia, E.M., Zhang, P.X., Satoh, A., Caputo, C., Medzhitov, R., Shenoy, A., Egan, M.E., and Krause, D.S. (2011). Abnormal trafficking and degradation of TLR4 underlie the elevated inflammatory response in cystic fibrosis. Journal of immunology *186*, 6990-6998.

Bug, M., and Meyer, H. (2012). Expanding into new markets - VCP/p97 in endocytosis and autophagy. Journal of structural biology *179*, 78-82.

Bushman, F.D., Malani, N., Fernandes, J., D'Orso, I., Cagney, G., Diamond, T.L., Zhou, H., Hazuda, D.J., Espeseth, A.S., Konig, R., *et al*. (2009). Host cell factors in HIV replication: meta-analysis of genome-wide studies. PLoS pathogens *5*, e1000437.

Buxton, P., Zhang, X.M., Walsh, B., Sriratana, A., Schenberg, I., Manickam, E., and Rowe, T. (2003). Identification and characterization of Snapin as a ubiquitously expressed SNARE-binding protein that interacts with SNAP23 in non-neuronal cells. The Biochemical journal *375*, 433-440.

Cai, L., Holoweckyj, N., Schaller, M.D., and Bear, J.E. (2005). Phosphorylation of coronin 1B by protein kinase C regulates interaction with Arp2/3 and cell motility. The Journal of biological chemistry *280*, 31913-31923.

Cai, Q., Lu, L., Tian, J.H., Zhu, Y.B., Qiao, H., and Sheng, Z.H. (2010). Snapin-regulated late endosomal transport is critical for efficient autophagy-lysosomal function in neurons. Neuron *68*, 73-86.

Cambi, A., de Lange, F., van Maarseveen, N.M., Nijhuis, M., Joosten, B., van Dijk, E.M., de Bakker, B.I., Fransen, J.A., Bovee-Geurts, P.H., van Leeuwen, F.N., *et al*. (2004). Microdomains of the C-type lectin DC-SIGN are portals for virus entry into dendritic cells. The Journal of cell biology *164*, 145-155.

Castello, A., Franco, D., Moral-Lopez, P., Berlanga, J.J., Alvarez, E., Wimmer, E., and Carrasco, L. (2009). HIV- 1 protease inhibits Cap- and poly(A)-dependent translation upon eIF4GI and PABP cleavage. PloS one *4*, e7997.

Cavrois, M., De Noronha, C., and Greene, W.C. (2002). A sensitive and specific enzyme-based assay detecting HIV-1 virion fusion in primary T lymphocytes. Nature biotechnology *20*, 1151-1154.

Chan, D.C., and Kim, P.S. (1998). HIV entry and its inhibition. Cell *93*, 681-684.

Chan, E.Y., Qian, W.J., Diamond, D.L., Liu, T., Gritsenko, M.A., Monroe, M.E., Camp, D.G., 2nd, Smith, R.D., and Katze, M.G. (2007). Quantitative analysis of human immunodeficiency virus type 1-infected CD4+ cell proteome: dysregulated cell cycle progression and nuclear transport coincide with robust virus production. Journal of virology *81*, 7571-7583.

Chao, M.P., Alizadeh, A.A., Tang, C., Myklebust, J.H., Varghese, B., Gill, S., Jan, M., Cha, A.C., Chan, C.K., Tan, B.T., *et al*. (2010). Anti-CD47 antibody synergizes with rituximab to promote phagocytosis and eradicate non-Hodgkin lymphoma. Cell *142*, 699-713.

Chao, M.P., Tang, C., Pachynski, R.K., Chin, R., Majeti, R., and Weissman, I.L. (2011). Extranodal dissemination of non-Hodgkin lymphoma requires CD47 and is inhibited by anti-CD47 antibody therapy. Blood *118*, 4890-4901.

Chao, M.P., Weissman, I.L., and Majeti, R. (2012). The CD47-SIRPalpha pathway in cancer immune evasion and potential therapeutic implications. Current opinion in immunology *24*, 225-232.

Charrin, S., and Alcover, A. (2006). Role of ERM (ezrin-radixin-moesin) proteins in T lymphocyte polarization, immune synapse formation and in T cell receptor-mediated signaling. Frontiers in bioscience : a journal and virtual library *11*, 1987-1997.

Chen, Z., Chen, L., Qiao, S.W., Nagaishi, T., and Blumberg, R.S. (2008). Carcinoembryonic antigen-related cell adhesion molecule 1 inhibits proximal TCR signaling by targeting ZAP-70. Journal of immunology *180*, 6085-6093.

Chertova, E., Chertov, O., Coren, L.V., Roser, J.D., Trubey, C.M., Bess, J.W., Jr., Sowder, R.C., 2nd, Barsov, E., Hood, B.L., Fisher, R.J., *et al*. (2006). Proteomic and biochemical analysis of purified human immunodeficiency virus type 1 produced from infected monocyte-derived macrophages. Journal of virology *80*, 9039-9052.

Choi, S.C., Kim, K.D., Kim, J.T., Oh, S.S., Yoon, S.Y., Song, E.Y., Lee, H.G., Choe, Y.K., Choi, I., Lim, J.S., *et al*. (2010). NDRG2 is one of novel intrinsic factors for regulation of IL-10 production in human myeloid cell. Biochemical and biophysical research communications *396*, 684-690.

Choudhary, C., and Mann, M. (2010). Decoding signalling networks by mass spectrometry-based proteomics. Nature reviews Molecular cell biology *11*, 427-439.

Christian, F., Anthony, D.F., Vadrevu, S., Riddell, T., Day, J.P., McLeod, R., Adams, D.R., Baillie, G.S., and Houslay, M.D. (2010). p62 (SQSTM1) and cyclic AMP phosphodiesterase-4A4 (PDE4A4) locate to a novel, reversible protein aggregate with links to autophagy and proteasome degradation pathways. Cellular signalling *22*, 1576-1596.

Clapham, P.R., and McKnight, A. (2001). HIV-1 receptors and cell tropism. British medical bulletin *58*, 43-59.

Clements, J.L., Yang, B., Ross-Barta, S.E., Eliason, S.L., Hrstka, R.F., Williamson, R.A., and Koretzky, G.A. (1998). Requirement for the leukocyte-specific adapter protein SLP-76 for normal T cell development. Science *281*, 416-419.

Clippinger, A.J., and Alwine, J.C. (2012). Dynein mediates the localization and activation of mTOR in normal and human cytomegalovirus-infected cells. Genes & development *26*, 2015-2026.

Clippinger, A.J., Maguire, T.G., and Alwine, J.C. (2011). The changing role of mTOR kinase in the maintenance of protein synthesis during human cytomegalovirus infection. Journal of virology *85*, 3930-3939.

Coleman, S.H., Hitchin, D., Noviello, C.M., and Guatelli, J.C. (2006). HIV-1 Nef stabilizes AP-1 on membranes without inducing ARF1-independent de novo attachment. Virology *345*, 148-155.

Cooper, J., Liu, L., Woodruff, E.A., Taylor, H.E., Goodwin, J.S., D'Aquila, R.T., Spearman, P., Hildreth, J.E., and Dong, X. (2011). Filamin A protein interacts with human immunodeficiency virus type 1 Gag protein and contributes to productive particle assembly. The Journal of biological chemistry *286*, 28498-28510.

Craggs, G., and Kellie, S. (2001). A functional nuclear localization sequence in the C-terminal domain of SHP-1. The Journal of biological chemistry *276*, 23719-23725.

Craig, R., and Beavis, R.C. (2004). TANDEM: matching proteins with tandem mass spectra. Bioinformatics *20*, 1466-1467.

Crespo, P., Schuebel, K.E., Ostrom, A.A., Gutkind, J.S., and Bustelo, X.R. (1997). Phosphotyrosine-dependent activation of Rac-1 GDP/GTP exchange by the vav proto-oncogene product. Nature *385*, 169-172.

Cristea, I.M., Rozjabek, H., Molloy, K.R., Karki, S., White, L.L., Rice, C.M., Rout, M.P., Chait, B.T., and MacDonald, M.R. (2010). Host factors associated with the Sindbis virus RNA-dependent RNA polymerase: role for G3BP1 and G3BP2 in virus replication. Journal of virology *84*, 6720-6732.

Cui, Y., Li, X., Chen, Q., He, X., Yang, Q., Zhang, A., Yu, X., Chen, H., Liu, N., Xie, Q., *et al*. (2010). BLOS1, a putative BLOC-1 subunit, interacts with SNX1 and modulates root growth in Arabidopsis. Journal of cell science *123*, 3727-3733.

Cullinane, A.R., Curry, J.A., Golas, G., Pan, J., Carmona-Rivera, C., Hess, R.A., White, J.G., Huizing, M., and Gahl, W.A. (2012). A BLOC-1 mutation screen reveals a novel BLOC1S3 mutation in Hermansky-Pudlak Syndrome type 8. Pigment cell & melanoma research *25*, 584-591.

Dangl, J.L., and Jones, J.D. (2001). Plant pathogens and integrated defence responses to infection. Nature *411*, 826-833.

de Souza, G.A., Malen, H., Softeland, T., Saelensminde, G., Prasad, S., Jonassen, I., and Wiker, H.G. (2008). High accuracy mass spectrometry analysis as a tool to verify and improve gene annotation using Mycobacterium tuberculosis as an example. BMC genomics *9*, 316.

de Witte, L., de Vries, R.D., van der Vlist, M., Yuksel, S., Litjens, M., de Swart, R.L., and Geijtenbeek, T.B. (2008). DC-SIGN and CD150 have distinct roles in transmission of measles virus from dendritic cells to T-lymphocytes. PLoS pathogens *4*, e1000049.

Dell'Angelica, E.C. (2009). AP-3-dependent trafficking and disease: the first decade. Current opinion in cell biology *21*, 552-559.

Dengjel, J., Akimov, V., Olsen, J.V., Bunkenborg, J., Mann, M., Blagoev, B., and Andersen, J.S. (2007). Quantitative proteomic assessment of very early cellular signaling events. Nature biotechnology *25*, 566-568.

Di Pietro, S.M., and Dell'Angelica, E.C. (2005). The cell biology of Hermansky-Pudlak syndrome: recent advances. Traffic *6*, 525-533.

Diaz, L., Mao, H., Zhou, Y., Kohli, M., Cassella, J., Santos, D., Fesseha, Z., Weng, K., Chen, H., Bamba, D., *et al*. (2010). TSG101 exposure on the surface of HIV-1 infected cells: implications for monoclonal antibody therapy for HIV/AIDS. American journal of translational research *2*, 368-380.

Dickman, D.K., Tong, A., and Davis, G.W. (2012). Snapin is critical for presynaptic homeostatic plasticity. The Journal of neuroscience : the official journal of the Society for Neuroscience *32*, 8716-8724.

Dobrikov, M., Dobrikova, E., Shveygert, M., and Gromeier, M. (2011). Phosphorylation of eukaryotic translation initiation factor 4G1 (eIF4G1) by protein kinase C{alpha} regulates eIF4G1 binding to Mnk1. Molecular and cellular biology *31*, 2947-2959.

Dong, C., Janas, A.M., Wang, J.H., Olson, W.J., and Wu, L. (2007). Characterization of human immunodeficiency virus type 1 replication in immature and mature dendritic cells reveals dissociable cis- and trans-infection. Journal of virology *81*, 11352-11362.

Dong, L.W., Kong, X.N., Yan, H.X., Yu, L.X., Chen, L., Yang, W., Liu, Q., Huang, D.D., Wu, M.C., and Wang, H.Y. (2008). Signal regulatory protein alpha negatively regulates both TLR3 and cytoplasmic pathways in type I interferon induction. Molecular immunology *45*, 3025-3035.

Dong, Q., Siminovitch, K.A., Fialkow, L., Fukushima, T., and Downey, G.P. (1999). Negative regulation of myeloid cell proliferation and function by the SH2 domain-containing tyrosine phosphatase-1. Journal of immunology *162*, 3220-3230.

Douek, D.C., Roederer, M., and Koup, R.A. (2009). Emerging concepts in the immunopathogenesis of AIDS. Annual review of medicine *60*, 471-484.

Douglass, A.D., and Vale, R.D. (2005). Single-molecule microscopy reveals plasma membrane microdomains created by protein-protein networks that exclude or trap signaling molecules in T cells. Cell *121*, 937-950.

Dunn, S.J., Khan, I.H., Chan, U.A., Scearce, R.L., Melara, C.L., Paul, A.M., Sharma, V., Bih, F.Y., Holzmayer, T.A., Luciw, P.A., *et al*. (2004). Identification of cell surface targets for HIV-1 therapeutics using genetic screens. Virology *321*, 260-273.

Eggeling, C., Ringemann, C., Medda, R., Schwarzmann, G., Sandhoff, K., Polyakova, S., Belov, V.N., Hein, B., von Middendorff, C., Schonle, A., *et al*. (2009). Direct observation of the nanoscale dynamics of membrane lipids in a living cell. Nature *457*, 1159-1162.

Elias, J.E., and Gygi, S.P. (2007). Target-decoy search strategy for increased confidence in large-scale protein identifications by mass spectrometry. Nature methods *4*, 207-214.

Falcon-Perez, J.M., Starcevic, M., Gautam, R., and Dell'Angelica, E.C. (2002). BLOC-1, a novel complex containing the pallidin and muted proteins involved in the biogenesis of melanosomes and platelet-dense granules. The Journal of biological chemistry *277*, 28191-28199.

Fawcett, V.C., and Lorenz, U. (2005). Localization of Src homology 2 domain-containing phosphatase 1 (SHP-1) to lipid rafts in T lymphocytes: functional implications and a role for the SHP-1 carboxyl terminus. Journal of immunology *174*, 2849-2859.

Fortin, G., Raymond, M., Van, V.Q., Rubio, M., Gautier, P., Sarfati, M., and Franchimont, D. (2009). A role for CD47 in the development of experimental colitis mediated by SIRPalpha+CD103- dendritic cells. The Journal of experimental medicine *206*, 1995-2011.

Fortin, J.F., Barbeau, B., Hedman, H., Lundgren, E., and Tremblay, M.J. (1999). Role of the leukocyte function antigen-1 conformational state in the process of human immunodeficiency virus type 1-mediated syncytium formation and virus infection. Virology *257*, 228-238.

Fortin, J.F., Barbeau, B., Robichaud, G.A., Pare, M.E., Lemieux, A.M., and Tremblay, M.J. (2001). Regulation of nuclear factor of activated T cells by phosphotyrosyl-specific

phosphatase activity: a positive effect on HIV-1 long terminal repeat-driven transcription and a possible implication of SHP-1. Blood *97*, 2390-2400.

Foster, L.J., Yeung, B., Mohtashami, M., Ross, K., Trimble, W.S., and Klip, A. (1998). Binary interactions of the SNARE proteins syntaxin-4, SNAP23, and VAMP-2 and their regulation by phosphorylation. Biochemistry *37*, 11089-11096.

Fournier, M.L., Gilmore, J.M., Martin-Brown, S.A., and Washburn, M.P. (2007). Multidimensional separations-based shotgun proteomics. Chemical reviews *107*, 3654-3686.

Fowler, C.C., Pao, L.I., Blattman, J.N., and Greenberg, P.D. (2010). SHP-1 in T cells limits the production of CD8 effector cells without impacting the formation of long-lived central memory cells. Journal of immunology *185*, 3256-3267.

Frank, C., Keilhack, H., Opitz, F., Zschornig, O., and Bohmer, F.D. (1999). Binding of phosphatidic acid to the protein-tyrosine phosphatase SHP-1 as a basis for activity modulation. Biochemistry *38*, 11993-12002.

Franke, E.K., and Luban, J. (1996). Inhibition of HIV-1 replication by cyclosporine A or related compounds correlates with the ability to disrupt the Gag-cyclophilin A interaction. Virology *222*, 279-282.

Franke, E.K., Yuan, H.E., and Luban, J. (1994). Specific incorporation of cyclophilin A into HIV-1 virions. Nature *372*, 359-362.

Freed, E.O. (2001). HIV-1 replication. Somatic cell and molecular genetics *26*, 13-33.

Freed, E.O. (2004). HIV-1 and the host cell: an intimate association. Trends in microbiology *12*, 170-177.

Fujioka, Y., Tsuda, M., Hattori, T., Sasaki, J., Sasaki, T., Miyazaki, T., and Ohba, Y. (2011). The Ras-PI3K signaling pathway is involved in clathrin-independent endocytosis and the internalization of influenza viruses. PloS one *6*, e16324.

Fusaki, N., Iwamatsu, A., Iwashima, M., and Fujisawa, J. (1997). Interaction between Sam68 and Src family tyrosine kinases, Fyn and Lck, in T cell receptor signaling. The Journal of biological chemistry *272*, 6214-6219.

Ganju, R.K., Brubaker, S.A., Chernock, R.D., Avraham, S., and Groopman, J.E. (2000). Beta-chemokine receptor CCR5 signals through SHP1, SHP2, and Syk. The Journal of biological chemistry *275*, 17263-17268.

Garcia, E., Pion, M., Pelchen-Matthews, A., Collinson, L., Arrighi, J.F., Blot, G., Leuba, F., Escola, J.M., Demaurex, N., Marsh, M., *et al*. (2005). HIV-1 trafficking to the dendritic cell-T-cell infectious synapse uses a pathway of tetraspanin sorting to the immunological synapse. Traffic *6*, 488-501.

Gaus, K., Chklovskaia, E., Fazekas de St Groth, B., Jessup, W., and Harder, T. (2005). Condensation of the plasma membrane at the site of T lymphocyte activation. The Journal of cell biology *171*, 121-131.

Gautier, V.W., Gu, L., O'Donoghue, N., Pennington, S., Sheehy, N., and Hall, W.W. (2009). In vitro nuclear interactome of the HIV-1 Tat protein. Retrovirology *6*, 47.

Geer, L.Y., Markey, S.P., Kowalak, J.A., Wagner, L., Xu, M., Maynard, D.M., Yang, X., Shi, W., and Bryant, S.H. (2004). Open mass spectrometry search algorithm. Journal of proteome research *3*, 958-964.

Geijtenbeek, T.B., Kwon, D.S., Torensma, R., van Vliet, S.J., van Duijnhoven, G.C., Middel, J., Cornelissen, I.L., Nottet, H.S., KewalRamani, V.N., Littman, D.R., *et al.* (2000). DC-SIGN, a dendritic cell-specific HIV-1-binding protein that enhances trans-infection of T cells. Cell *100*, 587-597.

Giguere, J.F., Paquette, J.S., Bounou, S., Cantin, R., and Tremblay, M.J. (2002). New insights into the functionality of a virion-anchored host cell membrane protein: CD28 versus HIV type 1. Journal of immunology *169*, 2762-2771.

Gilfillan, S., Stelzer, G., Piaia, E., Hofmann, M.G., and Meisterernst, M. (2005). Efficient binding of NC2.TATA-binding protein to DNA in the absence of TATA. The Journal of biological chemistry *280*, 6222-6230.

Goldenberg, S.J., Cascio, T.C., Shumway, S.D., Garbutt, K.C., Liu, J., Xiong, Y., and Zheng, N. (2004). Structure of the Cand1-Cul1-Roc1 complex reveals regulatory mechanisms for the assembly of the multisubunit cullin-dependent ubiquitin ligases. Cell *119*, 517-528.

Goldstone, D.C., Ennis-Adeniran, V., Hedden, J.J., Groom, H.C., Rice, G.I., Christodoulou, E., Walker, P.A., Kelly, G., Haire, L.F., Yap, M.W., *et al.* (2011). HIV-1 restriction factor SAMHD1 is a deoxynucleoside triphosphate triphosphohydrolase. Nature *480*, 379-382.

Gomez, C.P., Tiemi Shio, M., Duplay, P., Olivier, M., and Descoteaux, A. (2012). The Protein Tyrosine Phosphatase SHP-1 Regulates Phagolysosome Biogenesis. Journal of immunology *189*, 2203-2210.

Greene, W.C., and Peterlin, B.M. (2002). Charting HIV's remarkable voyage through the cell: Basic science as a passport to future therapy. Nature medicine *8*, 673-680.

Griffin, N.M., Yu, J., Long, F., Oh, P., Shore, S., Li, Y., Koziol, J.A., and Schnitzer, J.E. (2010). Label-free, normalized quantification of complex mass spectrometry data for proteomic analysis. Nature biotechnology *28*, 83-89.

Gringhuis, S.I., den Dunnen, J., Litjens, M., van der Vlist, M., and Geijtenbeek, T.B. (2009). Carbohydrate-specific signaling through the DC-SIGN signalosome tailors immunity to Mycobacterium tuberculosis, HIV-1 and Helicobacter pylori. Nature immunology *10*, 1081-1088.

Gringhuis, S.I., van der Vlist, M., van den Berg, L.M., den Dunnen, J., Litjens, M., and Geijtenbeek, T.B. (2010). HIV-1 exploits innate signaling by TLR8 and DC-SIGN for productive infection of dendritic cells. Nature immunology *11*, 419-426.

Guery, L., Benikhlef, N., Gautier, T., Paul, C., Jego, G., Dufour, E., Jacquel, A., Cally, R., Manoury, B., Vanden Berghe, T., *et al.* (2011). Fine-tuning nucleophosmin in macrophage differentiation and activation. Blood *118*, 4694-4704.

Gummuluru, S., Rogel, M., Stamatatos, L., and Emerman, M. (2003). Binding of human immunodeficiency virus type 1 to immature dendritic cells can occur independently of DC-SIGN and mannose binding C-type lectin receptors via a cholesterol-dependent pathway. Journal of virology *77*, 12865-12874.

Guo, D., Han, J., Adam, B.L., Colburn, N.H., Wang, M.H., Dong, Z., Eizirik, D.L., She, J.X., and Wang, C.Y. (2005). Proteomic analysis of SUMO4 substrates in HEK293 cells under serum starvation-induced stress. Biochemical and biophysical research communications *337*, 1308-1318.

Haase, A.T. (2010). Targeting early infection to prevent HIV-1 mucosal transmission. Nature *464*, 217-223.

Handley, M.E., Pollara, G., Chain, B.M., and Katz, D.R. (2005). The use of targeted microbeads for quantitative analysis of the phagocytic properties of human monocyte-derived dendritic cells. Journal of immunological methods *297*, 27-38.

Harman, A.N., Kraus, M., Bye, C.R., Byth, K., Turville, S.G., Tang, O., Mercier, S.K., Nasr, N., Stern, J.L., Slobedman, B., *et al*. (2009). HIV-1-infected dendritic cells show 2 phases of gene expression changes, with lysosomal enzyme activity decreased during the second phase. Blood *114*, 85-94.

Harmon, B., Campbell, N., and Ratner, L. (2010). Role of Abl kinase and the Wave2 signaling complex in HIV-1 entry at a post-hemifusion step. PLoS pathogens *6*, e1000956.

Hashimoto-Tane, A., Yokosuka, T., Sakata-Sogawa, K., Sakuma, M., Ishihara, C., Tokunaga, M., and Saito, T. (2011). Dynein-driven transport of T cell receptor microclusters regulates immune synapse formation and T cell activation. Immunity *34*, 919-931.

Hatherley, D., Graham, S.C., Turner, J., Harlos, K., Stuart, D.I., and Barclay, A.N. (2008). Paired receptor specificity explained by structures of signal regulatory proteins alone and complexed with CD47. Molecular cell *31*, 266-277.

Hayes, M.J., Bryon, K., Satkurunathan, J., and Levine, T.P. (2011). Yeast homologues of three BLOC-1 subunits highlight KxDL proteins as conserved interactors of BLOC-1. Traffic *12*, 260-268.

He, J.J., Henao-Mejia, J., and Liu, Y. (2009). Sam68 functions in nuclear export and translation of HIV-1 RNA. RNA biology *6*, 384-386.

Heil, F., Hemmi, H., Hochrein, H., Ampenberger, F., Kirschning, C., Akira, S., Lipford, G., Wagner, H., and Bauer, S. (2004). Species-specific recognition of single-stranded RNA via toll-like receptor 7 and 8. Science *303*, 1526-1529.

Henao-Mejia, J., Liu, Y., Park, I.W., Zhang, J., Sanford, J., and He, J.J. (2009). Suppression of HIV-1 Nef translation by Sam68 mutant-induced stress granules and nef mRNA sequestration. Molecular cell *33*, 87-96.

Hers, I., Vincent, E.E., and Tavare, J.M. (2011). Akt signalling in health and disease. Cellular signalling *23*, 1515-1527.

Hodges, A., Sharrocks, K., Edelmann, M., Baban, D., Moris, A., Schwartz, O., Drakesmith, H., Davies, K., Kessler, B., McMichael, A., *et al*. (2007). Activation of the lectin DC-SIGN induces an immature dendritic cell phenotype triggering Rho-GTPase activity required for HIV-1 replication. Nature immunology *8*, 569-577.

Hof, P., Pluskey, S., Dhe-Paganon, S., Eck, M.J., and Shoelson, S.E. (1998). Crystal structure of the tyrosine phosphatase SHP-2. Cell *92*, 441-450.

Hong, P.W., Nguyen, S., Young, S., Su, S.V., and Lee, B. (2007). Identification of the optimal DC-SIGN binding site on human immunodeficiency virus type 1 gp120. Journal of virology *81*, 8325-8336.

Hou, H., Wang, F., Zhang, W., Wang, D., Li, X., Bartlam, M., Yao, X., and Rao, Z. (2011). Structure-functional analyses of CRHSP-24 plasticity and dynamics in oxidative stress response. The Journal of biological chemistry *286*, 9623-9635.

Hsu, P.P., Kang, S.A., Rameseder, J., Zhang, Y., Ottina, K.A., Lim, D., Peterson, T.R., Choi, Y., Gray, N.S., Yaffe, M.B., *et al.* (2011). The mTOR-regulated phosphoproteome reveals a mechanism of mTORC1-mediated inhibition of growth factor signaling. Science *332*, 1317-1322.

Hunter, T. (1995). Protein kinases and phosphatases: the yin and yang of protein phosphorylation and signaling. Cell *80*, 225-236.

Ito, S., Takahara, Y., Hyodo, T., Hasegawa, H., Asano, E., Hamaguchi, M., and Senga, T. (2010). The roles of two distinct regions of PINCH-1 in the regulation of cell attachment and spreading. Molecular biology of the cell *21*, 4120-4129.

Iwasaki, A. (2012). Innate Immune Recognition of HIV-1. Immunity *37*, 389-398.

Izmailova, E., Bertley, F.M., Huang, Q., Makori, N., Miller, C.J., Young, R.A., and Aldovini, A. (2003). HIV-1 Tat reprograms immature dendritic cells to express chemoattractants for activated T cells and macrophages. Nature medicine *9*, 191-197.

Jager, S., Cimermancic, P., Gulbahce, N., Johnson, J.R., McGovern, K.E., Clarke, S.C., Shales, M., Mercenne, G., Pache, L., Li, K., *et al.* (2012). Global landscape of HIV-human protein complexes. Nature *481*, 365-370.

Ji, S., Liu, X., Li, S., Shen, L., Li, F., Wang, J., Han, J., and Yao, L. (2003). PH domain of G protein-coupled receptor kinase-2 binds to protein kinase C (PKC) and negatively regulates activity of PKC kinase. Frontiers in bioscience : a journal and virtual library *8*, a34-39.

Jolly, C., Welsch, S., Michor, S., and Sattentau, Q.J. (2011). The regulated secretory pathway in CD4(+) T cells contributes to human immunodeficiency virus type-1 cell-to-cell spread at the virological synapse. PLoS pathogens *7*, e1002226.

Jones, A.M., and Nuhse, T.S. (2011). Phosphoproteomics using iTRAQ. Methods in molecular biology *779*, 287-302.

Jouve, M., Sol-Foulon, N., Watson, S., Schwartz, O., and Benaroch, P. (2007). HIV-1 buds and accumulates in "nonacidic" endosomes of macrophages. Cell host & microbe *2*, 85-95.

Ju, J.S., and Weihl, C.C. (2010). p97/VCP at the intersection of the autophagy and the ubiquitin proteasome system. Autophagy *6*, 283-285.

Kanazawa, N., Tashiro, K., and Miyachi, Y. (2004). Signaling and immune regulatory role of the dendritic cell immunoreceptor (DCIR) family lectins: DCIR, DCAR, dectin-2 and BDCA-2. Immunobiology *209*, 179-190.

Kapoor, N., Gupta, R., Menon, S.T., Folta-Stogniew, E., Raleigh, D.P., and Sakmar, T.P. (2010). Nucleobindin 1 is a calcium-regulated guanine nucleotide dissociation inhibitor of G{alpha}i1. The Journal of biological chemistry *285*, 31647-31660.

Katoh, Y., Imakagura, H., Futatsumori, M., and Nakayama, K. (2006). Recruitment of clathrin onto endosomes by the Tom1-Tollip complex. Biochemical and biophysical research communications *341*, 143-149.

Katoh, Y., Shiba, Y., Mitsuhashi, H., Yanagida, Y., Takatsu, H., and Nakayama, K. (2004). Tollip and Tom1 form a complex and recruit ubiquitin-conjugated proteins onto early endosomes. The Journal of biological chemistry *279*, 24435-24443.

Kaur, S., Kuznetsova, S.A., Pendrak, M.L., Sipes, J.M., Romeo, M.J., Li, Z., Zhang, L., and Roberts, D.D. (2011). Heparan sulfate modification of the transmembrane receptor CD47 is necessary for inhibition of T cell receptor signaling by thrombospondin-1. The Journal of biological chemistry *286*, 14991-15002.

Keller, A., Eng, J., Zhang, N., Li, X.J., and Aebersold, R. (2005). A uniform proteomics MS/MS analysis platform utilizing open XML file formats. Molecular systems biology *1*, 2005 0017.

Keppler, O.T., Tibroni, N., Venzke, S., Rauch, S., and Fackler, O.T. (2006). Modulation of specific surface receptors and activation sensitization in primary resting CD4+ T lymphocytes by the Nef protein of HIV-1. Journal of leukocyte biology *79*, 616-627.

Kikuchi, Y., Uno, S., Yoshimura, Y., Otabe, K., Iida, S., Oheda, M., Fukushima, N., and Tsuchiya, M. (2004). A bivalent single-chain Fv fragment against CD47 induces apoptosis for leukemic cells. Biochemical and biophysical research communications *315*, 912-918.

Koethe, S., Avota, E., and Schneider-Schaulies, S. (2012). Measles virus transmission from dendritic cells to T cells: formation of synapse-like interfaces concentrating viral and cellular components. Journal of virology *86*, 9773-9781.

Kon-Kozlowski, M., Pani, G., Pawson, T., and Siminovitch, K.A. (1996). The tyrosine phosphatase PTP1C associates with Vav, Grb2, and mSos1 in hematopoietic cells. The Journal of biological chemistry *271*, 3856-3862.

Koncz, G., Kerekes, K., Chakrabandhu, K., and Hueber, A.O. (2008). Regulating Vav1 phosphorylation by the SHP-1 tyrosine phosphatase is a fine-tuning mechanism for the negative regulation of DISC formation and Fas-mediated cell death signaling. Cell death and differentiation *15*, 494-503.

Kong, X.N., Yan, H.X., Chen, L., Dong, L.W., Yang, W., Liu, Q., Yu, L.X., Huang, D.D., Liu, S.Q., Liu, H., *et al*. (2007). LPS-induced down-regulation of signal regulatory protein {alpha} contributes to innate immune activation in macrophages. The Journal of experimental medicine *204*, 2719-2731.

Konig, R., Zhou, Y., Elleder, D., Diamond, T.L., Bonamy, G.M., Irelan, J.T., Chiang, C.Y., Tu, B.P., De Jesus, P.D., Lilley, C.E., *et al*. (2008). Global analysis of host-pathogen interactions that regulate early-stage HIV-1 replication. Cell *135*, 49-60.

Krause, M., Sechi, A.S., Konradt, M., Monner, D., Gertler, F.B., and Wehland, J. (2000). Fyn-binding protein (Fyb)/SLP-76-associated protein (SLAP), Ena/vasodilator-stimulated phosphoprotein (VASP) proteins and the Arp2/3 complex link T cell receptor (TCR) signaling to the actin cytoskeleton. The Journal of cell biology *149*, 181-194.

Krautkramer, E., Giese, S.I., Gasteier, J.E., Muranyi, W., and Fackler, O.T. (2004). Human immunodeficiency virus type 1 Nef activates p21-activated kinase via recruitment into lipid rafts. Journal of virology *78*, 4085-4097.

Kubo, Y., Yoshii, H., Kamiyama, H., Tominaga, C., Tanaka, Y., Sato, H., and Yamamoto, N. (2008). Ezrin, Radixin, and Moesin (ERM) proteins function as pleiotropic regulators of human immunodeficiency virus type 1 infection. Virology *375*, 130-140.

Kutner, R.H., Zhang, X.Y., and Reiser, J. (2009). Production, concentration and titration of pseudotyped HIV-1-based lentiviral vectors. Nature protocols *4*, 495-505.

Kwon, D.S., Gregorio, G., Bitton, N., Hendrickson, W.A., and Littman, D.R. (2002). DC-SIGN-mediated internalization of HIV is required for trans-enhancement of T cell infection. Immunity *16*, 135-144.

Laguette, N., Sobhian, B., Casartelli, N., Ringeard, M., Chable-Bessia, C., Segeral, E., Yatim, A., Emiliani, S., Schwartz, O., and Benkirane, M. (2011). SAMHD1 is the dendritic- and myeloid-cell-specific HIV-1 restriction factor counteracted by Vpx. Nature *474*, 654-657.

Lambert, A.A., Barabe, F., Gilbert, C., and Tremblay, M.J. (2011). DCIR-mediated enhancement of HIV-1 infection requires the ITIM-associated signal transduction pathway. Blood *117*, 6589-6599.

Lambert, A.A., Gilbert, C., Richard, M., Beaulieu, A.D., and Tremblay, M.J. (2008). The C-type lectin surface receptor DCIR acts as a new attachment factor for HIV-1 in dendritic cells and contributes to trans- and cis-infection pathways. Blood *112*, 1299-1307.

Lambert, C., Doring, T., and Prange, R. (2007). Hepatitis B virus maturation is sensitive to functional inhibition of ESCRT-III, Vps4, and gamma 2-adaptin. Journal of virology *81*, 9050-9060.

Lankester, A.C., van Schijndel, G.M., and van Lier, R.A. (1995). Hematopoietic cell phosphatase is recruited to CD22 following B cell antigen receptor ligation. The Journal of biological chemistry *270*, 20305-20308.

Lee, H.H., Nemecek, D., Schindler, C., Smith, W.J., Ghirlando, R., Steven, A.C., Bonifacino, J.S., and Hurley, J.H. (2012). Assembly and architecture of biogenesis of lysosome-related organelles complex-1 (BLOC-1). The Journal of biological chemistry *287*, 5882-5890.

Lee, H.K., Lund, J.M., Ramanathan, B., Mizushima, N., and Iwasaki, A. (2007a). Autophagy-dependent viral recognition by plasmacytoid dendritic cells. Science *315*, 1398-1401.

Lee, W.Y., Weber, D.A., Laur, O., Severson, E.A., McCall, I., Jen, R.P., Chin, A.C., Wu, T., Gernert, K.M., and Parkos, C.A. (2007b). Novel structural determinants on SIRP alpha that mediate binding to CD47. Journal of immunology *179*, 7741-7750.

Li, B., Zhuang, L., and Trueb, B. (2004a). Zyxin interacts with the SH3 domains of the cytoskeletal proteins LIM-nebulette and Lasp-1. The Journal of biological chemistry *279*, 20401-20410.

Li, Q., Estes, J.D., Schlievert, P.M., Duan, L., Brosnahan, A.J., Southern, P.J., Reilly, C.S., Peterson, M.L., Schultz-Darken, N., Brunner, K.G., *et al.* (2009). Glycerol monolaurate prevents mucosal SIV transmission. Nature *458*, 1034-1038.

Li, W., Rusiniak, M.E., Chintala, S., Gautam, R., Novak, E.K., and Swank, R.T. (2004b). Murine Hermansky-Pudlak syndrome genes: regulators of lysosome-related organelles. BioEssays : news and reviews in molecular, cellular and developmental biology *26*, 616-628.

Li, W., Zhang, Q., Oiso, N., Novak, E.K., Gautam, R., O'Brien, E.P., Tinsley, C.L., Blake, D.J., Spritz, R.A., Copeland, N.G., *et al*. (2003). Hermansky-Pudlak syndrome type 7 (HPS-7) results from mutant dysbindin, a member of the biogenesis of lysosome-related organelles complex 1 (BLOC-1). Nature genetics *35*, 84-89.

Lin, S.Y., Raval, S., Zhang, Z., Deverill, M., Siminovitch, K.A., Branch, D.R., and Haimovich, B. (2004). The protein-tyrosine phosphatase SHP-1 regulates the phosphorylation of alpha-actinin. The Journal of biological chemistry *279*, 25755-25764.

Lindberg, F.P., Gresham, H.D., Reinhold, M.I., and Brown, E.J. (1996). Integrin-associated protein immunoglobulin domain is necessary for efficient vitronectin bead binding. The Journal of cell biology *134*, 1313-1322.

Liu, L., Sutton, J., Woodruff, E., Villalta, F., Spearman, P., and Dong, X. (2012). Defective HIV-1 Particle Assembly in AP-3-Deficient Cells Derived from Patients with Hermansky-Pudlak Syndrome Type 2. Journal of virology *86*, 11242-11253.

Liu, Y., Kruhlak, M.J., Hao, J.J., and Shaw, S. (2007a). Rapid T cell receptor-mediated SHP-1 S591 phosphorylation regulates SHP-1 cellular localization and phosphatase activity. Journal of leukocyte biology *82*, 742-751.

Liu, Y., Tan, H., Tian, H., Liang, C., Chen, S., and Liu, Q. (2011). Autoantigen La promotes efficient RNAi, antiviral response, and transposon silencing by facilitating multiple-turnover RISC catalysis. Molecular cell *44*, 502-508.

Liu, Y., Tong, Q., Zhou, Y., Lee, H.W., Yang, J.J., Buhring, H.J., Chen, Y.T., Ha, B., Chen, C.X., Yang, Y., *et al*. (2007b). Functional elements on SIRPalpha IgV domain mediate cell surface binding to CD47. Journal of molecular biology *365*, 680-693.

Lorenz, U. (2009). SHP-1 and SHP-2 in T cells: two phosphatases functioning at many levels. Immunological reviews *228*, 342-359.

Lorenz, U., Ravichandran, K.S., Pei, D., Walsh, C.T., Burakoff, S.J., and Neel, B.G. (1994). Lck-dependent tyrosyl phosphorylation of the phosphotyrosine phosphatase SH-PTP1 in murine T cells. Molecular and cellular biology *14*, 1824-1834.

Loschi, M., Leishman, C.C., Berardone, N., and Boccaccio, G.L. (2009). Dynein and kinesin regulate stress-granule and P-body dynamics. Journal of cell science *122*, 3973-3982.

Ma, X.Z., Jin, T., Sakac, D., Fahim, S., Zhang, X., Katsman, Y., Bali, M., and Branch, D.R. (2003). Abnormal splicing of SHP-1 protein tyrosine phosphatase in human T cells. Implications for lymphomagenesis. Experimental hematology *31*, 131-142.

MacDonald, M.R., Machlin, E.S., Albin, O.R., and Levy, D.E. (2007). The zinc finger antiviral protein acts synergistically with an interferon-induced factor for maximal activity against alphaviruses. Journal of virology *81*, 13509-13518.

Magadan, J.G., Perez-Victoria, F.J., Sougrat, R., Ye, Y., Strebel, K., and Bonifacino, J.S. (2010). Multilayered mechanism of CD4 downregulation by HIV-1 Vpu involving distinct ER retention and ERAD targeting steps. PLoS pathogens *6*, e1000869.

Majeti, R., Chao, M.P., Alizadeh, A.A., Pang, W.W., Jaiswal, S., Gibbs, K.D., Jr., van Rooijen, N., and Weissman, I.L. (2009). CD47 is an adverse prognostic factor and therapeutic antibody target on human acute myeloid leukemia stem cells. Cell *138*, 286-299.

Manel, N., Hogstad, B., Wang, Y., Levy, D.E., Unutmaz, D., and Littman, D.R. (2010). A cryptic sensor for HIV-1 activates antiviral innate immunity in dendritic cells. Nature *467*, 214-217.

Manel, N., and Littman, D.R. (2011). Hiding in plain sight: how HIV evades innate immune responses. Cell *147*, 271-274.

Manicassamy, S., Reizis, B., Ravindran, R., Nakaya, H., Salazar-Gonzalez, R.M., Wang, Y.C., and Pulendran, B. (2010). Activation of beta-catenin in dendritic cells regulates immunity versus tolerance in the intestine. Science *329*, 849-853.

Mann, M., and Jensen, O.N. (2003). Proteomic analysis of post-translational modifications. Nature biotechnology *21*, 255-261.

Mao, L., Yang, L., Arora, A., Choe, E.S., Zhang, G., Liu, Z., Fibuch, E.E., and Wang, J.Q. (2005). Role of protein phosphatase 2A in mGluR5-regulated MEK/ERK phosphorylation in neurons. The Journal of biological chemistry *280*, 12602-12610.

Martin-Serrano, J., and Neil, S.J. (2011). Host factors involved in retroviral budding and release. Nature reviews Microbiology *9*, 519-531.

Mason, J.M., and Arndt, K.M. (2004). Coiled coil domains: stability, specificity, and biological implications. Chembiochem : a European journal of chemical biology *5*, 170-176.

Matozaki, T., Murata, Y., Okazawa, H., and Ohnishi, H. (2009). Functions and molecular mechanisms of the CD47-SIRPalpha signalling pathway. Trends in cell biology *19*, 72-80.

Matza, D., Badou, A., Jha, M.K., Willinger, T., Antov, A., Sanjabi, S., Kobayashi, K.S., Marchesi, V.T., and Flavell, R.A. (2009). Requirement for AHNAK1-mediated calcium signaling during T lymphocyte cytolysis. Proceedings of the National Academy of Sciences of the United States of America *106*, 9785-9790.

McDonald, D., Vodicka, M.A., Lucero, G., Svitkina, T.M., Borisy, G.G., Emerman, M., and Hope, T.J. (2002). Visualization of the intracellular behavior of HIV in living cells. The Journal of cell biology *159*, 441-452.

McDonald, D., Wu, L., Bohks, S.M., KewalRamani, V.N., Unutmaz, D., and Hope, T.J. (2003). Recruitment of HIV and its receptors to dendritic cell-T cell junctions. Science *300*, 1295-1297.

McGettrick, A.F., and O'Neill, L.A. (2010). Localisation and trafficking of Toll-like receptors: an important mode of regulation. Current opinion in immunology *22*, 20-27.

McMahon, H.T., and Boucrot, E. (2011). Molecular mechanism and physiological functions of clathrin-mediated endocytosis. Nature reviews Molecular cell biology *12*, 517-533.

Medzhitov (2011). Innovating immunology: an interview with Ruslan Medzhitov. Dis Model Mech *4(4)*, 430-432.

Medzhitov, R., and Janeway, C.A., Jr. (2000). How does the immune system distinguish self from nonself? Seminars in immunology *12*, 185-188; discussion 257-344.

Medzhitov, R., and Janeway, C.A., Jr. (2002). Decoding the patterns of self and nonself by the innate immune system. Science *296*, 298-300.

Meerang, M., Ritz, D., Paliwal, S., Garajova, Z., Bosshard, M., Mailand, N., Janscak, P., Hubscher, U., Meyer, H., and Ramadan, K. (2011). The ubiquitin-selective segregase VCP/p97 orchestrates the response to DNA double-strand breaks. Nature cell biology *13*, 1376-1382.

Mehla, R., and Ayyavoo, V. (2012). Gene array studies in HIV-1 infection. Current HIV/AIDS reports *9*, 34-43.

Mellman, I., and Steinman, R.M. (2001). Dendritic cells: specialized and regulated antigen processing machines. Cell *106*, 255-258.

Meng, X., Krishnan, J., She, Y., Ens, W., Standing, K., and Wilkins, J.A. (2004). Association of rasGAPSH3 binding protein 1, G3BP1, and rasGap120 with integrin containing complexes induced by an adhesion blocking antibody. Journal of proteome research *3*, 506-516.

Minoo, P., Zadeh, M.M., Rottapel, R., Lebrun, J.J., and Ali, S. (2004). A novel SHP-1/Grb2-dependent mechanism of negative regulation of cytokine-receptor signaling: contribution of SHP-1 C-terminal tyrosines in cytokine signaling. Blood *103*, 1398-1407.

Miyauchi, K., Kim, Y., Latinovic, O., Morozov, V., and Melikyan, G.B. (2009). HIV enters cells via endocytosis and dynamin-dependent fusion with endosomes. Cell *137*, 433-444.

Monfregola, J., Napolitano, G., D'Urso, M., Lappalainen, P., and Ursini, M.V. (2010). Functional characterization of Wiskott-Aldrich syndrome protein and scar homolog (WASH), a bi-modular nucleation-promoting factor able to interact with biogenesis of lysosome-related organelle subunit 2 (BLOS2) and gamma-tubulin. The Journal of biological chemistry *285*, 16951-16957.

Morgan, N.V., Pasha, S., Johnson, C.A., Ainsworth, J.R., Eady, R.A., Dawood, B., McKeown, C., Trembath, R.C., Wilde, J., Watson, S.P., *et al*. (2006). A germline mutation in BLOC1S3/reduced pigmentation causes a novel variant of Hermansky-Pudlak syndrome (HPS8). American journal of human genetics *78*, 160-166.

Mori, T., Li, Y., Hata, H., and Kochi, H. (2004). NIRF is a ubiquitin ligase that is capable of ubiquitinating PCNP, a PEST-containing nuclear protein. FEBS letters *557*, 209-214.

Morita, E., Sandrin, V., McCullough, J., Katsuyama, A., Baci Hamilton, I., and Sundquist, W.I. (2011). ESCRT-III protein requirements for HIV-1 budding. Cell host & microbe *9*, 235-242.

Mosca, J.D., Chang, Y.N., and Williams, G. (2007). Antigen-presenting particle technology using inactivated surface-engineered viruses: induction of immune responses against infectious agents. Retrovirology *4*, 32.

Mukerji, J., Olivieri, K.C., Misra, V., Agopian, K.A., and Gabuzda, D. (2012). Proteomic analysis of HIV-1 Nef cellular binding partners reveals a role for exocyst complex proteins in mediating enhancement of intercellular nanotube formation. Retrovirology *9*, 33.

Mullin, A.P., Gokhale, A., Larimore, J., and Faundez, V. (2011). Cell biology of the BLOC-1 complex subunit dysbindin, a schizophrenia susceptibility gene. Molecular neurobiology *44*, 53-64.

Mumby, M., and Brekken, D. (2005). Phosphoproteomics: new insights into cellular signaling. Genome biology *6*, 230.

Munk, C., Sommer, A.F., and Konig, R. (2011). Systems-biology approaches to discover anti-viral effectors of the human innate immune response. Viruses *3*, 1112-1130.

Murai-Takebe, R., Noguchi, T., Ogura, T., Mikami, T., Yanagi, K., Inagaki, K., Ohnishi, H., Matozaki, T., and Kasuga, M. (2004). Ubiquitination-mediated regulation of biosynthesis of the adhesion receptor SHPS-1 in response to endoplasmic reticulum stress. The Journal of biological chemistry *279*, 11616-11625.

Nagaraja, T., Anand, A.R., Zhao, H., and Ganju, R.K. (2012). The adaptor protein SLP-76 regulates HIV-1 release and cell-to-cell transmission in T cells. Journal of immunology *188*, 2769-2777.

Naghavi, M.H., and Goff, S.P. (2007). Retroviral proteins that interact with the host cell cytoskeleton. Current opinion in immunology *19*, 402-407.

Naik, S.H., Proietto, A.I., Wilson, N.S., Dakic, A., Schnorrer, P., Fuchsberger, M., Lahoud, M.H., O'Keeffe, M., Shao, Q.X., Chen, W.F., *et al*. (2005). Cutting edge: generation of splenic CD8+ and CD8- dendritic cell equivalents in Fms-like tyrosine kinase 3 ligand bone marrow cultures. Journal of immunology *174*, 6592-6597.

Nakaishi, A., Hirose, M., Yoshimura, M., Oneyama, C., Saito, K., Kuki, N., Matsuda, M., Honma, N., Ohnishi, H., Matozaki, T., *et al*. (2008). Structural insight into the specific interaction between murine SHPS-1/SIRP alpha and its ligand CD47. Journal of molecular biology *375*, 650-660.

Nakatogawa, H., Ichimura, Y., and Ohsumi, Y. (2007). Atg8, a ubiquitin-like protein required for autophagosome formation, mediates membrane tethering and hemifusion. Cell *130*, 165-178.

Nakayama, K., Takahashi, K., Shultz, L.D., Miyakawa, K., and Tomita, K. (1997). Abnormal development and differentiation of macrophages and dendritic cells in viable motheaten mutant mice deficient in haematopoietic cell phosphatase. International journal of experimental pathology *78*, 245-257.

Naldini, L., Blomer, U., Gallay, P., Ory, D., Mulligan, R., Gage, F.H., Verma, I.M., and Trono, D. (1996). In vivo gene delivery and stable transduction of nondividing cells by a lentiviral vector. Science *272*, 263-267.

Narita, M., Young, A.R., Arakawa, S., Samarajiwa, S.A., Nakashima, T., Yoshida, S., Hong, S., Berry, L.S., Reichelt, S., Ferreira, M., *et al*. (2011). Spatial coupling of mTOR and autophagy augments secretory phenotypes. Science *332*, 966-970.

Navare, A.T., Sova, P., Purdy, D.E., Weiss, J.M., Wolf-Yadlin, A., Korth, M.J., Chang, S.T., Proll, S.C., Jahan, T.A., Krasnoselsky, A.L., *et al*. (2012). Quantitative proteomic analysis of HIV-1 infected CD4+ T cells reveals an early host response in important biological pathways: protein synthesis, cell proliferation, and T-cell activation. Virology *429*, 37-46.

Nesvizhskii, A.I., Keller, A., Kolker, E., and Aebersold, R. (2003). A statistical model for identifying proteins by tandem mass spectrometry. Analytical chemistry *75*, 4646-4658.

Newell-Litwa, K., Salazar, G., Smith, Y., and Faundez, V. (2009). Roles of BLOC-1 and adaptor protein-3 complexes in cargo sorting to synaptic vesicles. Molecular biology of the cell *20*, 1441-1453.

Nolz, J.C., Medeiros, R.B., Mitchell, J.S., Zhu, P., Freedman, B.D., Shimizu, Y., and Billadeau, D.D. (2007). WAVE2 regulates high-affinity integrin binding by recruiting vinculin and talin to the immunological synapse. Molecular and cellular biology *27*, 5986-6000.

O'Neill, L.A. (2008). 'Fine tuning' TLR signaling. Nature immunology *9*, 459-461.

Oldenborg, P.A., Zheleznyak, A., Fang, Y.F., Lagenaur, C.F., Gresham, H.D., and Lindberg, F.P. (2000). Role of CD47 as a marker of self on red blood cells. Science *288*, 2051-2054.

Olinger, G.G., Saifuddin, M., Hart, M.L., and Spear, G.T. (2002). Cellular factors influence the binding of HIV type 1 to cells. AIDS research and human retroviruses *18*, 259-267.

Olsen, J.V., Blagoev, B., Gnad, F., Macek, B., Kumar, C., Mortensen, P., and Mann, M. (2006). Global, in vivo, and site-specific phosphorylation dynamics in signaling networks. Cell *127*, 635-648.

Olsen, J.V., Schwartz, J.C., Griep-Raming, J., Nielsen, M.L., Damoc, E., Denisov, E., Lange, O., Remes, P., Taylor, D., Splendore, M., *et al*. (2009). A dual pressure linear ion trap Orbitrap instrument with very high sequencing speed. Molecular & cellular proteomics : MCP *8*, 2759-2769.

Ott, D.E. (2002). Potential roles of cellular proteins in HIV-1. Reviews in medical virology *12*, 359-374.

Paling, N.R., and Welham, M.J. (2005). Tyrosine phosphatase SHP-1 acts at different stages of development to regulate hematopoiesis. Blood *105*, 4290-4297.

Palmowski, M.J., Lopes, L., Ikeda, Y., Salio, M., Cerundolo, V., and Collins, M.K. (2004). Intravenous injection of a lentiviral vector encoding NY-ESO-1 induces an effective CTL response. Journal of immunology *172*, 1582-1587.

Pan, P.Y., Tian, J.H., and Sheng, Z.H. (2009). Snapin facilitates the synchronization of synaptic vesicle fusion. Neuron *61*, 412-424.

Paquette, J.S., Fortin, J.F., Blanchard, L., and Tremblay, M.J. (1998). Level of ICAM-1 surface expression on virus producer cells influences both the amount of virion-bound host ICAM-1 and human immunodeficiency virus type 1 infectivity. Journal of virology *72*, 9329-9336.

Pashov, A., Garimalla, S., Monzavi-Karbassi, B., and Kieber-Emmons, T. (2009). Carbohydrate targets in HIV vaccine research: lessons from failures. Immunotherapy *1*, 777-794.

Perez-Villar, J.J., Whitney, G.S., Bowen, M.A., Hewgill, D.H., Aruffo, A.A., and Kanner, S.B. (1999). CD5 negatively regulates the T-cell antigen receptor signal transduction pathway: involvement of SH2-containing phosphotyrosine phosphatase SHP-1. Molecular and cellular biology *19*, 2903-2912.

Petit, M.M., Fradelizi, J., Golsteyn, R.M., Ayoubi, T.A., Menichi, B., Louvard, D., Van de Ven, W.J., and Friederich, E. (2000). LPP, an actin cytoskeleton protein related to zyxin, harbors a nuclear export signal and transcriptional activation capacity. Molecular biology of the cell *11*, 117-129.

Petroski, M.D., and Deshaies, R.J. (2005). Function and regulation of cullin-RING ubiquitin ligases. Nature reviews Molecular cell biology *6*, 9-20.

Pfirsch-Maisonnas, S., Aloulou, M., Xu, T., Claver, J., Kanamaru, Y., Tiwari, M., Launay, P., Monteiro, R.C., and Blank, U. (2011). Inhibitory ITAM signaling traps activating receptors with the phosphatase SHP-1 to form polarized "inhibisome" clusters. Science signaling *4*, ra24.

Piguet, V., and Blauvelt, A. (2002). Essential roles for dendritic cells in the pathogenesis and potential treatment of HIV disease. The Journal of investigative dermatology *119*, 365-369.

Piguet, V., and Steinman, R.M. (2007). The interaction of HIV with dendritic cells: outcomes and pathways. Trends in immunology *28*, 503-510.

Plas, D.R., Johnson, R., Pingel, J.T., Matthews, R.J., Dalton, M., Roy, G., Chan, A.C., and Thomas, M.L. (1996). Direct regulation of ZAP-70 by SHP-1 in T cell antigen receptor signaling. Science *272*, 1173-1176.

Plas, D.R., Williams, C.B., Kersh, G.J., White, L.S., White, J.M., Paust, S., Ulyanova, T., Allen, P.M., and Thomas, M.L. (1999). Cutting edge: the tyrosine phosphatase SHP-1 regulates thymocyte positive selection. Journal of immunology *162*, 5680-5684.

Pontillo, A., Silva, L.T., Oshiro, T.M., Finazzo, C., Crovella, S., and Duarte, A.J. (2012). HIV-1 induces NALP3-inflammasome expression and interleukin-1beta secretion in dendritic cells from healthy individuals but not from HIV-positive patients. AIDS *26*, 11-18.

Poole, A.W., and Jones, M.L. (2005). A SHPing tale: perspectives on the regulation of SHP-1 and SHP-2 tyrosine phosphatases by the C-terminal tail. Cellular signalling *17*, 1323-1332.

Popik, W., Alce, T.M., and Au, W.C. (2002). Human immunodeficiency virus type 1 uses lipid raft-colocalized CD4 and chemokine receptors for productive entry into CD4(+) T cells. Journal of virology *76*, 4709-4722.

Ptak, R.G., Fu, W., Sanders-Beer, B.E., Dickerson, J.E., Pinney, J.W., Robertson, D.L., Rozanov, M.N., Katz, K.S., Maglott, D.R., Pruitt, K.D., *et al.* (2008). Cataloguing the HIV type 1 human protein interaction network. AIDS research and human retroviruses *24*, 1497-1502.

Ramachandran, I.R., Song, W., Lapteva, N., Seethammagari, M., Slawin, K.M., Spencer, D.M., and Levitt, J.M. (2011). The phosphatase SRC homology region 2 domain-containing phosphatase-1 is an intrinsic central regulator of dendritic cell function. Journal of immunology *186*, 3934-3945.

Raman, D., Sai, J., Neel, N.F., Chew, C.S., and Richmond, A. (2010). LIM and SH3 protein-1 modulates CXCR2-mediated cell migration. PloS one *5*, e10050.

Ramanathan, H.N., and Ye, Y. (2012). The p97 ATPase associates with EEA1 to regulate the size of early endosomes. Cell research *22*, 346-359.

Raposo, G., and Marks, M.S. (2007). Melanosomes--dark organelles enlighten endosomal membrane transport. Nature reviews Molecular cell biology *8*, 786-797.

Rebres, R.A., Vaz, L.E., Green, J.M., and Brown, E.J. (2001). Normal ligand binding and signaling by CD47 (integrin-associated protein) requires a long range disulfide bond between

the extracellular and membrane-spanning domains. The Journal of biological chemistry *276*, 34607-34616.

Ringrose, J.H., Jeeninga, R.E., Berkhout, B., and Speijer, D. (2008). Proteomic studies reveal coordinated changes in T-cell expression patterns upon infection with human immunodeficiency virus type 1. Journal of virology *82*, 4320-4330.

Ritz, D., Vuk, M., Kirchner, P., Bug, M., Schutz, S., Hayer, A., Bremer, S., Lusk, C., Baloh, R.H., Lee, H., *et al*. (2011). Endolysosomal sorting of ubiquitylated caveolin-1 is regulated by VCP and UBXD1 and impaired by VCP disease mutations. Nature cell biology *13*, 1116-1123.

Saito, Y., Iwamura, H., Kaneko, T., Ohnishi, H., Murata, Y., Okazawa, H., Kanazawa, Y., Sato-Hashimoto, M., Kobayashi, H., Oldenborg, P.A., *et al*. (2010). Regulation by SIRPalpha of dendritic cell homeostasis in lymphoid tissues. Blood *116*, 3517-3525.

Saitoh, T., Fujita, N., Jang, M.H., Uematsu, S., Yang, B.G., Satoh, T., Omori, H., Noda, T., Yamamoto, N., Komatsu, M., *et al*. (2008). Loss of the autophagy protein Atg16L1 enhances endotoxin-induced IL-1beta production. Nature *456*, 264-268.

Saitoh, T., Fujita, N., Yoshimori, T., and Akira, S. (2010). Regulation of dsDNA-induced innate immune responses by membrane trafficking. Autophagy *6*, 430-432.

Sancak, Y., Bar-Peled, L., Zoncu, R., Markhard, A.L., Nada, S., and Sabatini, D.M. (2010). Ragulator-Rag complex targets mTORC1 to the lysosomal surface and is necessary for its activation by amino acids. Cell *141*, 290-303.

Sancak, Y., Peterson, T.R., Shaul, Y.D., Lindquist, R.A., Thoreen, C.C., Bar-Peled, L., and Sabatini, D.M. (2008). The Rag GTPases bind raptor and mediate amino acid signaling to mTORC1. Science *320*, 1496-1501.

Santos, S., Obukhov, Y., Nekhai, S., Bukrinsky, M., and Iordanskiy, S. (2012). Virus-producing cells determine the host protein profiles of HIV-1 virion cores. Retrovirology *9*, 65.

Saphire, A.C., Gallay, P.A., and Bark, S.J. (2006). Proteomic analysis of human immunodeficiency virus using liquid chromatography/tandem mass spectrometry effectively distinguishes specific incorporated host proteins. Journal of proteome research *5*, 530-538.

Sarfati, M., Fortin, G., Raymond, M., and Susin, S. (2008). CD47 in the immune response: role of thrombospondin and SIRP-alpha reverse signaling. Current drug targets *9*, 842-850.

Sasai, M., Linehan, M.M., and Iwasaki, A. (2010). Bifurcation of Toll-like receptor 9 signaling by adaptor protein 3. Science *329*, 1530-1534.

Savina, A., Jancic, C., Hugues, S., Guermonprez, P., Vargas, P., Moura, I.C., Lennon-Dumenil, A.M., Seabra, M.C., Raposo, G., and Amigorena, S. (2006). NOX2 controls phagosomal pH to regulate antigen processing during crosspresentation by dendritic cells. Cell *126*, 205-218.

Scanlan, C.N., Offer, J., Zitzmann, N., and Dwek, R.A. (2007). Exploiting the defensive sugars of HIV-1 for drug and vaccine design. Nature *446*, 1038-1045.

Schaeffer-Reiss, C. (2008). A brief summary of the different types of mass spectrometers used in proteomics. Methods in molecular biology *484*, 3-16.

Schelhaas, M. (2010). Come in and take your coat off - how host cells provide endocytosis for virus entry. Cellular microbiology *12*, 1378-1388.

Scott, C.L., Aumeunier, A.M., and Mowat, A.M. (2011). Intestinal CD103+ dendritic cells: master regulators of tolerance? Trends in immunology *32*, 412-419.

Shaw, M.L., Stone, K.L., Colangelo, C.M., Gulcicek, E.E., and Palese, P. (2008). Cellular proteins in influenza virus particles. PLoS pathogens *4*, e1000085.

Shevchenko, A., Wilm, M., Vorm, O., and Mann, M. (1996). Mass spectrometric sequencing of proteins silver-stained polyacrylamide gels. Analytical chemistry *68*, 850-858.

Shi, B., Huang, Q., Tak, P.P., Vervoordeldonk, M.J., Huang, C.C., Dorfleutner, A., Stehlik, C., and Pope, R.M. (2012). SNAPIN: an endogenous Toll-like receptor ligand in rheumatoid arthritis. Annals of the rheumatic diseases *71*, 1411-1417.

Shio, M.T., Hassani, K., Isnard, A., Ralph, B., Contreras, I., Gomez, M.A., Abu-Dayyeh, I., and Olivier, M. (2012). Host cell signalling and leishmania mechanisms of evasion. Journal of tropical medicine *2012*, 819512.

Shirasaki, T., Honda, M., Mizuno, H., Shimakami, T., Okada, H., Sakai, Y., Murakami, S., Wakita, T., and Kaneko, S. (2010). La protein required for internal ribosome entry site-directed translation is a potential therapeutic target for hepatitis C virus replication. The Journal of infectious diseases *202*, 75-85.

Shultz, L.D., and Green, M.C. (1976). Motheaten, an immunodeficient mutant of the mouse. II. Depressed immune competence and elevated serum immunoglobulins. Journal of immunology *116*, 936-943.

Simoneau, M., Coulombe, G., Vandal, G., Vezina, A., and Rivard, N. (2011). SHP-1 inhibits beta-catenin function by inducing its degradation and interfering with its association with TATA-binding protein. Cellular signalling *23*, 269-279.

Smith, A.J., Li, Q., Wietgrefe, S.W., Schacker, T.W., Reilly, C.S., and Haase, A.T. (2010). Host genes associated with HIV-1 replication in lymphatic tissue. Journal of immunology *185*, 5417-5424.

Snyder, D.A., Kelly, M.L., and Woodbury, D.J. (2006). SNARE complex regulation by phosphorylation. Cell biochemistry and biophysics *45*, 111-123.

Solis, M., Wilkinson, P., Romieu, R., Hernandez, E., Wainberg, M.A., and Hiscott, J. (2006). Gene expression profiling of the host response to HIV-1 B, C, or A/E infection in monocyte-derived dendritic cells. Virology *352*, 86-99.

Sowa, M.E., Bennett, E.J., Gygi, S.P., and Harper, J.W. (2009). Defining the human deubiquitinating enzyme interaction landscape. Cell *138*, 389-403.

Spaargaren, M. (2011). Lymphoma spread? Target CD47-SIRPalpha! Blood *118*, 4762-4764.

Spurgers, K.B., Alefantis, T., Peyser, B.D., Ruthel, G.T., Bergeron, A.A., Costantino, J.A., Enterlein, S., Kota, K.P., Boltz, R.C., Aman, M.J., *et al.* (2010). Identification of essential filovirion-associated host factors by serial proteomic analysis and RNAi screen. Molecular & cellular proteomics : MCP *9*, 2690-2703.

Spurrell, D.R., Luckashenak, N.A., Minney, D.C., Chaplin, A., Penninger, J.M., Liwski, R.S., Clements, J.L., and West, K.A. (2009). Vav1 regulates the migration and adhesion of dendritic cells. Journal of immunology *183*, 310-318.

Starcevic, M., and Dell'Angelica, E.C. (2004). Identification of snapin and three novel proteins (BLOS1, BLOS2, and BLOS3/reduced pigmentation) as subunits of biogenesis of lysosome-related organelles complex-1 (BLOC-1). The Journal of biological chemistry *279*, 28393-28401.

Stauber, R.H., Rulong, S., Palm, G., and Tarasova, N.I. (1999). Direct visualization of HIV-1 entry: mechanisms and role of cell surface receptors. Biochemical and biophysical research communications *258*, 695-702.

Stefanova, I., Hemmer, B., Vergelli, M., Martin, R., Biddison, W.E., and Germain, R.N. (2003). TCR ligand discrimination is enforced by competing ERK positive and SHP-1 negative feedback pathways. Nature immunology *4*, 248-254.

Stevens, R.J., and Littleton, J.T. (2011). Synaptic growth: dancing with adducin. Current biology : CB *21*, R402-405.

Stolp, B., and Fackler, O.T. (2011). How HIV takes advantage of the cytoskeleton in entry and replication. Viruses *3*, 293-311.

Stuchell-Brereton, M.D., Skalicky, J.J., Kieffer, C., Karren, M.A., Ghaffarian, S., and Sundquist, W.I. (2007). ESCRT-III recognition by VPS4 ATPases. Nature *449*, 740-744.

Takahara, T., and Maeda, T. (2012). Transient sequestration of TORC1 into stress granules during heat stress. Molecular cell *47*, 242-252.

Takahashi, K., Shibata, T., Akashi-Takamura, S., Kiyokawa, T., Wakabayashi, Y., Tanimura, N., Kobayashi, T., Matsumoto, F., Fukui, R., Kouro, T., *et al*. (2007). A protein associated with Toll-like receptor (TLR) 4 (PRAT4A) is required for TLR-dependent immune responses. The Journal of experimental medicine *204*, 2963-2976.

Takenaka, K., Prasolava, T.K., Wang, J.C., Mortin-Toth, S.M., Khalouei, S., Gan, O.I., Dick, J.E., and Danska, J.S. (2007). Polymorphism in Sirpa modulates engraftment of human hematopoietic stem cells. Nature immunology *8*, 1313-1323.

Talbot, K., Cho, D.S., Ong, W.Y., Benson, M.A., Han, L.Y., Kazi, H.A., Kamins, J., Hahn, C.G., Blake, D.J., and Arnold, S.E. (2006). Dysbindin-1 is a synaptic and microtubular protein that binds brain snapin. Human molecular genetics *15*, 3041-3054.

Tamir, I., Dal Porto, J.M., and Cambier, J.C. (2000). Cytoplasmic protein tyrosine phosphatases SHP-1 and SHP-2: regulators of B cell signal transduction. Current opinion in immunology *12*, 307-315.

Tayyari, F., Marchant, D., Moraes, T.J., Duan, W., Mastrangelo, P., and Hegele, R.G. (2011). Identification of nucleolin as a cellular receptor for human respiratory syncytial virus. Nature medicine *17*, 1132-1135.

Thakur, P., Stevens, D.R., Sheng, Z.H., and Rettig, J. (2004). Effects of PKA-mediated phosphorylation of Snapin on synaptic transmission in cultured hippocampal neurons. The Journal of neuroscience : the official journal of the Society for Neuroscience *24*, 6476-6481.

Thali, M., Bukovsky, A., Kondo, E., Rosenwirth, B., Walsh, C.T., Sodroski, J., and Gottlinger, H.G. (1994). Functional association of cyclophilin A with HIV-1 virions. Nature *372*, 363-365.

Thomas, M.G., Loschi, M., Desbats, M.A., and Boccaccio, G.L. (2011). RNA granules: the good, the bad and the ugly. Cellular signalling *23*, 324-334.

Tresse, E., Salomons, F.A., Vesa, J., Bott, L.C., Kimonis, V., Yao, T.P., Dantuma, N.P., and Taylor, J.P. (2010). VCP/p97 is essential for maturation of ubiquitin-containing autophagosomes and this function is impaired by mutations that cause IBMPFD. Autophagy *6*, 217-227.

Trudgian, D.C., Ridlova, G., Fischer, R., Mackeen, M.M., Ternette, N., Acuto, O., Kessler, B.M., and Thomas, B. (2011). Comparative evaluation of label-free SINQ normalized spectral index quantitation in the central proteomics facilities pipeline. Proteomics *11*, 2790-2797.

Trudgian, D.C., Thomas, B., McGowan, S.J., Kessler, B.M., Salek, M., and Acuto, O. CPFP: a central proteomics facilities pipeline. Bioinformatics *26*, 1131-1132.

Trudgian, D.C., Thomas, B., McGowan, S.J., Kessler, B.M., Salek, M., and Acuto, O. (2010). CPFP: a central proteomics facilities pipeline. Bioinformatics *26*, 1131-1132.

Tsai, N.P., Tsui, Y.C., and Wei, L.N. (2009). Dynein motor contributes to stress granule dynamics in primary neurons. Neuroscience *159*, 647-656.

Tsuda, M., Matozaki, T., Fukunaga, K., Fujioka, Y., Imamoto, A., Noguchi, T., Takada, T., Yamao, T., Takeda, H., Ochi, F., *et al*. (1998). Integrin-mediated tyrosine phosphorylation of SHPS-1 and its association with SHP-2. Roles of Fak and Src family kinases. The Journal of biological chemistry *273*, 13223-13229.

Tsui, F.W., Martin, A., Wang, J., and Tsui, H.W. (2006). Investigations into the regulation and function of the SH2 domain-containing protein-tyrosine phosphatase, SHP-1. Immunologic research *35*, 127-136.

Turville, S.G., Santos, J.J., Frank, I., Cameron, P.U., Wilkinson, J., Miranda-Saksena, M., Dable, J., Stossel, H., Romani, N., Piatak, M., Jr., *et al*. (2004). Immunodeficiency virus uptake, turnover, and 2-phase transfer in human dendritic cells. Blood *103*, 2170-2179.

Uchida, T., Matozaki, T., Noguchi, T., Yamao, T., Horita, K., Suzuki, T., Fujioka, Y., Sakamoto, C., and Kasuga, M. (1994). Insulin stimulates the phosphorylation of Tyr538 and the catalytic activity of PTP1C, a protein tyrosine phosphatase with Src homology-2 domains. The Journal of biological chemistry *269*, 12220-12228.

Uematsu, S., Sato, S., Yamamoto, M., Hirotani, T., Kato, H., Takeshita, F., Matsuda, M., Coban, C., Ishii, K.J., Kawai, T., *et al*. (2005). Interleukin-1 receptor-associated kinase-1 plays an essential role for Toll-like receptor (TLR)7- and TLR9-mediated interferon-{alpha} induction. The Journal of experimental medicine *201*, 915-923.

Uno, S., Kinoshita, Y., Azuma, Y., Tsunenari, T., Yoshimura, Y., Iida, S., Kikuchi, Y., Yamada-Okabe, H., and Fukushima, N. (2007). Antitumor activity of a monoclonal antibody against CD47 in xenograft models of human leukemia. Oncology reports *17*, 1189-1194.

Vaggi, F., Disanza, A., Milanesi, F., Di Fiore, P.P., Menna, E., Matteoli, M., Gov, N.S., Scita, G., and Ciliberto, A. (2011). The Eps8/IRSp53/VASP network differentially controls actin capping and bundling in filopodia formation. PLoS computational biology *7*, e1002088.

van 't Wout, A.B., Lehrman, G.K., Mikheeva, S.A., O'Keeffe, G.C., Katze, M.G., Bumgarner, R.E., Geiss, G.K., and Mullins, J.I. (2003). Cellular gene expression upon human immunodeficiency virus type 1 infection of CD4(+)-T-cell lines. Journal of virology *77*, 1392-1402.

Van den Broeke, C., Radu, M., Chernoff, J., and Favoreel, H.W. (2010). An emerging role for p21-activated kinases (Paks) in viral infections. Trends in cell biology *20*, 160-169.

von Holleben, M., Gohla, A., Janssen, K.P., Iritani, B.M., and Beer-Hammer, S. (2011). Immunoinhibitory adapter protein Src homology domain 3 lymphocyte protein 2 (SLy2) regulates actin dynamics and B cell spreading. The Journal of biological chemistry *286*, 13489-13501.

Wakabayashi, Y., Kobayashi, M., Akashi-Takamura, S., Tanimura, N., Konno, K., Takahashi, K., Ishii, T., Mizutani, T., Iba, H., Kouro, T., *et al*. (2006). A protein associated with toll-like receptor 4 (PRAT4A) regulates cell surface expression of TLR4. Journal of immunology *177*, 1772-1779.

Walter, R.B., Raden, B.W., Zeng, R., Hausermann, P., Bernstein, I.D., and Cooper, J.A. (2008). ITIM-dependent endocytosis of CD33-related Siglecs: role of intracellular domain, tyrosine phosphorylation, and the tyrosine phosphatases, Shp1 and Shp2. Journal of leukocyte biology *83*, 200-211.

Wang, N., Dong, Q., Li, J., Jangra, R.K., Fan, M., Brasier, A.R., Lemon, S.M., Pfeffer, L.M., and Li, K. (2010a). Viral induction of the zinc finger antiviral protein is IRF3-dependent but NF-kappaB-independent. The Journal of biological chemistry *285*, 6080-6090.

Wang, T., Liu, N.S., Seet, L.F., and Hong, W. (2010b). The emerging role of VHS domain-containing Tom1, Tom1L1 and Tom1L2 in membrane trafficking. Traffic *11*, 1119-1128.

Watson, R.O., Manzanillo, P.S., and Cox, J.S. (2012). Extracellular M. tuberculosis DNA Targets Bacteria for Autophagy by Activating the Host DNA-Sensing Pathway. Cell *150*, 803-815.

Wei, M.L. (2006). Hermansky-Pudlak syndrome: a disease of protein trafficking and organelle function. Pigment cell research / sponsored by the European Society for Pigment Cell Research and the International Pigment Cell Society *19*, 19-42.

Weidberg, H., Shvets, E., Shpilka, T., Shimron, F., Shinder, V., and Elazar, Z. (2010). LC3 and GATE-16/GABARAP subfamilies are both essential yet act differently in autophagosome biogenesis. The EMBO journal *29*, 1792-1802.

Wilm, M. (2011). Principles of electrospray ionization. Molecular & cellular proteomics : MCP.

Worby, C.A., and Dixon, J.E. (2002). Sorting out the cellular functions of sorting nexins. Nature reviews Molecular cell biology *3*, 919-931.

Wu, J., Lu, L.Y., and Yu, X. (2010). The role of BRCA1 in DNA damage response. Protein & cell *1*, 117-123.

Xie, R., Wang, F., McKeehan, W.L., and Liu, L. (2011). Autophagy enhanced by microtubule- and mitochondrion-associated MAP1S suppresses genome instability and hepatocarcinogenesis. Cancer research *71*, 7537-7546.

Xu, Y., Liu, Y., Ridgway, N.D., and McMaster, C.R. (2001). Novel members of the human oxysterol-binding protein family bind phospholipids and regulate vesicle transport. The Journal of biological chemistry *276*, 18407-18414.

Yamaguchi, H., Shiraishi, M., Fukami, K., Tanabe, A., Ikeda-Matsuo, Y., Naito, Y., and Sasaki, Y. (2009). MARCKS regulates lamellipodia formation induced by IGF-I via association with PIP2 and beta-actin at membrane microdomains. Journal of cellular physiology *220*, 748-755.

Yan, G., Lai, Y., and Jiang, Y. (2012). The TOR complex 1 is a direct target of Rho1 GTPase. Molecular cell *45*, 743-753.

Yan, N., and Lieberman, J. (2011). Gaining a foothold: how HIV avoids innate immune recognition. Current opinion in immunology *23*, 21-28.

Yan, N., Regalado-Magdos, A.D., Stiggelbout, B., Lee-Kirsch, M.A., and Lieberman, J. (2010). The cytosolic exonuclease TREX1 inhibits the innate immune response to human immunodeficiency virus type 1. Nature immunology *11*, 1005-1013.

Yang, J., Liu, L., He, D., Song, X., Liang, X., Zhao, Z.J., and Zhou, G.W. (2003). Crystal structure of human protein-tyrosine phosphatase SHP-1. The Journal of biological chemistry *278*, 6516-6520.

Yang, P., An, H., Liu, X., Wen, M., Zheng, Y., Rui, Y., and Cao, X. (2010). The cytosolic nucleic acid sensor LRRFIP1 mediates the production of type I interferon via a beta-catenin-dependent pathway. Nature immunology *11*, 487-494.

Yates, J.R., Ruse, C.I., and Nakorchevsky, A. (2009). Proteomics by mass spectrometry: approaches, advances, and applications. Annual review of biomedical engineering *11*, 49-79.

Yi, Z., Pan, T., Wu, X., Song, W., Wang, S., Xu, Y., Rice, C.M., Macdonald, M.R., and Yuan, Z. (2011). Hepatitis C virus co-opts Ras-GTPase-activating protein-binding protein 1 for its genome replication. Journal of virology *85*, 6996-7004.

You, M., and Zhao, Z. (1997). Positive effects of SH2 domain-containing tyrosine phosphatase SHP-1 on epidermal growth factor- and interferon-gamma-stimulated activation of STAT transcription factors in HeLa cells. The Journal of biological chemistry *272*, 23376-23381.

Yu, C.C., Tsui, H.W., Ngan, B.Y., Shulman, M.J., Wu, G.E., and Tsui, F.W. (1996). B and T cells are not required for the viable motheaten phenotype. The Journal of experimental medicine *183*, 371-380.

Yu, Y., Yoon, S.O., Poulogiannis, G., Yang, Q., Ma, X.M., Villen, J., Kubica, N., Hoffman, G.R., Cantley, L.C., Gygi, S.P., *et al*. (2011). Phosphoproteomic analysis identifies Grb10 as an mTORC1 substrate that negatively regulates insulin signaling. Science *332*, 1322-1326.

Yuzaki, M. (2010). Snapin snaps into the dynein complex for late endosome-lysosome trafficking and autophagy. Neuron *68*, 4-6.

Zhang, J., Somani, A.K., and Siminovitch, K.A. (2000). Roles of the SHP-1 tyrosine phosphatase in the negative regulation of cell signalling. Seminars in immunology *12*, 361-378.

Zhang, L., Zhang, X., Ma, Q., and Zhou, H. (2010). Host proteome research in HIV infection. Genomics, proteomics & bioinformatics *8*, 1-9.

Zhang, Z., Shen, K., Lu, W., and Cole, P.A. (2003). The role of C-terminal tyrosine phosphorylation in the regulation of SHP-1 explored via expressed protein ligation. The Journal of biological chemistry *278*, 4668-4674.

Zhou, H., Xu, M., Huang, Q., Gates, A.T., Zhang, X.D., Castle, J.C., Stec, E., Ferrer, M., Strulovici, B., Hazuda, D.J., *et al*. (2008). Genome-scale RNAi screen for host factors required for HIV replication. Cell host & microbe *4*, 495-504.

Zhu, P., Liu, J., Bess, J., Jr., Chertova, E., Lifson, J.D., Grise, H., Ofek, G.A., Taylor, K.A., and Roux, K.H. (2006). Distribution and three-dimensional structure of AIDS virus envelope spikes. Nature *441*, 847-852.

Zhu, Y., Chen, G., Lv, F., Wang, X., Ji, X., Xu, Y., Sun, J., Wu, L., Zheng, Y.T., and Gao, G. (2011). Zinc-finger antiviral protein inhibits HIV-1 infection by selectively targeting multiply spliced viral mRNAs for degradation. Proceedings of the National Academy of Sciences of the United States of America *108*, 15834-15839.

Zoncu, R., Efeyan, A., and Sabatini, D.M. (2011). mTOR: from growth signal integration to cancer, diabetes and ageing. Nature reviews Molecular cell biology *12*, 21-35.

Zoncu, R., and Sabatini, D.M. (2011). Cell biology. The TASCC of secretion. Science *332*, 923-925.

Zufferey, R., Nagy, D., Mandel, R.J., Naldini, L., and Trono, D. (1997). Multiply attenuated lentiviral vector achieves efficient gene delivery in vivo. Nature biotechnology *15*, 871-875.

Appendix

Preliminary data obtained from LC-MS/MS and CPFP analysis of DCs infected with HIV-1 or mock.

Table A1

Proteins exclusively phosphorylated following HIV-1 infection	SwissProt Number	Number peptide matches
Heat shock protein HSP 90-alpha	P07900	11
60S acidic ribosomal protein P0	P05388	9
Casein kinase II subunit alpha	P68400	8
Septin-7	Q16181	8
60S acidic ribosomal protein P1	P05387	7
Acidic leucine-rich nuclear phosphoprotein 32 family member A	P39687	7
Neuroblast differentiation-associated protein AHNAK	Q09666	6
Proliferation-associated protein 2G4	Q9UQ80	6
Proteasome subunit beta type-2	P49721	6
Tubulin beta-6 chain	Q9BUF5	6
Lamin-A/C	P02545	5
Stress-induced-phosphoprotein 1	P31948	5
Zyxin	Q15942	5
14-3-3 protein zeta/delta	P63104	4
Cytosolic purine 5'-nucleotidase	P49902	4
Eukaryotic translation initiation factor 2 subunit 2-like protein	P20042	4
Hematopoietic lineage cell-specific protein	P14317	4
Heterogeneous nuclear ribonucleoprotein U-like protein 2	Q1KMD3	4
HLA class II histocompatibility antigen, DR alpha chain	P01903	4
LIM and SH3 domain protein 1	Q14847	4
Plasminogen activator inhibitor 1 RNA-binding protein	Q8NC51	4
Pyruvate dehydrogenase E1 component subunit beta	P11177	4
Serum albumin	P02769	4
Splicing factor 1	Q15637	4
Synapse-associated protein 1	Q96A49	4
Tubulin alpha-4A chain	P68366	4
AMP deaminase 2	Q01433	3
Calumenin	O35783	3
cAMP-dependent protein kinase catalytic subunit alpha C-beta	P17612	3
Dihydropyrimidinase-related protein 2	Q16555	3
Eukaryotic translation initiation factor 4B (F2)	P23588	3
Histone H2A type 2-C	Q16777	3
Interferon regulatory factor 2-binding protein 2	Q7Z5L9	3
Proteasome activator complex subunit 1	Q06323	3
Putative adenosylhomocysteinase 2	O43865	3
Ras-related GTP-binding protein C	Q9HB90	3
Septin-6	Q14141	3
Serine/threonine-protein kinase PAK 2	Q13177	3
Splicing factor, arginine/serine-rich 1	Q07955	3
Transcription factor BTF3 homolog 4	Q96K17	3
Ubiquitin	P62988	3
14-3-3 protein epsilon	P62258	2
26S proteasome non-ATPase regulatory subunit 7	P51665	2
28 kDa heat- and acid-stable phosphoprotein	Q13442	2
5'-AMP-activated protein kinase subunit gamma-1	P54619	2
Acidic leucine-rich nuclear phosphoprotein 32 family member B	Q92688	2
Activated RNA polymerase II transcriptional coactivator p15	P53999	2
Aspartyl aminopeptidase	Q9ULA0	2
Bcl-2-like protein 13 (F1)	Q9BXK5	2
cAMP-dependent protein kinase type II-alpha regulatory subunit	P13861	2
Capz-interacting protein	Q6JBY9	2
Coatomer subunit epsilon	O14579	2
Coronin-1C	Q9ULV4	2
DnaJ homolog subfamily A member 1	P31689	2
Heterogeneous nuclear ribonucleoprotein C	P07910	2
Histone H2A.x	P16104	2
HLA class II histocompatibility antigen, DRB1-3 chain	P01912	2
Importin subunit alpha-3	O00505	2
Importin subunit alpha-4	O00629	2
Lipoma-preferred partner homolog	Q93052	2
Programmed cell death protein 10	Q9BUL8	2
Proteasome activator complex subunit 2	Q9UL46	2
Protein CutA	O60888	2

Proteins exclusively phosphorylated following HIV-1 infection	SwissProt Number	Number peptide matches
Protein NDRG2	Q9UN36	2
Ras GTPase-activating protein-binding protein 1	Q13283	2
Ras GTPase-activating protein-binding protein 2	Q9UN86	2
Ras-related GTP-binding protein A	Q7L523	2
Reticulon-4	Q9NQC3	2
Serine/threonine-protein kinase PAK 1	Q13153	2
Triosephosphate isomerase	P60174	2
Uncharacterized protein C22orf9	Q6ICG6	2
UPF0687 protein C20orf27	Q9GZN8	2
Wiskott-Aldrich syndrome protein family member 2	Q9Y6W5	2
14-3-3 protein beta/alpha	P31946	1
14-3-3 protein gamma	P61981	1
26S protease regulatory subunit 6A homolog B	P17980	1
26S proteasome non-ATPase regulatory subunit 9	O00233	1
A-kinase anchor protein 12	Q02952	1
Alpha-adducin	P35611	1
Annexin A2	P07355	1
AP-1 complex subunit beta-1	Q10567	1
ATP synthase subunit alpha, mitochondrial	P25705	1
Autophagy-related protein 7	O95352	1
Beta-arrestin-1	P49407	1
BRCA1-A complex subunit MERIT40	Q9NWV8	1
Breast carcinoma-amplified sequence 3	Q9H6U6	1
Calcium-regulated heat stable protein 1	Q9Y2V2	1
Calpain small subunit 1	P04632	1
Calpain-2 catalytic subunit	P17655	1
Calreticulin-3	Q9D9Q6	1
Charged multivesicular body protein 4b (F3)	Q9H444	1
Clathrin light chain A	P09496	1
Cyclin-K	O75909	1
Cytosol aminopeptidase	P28838	1
Dr1-associated corepressor	Q14919	1
Drebrin-like protein	Q9UJU6	1
Elongation factor Tu, mitochondrial	P49411	1
Eukaryotic translation initiation factor 2 subunit 1	P05198	1
Exportin-2	P55060	1
Filamin-A	P21333	1
Fructose-bisphosphate aldolase A	P04075	1
Gamma-adducin	Q9UEY8	1
Gamma-aminobutyric acid receptor-associated protein	O95166	1
Heterogeneous nuclear ribonucleoprotein A3	P51991	1
Heterogeneous nuclear ribonucleoprotein G	P38159	1
High mobility group nucleosome-binding domain-containing protein 3	Q15651	1
High mobility group protein B3	O15347	1
Histone deacetylase 2	Q92769	1
HLA class II histocompatibility antigen, DR-1 beta chain	P01914	1
Isocitrate dehydrogenase [NADP], mitochondrial	P48735	1
KH domain-containing, RNA-binding, signal transduction-associated protein	Q07666	1
LIM domain and actin-binding protein 1	Q9UHB6	1
Lys-63-specific deubiquitinase BRCC36	P46736	1
Methylosome protein 50	Q9BQA1	1
Microtubule-associated protein 1S	Q66K74	1
Myosin light chain 1/3, skeletal muscle isoform	P05976	1
Na(+)/H(+) exchange regulatory cofactor NHE-RF1	O14745	1
NAD kinase	O95544	1
Nascent polypeptide-associated complex subunit alpha-2	Q9H009	1
Nuclear receptor coactivator 5	Q9HCD5	1
Nucleobindin-1	Q02818	1
Nucleolin	P19338	1
Pantothenate kinase 2, mitochondrial	Q9BZ23	1
Peroxiredoxin-4	Q13162	1
Pallidin	Q9UL45	1
Peroxisomal biogenesis factor 19	P40855	1
PEST proteolytic signal-containing nuclear protein;	Q8WW12	1
Phosphoglycerate kinase 1	P00558	1
Phostensin	Q6NYC8	1
PRA1 family protein 3	O75915	1
Proactivator polypeptide	P07602	1
Proteasome subunit beta type-10	P40306	1
Proteasome subunit beta type-7	Q99436	1
Protein arginine N-methyltransferase 5	O14744	1
Protein canopy homolog 3 (F5)	Q9BT09	1

Proteins exclusively phosphorylated following HIV-1 infection	SwissProt Number	Number peptide matches
Protein cappuccino homolog	Q9NUP1	1
Protein numb homolog	P49757	1
Protein phosphatase 1F	P49593	1
Putative heat shock protein HSP 90-alpha A4	Q58FG1	1
Pyruvate dehydrogenase E1 component subunit beta, mitochondrial	Q09171	1
Quinone oxidoreductase	Q08257	1
Reticulocalbin-1	Q15293	1
Serine/threonine-protein kinase 24	Q9Y6E0	1
Small nuclear ribonucleoprotein Sm D1	P62314	1
Small nuclear ribonucleoprotein Sm D3	P62318	1
Stromal cell-derived factor 2-like protein 1	Q9HCN8	1
Target of Myb protein 1	O60784	1
Transcription factor Sp3	Q02447	1
Transcriptional activator protein Pur-alpha	Q00577	1
tRNA modification GTPase mnmE	Q39ZT0	1
U1 small nuclear ribonucleoprotein 70 kDa	P08621	1
UV excision repair protein RAD23 homolog A	P54725	1
Vinculin	P18206	1
Voltage-gated potassium channel subunit beta-2	Q13303	1
WD repeat-containing protein 82-B	Q6UXN9	1
Zinc finger protein 428	Q96B54	1

Table A2

Proteins exclusively dephosphorylated following HIV-1 infection	SwissProt Number	Number unique peptide matches
Heat shock protein HSP 90-alpha	P46633	14
Eukaryotic translation initiation factor 2 subunit 3	P41091	11
Probable ATP-dependent RNA helicase DDX17	Q92841	11
Protein disulfide-isomerase A4	Q29RV1	7
Ribonuclease inhibitor	P13489	6
Heat shock protein beta-1	P04792	5
Proteasome subunit alpha type-4	P25789	5
Histone H2A type 2-C	A1A4R1	4
Myosin-9	P35579	4
Cleavage and polyadenylation specificity factor subunit 5	O43809	3
Elongation factor 1-alpha 1	P68104	3
Hepatoma-derived growth factor	P51858	3
Septin-7	Q16181	3
Vacuolar protein sorting-associated protein 4B	O75351	3
40S ribosomal protein S6	P62753	2
Calnexin	P27824	2
Chaperone protein htpG	A0L8B0	2
Heat shock protein 105 kDa	Q92598	2
Heterogeneous nuclear ribonucleoproteins A2/B1	P22626	2
Hsc70-interacting protein	P50502	2
Myosin regulatory light chain 12B	O14950	2
Nascent polypeptide-associated complex subunit alpha, muscle-specific form	Q13765	2
Protein disulfide-isomerase A3	P30101	2
RNA-binding protein Raly	Q9UKM9	2
Septin-6	Q14141	2
Serine/threonine-protein phosphatase 6 regulatory ankyrin repeat subunit B	Q8N8A2	2
Tropomyosin alpha-3 chain	P06753	2
Tubulin beta-1 chain	P07436	2
Tyrosine-protein phosphatase non-receptor type 6	P29350	2
RAC-alpha serine/threonine-protein kinase	P31749	1
ATP synthase subunit beta, mitochondrial	P06576	1
Biogenesis of lysosome-related organelles complex 1 subunit 1	P78537	1
BRCA1-A complex subunit BRE	Q9NXR7	1
BRCA2 and CDKN1A-interacting protein	Q2NL37	1
Bridging integrator 2	Q9UBW5	1
Calumenin-B	O43852	1
Chromobox protein homolog 3	P83916	1
Cleavage and polyadenylation specificity factor subunit 6	Q16630	1
Coronin-1A	P31146	1
CTP synthase 1	P17812	1
Factor VIII intron 22 protein	P23610	1
Glycogen phosphorylase, muscle form	P11217	1
Heat shock cognate 71 kDa protein	P11142	1
Heat shock protein SSB	Q75E44	1
Histone H2B type 1-K	O60814	1
LIM and senescent cell antigen-like-containing domain protein 1	P48059	1
Myeloperoxidase	P05164	1
Myosin light chain 6B	P14649	1
Neutral alpha-glucosidase AB	Q14697	1
Nucleobindin-2	P80303	1
Probable heat shock protein ssa2	P08107	1
Proteasome subunit alpha type-7	Q9SXU1	1
Proteasome subunit beta type-5	P28074	1
Protein phosphatase 1 regulatory subunit 7	Q15435	1
Pyruvate dehydrogenase E1 component subunit alpha, somatic form, mitochondrial	P08559	1
Nuclease-sensitive element-binding protein 1	P67809	1
Rho GTPase-activating protein 17	Q68EM7	1
RNA-binding Raly-like protein	Q86SE5	1
SAM domain-containing protein SAMSN-1	Q9NSI8	1
Small glutamine-rich tetratricopeptide repeat-containing protein alpha (F2)	O43765	1
Tubulin alpha-3 chain	P09734	1
Vasodilator-stimulated phosphoprotein	P70460	1
Zinc finger CCCH-type antiviral protein 1	Q7Z2W4	1
Zinc import ATP-binding protein znuC	Q68Y13	1

Appendix

Preliminary data obtained from LC-MS/MS and CPFP analysis of DCs infected with HIV-1 or mock.

Table A1

Proteins exclusively phosphorylated following HIV-1 infection	SwissProt Number	Number peptide matches
Heat shock protein HSP 90-alpha	P07900	11
60S acidic ribosomal protein P0	P05388	9
Casein kinase II subunit alpha	P68400	8
Septin-7	Q16181	8
60S acidic ribosomal protein P1	P05387	7
Acidic leucine-rich nuclear phosphoprotein 32 family member A	P39687	7
Neuroblast differentiation-associated protein AHNAK	Q09666	6
Proliferation-associated protein 2G4	Q9UQ80	6
Proteasome subunit beta type-2	P49721	6
Tubulin beta-6 chain	Q9BUF5	6
Lamin-A/C	P02545	5
Stress-induced-phosphoprotein 1	P31948	5
Zyxin	Q15942	5
14-3-3 protein zeta/delta	P63104	4
Cytosolic purine 5'-nucleotidase	P49902	4
Eukaryotic translation initiation factor 2 subunit 2-like protein	P20042	4
Hematopoietic lineage cell-specific protein	P14317	4
Heterogeneous nuclear ribonucleoprotein U-like protein 2	Q1KMD3	4
HLA class II histocompatibility antigen, DR alpha chain	P01903	4
LIM and SH3 domain protein 1	Q14847	4
Plasminogen activator inhibitor 1 RNA-binding protein	Q8NC51	4
Pyruvate dehydrogenase E1 component subunit beta	P11177	4
Serum albumin	P02769	4
Splicing factor 1	Q15637	4
Synapse-associated protein 1	Q96A49	4
Tubulin alpha-4A chain	P68366	4
AMP deaminase 2	Q01433	3
Calumenin	O35783	3
cAMP-dependent protein kinase catalytic subunit alpha C-beta	P17612	3
Dihydropyrimidinase-related protein 2	Q16555	3
Eukaryotic translation initiation factor 4B (F2)	P23588	3
Histone H2A type 2-C	Q16777	3
Interferon regulatory factor 2-binding protein 2	Q7Z5L9	3
Proteasome activator complex subunit 1	Q06323	3
Putative adenosylhomocysteinase 2	O43865	3
Ras-related GTP-binding protein C	Q9HB90	3
Septin-6	Q14141	3
Serine/threonine-protein kinase PAK 2	Q13177	3
Splicing factor, arginine/serine-rich 1	Q07955	3
Transcription factor BTF3 homolog 4	Q96K17	3
Ubiquitin	P62988	3
14-3-3 protein epsilon	P62258	2
26S proteasome non-ATPase regulatory subunit 7	P51665	2
28 kDa heat- and acid-stable phosphoprotein	Q13442	2
5'-AMP-activated protein kinase subunit gamma-1	P54619	2
Acidic leucine-rich nuclear phosphoprotein 32 family member B	Q92688	2
Activated RNA polymerase II transcriptional coactivator p15	P53999	2
Aspartyl aminopeptidase	Q9ULA0	2
Bcl-2-like protein 13 (F1)	Q9BXK5	2
cAMP-dependent protein kinase type II-alpha regulatory subunit	P13861	2
Capz-interacting protein	Q6JBY9	2
Coatomer subunit epsilon	O14579	2
Coronin-1C	Q9ULV4	2
DnaJ homolog subfamily A member 1	P31689	2
Heterogeneous nuclear ribonucleoprotein C	P07910	2
Histone H2A.x	P16104	2
HLA class II histocompatibility antigen, DRB1-3 chain	P01912	2
Importin subunit alpha-3	O00505	2
Importin subunit alpha-4	O00629	2
Lipoma-preferred partner homolog	Q93052	2
Programmed cell death protein 10	Q9BUL8	2
Proteasome activator complex subunit 2	Q9UL46	2
Protein CutA	O60888	2

Proteins exclusively phosphorylated following HIV-1 infection	SwissProt Number	Number peptide matches
Protein NDRG2	Q9UN36	2
Ras GTPase-activating protein-binding protein 1	Q13283	2
Ras GTPase-activating protein-binding protein 2	Q9UN86	2
Ras-related GTP-binding protein A	Q7L523	2
Reticulon-4	Q9NQC3	2
Serine/threonine-protein kinase PAK 1	Q13153	2
Triosephosphate isomerase	P60174	2
Uncharacterized protein C22orf9	Q6ICG6	2
UPF0687 protein C20orf27	Q9GZN8	2
Wiskott-Aldrich syndrome protein family member 2	Q9Y6W5	2
14-3-3 protein beta/alpha	P31946	1
14-3-3 protein gamma	P61981	1
26S protease regulatory subunit 6A homolog B	P17980	1
26S proteasome non-ATPase regulatory subunit 9	O00233	1
A-kinase anchor protein 12	Q02952	1
Alpha-adducin	P35611	1
Annexin A2	P07355	1
AP-1 complex subunit beta-1	Q10567	1
ATP synthase subunit alpha, mitochondrial	P25705	1
Autophagy-related protein 7	O95352	1
Beta-arrestin-1	P49407	1
BRCA1-A complex subunit MERIT40	Q9NWV8	1
Breast carcinoma-amplified sequence 3	Q9H6U6	1
Calcium-regulated heat stable protein 1	Q9Y2V2	1
Calpain small subunit 1	P04632	1
Calpain-2 catalytic subunit	P17655	1
Calreticulin-3	Q9D9Q6	1
Charged multivesicular body protein 4b (F3)	Q9H444	1
Clathrin light chain A	P09496	1
Cyclin-K	O75909	1
Cytosol aminopeptidase	P28838	1
Dr1-associated corepressor	Q14919	1
Drebrin-like protein	Q9UJU6	1
Elongation factor Tu, mitochondrial	P49411	1
Eukaryotic translation initiation factor 2 subunit 1	P05198	1
Exportin-2	P55060	1
Filamin-A	P21333	1
Fructose-bisphosphate aldolase A	P04075	1
Gamma-adducin	Q9UEY8	1
Gamma-aminobutyric acid receptor-associated protein	O95166	1
Heterogeneous nuclear ribonucleoprotein A3	P51991	1
Heterogeneous nuclear ribonucleoprotein G	P38159	1
High mobility group nucleosome-binding domain-containing protein 3	Q15651	1
High mobility group protein B3	O15347	1
Histone deacetylase 2	Q92769	1
HLA class II histocompatibility antigen, DR-1 beta chain	P01914	1
Isocitrate dehydrogenase [NADP], mitochondrial	P48735	1
KH domain-containing, RNA-binding, signal transduction-associated protein	Q07666	1
LIM domain and actin-binding protein 1	Q9UHB6	1
Lys-63-specific deubiquitinase BRCC36	P46736	1
Methylosome protein 50	Q9BQA1	1
Microtubule-associated protein 1S	Q66K74	1
Myosin light chain 1/3, skeletal muscle isoform	P05976	1
Na(+)/H(+) exchange regulatory cofactor NHE-RF1	O14745	1
NAD kinase	O95544	1
Nascent polypeptide-associated complex subunit alpha-2	Q9H009	1
Nuclear receptor coactivator 5	Q9HCD5	1
Nucleobindin-1	Q02818	1
Nucleolin	P19338	1
Pantothenate kinase 2, mitochondrial	Q9BZ23	1
Peroxiredoxin-4	Q13162	1
Pallidin	Q9UL45	1
Peroxisomal biogenesis factor 19	P40855	1
PEST proteolytic signal-containing nuclear protein;	Q8WW12	1
Phosphoglycerate kinase 1	P00558	1
Phostensin	Q6NYC8	1
PRA1 family protein 3	O75915	1
Proactivator polypeptide	P07602	1
Proteasome subunit beta type-10	P40306	1
Proteasome subunit beta type-7	Q99436	1
Protein arginine N-methyltransferase 5	O14744	1
Protein canopy homolog 3 (F5)	Q9BT09	1

Proteins exclusively phosphorylated following HIV-1 infection	SwissProt Number	Number peptide matches
Protein cappuccino homolog	Q9NUP1	1
Protein numb homolog	P49757	1
Protein phosphatase 1F	P49593	1
Putative heat shock protein HSP 90-alpha A4	Q58FG1	1
Pyruvate dehydrogenase E1 component subunit beta, mitochondrial	Q09171	1
Quinone oxidoreductase	Q08257	1
Reticulocalbin-1	Q15293	1
Serine/threonine-protein kinase 24	Q9Y6E0	1
Small nuclear ribonucleoprotein Sm D1	P62314	1
Small nuclear ribonucleoprotein Sm D3	P62318	1
Stromal cell-derived factor 2-like protein 1	Q9HCN8	1
Target of Myb protein 1	O60784	1
Transcription factor Sp3	Q02447	1
Transcriptional activator protein Pur-alpha	Q00577	1
tRNA modification GTPase mnmE	Q39ZT0	1
U1 small nuclear ribonucleoprotein 70 kDa	P08621	1
UV excision repair protein RAD23 homolog A	P54725	1
Vinculin	P18206	1
Voltage-gated potassium channel subunit beta-2	Q13303	1
WD repeat-containing protein 82-B	Q6UXN9	1
Zinc finger protein 428	Q96B54	1

Table A2

Proteins exclusively dephosphorylated following HIV-1 infection	SwissProt Number	Number unique peptide matches
Heat shock protein HSP 90-alpha	P46633	14
Eukaryotic translation initiation factor 2 subunit 3	P41091	11
Probable ATP-dependent RNA helicase DDX17	Q92841	11
Protein disulfide-isomerase A4	Q29RV1	7
Ribonuclease inhibitor	P13489	6
Heat shock protein beta-1	P04792	5
Proteasome subunit alpha type-4	P25789	5
Histone H2A type 2-C	A1A4R1	4
Myosin-9	P35579	4
Cleavage and polyadenylation specificity factor subunit 5	O43809	3
Elongation factor 1-alpha 1	P68104	3
Hepatoma-derived growth factor	P51858	3
Septin-7	Q16181	3
Vacuolar protein sorting-associated protein 4B	O75351	3
40S ribosomal protein S6	P62753	2
Calnexin	P27824	2
Chaperone protein htpG	A0L8B0	2
Heat shock protein 105 kDa	Q92598	2
Heterogeneous nuclear ribonucleoproteins A2/B1	P22626	2
Hsc70-interacting protein	P50502	2
Myosin regulatory light chain 12B	O14950	2
Nascent polypeptide-associated complex subunit alpha, muscle-specific form	Q13765	2
Protein disulfide-isomerase A3	P30101	2
RNA-binding protein Raly	Q9UKM9	2
Septin-6	Q14141	2
Serine/threonine-protein phosphatase 6 regulatory ankyrin repeat subunit B	Q8N8A2	2
Tropomyosin alpha-3 chain	P06753	2
Tubulin beta-1 chain	P07436	2
Tyrosine-protein phosphatase non-receptor type 6	P29350	2
RAC-alpha serine/threonine-protein kinase	P31749	1
ATP synthase subunit beta, mitochondrial	P06576	1
Biogenesis of lysosome-related organelles complex 1 subunit 1	P78537	1
BRCA1-A complex subunit BRE	Q9NXR7	1
BRCA2 and CDKN1A-interacting protein	Q2NL37	1
Bridging integrator 2	Q9UBW5	1
Calumenin-B	O43852	1
Chromobox protein homolog 3	P83916	1
Cleavage and polyadenylation specificity factor subunit 6	Q16630	1
Coronin-1A	P31146	1
CTP synthase 1	P17812	1
Factor VIII intron 22 protein	P23610	1
Glycogen phosphorylase, muscle form	P11217	1
Heat shock cognate 71 kDa protein	P11142	1
Heat shock protein SSB	Q75E44	1
Histone H2B type 1-K	O60814	1
LIM and senescent cell antigen-like-containing domain protein 1	P48059	1
Myeloperoxidase	P05164	1
Myosin light chain 6B	P14649	1
Neutral alpha-glucosidase AB	Q14697	1
Nucleobindin-2	P80303	1
Probable heat shock protein ssa2	P08107	1
Proteasome subunit alpha type-7	Q9SXU1	1
Proteasome subunit beta type-5	P28074	1
Protein phosphatase 1 regulatory subunit 7	Q15435	1
Pyruvate dehydrogenase E1 component subunit alpha, somatic form, mitochondrial	P08559	1
Nuclease-sensitive element-binding protein 1	P67809	1
Rho GTPase-activating protein 17	Q68EM7	1
RNA-binding Raly-like protein	Q86SE5	1
SAM domain-containing protein SAMSN-1	Q9NSI8	1
Small glutamine-rich tetratricopeptide repeat-containing protein alpha (F2)	O43765	1
Tubulin alpha-3 chain	P09734	1
Vasodilator-stimulated phosphoprotein	P70460	1
Zinc finger CCCH-type antiviral protein 1	Q7Z2W4	1
Zinc import ATP-binding protein znuC	Q68Y13	1